#540527

**Sandia National Laboratories
Waste Isolation Pilot Plant**

**Analysis Package for BRAGFLO: 2004 Compliance
Recertification Application Performance
Assessment Baseline Calculation**

Author:	Martin Nemer (6821)		7/27/05
	Print	Signature	Date
Author:	Joshua Stein (6852)	Joshua S. Stein	7/28/2005
	Print	Signature	Date
Technical Review:	Christi Leigh (6821)		July 27 2005
	Print	Signature	Date
QA Review:	Mario Chavez (6820)	Mario Chavez	7/27/05
	Print	Signature	Date
Management Review:	Mark Rigali (6822)		7/27/05
	Print	Signature	Date
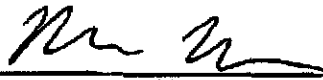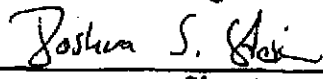
WIPP:1.4.1.1:PA:QA-L:540232

Table of Contents

List of Tables

List of Figures

Acronyms

AP	Analysis Plan
BNL	Brookhaven National Laboratory
CCA	Compliance Certification Application
CCDF	Complementary Cumulative Distribution Function
CMS	Code Management System
CDB	Camdat database file
CRA	Compliance Recertification Application
CPR	Cellulose, plastic, and rubber
DCL	Digital Command Language
DOE	U.S. Department of Energy
DRZ	Disturbed Rock Zone
EPA	U.S. Environmental Protection Agency
LHS	Software that performs Latin Hypercube sampling
LWB	Land Withdrawal Boundary
MB	Marker Bed
OC	Organic Carbon
PA	Performance Assessment
PAPDB	Performance Assessment Parameter Database
PAVT	Performance Assessment Verification Test
PC	Personal Computer
PCS	Panel Closure System
POD	Parameter Output Database
PRCC	Partial Rank Correlation Coefficient
RoR	Rest of Repository
SNL	Sandia National Laboratories
TBM	Technical Baseline Migration
TRU	Transuranic Waste
WIPP	Waste Isolation Pilot Plant

1 EXECUTIVE SUMMARY

This report describes and compares the results of BRAGFLO calculations for the CRA 2004 PABC to results of earlier analyses including the CRA 2004 and the 1997 PAVT. Significant changes to the BRAGFLO model include new significantly lower microbial gas generation rates and the removal of methanogenesis from the microbial-gas-generation model. The new lower gas generation rates lead to a slower rate of pressurization of the repository but the overall pressure at 10,000 years is not significantly different from the CRA 2004. The effect of the removal of methanogenesis on BRAGFLO results is negligible.

2 INTRODUCTION

2.1 BACKGROUND

The Waste Isolation Pilot Plant (WIPP) is located in southeastern New Mexico and has been developed by the U.S. Department of Energy (DOE) for the geologic (deep underground) disposal of transuranic (TRU) waste (U. S. DOE, 1980; U. S. DOE, 1990; U. S. DOE, 1993). In 1992, Congress designated the U.S. Environmental Protection Agency (EPA) as WIPP's official certifier, and mandated that once DOE demonstrated to EPA's satisfaction that WIPP complied with Title 40 of the Code of Federal Regulations, Part 191 (U.S. DOE, 1996; U.S. EPA, 1996), EPA would certify the repository. To show compliance with the regulations the DOE had their scientific advisor, Sandia National Laboratories (SNL) develop a computational modeling system to predict the future performance of the repository for 10,000 years after closure, given the conceptual models of E1/E2 intrusions (see §6.4.1) being the primary pathways for releases. SNL has developed a system called WIPP Performance Assessment (PA), which examines failure scenarios, quantifies their likelihoods, estimates potential releases to the surface or the site boundary, and evaluates the potential consequences, including uncertainties. The regulation also requires that these models be maintained and updated with new information to be part of a recertification process that occurs at five-year intervals after the first waste is received at the site.

The WIPP PA consists of a suite of software designed to predict conditions in and around the repository over a period of 10,000 years. The first model that is run for the PA is the BRAGFLO software (Stein, 2003a), which simulates brine and gas flow in and around the repository. BRAGFLO includes the effects of processes such as gas generation and creep closure. Outputs from the BRAGFLO simulations describe the conditions (pressure, brine saturation, porosity) and flow patterns (brine flow up an intrusion borehole and out anhydrite marker beds to the accessible environment) that are used by other software to predict radionuclide releases.

This report documents the BRAGFLO simulations and results that support the baseline PA calculations for the first recertification of the repository as described below.

2.1.1 Compliance Certification Application

In October 1996, DOE submitted the Compliance Certification Application (CCA) to the EPA, which included the results of the WIPP PA system. During the review of the CCA, EPA mandated an additional Performance Assessment Verification Test (PAVT), which revised selected CCA inputs to the PA (SNL, 1997). The PAVT analysis ran the full suite of WIPP PA software and confirmed the conclusions of the CCA analysis that the repository design met the regulations. Following the receipt of the PAVT analysis, EPA ruled in May 1997 that WIPP had met the regulations for permanent disposal of transuranic waste. Several lawsuits in opposition to the EPA's ruling were filed in court and were eventually dismissed. The first shipment of radioactive waste from the nation's nuclear weapons complex arrived at the WIPP site in late March 1999, starting the five-year clock for the site's required recertification. The results of CCA PA analyses were subsequently summarized in a SNL report (Helton et al., 1998).

2.1.2 Technical Baseline Migration

The Technical Baseline Migration (TBM) was an effort begun in 2001 to merge the CCA (U. S. DOE, 1996) and PAVT (SNL, 1997) PA baselines while at the same time implementing conceptual model changes being reviewed by the Salado Flow Peer Review in preparation for the first recertification PA. The TBM analysis eventually consisted of a full PA calculation which implemented several changes from the PAVT PA baseline. As part of this migration, a new BRAGFLO numerical grid (mesh) was developed and is described in Hansen et al. (2002). The new TBM BRAGFLO grid replaced the CCA/PAVT BRAGFLO grid. The most important changes with respect to the TBM BRAGFLO grid were the implementation of the Option D panel closure design, which was mandated by the EPA as a condition to their final rule, and the removal of an explicit representation of the shaft seal system in the grid. Additional grid refinements were implemented to increase numerical accuracy and computational efficiency and to reduce numerical dispersion in transport simulations that used the same grid as BRAGFLO.

In May, 2002, the Salado Flow Peer Review panel met in Carlsbad to evaluate the proposed changes to conceptual models for the TBM. A set of PA calculations (TBM) was run to demonstrate the effects of these changes on BRAGFLO results. The peer review panel judged the changes to be "generally sound in their structure, reasonableness, and relationship to the original models". However the panel required that a total systems PA be run and complementary cumulative distribution functions (CCDFs) be generated before they would agree to the changes (Caporuscio et al., 2002).

2.1.3 Analysis Plan 106 (AP106)

After the first meeting of the Salado Flow Peer Review, the conceptual models were revised to address new concerns of the EPA and to incorporate new technical information from laboratory and field investigations (Stein and Zelinski, 2003b). The Salado Flow Peer Review Panel held a second and final meeting in Carlsbad in February 2003 to consider the results of the total systems PA using the new revised BRAGFLO grid and modeling assumptions. The panel approved the proposed conceptual model changes (Caporuscio et al., 2003) permitting the start of PA analyses for the 2004 Compliance Recertification

Information Only

Application (CRA-2004) beginning with the Salado Flow Analysis of gas and brine flow in the vicinity of the repository.

2.1.4 2004 Compliance Recertification Application

The first compliance recertification application (CRA-2004) was submitted to the EPA by the DOE in March 2004 (U.S. DOE, 2004). During its review of CRA-2004, the EPA raised several questions regarding its completeness and technical adequacy (Cotsworth, 2004a; Cotsworth, 2004b; Cotsworth, 2004c; Cotsworth, 2004d), (Gitlin, 2005). The DOE and SNL responded to EPA questions in writing (Detwiler, 2004a; Detwiler, 2004b; Detwiler, 2004c; Detwiler, 2004d; Detwiler, 2004e; Detwiler, 2004f; Piper, 2004; U.S. DOE, 2004; Patterson, 2005; Triay, 2005) and by engaging in technical meetings with EPA staff. The result of these technical interactions was that the EPA required that SNL revise the CRA-2004 PA analysis and run a new PA analysis, which would be considered the PA new baseline following recertification. The BRAGFLO results of this revised calculation (CRA-2004 PABC) are the subject of this report.

2.2 OBJECTIVES FOR THE CRA-2004 PABC BRAGFLO ANALYSIS

The EPA required that DOE revise the CRA-2004 analysis and present results before EPA would judge the CRA-2004 complete (Cotsworth, 2005). The EPA noted a number of technical changes and corrections to the CRA-2004 PA that it deemed necessary. Additionally, the EPA stated that a number of modeling assumptions used in CRA-2004 have not been sufficiently justified and that alternative modeling assumptions must be used. The issues and changes mandated by the EPA that effect the BRAGFLO portion of WIPP PA include the following:

1) Inventory information was updated.
2) Changes to the parameter describing the probability of microbial gas generation in the repository were made.
3) Methanogenesis was no longer assumed to be the primary microbial gas generation reaction.

Minor corrections were also made in the CRA-2004 PABC to the LHS's parameter sampling step to correct an error that was discovered after completion of the CRA-2004 (Vugrin et al., 2005). The work contained in this report was performed under AP-122 (Kanney and Leigh, 2005).

3 CONCEPTUAL APPROACH FOR SALADO FLOW ANALYSIS

The conceptual models implemented in the BRAGFLO simulations for the CRA-2004 PABC are unchanged from those approved by peer review for the CRA-2004.

3.1 MODEL GEOMETRY

Information Only

The BRAGFLO grid used for CRA-2004 PABC BRAGFLO calculations is the same as that used for the CRA-2004 (Stein and Zelinski, 2003a). This grid is shown as a logical grid with dimensions in Figure 3-1 and it is shown from the top, displaying its radial flaring in Figure 3-2. It should be noted that there were minor errors in the figure presented in the CRA-2004 BRAGFLO analysis report (Stein and Zelinski, 2003a), which have been corrected in this report. The erroneous figure in the Stein and Zelinski report (2003a) displayed more significant figures in the ΔY dimensions than were being used in the GENMESH input file. In addition, the DX dimensions for columns 20 and 48 were labeled as 4.21 m rather then 4.20 m, which is used in the GENMESH input file. These errors in the figures are corrected in this report. Despite this correction in this report the BRAGFLO grids used in the CRA-2004 and the CRA-2004 PABC are identical in regards to the dimensions of the grid cells.

Figure 3-1. CRA-2004 PABC BRAGFLO grid (Δx, Δy, and Δz dimensions in meters). Note that "north of the repository" is to the right of the Exp area on the above graph and "south of the repository" is to the left of the Panel area.
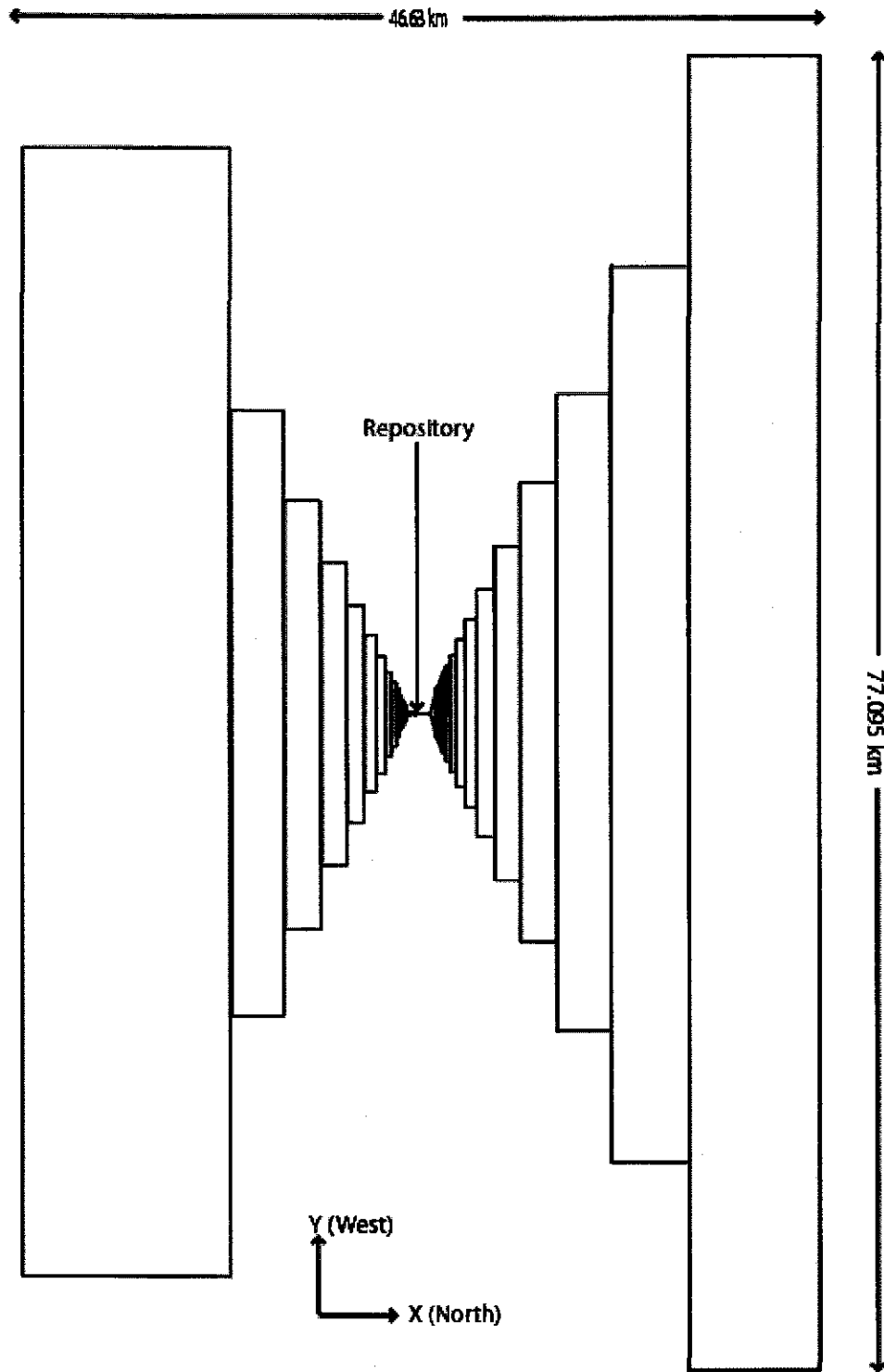
Figure 3-2. Top view of CRA-2004, CRA-2004 PABC logical grid showing the radial flaring.

The primary objective in creating the modeling grid for BRAGFLO is to capture the effects of known and significant hydrologic features in and around the repository. This is accomplished by using a vertical, two-dimensional grid, oriented south to north through the repository and surrounding strata (Figure 3-1). The lengths (Δx), the widths (Δz), and the heights (Δy) of each grid cell are indicated in Figure 3-1. The wide variation in grid cell dimensions captures a relatively large amount of detail with a relatively small number of grid cells.

The two dimensional BRAGFLO grid captures three-dimensional flow effects by employing the technique of "radial flaring." This flaring is visible when looking down on the grid from the top as shown in Figure 3-2. In this figure, the width of each grid cell to the north and south of the repository increases with distance away from the center of the waste filled region. The flaring simulates convergent or divergent flow to the north and south centered on the repository, and laterally away from the repository. The flaring methodology used to create the grid is discussed in a separate memorandum (Stein, 2002). This general methodology was tested in WIPP PA (SNL, 1996) and shown to adequately represent fluid releases when compared to an alternative three dimensional approach, which is more computationally expensive.

The Salado flow grid incorporates the repository, the Castile brine reservoir, the Salado Formation, bedded units above the Salado, the shaft, panel seals, and an intrusion borehole, used for disturbed scenarios. The analysis report for CRA-2004 (Stein and Zelinski, 2003a) provides a detailed explanation of all the stratagraphic and other materials used to represent the repository and surrounding units.

The CRA-2004 grid has been designed to address a variety of issues that have arisen since the CCA. Some of these changes were evaluated in the TBM analysis, and others in the CRA-2004 (introduced for AP106). The following changes from the CCA grid were peer reviewed and incorporated into the CRA-2004 grid, as described in the CRA-2004 BRAGFLO analysis report (Stein and Zelinski, 2003a):

1. Refinement of grid outside the excavated area to improve computational accuracy and efficiency,
2. Simplification of the shaft seal model,
3. Implementation of Option D panel closures,
4. Increased segmentation in Rest of Repository (south RoR and north RoR)

3.2 INITIAL CONDITIONS

BRAGFLO simulation of brine and gas flow in the vicinity of the WIPP site requires the assignment of initial conditions including brine pressure, brine saturation, and concentrations of iron and biodegradable material. These initial conditions are provided to BRAGFLO through various pre-processing steps during which values are extracted or sampled from the WIPP PA Performance Assessment Parameter Database (WIPP PAPDB).

At the beginning of each BRAGFLO run (scenario-vector combination), the model simulates a short period of time representing disposal operations. This portion of the run is called the initialization period and lasts for 5 years (from t = -5 to 0 years), corresponding to the time a typical waste panel is expected to be open during disposal operations. All grid blocks require initial pressure and saturation at the beginning of the run (t = -5 years). At the beginning of the regulatory period (0 to 10,000 years), BRAGFLO resets initial conditions within the excavated regions and in the shaft.

The initial conditions at -5 years for BRAGFLO modeling are listed below:

- Brine pressure in all non-excavated regions is equal to lithostatic pressure (sampled at one location and assumed hydrostatic at all other locations).
- Pressure within the repository is set to 1.01325×10^5 Pa (1 atm).
- Brine saturation within the non-excavated regions is set to 1.0.
- Brine saturation within the excavated regions is set to 0.0.

During the initialization period brine tends to flow into the excavated areas and the shaft, resulting in decreased pressure and saturation in the rock immediately adjacent to the excavations. At time, t = 0, the pressure and saturation in all the excavations is reset to initial conditions for the materials used to represent these regions for the regulatory period. This practice is intended to capture the effect of evaporation of brine inflow during the operational period and the transport of this brine up the shaft ventilation system.

For the CRA-2004 PABC, an additional pressure increment is added to the atmospheric pressure initial conditions. This increment of 26,714 Pa is intended to account for a short period of time with a higher microbial gas generation rate (Nemer et al., 2005). This is a change from the CRA-2004 in which the initial pressure was set to 1 atmosphere (101,325 Pa). Microbial gas generation is discussed in greater detail in Section §5.5.

3.3   BOUNDARY CONDITIONS

The boundary conditions assigned for the BRAGFLO calculations are unchanged from the CRA-2004 and are as follows:

- Constant pressure at the north and south ends of the Culebra and Magenta Dolomites.
- Constant pressure (1.01325×10^5 Pa) and saturation (0.08363 dimensionless) conditions at the land surface boundary of the grid.
- No flow conditions at all other grid boundaries.

4   SALADO FLOW MODELING METHODOLOGY

The BRAGFLO software calculates the flow of brine and gas in the vicinity of the WIPP repository over a 10,000-year regulatory compliance period. The results of these

calculations are used by other software to calculate potential radionuclide releases to the accessible environment. Some of the specific processes included in the BRAGFLO calculations include:

- Brine and gas flow
- Creep closure of the waste filled regions within the repository,
- Gas generation due to corrosion of steel and degradation of biodegradable materials (cellulosics, plastics, and rubbers),
- Physical changes (e.g. permeability and porosity) in the modeling domain over time,
- The consequences of rock fracturing due to high pressure.

There is a significant amount of uncertainty associated with characterizing the physical properties of geologic materials that influence these processes. WIPP PA deals with these uncertainties in two ways. Properties such as permeability and porosity are usually measured indirectly and vary significantly depending upon location. This uncertainty in the appropriate value to assign to certain physical properties is called subjective uncertainty. Subjective uncertainty can, in theory, be reduced by further study of the system. Subjective uncertainty is dealt with in WIPP PA (and in BRAGFLO) by running multiple realizations in which the values of uncertain parameters are varied. To reduce the number of realizations required and to ensure that low probability (and possibly high consequence) combinations are represented, Latin Hypercube sampling is used to create the realizations. For the WIPP PA, the LHS software (Vugrin, 2005f) is used to create a "replicate" of 100 distinct parameter sets ("vectors") that span the full range of parameter uncertainty. To ensure that the Latin Hypercube replicates are representative, a total of three replicates are run for a total of 300 separate vectors.

Another type of uncertainty faced by WIPP PA is what is called "stochastic" uncertainty, or the uncertainty in what will happen in the future. Unlike subjective uncertainty, stochastic uncertainty cannot be reduced by further study. To deal with this type of uncertainty, WIPP PA employs a Monte Carlo method of sampling on random "futures". A future is defined as one possible sequence of events. In the context of the BRAGFLO calculations, stochastic uncertainty is included by defining a set of six scenarios for which brine and gas flow is calculated for each of the vectors generated by the LHS software. Another software (CCDFGF) run after BRAGFLO and other PA software use the results of these scenarios to construct the individual futures. The total number of BRAGFLO simulations that have to be run for a WIPP PA calculation is 300 vectors times 6 scenarios, or 1800 BRAGFLO model runs.

4.1 SALADO FLOW MODELING PROCESS

To run each of these 1800 separate BRAGFLO simulations requires a series of preprocessing steps to be performed:

- A numerical modeling grid must be defined.
- Material types need to be assigned to regions

- Physical properties for all material types must be defined
- Other parameters required by BRAGFLO (e.g. gas generation rates, etc ...) must be defined.

These tasks are accomplished in five discrete computer-modeling steps, which are summarized in Table 4-1. This table also includes the software names and version numbers used for the CRA-2004 PABC BRAGFLO analysis. Additional information can be found in Long (2005).

4.1.1 SANTOS

Several steps must be complete before the BRAGFLO analysis can start. Creep closure calculations (SANTOS) must be complete and an ASCII input file created that contains information about the porosity surface(s) to be used in the BRAGFLO calculation. The ASCII file used for the CRA-2004 PABC is named BF2_CRA1BC_CLOSURE.DAT and is located in the Code Management System (CMS) library: LIBCRA1BC_BF. This file is identical to the one used for the CRA-2004 calculations. The porosity surface data contained in the file is identical to that used for the 1996 CCA and 1997 PAVT PA calculations as well.

4.1.2 LHS

In addition, the LHS software is run before BRAGFLO calculations can start. The LHS software obtains information from the WIPP PAPDB via the preprocessing software PRELHS. This software reads from an ASCII input file, finds in the database the parameters that describe the probability distributions used in the WIPP PA analysis, and creates an ASCII output file, which is used as input to the LHS software, which does the actual parameter sampling. There are three ASCII input files read by PRELHS (one for each replicate) for the CRA-2004 PABC. These files are named: LHS1_CRA1BC_R1.INP, LHS1_CRA1BC_R2.INP, and LHS1_CRA1BC_R3.INP. They are stored in the CMS library: LIBCRA1BC_LHS.

4.1.3 GENMESH

The first step in the BRAGFLO modeling process (Step 1 in Table 4-1) is the definition of the modeling grid using the software, GENMESH (Shuldberg, 1995). The parameters required to define the mesh include grid cell dimensions and region definitions. The analyst supplies these parameters in an ASCII input file. The CRA-2004 PABC analysis uses the file: GM_BF_CRA1BC.INP located in CMS library: LIBCRA1BC_BF.

4.1.4 MATSET

Details of the functionality of MATSET are discussed in the MATSET Users Manual (Gilkey, 2001). MATSET is the first step for assigning the material property values needed by BRAGFLO (Step 1 in Table 4-1). The GENMESH binary output file, which

is required as input for the MATSET software, provides the initial material map. All materials and properties that are used in BRAGFLO modeling should be specified in this modeling step, although the values may be changed in subsequent steps. For example, the parameters that are assigned sampled values by the LHS software in modeling Steps 3 through 5, must be assigned initial values by MATSET so that they can be reassigned in later steps.

Each property assignment requires specification of both the material (e.g. Salado halite) and the property (e.g. bulk compressibility) to be associated with that material. For PA analyses, MATSET extracts the information from the WIPP PAPDB according to instructions in the user-supplied input control file. If the database contains information defining a distribution of values for a material/property pair, MATSET retrieves the median value. The MATSET input file used for the CRA-2004 PABC is MS_BF_CRA1BC.INP and is located in the CMS library: LIBCRA1BC_BF.

4.1.5   POSTLHS

Modeling Step 2 (Table 4-1) employs the software, POSTLHS, which takes the binary output from MATSET and creates 100 copies of this file replacing median values with the sampled values from the LHS software for every sampled parameter in each vector. Table 4-2 summarizes the parameters that are assigned sampled values by the LHS software. The independent variable name in the right hand column of the table is used in the analysis of BRAGFLO and is simply an alternative single-word name for each sampled MATERIAL/PROPERTY pair. These "independent variable" names are used in the sensitivity analysis described in section 4.1.12. POSTLHS requires that a dummy ASCII file be specified, which is not used in the calculations. The dummy file used for the CRA-2004 PABC is LHS3_DUMMY.INP and is located in CMS library: LIBCRA1BC_BF.

4.1.6   ICSET

Initial conditions required by BRAGFLO include pressure, saturation, and steel and biodegradable material concentrations in all grid cells. Modeling Step 3 (Table 4-1) uses the application, ICSET (provide reference) to define some of these initial conditions. The functionality of ICSET is described in the Users Manual (Rath, 1995). The software requires a user-supplied input control file defining how initial conditions are to be set and the POSTLHS binary (.CDB) file from Step 2. ICSET updates the input CDB file with the user supplied initial conditions creating a new output CDB file. The ICSET input file used for the CRA-2004 PABC is IC_BF_CRA1BC.INP and is stored in the CMS library: LIBCRA1BC_BF.

Table 4-1. BRAGFLO model preprocessing steps used for the CRA-2004 PABC

Modeling Step	Software	Version	WIPP Prefix	Function	Interaction
0	SANTOS	2.1.7		Run prior to BRAGFLO analyses to provide porosity in waste-filled areas as a function of pressure and time. The porosity surface has not changed from the CCA.	
0	PRELHS	2.30	LHS1	Beginning with the CRA-2004 PABC, this software is run for all PA analyses software once, prior to BRAGFLO analysis. Identifies correlated properties. Retrieves property distribution data from WIPP database. User identifies properties to be sampled. Accepts user specified "seed" number that is used by LHS2 to randomly select values of sampled variables.	User Input Control File & Input from MATSET
0	LHS	2.42	LHS2	Beginning with the CRA-2004 PABC, this software is run for all PA analyses software once, prior to BRAGFLO analysis. Latin hypercube sampling is performed creating 100 "vectors" of sampled data. Each vector is defined by a set of randomly generated values for sampled variable based upon the distribution information retrieved by LHS1 from the WIPP database.	No direct user interaction. Input from LHS1.
1	GENMESH	6.08	GM	Generates the modeling grid and defines groups of cells as regions that are stored as material "blocks" in the output file.	User Input Control File
1	MATSET	9.10	MS	Defines additional material blocks and extracts properties from the WIPP database and assigns material-property values.	User Input Control File & Input from GENMESH
2	POSTLHS	4.07A	LHS3	Generates 100 CAMDAT output files (one for each vector).	No direct user interaction. Input from LHS2.
3	ICSET	2.22	IC	Sets selected initial conditions such as initial brine saturation, and initial pressure in the Culebra and Magenta units at the edge of the grid. Other initial conditions are set in the next step.	User Input Control File & Input from LHS3

Table 4-1. BRAGFLO model preprocessing steps used for the CRA-2004 PABC (continued)

Modeling Step	Software	Version	WIPP Prefix	Function	Interaction
3	*ALGEGRACDB*	*2.35*	*ALG1*	User can use ALGEBRACDB to calculate values for specified material properties from other input information (e.g. log permeability to permeability, bulk compressibility to pore compressibility, etc.). Calculations defining initial pressures, steel and biodegradable concentrations, gas generation rates, etc. are made.	User Input Control File & Input from ICSET
4	*PREBRAG*	*7.00*	*BF1*	User specifies temporal parameters for BRAGFLO including drilling location and time and changes in material properties over time. This is the step where each scenario is defined.	User Input Control File & Input from ALG1
5	*BRAGFLO*	*5.00*	*BF2*	Performs calculations for gas generations and gas/brine flow in a porous medium.	No direct user interaction. Input from BF1.
5	*POSTBRAG*	*4.00*	*BF3*	Converts BF2 binary output file into the binary WIPP database format.	No direct user interaction. Input from BF2.
5	*ALGEBRACDB*	*2.35*	*ALG2*	User defines time-integrated output variables used in the analysis of results (e.g. volume averaged pressures and saturations).	User Input Control File & Input from BF3.
	SUMMARIZE	*2.20*	*SUM*	Generates ASCII tables of output variables.	User Input Control File & Input from ALG2
	SPLAT	*1.02*		Creates plots of output variables for each vector (usually 100)	User Input control File & Input from SUMMARIZE
	PCCSRC	*2.21*		Performs correlation and regression analyses	User Input control File & Input from SUMMARIZE & LHS

Steps with user interaction are indicated with bold italics lettering

Table 4-2. List of sampled material/property pairs with distribution type. Label in parenthesis in MATERIAL column refers to label in Figure 3-1.

INDEPENDENT VARIABLE	MATERIAL	PROPERTY	DISTRIBUTION	DESCRIPTION
			Unchanged From CRA-2004	
ANHBCEXP	S_MB139 (MB-138, MB-139, Anhydrite AB)	PORE_DIS	Student's T	Brooks-Corey pore distribution parameter for anhydrite (dimensionless).
ANHBCVGP	S_MB139 (MB-138, MB-139, Anhydrite AB)	RELP_MOD	Cumulative	Pointer variable for selection of relative permeability model for use in anhydrite (dimensionless).
ANHPRM	S_MB139 (MB-138, MB-139, Anhydrite AB)	PRMX_LOG	Student's T	Logarithm of intrinsic anhydrite permeability, x-direction (m^2).
ANRBRSAT	S_MB139 (MB-138, MB-139, Anhydrite AB)	SAT_RBRN	Student's T	Residual brine saturation in anhydrite (dimensionless).
BHPERM	BH_SAND (Borehole)	PRMX_LOG	Uniform	Logarithm of intrinsic borehole permeability, x-direction (m^2).
BPCOMP[1]	CASTILER (Castile Brine Reservoir)	COMP_RCK	Triangular	Logarithm of bulk compressibility of brine pocket (Pa^{-1}).
BPINTPRS	CASTILER (Castile Brine Reservoir)	PRESSURE	Triangular	Initial pressure in brine pocket (Pa).
BPPRM[1]	CASTILER (Castile Brine Reservoir)	PRMX_LOG	Triangular	Logarithm of intrinsic brine pocket permeability, x-direction (m^2).
CONBCEXP	CONC_PCS (CONC_PCS)	PORE_DIS	Cumulative	Brooks-Corey pore distribution parameter for the concrete portion of Panel Closure System (PCS) (dimensionless).
CONBRSAT	CONC_PCS (CONC_PCS)	SAT_RBRN	Cumulative	Residual brine saturation in the concrete portion of PCS (dimensionless).

---

[1] BPPRM and BPCOMP are assumed to be correlated with a correlation coefficient equal to -0.75

Table 4-2. List of sampled material/property pairs with distribution type. (continued)

INDEPENDENT VARIABLE	MATERIAL	PROPERTY	DISTRIBUTION	DESCRIPTION
CONGSSAT	CONC_PCS (CONC_PCS)	SAT_RGAS	Uniform	Residual gas saturation in the concrete portion of PCS (dimensionless).
CONPRM	CONC_PCS (CONC_PCS)	PRMX_LOG	Triangular	Logarithm of concrete permeability, x-direction, in concrete portion of the PCS (m^2).
DRZPCPRM	DRZ_PCS (DRZ_PCS)	PRMX_LOG	Triangular	Logarithm of concrete permeability, x-direction, in the DRZ above the PCS (m^2).
DRZPRM	DRZ_1 (Upper DRZ, Lower DRZ)	PRMX_LOG	Uniform	Logarithm of DRZ permeability, x-direction (m^2).
HALCOMP[2]	S_HALITE (Salado)	COMP_RCK	Uniform	Bulk compressibility of halite (Pa^{-1}).
HALPOR	S_HALITE (Salado)	POROSITY	Cumulative	Halite porosity (dimensionless).
HALPRM[2]	S_HALITE (Salado)	PRMX_LOG	Uniform	Logarithm of halite permeability, x-direction (m^2).
PLGPRM	CONC_PLG (Conc_Mon)	PRMX_LOG	Uniform	Logarithm of concrete plug permeability, x-direction (m^2).
SALPRES	S_HALITE (Salado)	PRESSURE	Uniform	Initial brine pressure, without the repository being present, at a reference point located in the center of the combined shafts at the elevation of the midpoint of Marker Bed (MB) 139 (Pa).
SHLPRM2	SHFTL_T1 (SHFTL_T1)	PRMX_LOG	Cumulative	Logarithm of intrinsic permeability of the lower portion of the simplified shaft (0-200 years)(m^2).
SHLPRM3	SHFTL_T2 (SHFTL_T2)	PRMX_LOG	Cumulative	Logarithm of intrinsic permeability of the lower portion of the simplified shaft (after 200 years)(m^2).
SHUPRM	SHFTU (SHFTU)	PRMX_LOG	Cumulative	Logarithm of intrinsic permeability of the upper portion of the simplified shaft (m^2).
SHURBRN	SHFTU (SHFTU)	SAT_RBRN	Cumulative	Residual brine saturation of the upper portion of the simplified shaft (dimensionless)
SHURGAS	SHFTU (SHFTU)	SAT_RGAS	Uniform	Residual gas saturation of the upper portion of the simplified shaft (dimensionless)

---

[2] HALPRM and HALCOMP are assumed to be correlated with a correlation coefficient equal to -0.99

Table 4-2. List of sampled material/property pairs with distribution type. (continued)

INDEPENDENT VARIABLE	MATERIAL	PROPERTY	DISTRIBUTION	DESCRIPTION
WASTWICK	WAS_AREA (Panel)	SAT_WICK	Uniform	Increase in brine saturation of waste due to capillary forces (dimensionless).
WFBETCEL	CELLULS	FBETA	Uniform	Scale factor used in definition of stoichiometric coefficient for microbial gas generation (dimensionless).
WGRCOR	STEEL	CORRMCO2	Uniform	Corrosion rate for steel under inundated conditions in the absence of CO_2 (m/s).
WGRMICH	WAS_AREA (Panel)	GRATMICH	Uniform	Microbial degradation rate for cellulose under humid conditions (mol/kg·s).
WGRMICI	WAS_AREA (Panel)	GRATMICI	Uniform	Microbial degradation rate for cellulose under inundated conditions (mol/kg·s).
WMICDFLG	WAS_AREA (Panel)	PROBDEG	Cumulative	Categorical variable for microbial degradation of cellulose (dimensionless).
WRBRNSAT	WAS_AREA (Panel)	SAT_RBRN	Uniform	Residual brine saturation in waste (dimensionless).
WRGSSAT	WAS_AREA (Panel)	SAT_RGAS	Uniform	Residual gas saturation in waste (dimensionless).
Changes for CRA-2004 PABC				
ANHCOMP	S_MB139 (MB-138, MB-139, Anhydrite AB)	COMP_RCK	Made constant for the CRA-2004 PABC	Bulk compressibility of anhydrite (Pa^{-1}) (Vugrin et al., 2005).
ANRGSSAT	S_MB139 (MB-138, MB-139, Anhydrite AB)	SAT_RGAS	Made constant for the CRA-2004 PABC	Residual gas saturation in anhydrite (dimensionless) (Vugrin et al., 2005).
BIOGENFC	WAS_AREA (Panel)	BIOGENFC	Added for CRA-2004 PABC	Probability of attaining sampled microbial gas generation rate (dimensionless) (Nemer et al., 2005).

4.1.7 ALGEBRACDB

Modeling Step 3 (Table 4-1) employs the ALGEBRACDB software, which is used to manipulate data from the binary (.CDB) output file from ICSET. ALGEBRACDB is capable of performing most common algebraic manipulations and evaluating most common transcendental functions (trigonometric, logarithmic, exponential, etc.). Its functionality is discussed in the Users Manual (Gilkey, 1996).

ALGEBRACDB reads its instructions from a user-supplied ASCII input file that employs an algebraic syntax that is similar in appearance to FORTRAN syntax. It then executes the mathematical instructions to modify input data from ICSET and to calculate new parameters needed by the BRAGFLO software. These parameters are derived by calculation given data from the WIPP parameter database and not directly from experimental data. The results are written to a new binary (.CDB) output file. Files associated with this step are designated with ALG1 in the filename, because ALGEBRACDB is also used in post-BRAGFLO processing (see §4.1.10).

Calculations performed in this step include:
- Calculation of total amount of steel and biodegradable organic materials from densities reported in the inventory.
- Conversion between units stored in the WIPP PAPDB and units required by BRAGFLO.
- Assignment of parameters sampled for one material to another material (e.g. hydraulic properties are sampled for anhydrite marker bed 139 and assigned to the other marker bed materials in the model).
- Assignment of gas generation parameters including initial concentration, humid and inundated gas generation rates that depend on inventory and sampled parameters.
- Calculation and application of the $1°$ stratigraphic dip of the Salado Formation.

The ALGEBRACDB input file used for this step of the CRA-2004 PABC is ALG1_BF_CRA1BC.INP and is located in CMS library: LIBCRA1BC_BF.

4.1.8 PREBRAG

The final pre-processing step for BRAGFLO modeling (Step 4 in Table 4-1) employs the software, PREBRAG, which accepts the binary (.CDB) output file from ALGEBRACDB (ALG1) and creates the ASCII file used as input to the BRAGFLO software. The functionality of PREBRAG is discussed in the User's Manual (Stein, 2003b). The user supplies instructions to PREBRAG in an ASCII input file to specify changes in modeling conditions at different times and to identify what information should be calculated and written by BRAGFLO to the output files. This is the modeling step in which scenarios are defined by specifying changes in materials and properties at different times (e.g. "create" a borehole at 350 or 1000 years by redefining the material map at that time in the

simulation). The PREBRAG input files the CRA-2004 PABC are BF1_CRA1BC_Ss.INP, where s = 1, ...6, and are located in CMS library: LIBCRA1BC_BF

4.1.9 BRAGFLO

The final step in the BRAGFLO analysis (Step 5 in Table 4-1) is to run the BRAGFLO software for each vector / scenario / replicate combination (1800 model runs). The functionality and the theory on which BRAGFLO is based are discussed in the Users Manual (Stein, 2003a). The results of BRAGFLO include calculated values for variables such as pressure, brine saturation, porosity, and fluid flow at times and grid locations that are specified in the PREBRAG input control file. The output data is written to ASCII and binary output files. Only the binary files are used for Salado Flow analysis and for input to subsequent WIPP PA activities (e.g. NUTS, DRSPALL, etc.). The ASCII input files used for the CRA-2004 PABC runs are named BF2_CRA1BC_R#_S#_V###.INP, where R# is R1, R2, or R3, depending on the replicate, S# is S1-S6, depending on the scenario, and V### is V001 to V100, depending on the vector. These files are stored in 18 separate CMS libraries with the naming convention: LIBCRA1BC_BFR#S#, where R# and S# are described above.

4.1.10 POSTBRAG & ALGEBRACDB (ALG2)

The post-BRAGFLO processing application, POSTBRAG, is used to convert the BRAGFLO binary output file (.BIN) into the CAMDAT (Rechard et al., 1990) database file (.CDB) that is used by other WIPP PA software (Step 5 in Table 4-1). The software ALGEBRACDB is again used to calculate cumulative and/or volume-averaged values for specific regions in the grid. The output is written to a binary (.CDB) file (modeling Step 5 in Table 4-1). Files associated with post-BRAGFLO processing using ALGEBRACDB are identified with ALG2 in their names. The ALGEBRACDB input file used for this post-processing step of the CRA-2004 PABC is ALG2_BF_CRA1BC.INP and is located in CMS library: LIBCRA1BC_BF.

4.1.11 SUMMARIZE and SPLAT

The software, SUMMARIZE (see Table 4-1) is used to extract data from the binary output files (.CDB) from POSTBRAG or ALGEBRACDB (ALG2) to produce ASCII tables organized according to analytical needs. One common use of SUMMARIZE is to create a table of output variables with values for all 100 vectors reported at specified time intervals. In this case, SUMMARIZE will linearly interpolate output values at specific times from the nearest times included in the binary file. This interpolation is necessary because BRAGFLO uses a variable time-step and thus vectors do not have output at exactly the same times. SUMMARIZE can take input from each vector and combine it into a single table file.

Tables from SUMMARIZE are used to make horsetail plots that show the values of output variables for each of the 100 vectors in a scenario over time (usually the full 10,000 year regulatory period). These plots are generated using the software, SPLAT (see Table 4-1).

4.1.12 PCCSRC

Several approaches are used in this analysis to evaluate the effects of sampled input parameters on BRAGFLO results. The simplest method is to use scatter plots to visually evaluate relationships of an output variable with a single input parameter (or another output variable).

Excel is used to calculate Pearson sample correlation coefficients for pairings of variables and input parameters. Pearson correlation coefficients were calculated to determine the relative importance of various input parameters to annualized brine outflow rates during this stage. The Pearson correlation coefficient, r, for two arrays, X and Y containing n elements is:

$$r = \frac{n\left(\sum XY\right) - \left(\sum X\right)\left(\sum Y\right)}{\sqrt{\left[n\sum X^2 - \left(\sum X\right)^2\right]\left[n\sum Y^2 - \left(\sum Y\right)^2\right]}}. \tag{1}$$

Pearson correlation coefficients vary from -1.0 to 1.0 and indicate the extent of a linear relationship between the two arrays.

The application, PCCSRC is a systematic approach to identifying the most important input parameters that explain the variability in model outputs (Gilkey, 1995) (see Table 4-1). PCCSRC produces plots of correlation statistics for selected output variables (dependent variables) relative to sampled input parameters (independent variables). Partial rank correlation coefficients (PRCC's) are used in the Salado Flow Analysis, because some relationships may be non-linear over the full range of conditions represented in 100 vectors. These correlation calculations are performed on the ranks of the variables rather than their values, which reduces problems due to larger differences in the magnitudes of input parameters. Partial correlation coefficients are calculated by excluding the influence of all other parameters. Each PRCC explains how much of the ranking for the output variable can be explained by the ranking of the input variable with the linear effects of the other variables removed (Helton et al., 1998).

PRCC's are calculated at selected times to produce plots of PRCC's over an extended period of time. Only the input parameters with the top five PRCC's are plotted, and any variable with a PRCC below 0.25 is disregarded. The correlations may be positive or negative, and the absolute value of the PRCC indicates the relative importance of each input parameter to the uncertainty in the output variable.

4.1.13 Execution and Run Control

Digital Command Language (DCL) scripts, referred to here as EVAL run scripts, are used to implement and document the running of all software. These scripts, which are the basis for the WIPP PA run control system, are stored in the CRA1BC_EVAL CMS library. All inputs are fetched at run time by the scripts, and outputs and run logs are automatically stored by the scripts in class CRA1BC-0 of the CMS libraries.

4.2 MODELING SCENARIOS

A total of six scenarios (S1-S6) are considered in the BRAGFLO modeling for the WIPP PA. These scenarios are unchanged from those used for the 1996 CCA, the 1997 PAVT, and CRA-2004. The scenarios include one undisturbed scenario (S1), four scenarios that include a single inadvertent future drilling intrusion into the repository in 10,000 years, and one scenario that investigates the effect of two intrusions into a single waste panel. Two types of intrusions are considered. An E1 intrusion assumes the borehole passes through a waste-filled panel and into a pressurized brine pocket that may exist under the repository in the Castile formation. An E2 intrusion assumes that the borehole passes through the repository but does not encounter a brine pocket. Scenarios S2 and S3 model the effect of an E1 intrusion occurring at 350 years and 1000 years, respectively, after the repository is closed. Scenarios S4 and S5 model the effect of an E2 intrusion at 350 and 1000 years. Scenario S6 models an E2 intrusion occurring at 1000 years, followed by an E1 into the same panel at 2000 years. Table 4-3 summarizes the six scenarios used in this analysis.

Table 4-3. BRAGFLO modeling scenarios

Scenario	Description
S1	Undisturbed Repository
S2	E1 intrusion at 350 years
S3	E1 intrusion at 1000 years
S4	E2 intrusion at 350 years
S5	E2 intrusion at 1000 years
S6	E2 intrusion at 1000 years; E1 intrusion at 2000 years.

E1: Borehole penetrates through the repository and into a hypothetical pressurized brine reservoir in the Castile Formation.
E2: Borehole penetrates the repository, but does not encounter brine in the Castile Formation.

5 METHODS AND INPUT INFORMATION SPECIFIC TO THE CRA-2004 PABC

This section describes changes to the CRA-2004 BRAGFLO modeling made for the CRA-2004 PABC calculation. These changes include the following:

1) Inventory information was updated (Crawford, 2005).
2) Parameters describing the bulk compressibility and residual gas saturation for the marker bed materials were changed to constants (Vugrin et al., 2005).
3) The LHS software was revised (Vugrin, 2004).
4) Changes to the parameter describing the probability of microbial gas generation in the repository were made (Nemer, 2005).
5) Methanogenesis is no longer assumed to be the primary microbial gas generation reaction (Nemer and Zelinski, 2005).
6) Microbial gas generation rates were revised to be consistent with, long-term laboratory experimental results (Stein and Nemer, 2005).

5.1 REVISED INVENTORY

Waste inventory information used for the CRA-2004 PABC BRAGFLO simulations has been updated to reflect corrections and changes that have occurred while the EPA completeness review of CRA-2004 was being performed (Crawford, 2005). These changes are reflected by changed inventory parameter values for parameters listed in Table 5-1.

Table 5-1. Inventory parameters revised for the CRA-2004 PABC

Material	Property	Description	CRA-2004 Value	CRA-2004 PABC Value
NITRATE	QINIT	Initial quantity of NO_3^- in waste (moles)	2.6100000E+007	4.3100000E+007
SULFATE	QINIT	Initial quantity of SO_4^{2-} in waste (moles)	6.5900000E+006	4.6100000E+006
WAS_AREA	DCELLCHW	Average density of cellulosics in CH (contact handled) waste (kg/m^3)	5.8000000E+001	6.0000000E+001
WAS_AREA	DCELLRHW	Average density of cellulosics in RH (remote handled) waste (kg/m^3)	4.5000000E+000	9.3000000E+000
WAS_AREA	DIRNCCHW	Bulk density of iron containers in CH waste (kg/m^3)	1.7000000E+002	1.7000000E+002
WAS_AREA	DIRNCRHW	Bulk density of iron containers in RH waste (kg/m^3)	4.8000000E+002	5.4000000E+002
WAS_AREA	DIRONCHW	Average density of iron-based material in CH waste (kg/m^3)	1.1000000E+002	1.1000000E+002
WAS_AREA	DIRONRHW	Average density of iron-based material in RH waste (kg/m^3)	1.1000000E+002	5.9000000E+001
WAS_AREA	DPLASCHW	Average density of plastics in CH waste (kg/m^3)	4.2000000E+001	4.3000000E+001
WAS_AREA	DPLASRHW	Average density of plastics in RH waste (kg/m^3)	4.9000000E+000	8.0000000E+000
WAS_AREA	DPLSCCHW	Bulk density of plastic liners in CH waste (kg/m^3)	1.6000000E+001	1.7000000E+001
WAS_AREA	DPLSCRHW	Bulk density of plastic liners in RH waste (kg/m^3)	4.1000000E+000	3.1000000E+000
WAS_AREA	DRUBBCHW	Average density of rubber in CH waste (kg/m^3)	1.4000000E+001	1.3000000E+001
WAS_AREA	DRUBBRHW	Average density of rubber in RH waste (kg/m^3)	3.1000000E+000	6.7000000E+000

Notes: Values for properties DIRNCCHW and DIRONCHW are unchanged from the CRA-2004.

5.2 CHANGING SAMPLED INPUT PARAMETERS TO CONSTANTS

An error was detected in how the LHS software, Version 2.41, sampled truncated normal distributions (Vugrin, 2004). Correction of this error led to a change in the technique that LHS Version 2.42 uses to sample truncated Student's T distributions, and this change in sampling necessitated a change in how the anhydrite rock compressibility and residual

gas saturation parameters, S_MB139:COMP_RCK and S_MB139:SAT_RGAS, are modeled. Material S_MB139 represents anhydrite marker bed 139 and many material properties defined for this material are applied to the other marker bed materials represented in the BRAGFLO grid (e.g., S_MB138 and S_ANH_AB). The property COMP_RCK is the bulk compressibility of the material. The property SAT_RGAS is the residual gas saturation of the material.

Analysis of results with constant values for the previously sampled input parameters, S_MB139:COMP_RCK and S_MB139:SAT_RGAS, showed no significant impact on pressure, brine saturation levels, or brine outflow results (Vugrin et al., 2005). Furthermore, direct brine release (DBR) volumes were only slightly affected (Vugrin et al., 2005). The impact of the modified parameters on total releases has not been determined in the present analysis. However, the results of the Vugrin et al. (2005) analysis suggest that total releases will not be significantly affected.

New constant values for S_MB139:COMP_RCK and S_MB139:SAT_RGAS were entered into the WIPP PAPDB before the CRA-2004 PABC controlled analysis runs. The values are extracted and assigned to materials in the MATSET analysis step (Step 1 in Table 4-1). The new constant values for these parameters are listed in Table 5-2.

Table 5-2. Parameters changed from sampled to constant values for the CRA-2004 PABC.

Material	Property	CRA-2004 PABC Value	Units
S_ANH_AB	COMP_RCK	2.2300000E-011	Pa^{-1}
S_ANH_AB	SAT_RGAS	5.4950000E-002	dimensionless
S_MB138	COMP_RCK	2.2300000E-011	Pa^{-1}
S_MB138	SAT_RGAS	5.4950000E-002	dimensionless
S_MB139	COMP_RCK	2.2300000E-011	Pa^{-1}
S_MB139	SAT_RGAS	5.4950000E-002	dimensionless

5.3 REVISION OF THE LHS SOFTWARE

Two errors (described below) were detected in the LHS software, Version 2.41 (Vugrin, 2004) , (Hansen, 2004). These errors have been corrected, and a new version of the LHS software (Version 2.42) has been released (Vugrin, 2005a). LHS Version 2.42 was used for the CRA-2004 PABC (Vugrin, 2005a; Vugrin, 2005b; Vugrin, 2005c; Vugrin, 2005d; Vugrin, 2005e; Vugrin, 2005f; Vugrin, 2005g).

The first error in LHS Version 2.41 (Hansen, 2004) affected the sampling of normal and lognormal distributions. The software is supposed to sample between the 1st and 99th quantiles, but due to how the sampling technique was implemented, it could return values outside of the specified sampling range.

The second error in LHS Version 2.41 (Vugrin, 2004) affected the sampling of Student's T and Log Student's T distributions. The software constrained sampled values to be within the range of data points supplied for the distribution by the WIPP PAPDB. The

technique that the software employed for sampling allowed multiple vectors to have the same value for a parameter. Additionally, constraining the sampled values by the data points may unnecessarily restrict the sampling range. LHS Version 2.42 corrected this error by sampling all Student's T and Log Student's T distributions between the 1st and 99th quantiles. Additionally, all vectors are ensured to have distinct values for Student's T and Log Student's T distributions.

5.4 PROBABILITY FOR MICROBIAL DEGRADATION OF DIFFERENT ORGANIC MATERIALS

During a technical exchange with EPA in January 2005, EPA expressed concerns about the parameter that defines the probability that microbial gas generation will occur in the WIPP. Advances in microbiology have found microbes existing in a wide variety of so-called "extreme" environments that were previously not considered to be conducive to supporting microbes. Based on these scientific advances, the EPA argued that the probability that microbial activity and resulting microbial gas generation would occur in the WIPP should be changed from 0.5, which corresponds to microbial activity in 50% of vectors to 1.0, which means that microbial activity could occur in every vector. The DOE responded that there is a significant probability that microbial activity would slow considerably as microbes use the available electron acceptors and the geochemical environment in the waste rooms changes with time. This expectation has been confirmed by long-term microbial gas-generation experiments performed at Brookhaven National Laboratory (BNL) (Francis et al., 1997; U. S. DOE, 2002). Microbial gas-generation rates used in PA for the CCA, the 1997 PAVT and the CRA-2004 Performance Assessment (CRA-2004) were based upon the first 1 to 3 years of data from these experiments, but approximately 10 years of data are now available. The full range of data from the experiments shows that rates of microbial gas generation decrease rapidly with time, slowing significantly after the first few years. During the January 2005 technical exchange, DOE accepted a probability of 1.0 for microbial activity for the CRA-2004 PABC but favored the use of gas-generation rates in the WIPP PA models that reflect the longer-term experimental results.

The probability that microbial degradation of cellulose, plastic, and rubber (CPR) will occur in the waste-filled areas is represented by the sampled input parameter, WAS_AREA:PROBDEG. In the CRA-2004 PA, WAS_AREA:PROBDEG was assigned a delta distribution of integer values and associated probabilities given in Table 5-3.

Table 5-3. Possible values for the parameter, WAS_AREA:PROBDEG, in CRA-2004.

WAS_AREA:PROBDEG value (probability)	Description
0 (0.5)	no microbial gas generation
1 (0.25)	microbial gas generation by consumption of cellulose only
2 (0.25)	microbial gas generation by consumption of CPR

For the CRA-2004 PABC, all vectors are considered to have the potential for microbial gas generation and therefore the case in which WAS_AREA:PROBDEG = 0 was not considered in the CRA-2004 PABC calculation. Instead the probability that only cellulose is susceptible to microbial degradation (WAS_AREA:PROBDEG = 1) was changed to 0.75 while the probability that all CPR is susceptible to degradation (WAS_AREA:PROBDEG = 2) remained at 0.25. The result of these changes is that in 100% of vectors run for the CRA-2004 PABC the effects of microbial degradation and gas generation are simulated. Table 5-4 summarizes the probabilities used to assign values to the parameter WAS_AREA:PROBDEG for the CRA-2004 and for the CRA-2004 PABC. (Nemer and Zelinski, 2005) wrote an analysis report discussing the impact of this change and of revised gas generation rates described in Section 5.5. An additional memorandum was written describing the current implementation of the sampled parameter WAS_AREA:PROBDEG (Nemer, 2005). The new values for WAS_AREA:PROBDEG have been entered into the WIPP PAPDB for use in CRA-2004 PABC analyses.

Table 5-4 Probabilities for biodegradation of different organic materials (WAS_AREA:PROBDEG)

WAS_AREA:PROBDEG	2004-CRA	2004-CRA PABC
0	0.5	0.0
1	0.25	0.75
2	0.25	0.25

5.5 REVISION OF MICROBIAL GAS GENERATION RATES

The microbial-gas-generation rates used in the CCA, the 1997 PAVT and the CRA-2004 PA were based upon the first 1 to 3 years of data from experiments performed at BNL (Francis et al., 1997). Looking over the entire 10 years of experimental data, the rates of microbial gas generation decrease significantly with time. An example of this behavior is shown in Figure 5-1. Gas generation rates are equal to the slope of the gas accumulation lines and it is obvious in the figure that rates decrease significantly over time. Such decreases in the rates of microbial activity is commonly observed in many microbial systems and is generally attributed to the sequential use of different electron acceptors, different substrates, and the build-up of microbial metabolites (Monod, 1949). For the

CRA-2004 PABC calculations the following three modifications were made to the way the gas generation rates are implemented:
1. Gas generation rate distributions were modified to reflect rates observed in long-term experiments run at BNL.
2. The brief initial period of faster gas generation rates was accounted for by adding additional gas to the repository as an initial condition.
3. An additional uncertainty factor was added to the calculation of the microbial gas generation rates for the WIPP to account for differences in conditions between the experiments and the WIPP underground.

5.5.1   New Microbial Gas Generation Rate Distributions

As described in an earlier analysis report (Nemer et al., 2005) and shown in Figure 5-1, the data for the amount of carbon dioxide accumulated versus time was fit using two least-square linear functions, in which the slopes of the best-fit lines correspond to the gas generation rates. The first least-squares fit corresponds to the short-term rapid increase in the amount of accumulated carbon dioxide which occurred during the first year of the experiment. The second line corresponds to the long-term accumulation rate observed from about 1 year to 10 years. A detailed description of the fitting procedure is given in (Nemer et al., 2005).

BRAGFLO requires two zeroth-order microbial-gas-generation rates: WAS_AREA:GRATMICI and WAS_AREA:GRATMICH. The rate WAS_AREA:GRATMICI accounts for the brine-inundated, microbial-gas-generation rate and WAS_AREA:GRATMICH accounts for the humid microbial-gas-generation rate. Additionally both rates are sampled on a uniform distribution between minimum and maximum values. In the CCA, 1997 PAVT, CRA-2004 PA and the current analysis the minimum humid rate (WAS_AREA:GRATMICH) was taken to be zero. A summary of numerical gas generation rates from the CCA, 1997 PAVT, CRA-2004 PA and the current CRA-2004 PABC analysis are given in Table 5-5.
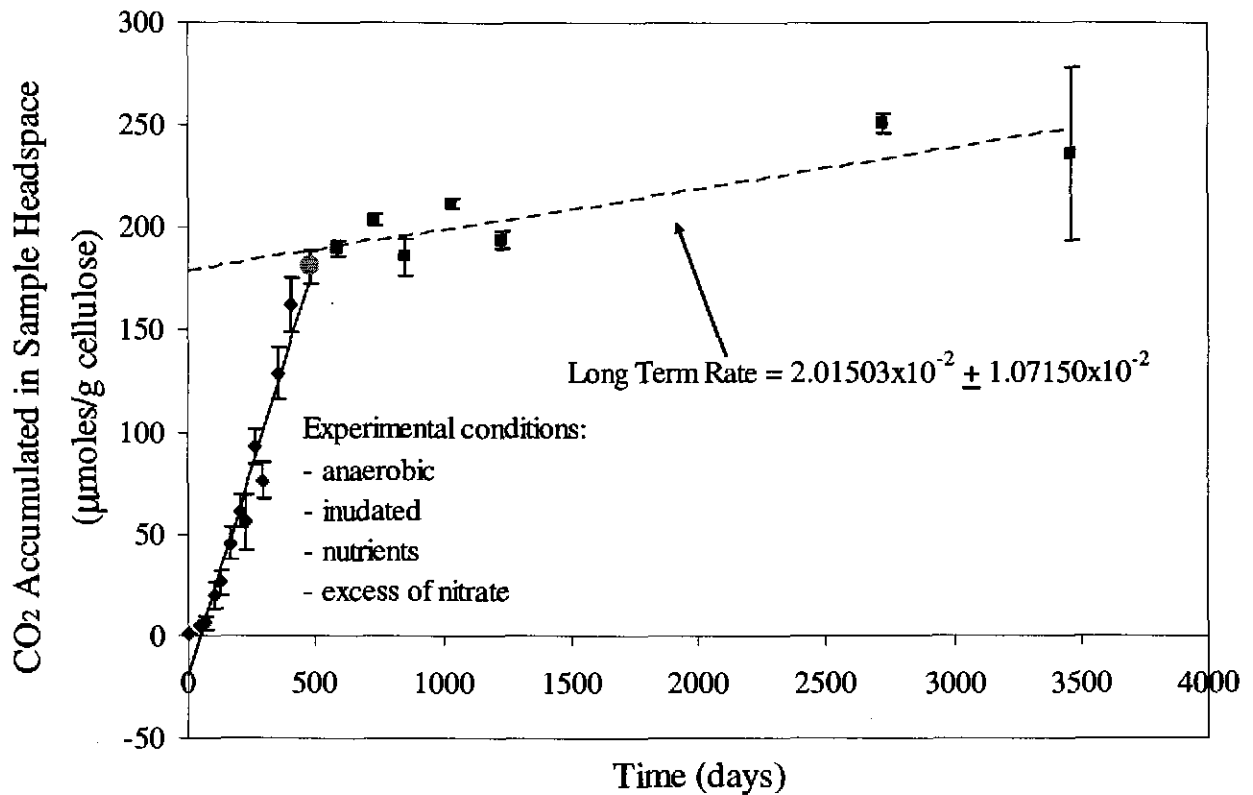
Figure 5-1. Carbon dioxide accumulated in experiments that were inundated, inoculated, amended, and with excess nitrate. This figure was taken from Nemer et al., (2005).

Table 5-5 Microbial gas generation rates from the CCA, PAVT, CRA-2004 PA, and this analysis. In the below table, mol C refers to the moles of organic carbon consumed.

	CCA, PAVT, CRA-2004 PA (mol C/kg/year) (Wang and Brush, 1996)	CRA-2004 PABC (mol C/kg/year) (Nemer et al., 2005)	CRA-2004 PABC BRAGFLO input units (mol C/kg/sec) (Nemer et al., 2005)
Max inundated rate	0.300	0.0175747	5.56921×10^{-10}
Min inundated rate	0.010	0.000972803	3.08269×10^{-11}
Max humid rate	0.040	0.0324142	1.02717×10^{-9}
Min humid rate	0.0	0.0	0.0

The experimental data for the gas generation experiments run under humid conditions indicate that the long-term maximum humid microbial gas-generation rate is greater than the long-term inundated rate. The DOE believes this to be physically unrealistic. Given the lack of water under humid experimental conditions, DOE expects the humid rate to be much less than the case where the microbes are inundated with brine. Thus in this analysis the sampled humid rate was constrained to always be less than or equal to the sampled inundated rate,

$$R_{mh} = \min(R_{mi}, R_{mh}),\qquad\qquad\qquad\qquad (2)$$

where R_{mh} is the sampled humid microbial-gas-generation rate and R_{mi} is the sampled inundated microbial-gas-generation rate. This was implemented in the ALGEBRACDB input file run before PREBRAG (Step 5, Table 4-1) using the following line:

GRATMICH = MIN(GRATMICH,GRATMICI).

5.5.2 Changes to the Initial Conditions

In order to accurately implement the long-term microbial-gas-generation rates in BRAGFLO it is necessary to account for the short-term accumulation of carbon dioxide (the amount of carbon dioxide produced under the solid line in Figure 5-1). Because the BRAGFLO software can only accept zeroth-order gas generation rates which are constant over time, it is not possible to directly simulate this brief period of faster gas generation. Instead, for the CRA-2004 PABC calculations, the gas produced over this brief period is assumed to already exist in the repository at the start of the calculations. This was accomplished by pre-charging the repository with the amount of gas produced by the maximum estimated short-term microbial rate up to the point in time where the rate changed from the short-term value to the long-term value. As described in (Nemer et al., 2005) this was accomplished by adding a pressure increment (26,714 Pa) to the initial atmospheric pressure (one atmosphere 101,325 Pa) in the repository, after closure. The pressure increment was calculated assuming ideal gas behavior and is described in the (Nemer et al., 2005) report. Thus the initial pressure in the waste-filled areas of the repository is defined as: $p_{initial} = (101,325 + 26,714)\,Pa = 128,039\,Pa$ in the current CRA-2004 PABC calculations. The increased initial pressure was implemented in the MATSET input file (Step 1, Table 4-1) with the following lines:

PROPERTY_VALUES, MAT=CAVITY_1, NAME*VALUE: PRESSURE = 1.28039e+005
PROPERTY_VALUES, MAT=CAVITY_2, NAME*VALUE: PRESSURE = 1.28039e+005

5.5.3 Addition of an Uncertainty Factor

The conditions inside the WIPP are likely to be quite different from the conditions represented in the BNL experiments, which were designed to promote microbial growth. Brush (Brush, 2004) indicates that uncertainty about WIPP conditions versus experimental conditions may cause microbial action to be reduced from that observed in the experiments. (Brush, 2004) mentions uncertainty in:

1. Whether microbes will survive for a significant fraction of the 10,000-year regulatory period
2. Whether sufficient H_2O will be present
3. Whether sufficient quantities of biodegradable substrates will be present
4. Whether sufficient electron acceptors will be present and available

5. Whether enough nutrients will be present and available.

Due to these and other uncertainties, an additional sampled parameter was added to theCRA-2004 PABC. This additional parameter is a multiplicative factor (BIOGENFC) that determines the effective microbial-gas-generation rates. BIOGENFC was created in the WIPP parameter database with a uniform distribution from 0 to 1. A uniform distribution was chosen to reflect the fact that there is no quantitative data on the effect of items 1-6 above on the probability of attaining the BNL gas generation rates in the WIPP. BIOGENFC was added to the MATSET and PRELHS input files as a property of the material WAS_AREA. The multiplication of gas generation rates by BIOGENFC was performed in the ALGEBRACDB modeling step. This was accomplished using the following lines in the ALGEBRACDB (Step 5, Table 4-1) input file:

$$KBGSI = GRATMICI*CONCBIO*BIOGENFC$$

$$KBGSH = GRATMICH*CONCBIO*BIOGENFC$$

Here KBGSI, and KBGSH are the inundated and humid microbial-gas-generation rates used by BRAGFLO.

5.6   REMOVAL OF METHANOGENESIS FROM THE MICROBIAL GAS GENERATION MODEL

As a consequence of its completeness review of the CRA-2004, the EPA dictated in comment G-14 of the Third Completeness Letter (Cotsworth, 2004b) that WIPP PA simulations will assume that microbial gas generation may occur only by denitrification and sulfate reduction and not by methanogenesis. EPA's concerns surround the availability of sulfate in the repository, such as in the DRZ, beyond what is initially available in the waste inventory. EPA does not feel that DOE has adequately shown that an excess of sulfate will not be available for the 10,000 year regulatory period. It is commonly accepted that methanogenesis only occurs when the availability of NO_3^- and SO_4^{2-} limits denitrification and sulfate reduction. The amount of nitrate available is limited to that initially in the waste (NITRATE:QINT, see

Table 5-1). Thus for the time being, DOE has accepted EPA's assertion and has removed methanogenesis from the gas generation model for the CRA-2004 PABC. An analysis report was written on the potential impacts of removing methanogenesis on PA (Nemer and Zelinski, 2005).

BRAGFLO gas generation calculations consider three reaction pathways (Wang and Brush, 1996):

$$C_6H_{10}O_5 + 4.8\ H^+ + 4.8\ NO_3^- \rightarrow 7.4\ H_2O + 6\ CO_2 + 2.4\ N_2 \quad \text{[denitrification]} \quad (3)$$

$$C_6H_{10}O_5 + 6\ H^+ + 3\ SO_4^{2-} \rightarrow 5\ H_2O + 6\ CO_2 + 3\ H_2S \quad \text{[sulfate reduction]} \quad (4)$$

$$C_6H_{10}O_5 + H_2O \rightarrow 3\ CH_4 + 3\ CO_2 \quad \text{[methanogenesis]} \quad (5)$$
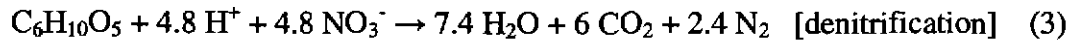
Reactions (3)-(5) are assumed to proceed sequentially according to the energy yield of each reaction. The reactions occur sequentially after concentrations of electron acceptors become depleted. In the CRA-2004, NO_3^- availability was limited such that approximately 2.5% of gas was produced through denitrification; SO_4^{2-} availability limited gas produced by sulfate reduction to approximately 1.2%; approximately 96.3% of microbial gas generation occurred by methanogenesis.

The calculations for this analysis assume that an excess of SO_4^{2-} is always present in the repository. Methanogenesis is removed from WIPP PA models. Given the new inventory for nitrate (NITRATE:QINT, see

Table 5-1), and the new inventory of CPR 4% (of total moles) of gas generation now occurs by denitrification and 96% of gas generation occurs by sulfate reduction; this calculation is performed in Appendix A. The net effect of the removal of methanogenesis on total microbial gas generation is small. This is because CO_2 from all three reactions (Equations 3-5) is absorbed by MgO (Wang and Brush, 2002), and the total moles of other gases produced through sulfate reduction and methanogenesis are equal.

Gas generation stoichiometry is calculated in BRAGFLO using the stoichiometric factor y, which is defined to represent the overall reaction

$$C + unknown \rightarrow y * gas + unknown. \tag{6}$$
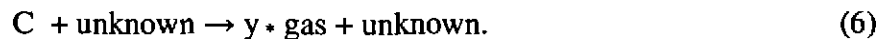
In BRAGFLO all gas is treated as hydrogen. The stoichiometric factor y is related to the cumulative amount of gas produced by 10,000 years. In PA calculations the stoichiometric factor is used to determine the amount of gas produced at any time. The removal of methanogenesis required changing the calculation of the stoichiometric factor.

For each BRAGFLO simulation, y is uniformly sampled over the range, [y_{min}, y_{max}]

$$y = y_{min} + \beta \times (y_{max} - y_{min}), \tag{7}$$

where β is a sampled input parameter ($0 \le \beta \le 1$) with a uniform distribution. Here we do not discuss the details of calculating y_{min} and y_{max}, rather we direct the reader to an analysis report (Nemer and Zelinski, 2005) which covers this calculation. A summary of the values of y_{min} and y_{max} for the CRA-2004 PA and the current analysis is given in Table 5-6. Two values of y_{min} and y_{max} are possible depending on the value of the sampled parameter WAS_AREA:PROBDEG. PA modeling considers two types of organic materials that could be subjected to biodegradation, cellulosics and CPR. Whether cellulose or CPR degrades depends on the value of WAS_AREA:PROBDEG as described in §5.4. Notice from Table 5-6 that y_{min} and y_{max} are equal in the CRA-2004 PABC and thus β is no longer used.

Table 5-6 Stoichiometric factor y. These values were obtained from the ALG1 files, in the ALG1 pre-processing step (see Table 4-1). The location of CRA-2004 data is given in section 6

PA Calculation	Biodegradable Organics	y_{min}	y_{max}
CRA-2004 PABC (no methanogenesis)	Cellulose only	0.486	0.486
CRA-2004	Cellulose only	0.473	0.491
CRA-2004 PABC (no methanogenesis)	CPR	0.495	0.495
CRA-2004	CPR	0.491	0.497

6 MODELING RESULTS

The parameter values (distributions for sampled parameters) used for the Salado Flow Analysis are stored in the WIPP PAPDB, which is accessible on line. The results of Salado Flow Analysis are stored in binary (.CDB) files that reside in CMS library LIBCRA1BC_BFRrSs, where r = 1,2,3, and s = 1,2,...6. The CMS class for these files is CRA1BC-0. These results include detailed and summarized information about:

- Creep closure of the excavated areas of the repository
- Gas generation by corrosion of metal and microbial consumption of organic material
- Pressure
- Fracturing of rock due to high pressure
- Permeability
- Brine and gas saturation
- Brine and gas flow

Other output may be selected by the user, but this may require adjustments to pre-processing steps. The Salado Flow output data are preserved for all cells and areas of the grid at incremental times between 0 and 10,000 years.

The application, ALGEBRACDB, is used to post-process numerical output from BRAGFLO resulting in data that are useful for analysis. The output variables from ALGEBRACDB are listed in Appendix B. Graphics are used extensively to demonstrate observations, relationships, and dependencies. "Horsetail" plots, which are produced using the application SPLAT, plot values of individual variables for all vectors in a scenario as a function of time for the entire 10,000-year regulatory compliance period. These plots are an effective method for demonstrating the potential range and behavior of results. "Composite" plots display the statistics for a replicate over time (e.g. median, mean, maximum and minimum over 100 vectors in a scenario at selected times). These plots are used to collectively view results for comparison purposes (e.g. comparing trends for two different output variables). The application PCCSRC is used to correlate output variables with sampled input parameters and to generate plots displaying the most prominent partial correlation coefficients (PRCC) over time.

In the following subsections, results from the CRA-2004 PABC are often compared to results from the CRA-2004 PA. The results of the CRA-2004 Salado Flow Analysis are stored in binary (.CDB) files that reside in CMS library LIBCRA1_BFRrSs, where r = 1,2,3, and s = 1,2,...6. The CMS class for these files is CRA1A. File names can be found in (Long, 2004).

6.1 *EXCEPTION VECTORS*

The ASCII input control file to BRAGFLO includes a series of input numerical control parameters that influence the way BRAGFLO performs calculations. The standard settings optimize calculations under most circumstances, but occasionally certain BRAGFLO vectors do not run to completion in the maximum number of timesteps (10,000) or encounter a fatal error. These "exception vectors" must be rerun with modified inputs so that they will complete the 10,000 year simulation. Exception vectors usually result from the combination of extreme conditions of coincident sampled variables and/or very small grid cells (e.g., the intersection of the borehole or shaft with a marker bed). These circumstances can lead to extreme spatial or temporal gradients within the model that exceed the default tolerances specified in the input control file. These conditions cause BRAGFLO to shorten its time step. For most vectors this is sufficient to solve the short-lived numerical problem, however for some exception vectors it is necessary to relax, tighten, or otherwise adjust BRAGFLO input numerical control parameters in order to complete the calculations.

The capability to make such adjustments is a normal part of any numerical modeling study including the BRAGFLO modeling process. The input control parameters are included in BRAGFLO software to permit the analyst to make adjustments for circumstances that fall outside of the typical range of modeling conditions and allow a difficult calculation to complete. Description of adjustments to input control parameters for exception vectors are included in the discussion of results for each replicate/scenario. Descriptions of the actual control parameters themselves are in the BRAGFLO user's manual (Stein, 2003a).

6.1.1 Replicate 1

In Replicate 1, BRAGFLO calculations for twelve vectors did not run to completion using standard input control values. Calculations for ten of these ("1" in Table 6-1) were completed by changing the value for ICONVTEST from "1" to "0". Two vectors also required changing the value of the input parameter, FTOLNORM(1), from 1.0E-2 to 1.0E-3. These changes are summarized in Table 6-1 below.

Table 6-1 Exception vectors, CRA-2004 PABC Replicate 1

Vector	S1	S2	S3	S4	S5	S6
22	1	1	1	2		
29	2			1		
46	1	1	1	1	1	1

1 (in table) ICONVTEST changed from "1" to "0"
2 (in table) ICONVTEST changed & FTOLNORM(1) changed from 1.0E-2 to 1.0E-3

6.1.2 Replicate 2

Twelve vectors were rerun with modified input control parameters in order to have BRAGFLO complete the calculations. Calculations for nine of these were

completed by changing the value for ICONVTEST from "1" to "0". Two vectors also required changing FTOLNORM(1). Two vectors required EPS_NORM(1) to be changed from 3 to 4. One vector, Scenario S1 Vector 95, was particularly difficult and also required changing DSATLIM to 0.4 from 0.2, SATLIMIT to 0.1 from 0.001 and MAXSTEPS to 20000 for all 10000. Vector S1 V095 became very dry (low brine saturation) early in the simulation which caused the software to converge very slowly.

Table 6-2 Exception vectors, CRA-2004 PABC Replicate 2

Vector	S1	S2	S3	S4	S5	S6
27	1	1	1	1	1	
55				3	1	
95	4	2				
99	1			1	1	

1 (in table) ICONVTEST set to 0 from 1
2 (in table) ICONVTEST set to 0 & FTOLNORM(1) changed from 1.0E-2 to 1.0E-3
3 (in table) ICONVTEST changed to 0 & FTOLNORM(1) changed to 1.0E-3 & EPS_NORM(1) changed to 4 from 3
4 Vector 95 in Replicate 2, Scenario 1 required setting ICONVTEST to 0, EPS_NORM(1) to 4, DSATLIM to 0.4, SATLIMIT to 0.1 and MAXSTEPS to 20000.

6.1.3 Replicate 3

Six vectors were rerun with modified input control parameters in order to have BRAGFLO complete the calculations. Calculations for five of these were completed by changing the value for ICONVTEST from "1" to "0". Vector 75 in Scenario S5 also required that EPS_NORM(1) be changed from 3 to 2.

Table 6-3 Exception vectors, CRA-2004 PABC Replicate 3

Vector	S1	S2	S3	S4	S5	S6
32	1	1	1			
71				1		
75				1	3	

1 (in table) ICONVTEST set to 0 from 1
3 (in table) ICONVTEST changed to 0 & EPS_NORM(1) changed to 3 from 2

6.2 OVERVIEW OF THE SALADO FLOW ANALYSIS

Repository behavior is characterized by interactions among creep closure, gas generation, and fluid and gas flow. The Salado Flow Analysis is divided into three replicates, and each is comprised of the same six modeling scenarios. Replicate 1 is the primary subject for analysis, and the other two are used to confirm the results for the most important output variables and to demonstrate statistical confidence in the results. Each scenario consists of 100 vectors that are defined by a unique set of sampled input values.

6.2.1 Organization

The discussion of results is organized by scenario or pair of scenarios as follows:

- Section 6.3: Undisturbed (Scenario S1)
- Section 6.4: E2 drilling intrusion at 350 years (Scenario S2), E1 drilling intrusion at 350 years (Scenario S4).
- Section 6.5: Comparison of the replicates for Scenario S1.
-

Each of the sections listed above includes an analysis of the following:

- *Halite Creep.* Plastic flow of salt will cause the pore volume of the repository to decrease over time by gradually compressing the waste-filled rooms and filling the empty space.

- *Brine Inflow.* Availability of brine is required for gas generation and for fluid flow away from the repository.

- *Gas Generation.* In some scenarios, gas generation results in high pressures within the repository.

- *Pressure.* High pressure within the repository can increase permeability of wall rock by causing hydro fracturing. This is a primary output variable to subsequent PA analyses.

- *Brine Saturation.* This affects the rate of corrosion of steel. This is also a primary output variable to subsequent PA analyses.

- *Rock Fracturing.* Caused by high gas pressure. Rock fracturing can increase the porosity and permeability of the wall rock in the DRZ and of anhydrite in the marker beds providing a conduit for local brine migration (e.g., around the panel closures and into the shaft).

- *Brine Outflow.* Brine outflow through the Salado to the accessible environment is a potential pathway for radionuclide transport. Brine flow is a BRAGFLO output variable that is used as input to analyses of radionuclide flow and transport in the Salado and Culebra.

6.2.2 Halite Creep

Creep closure of the excavated regions begins immediately because of excavated-induced loading. As rooms close, waste consolidation will occur and continue until back stresses imposed by compressed waste resist further closure or until fluid pressures become sufficiently high due to gas generation.

BRAGFLO calculates the porosity of materials that undergo creep closure by interpolating over a "porosity surface." The porosity surface gives porosity as a function of time and pressure, and was obtained by modeling deformation of a waste-filled room using the software SANTOS (Butcher et al., 1995 and Stone, 1995).

6.2.3 Coupling of Gas Generation and Brine/Gas Flow

Gas generation and brine/gas flow are coupled processes. Because moisture is required for both corrosion and microbial gas generation processes (and it is consumed by the corrosion of steel), the rate of brine inflow into the repository affects the total rate of gas generation. Brine inflow decreases as pressure increases, and brine may eventually be expelled from the repository if pressure exceeds brine pressure in the surrounding formation. This may result in the slowing or even stopping of gas generation in some vectors. Gas may flow away from the waste into areas with lower pressure, which may include the northern experimental and operations areas, the DRZ, the anhydrite interbeds and the shaft. Gas flow into intact halite is not significant because of the high threshold pressure of halite.

6.3 *MODELING RESULTS FOR UNDISTURBED PERFORMANCE (R1S1)*

Previous analyses (U. S. DOE, 1996; SNL, 1997; Helton et al., 1998; Hansen and Leigh, 2002) have identified two potential pathways for brine flow and radionuclide transport away from the repository in the undisturbed scenario. In the first pathway, brine may migrate through the panel seals and drifts or through the disturbed rock zone (DRZ) surrounding the repository to the shaft and then upwards towards the Culebra Dolomite Member of the Rustler Formation. The quantity of brine reaching the Culebra is important, because transport then may occur laterally towards the subsurface land withdrawal boundary. In the second pathway, brine may migrate from the repository through the DRZ and laterally towards the subsurface land withdrawal boundary through the anhydrite interbeds of the Salado formation.

In addition, pressure and brine saturation in the undisturbed scenario are important variables because conditions in this scenario are used as input for other software used to calculate direct releases from the first intrusion into the repository. Subsequent intrusions look to conditions in the other disturbed scenarios.

6.3.1 Sequence of Events

In scenario 1, there is a change in lower shaft material at 200 years after closure. This change primarily represents the consolidation and recrystallization of the crushed salt portion of the shaft seal system that is expected during this time.

6.3.2   Halite Creep

Halite creep causes the pore volume (void space), of the waste filled regions of the repository to decrease over time as halite flows to fill the excavated space and compresses the waste. Porosity is calculated by dividing the pore volume by total volume, and it can be expressed as a fraction or as pore volume percent of total volume.

The output variable, W_R_POR, is the volume-averaged porosity for all waste areas. Figure 6-1 compares horsetail plots of volume-averaged porosity in all waste-filled areas (W_R_POR) for the CRA-2004 and the CRA-2004 PABC. The distribution of values is similar, and the statistics are summarized in Table 6-4. There is slightly less variability of porosity in the CRA-2004 PABC compared to CRA-2004.

Table 6-4. Statistical comparison of volume averaged porosity in all waste-filled areas at 10,000 years in Replicate R1, Scenario S1 for the CRA-2004 and the CRA-2004 PABC. W_R_POR is a variable calculated in the ALG2 post-processing step (see Table 4-1 and Appendix B).

W_R_POR (dimensionless)	CRA-2004	CRA-2004 PABC
Minimum	7.99E-02	1.12E-01
Average	1.68E-01	1.64E-01
Maximum	2.30E-01	2.24E-01

In the CRA-2004 PABC, the porosity in all vectors drops from its initial value of 0.848 (Stein and Zelinski, 2003a) to a value that ranges from 0.112 to 0.224 at 10,000 years. Much of the reduction in pore volume occurs during the first 50 years. As in the CRA-2004, most vectors show expansion of pore volume due to gas generation.

6.3.3   Brine Inflow

The ALG2 (see Table 4-1, Appendix B) output variable, BRNREPTC, includes all brine that flows into the repository. Figure 6-2 compares horsetail plots of BRNREPTC from the CRA-2004 and the CRA-2004 PABC. Figure 6-3 shows horsetails of brine volume in the waste areas versus time from the CRA-2004 and the CRA-2004 PABC. The two analyses are not markedly different. Table 6-5 confirms the statistical similarity of brine inflow in the CRA-2004 PABC and the CRA-2004 for the undisturbed scenario, S1.

In the undisturbed scenario, S1, brine can only come in contact with the waste by flowing through or from the DRZ. The only significant potential external source of brine to the DRZ is from the anhydrite marker beds or from in situ brine within the DRZ. The permeability of undisturbed halite is too low to permit significant migration of brine. The CRA-2004 PABC analysis confirms the results of the CRA-2004 that brine inflow comes primarily from the DRZ.

Table 6-5. Statistical comparison of total cumulative brine inflow at 10,000 years for Replicate R1, Scenario S1 for the CRA-2004 and the CRA-2004 PABC. BRNREPTC is an output variable calculated in the ALG2 post-processing step (see Table 4-1 and Appendix B).

BRNREPTC (m³)	CRA-2004 (m³)	CRA-2004 PABC (m³)
Minimum	77	346
Average	10335	10050
Maximum	49258	45063

The sampled input parameter halite porosity, HALPOR (see Table 4-2), determines how much brine is available in the DRZ for each vector. A scatter plot of HALPOR versus BRNREPTC at 10,000 years, Figure 6-4, shows that vectors with high brine inflow have high HALPOR values. Permeability also influences brine inflow, but there are no vectors with high brine inflow that do not have relatively high HALPOR values.

The ALG2 (see Table 4-1) output variable, BRAALIC, is the cumulative total brine inflow from all marker beds into the DRZ. A scatter plot of BRAALIC versus BRNREPTC at 10,000 years shown in Figure 6-5 indicates no significant relationship between the two brine flows. In fact, brine flow from the marker beds into the DRZ (BRAALIC) appears to be about the same regardless of whether brine flow into the repository (BRNREPTC) is relatively high or low. This means that brine outside of the DRZ is not a major contributor to brine flow into the repository, which is coming almost entirely from the DRZ. Brine flow from the marker beds is not a significant contributor to brine in the repository.

6.3.4 Brine Saturation

Brine saturation is an important result of the BRAGFLO model, because (1) gas generation processes require the availability of brine to proceed and (2) Direct Brine Releases, which are modeled in another PA activity, depend on the brine saturation in the waste regions calculated by BRAGFLO. Figure 6-6 compares horsetail plots of brine saturation in the waste panel for the CRA-2004 and the CRA-2004 PABC. The patterns are similar, but the horsetail plots show that in the CRA-2004 PABC brine saturation goes up faster in the first few years (Figure 6-6). Table 6-6 contains a statistical comparison of brine saturation in the waste panel (ALG2 output variable WAS_SATB) at 10,000 years for the CRA-2004 PABC, the CRA-2004, and the PAVT. The CRA-2004 PABC and CRA-2004 values are similar, and the higher average brine saturation in the PAVT is due to more permeable panel closures.

Table 6-6. Volume-averaged brine saturation at 10,000 years in the waste panel for Replicate R1, Scenario S1 for the PAVT, the CRA-2004, and the CRA-2004 PABC. WAS_SATB is calculated in the ALG2 post-processing step (see Table 4-1 and Appendix B).

WAS_SATB (dimensionless)	PAVT	CRA-2004	CRA-2004 PABC
Minimum	5.96E-08	5.96E-08	1.01E-06
Average	2.30E-01	9.60E-02	8.13E-02
Maximum	9.94E-01	9.80E-01	9.59E-01

Statistics for volume-averaged brine saturation in different regions of the repository are summarized in Table 6-7. The Waste Panel has the widest range of volume-averaged brine saturation at 10,000 years (Figure 6-6) ranging from a low of 1 x 10^{-6} to a high of 0.96 (Table 6-7). Higher brine saturation in the Waste Panel than the RoR areas is due to the direct proximity of the Waste Panel to the markerbeds and the isolation of the RoR areas by the Option D panel closures. Many vectors show a sharp increase in brine saturation during the first 500 years followed by slowly declining brine saturation to 10,000 years (Figure 6-6).

Table 6-7. Volume-averaged brine saturation at 10,000 years in different areas of WIPP for Replicate R1, Scenario S1 for the CRA-2004 PABC. These brine saturations were calculated in the ALG2 post processing step (see Table 4-1 and Appendix B).

	Brine saturation (dimensionless)	Min	Avg	Max
Waste Panel	WAS_SATB	1.01E-06	8.13E-02	9.59E-01
RoR South	SRR_SATB	1.19E-07	1.80E-02	2.56E-01
RoR North	NRR_SATB	5.96E-08	1.83E-02	2.59E-01
Operations Area	OPS_SATB	1.91E-02	4.34E-01	1.00E+00
Experimental Area	EXP_SATB	9.97E-03	9.53E-02	8.02E-01

The Experimental (EXP_SATB) and Operations non-waste areas (OPS_SATB), at the north end of the grid, have the highest median and average brine saturations according to Table 6-7. The waste-filled and non-waste areas are separated by Option D panel closures, which impede the transfer of brine. These non-waste areas receive greater brine flow in from the marker beds than the isolated RoR areas. As in other areas of the repository, there is a sharp increase in brine saturation during the first 500 years, but the maximum saturations are lower than in the waste areas. This is due to the fact that there is no creep closure modeled in the non-waste areas. Creep closure decreases pore volume and thus causes brine saturation to increase.

Sensitivity analysis for BRAGFLO is complicated by the coupled, non-linear processes that are modeled. Generally the results of sensitivity analysis indicate which input parameters are most important for average performance, but often they will not explain anomalous modeling results. For example, the relationship between brine saturation and pressure changes as a function of pressure. At low pressures, which occur dominantly in early years of the model, there is a positive correlation between brine saturation and pressure, because increases in saturation accelerate the rate of gas generation, which results in increasing pressure. However, at higher pressures, which develop as a consequence of gas generation, the correlation decreases and becomes

negative, because increasing pressure tends to impede brine inflow and eventually, high pressure drives brine out of the repository thereby reducing brine saturation. Figure 6-7 shows brine saturation versus pressure in the Waste Area. This plot illustrates the relationship between pressure and brine saturation for Vector 28, which reaches the highest pressure of any vector in R1S1. As shown in the figure, the crossover from positive to negative slope between pressure and brine saturation occurs at about 4 to 5 MPa for Vector 28.

When all 100 vectors are used to evaluate Waste Area brine saturation dependencies on sampled input parameters, the PRCC's plotted in Figure 6-8 reflect a mixture of results from high and low pressure regimes. At 10,000 years, the high-pressure regime dominates. Consequently, Waste Area brine saturation has prominent PRCC's with the gas generation factors (e.g. DRZPRM, WGRCOR, HALPOR, and WASTWICK, see Table 4-2 for a description of these parameters).

Brine saturation in the Waste Panel has a moderate positive PRCC with the permeability of the DRZ, DRZPRM, and with the porosity of halite, HALPOR (see Table 4-2), because together these two input parameters determine how much brine can enter the repository at relatively low pressure. At high pressure DRZPRM determines how much brine can be forced out of the repository. Higher values of halite porosity result in more water being available in the DRZ for release to the repository, and higher permeability in the DRZ provides less resistance for brine flow into the repository. There are also moderate negative correlations to the gas generation factors for the corrosion rate of steel WGRCOR (see Table 4-2), because corrosion consumes brine. The weaker negative correlation with the wicking input parameter WASTWICK (see Table 4-2), the increase in effective brine saturation of waste due to capillary forces, is due to the increase in pressure associated with higher wicking factors. As discussed above, brine is forced out of the repository at higher pressures.

6.3.5 Gas Generation

There are two potential sources for gas generation in the Salado Flow Model. The corrosion of steel, in the presence of brine, generates hydrogen gas in the model, and microbial degradation of organic material in the waste, including cellulose, rubber, and plastic, may yield N_2, H_2S, and CO_2. However, all gas is assumed to have hydrogen properties in BRAGFLO. The carbon dioxide produced by microbial degradation is assumed to be sequestered by MgO and is thus not released into the repository.

6.3.5.1 Gas Generation by Corrosion

Gas generation by corrosion (Figure 6-9) continues until all steel or all brine is consumed (Figure 6-10). Gas generation by corrosion declines rapidly after 1,000 years, but it continues at a relatively slow rate in many vectors to the end of 10,000 years (Figure 6-9). Cumulative gas generated by corrosion is not generally limited by the availability of steel (Figure 6-10) since at least 12% of the steel remains in all vectors at 10,000 years. However, steel inventory in certain grid cells may be depleted before 10,000 years. Brine availability is the limiting factor for gas generation by corrosion for many vectors (Figure 6-11). Statistics of gas generation for the CRA-2004 PABC and the CRA-2004 are given below in Table 6-8.

Table 6-8. Gas generation statistics at 10,000 years for Replicate R1, Scenario S1 for the CRA-2004 and the 2004-CRA PABC[1]. The values in the table were calculated in the ALG2 post processing step (see Table 4-1 and Appendix B).

	CRA-2004	CRA-2004 PABC
FE_MOLE (moles)		
Minimum	5.29E+06	3.40E+07
Average	2.98E+08	2.99E+08
Maximum	7.98E+08	8.16E+08
CELL_MOL (moles)		
Minimum	0.00E+00	2.34E+05
Average	1.74E+08	1.14E+08
Maximum	5.32E+08	4.93E+08
GAS_MOLE (moles)		
Minimum	5.80E+07	1.58E+08
Average	4.72E+08	4.13E+08
Maximum	1.10E+09	1.06E+09

[1] Here FE_MOLE is the amount of gas (moles) produced by iron corrosion, CELL_MOL is the amount of gas (moles) produced by microbial gas generation, and GAS_MOLE is the total amount of gas (moles) produced. Note that the average GAS_MOLE is the sum of the average FE_MOLE and CELL_MOL, but the minimum and maximum typically correspond to different vectors and thus for different quantities and thus don't sum to the respective GAS_MOLE maximum or minimum.

Brine is consumed in the corrosion process and is impeded from flowing in or out of the repository at sufficiently high pressure. This is discussed in §6.3.4.

As shown in Figure 6-11, the porosity of halite HALPOR is the most important input parameter influencing corrosion. As discussed in §6.3.3, higher values of HALPOR means that more brine is available to flow into the repository from the DRZ at sufficiently low pressures.

6.3.5.2 Gas Generation by Microbial Activity

Microbial gas generation now occurs in all vectors, in contrast to the CRA-2004 where the probability of microbial gas-generation was 0.5 (see §5.4). Figure 6-12 shows the cumulative amount (in moles) of gas generated by microbial consumption of cellulose

or CPR versus time. In the CRA-2004, most of the cellulose or CPR was consumed within the first several thousand years, as shown in Figure 6-13. Using the updated microbial gas generation rates (see §5.5), many vectors now have cellulose or CPR remaining after 10,000 years. The cessation of microbial gas generation is indicated by horizontal lines for cumulative moles of gas.

Microbial gas generation requires the presence of some brine, and it continues at the humid rate at very low brine saturation values. However microbial gas generation ceases completely when brine saturation becomes zero. As shown in Figure 6-13, several vectors in Scenario 1 show that microbial degradation has all but stopped before all decomposable organic material is consumed. This occurs because brine saturation has dropped to levels very close to zero. Consumable organic material survives to the end of the 10,000-year regulatory period for these vectors.

Figure 6-14 shows the five most prominent correlations of microbial gas generation to sampled input parameters. The greatest positive correlation is with WBIOGENF (WAS_AREA:BIOGENFC) which is the scaling factor that is multiplied by the sampled gas-generation rates (see §5.5). The second greatest positive correlation is with WGRMICI (WAS_AREA:GRATMICI) which is the inundated gas-generation rate. This correlation reflects gas generation being more dependent on the inundated rate rather than the humid rate. The third largest positive correlation is with WMICDLF (WAS_AREA:PROBDEG) which influences the amount of CPR that is available and thus the rate of CO_2 production (see Nemer et al., (2005)). The two negative correlations are the inundated rate of iron corrosion WGRCOR (STEEL:CORRMCO2) and the wicking factor WASTWICK (WAS_AREA:SAT_WICK), see Stein (2003a). These two parameters will tend to increase the rate of iron corrosion which consumes water and hence dries out the repository slowing down the rate of microbial gas generation.

6.3.5.3 Total Gas Generation

Figure 6-15 shows the total gas generation obtained by combining gas generation due to corrosion and gas generation due to microbial degradation. Figure 6-17 shows the amount of gas generated versus time averaged over 100 vectors for corrosion, microbial, and total. On average, iron corrosion generates 2.5 times as much gas as microbial gas generation.

Figure 6-16 presents the most prominent PRCC's for total cumulative gas generation with sampled input parameters. Notable is HALPOR which, as described in §6.3.3 controls brine availability.

6.3.6 Pressure

Pressure within the repository is particularly important to WIPP PA because the release mechanisms Spallings and DBR are quite sensitive to this variable. In addition, pressure strongly influences the extent to which contaminated brine can migrate from the repository into the marker beds or up the shaft to the Culebra. As shown in Figure 6-18, pressures tend to increase more slowly in the CRA-2004 PABC compared to the CRA-2004 due to the updated microbial-gas-generation rates. However the pressure in the

Waste Area after 10,000 years is not very different from the CRA-2004 and the PAVT, as shown in Table 6-9.

Table 6-9. Pressure in the waste panel at 10,000 years for Replicate R1, Scenario S1 for the PAVT, the CRA-2004 and CRA-2004 PABC. The output variable WAS_PRES is calculated in the ALG2 post processing step (see Table 4-1 and Appendix B).

WAS_PRES (Pa)	PAVT	CRA-2004	CRA-2004 PABC
Minimum	4.52E+06	4.17E+06	6.18E+06
Average	1.05E+07	1.04E+07	9.95E+06
Maximum	1.68E+07	1.58E+07	1.55E+07

PCCR's for volume averaged pressure in the Waste Area are shown in Figure 6-19. The strongest positive correlation after around three thousand years is with HALPOR (halite permeability). Brine is consumed by corrosion and is required for microbial gas generation.

6.3.7 Rock Fracturing

If pressures in the DRZ or in the anhydrite marker beds exceed the initial pressure in these materials by 0.2 MPa, BRAGFLO treats the material as being fractured and increases the porosity and permeability of the material according to the fracture model described in the BRAGFLO users manual (Stein, 2003a). Figure 6-20 through Figure 6-25 show fracture length in the anhydrite marker beds versus time. Fracture length is arbitrarily defined in this analysis as the length of marker bed from the repository to the exterior edge of the furthest grid cell where the permeability has doubled from its initial value. Significant fracturing does not occur in all vectors. Looking at Figure 6-20 through Figure 6-25, the fracturing length is generally lower in the CRA-2004 PABC compared to the CRA-2004. Figure 6-20 shows that there was no fracturing in the CRA-2004 PABC in marker bed MB-138 north of the repository, although fracturing did occur in the CRA-2004. However only four vectors had fracturing in MB-138 North in the CRA-2004.

Vector 53 of S1 is an exception with a particularly large but transient fracture length at around 3700 years, shown in Figure 6-22 and Figure 6-24. This occurred because the initial anhydrite permeability in this vector was the largest of all vectors in this scenario and replicate and because the pressure in this vector was higher than vectors with similar anhydrite permeabilities in the CRA-2004. The intact permeability enters the equation for the fractured permeability

$$k = k_i \left[\frac{\phi}{\phi_i} \right]^n ,$$

(8)

where k is the fractured permeability, k_i is the intact permeability, φ is the porosity of the fractured material and φ_i is the porosity of the intact material at the fracture initiation pressure (see the BRAGFLO users manual: Stein, 2003a).

6.3.8 Brine Outflow

Figure 6-26 shows total cumulative brine flow out of repository areas for the CRA-2004 PABC and the CRA-2004. The amount of brine outflow is slightly larger in the CRA-2004 PABC than in the CRA-2004. Table 6-10 gives statistics for the CRA-2004 PABC and the CRA-2004 for cumulative brine outflow at 10,000 years.

Table 6-10. Statistics on cumulative brine flow out of the repository at 10,000 years for Replicate R1, Scenario S1 for the CRA-2004 and CRA-2004 PABC. BRNREPOC is an output variable calculated in the ALG2 post processing step (see Table 4-1 and Appendix B).

BRNREPOC (m³)	CRA-2004	CRA-2004 PABC
Minimum	1.22E+00	1.49E+00
Average	6.46E+02	7.16E+02
Maximum	1.96E+04	2.11E+04

Correlations of total cumulative brine flow away from the repository, BRNREPOC (an ALG2 output variable, see Table 4-1), are shown in Figure 6-27. The strongest positive correlation is with the permeability of the DRZ. The second strongest positive correlation is with CONPRM, the permeability for concrete (see Table 4-2). The positive PRCC indicates that increased flow through concrete corresponds to increased outflow from the repository, because the brine can pass more quickly thorough internal barriers within the repository.

Figure 6-28 shows the cumulative brine release to the Land Withdrawal Boundary (LWB); releases to the Culebra are negligible for scenario S1. In both the CRA-2004 and the CRA-2004 PABC only a few vectors had significant brine releases to the LWB. Table 6-11 gives statistics for cumulative brine outflows for 10,000 years at the LWB. The maximum brine outflow for the CRA-2004 PABC analysis is about three times larger than the largest outflow in the CRA-2004.

Table 6-11. Statistics on cumulative brine outflow to the LWB for Replicate R1, Scenario S1 for the CRA-2004 and CRA-2004 PABC. BRAALLWC is an output variable calculated in the ALG2 post processing step (see Table 4-1 and Appendix B).

BRAALLWC (m³)	CRA-2004	CRA-2004 PABC
Minimum	2.99E-06	4.96E-05
Average	7.22E+00	1.21E+01
Maximum	4.33E+02	1.21E+03

6.3.9 Figures for Section 6.3

R1S1: Volume Averaged Porosity in All Waste Regions

a) PABC: Porosity range displayed = 0 to 1.0

b) CRA1: Porosity range displayed = 0 to 1.0

c) PABC: Porosity range displayed = 0.05 to 0.25

d) CRA1: Porosity range displayed = 0.05 to 0.25
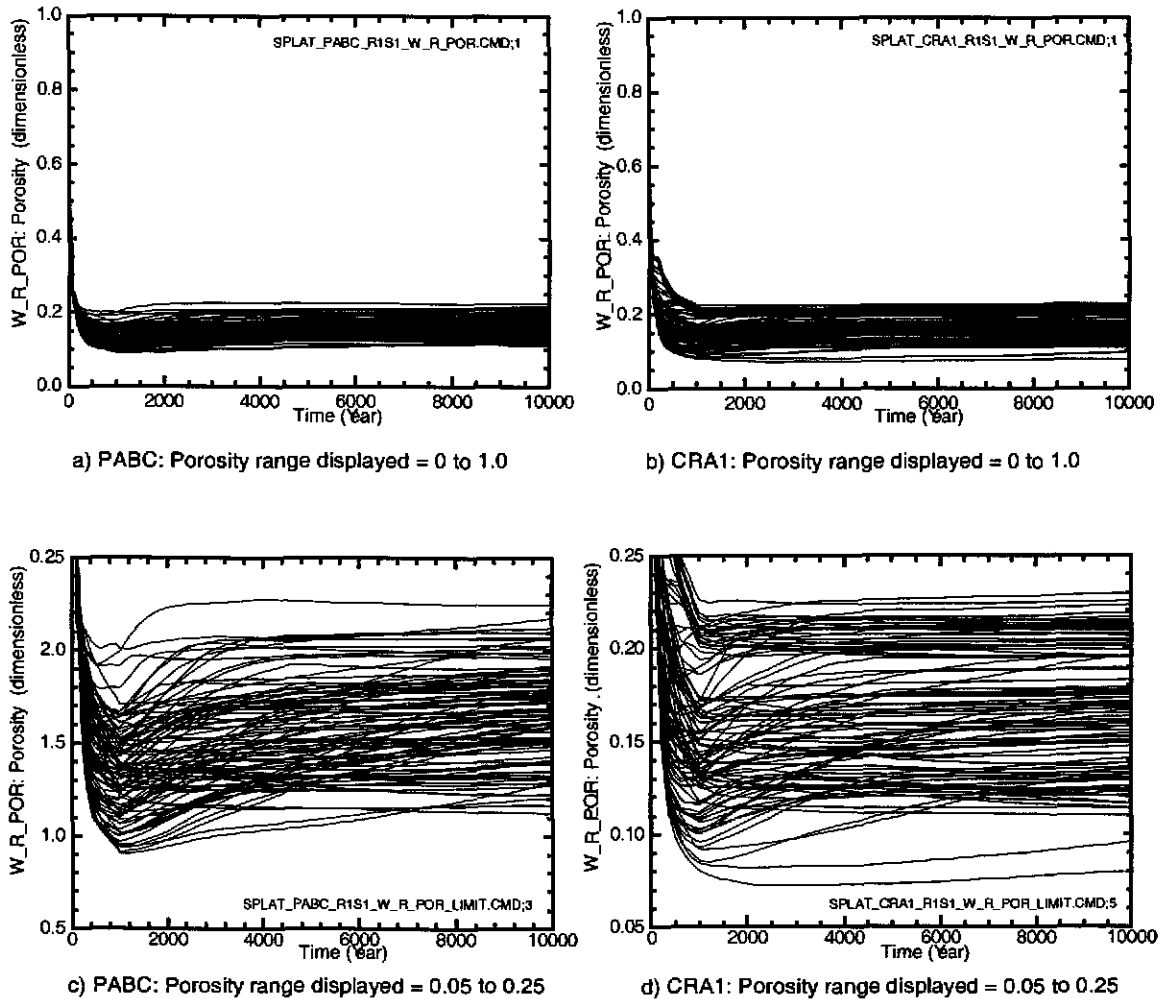
Figure 6-1. Volume averaged porosity (dimensionless) in all waste regions versus time (years) for all 100 vectors in Replicate 1, Scenario S1. Figures a) and c) show results from the CRA-2004 PABC. Figures b) and d) show results from the CRA-2004.
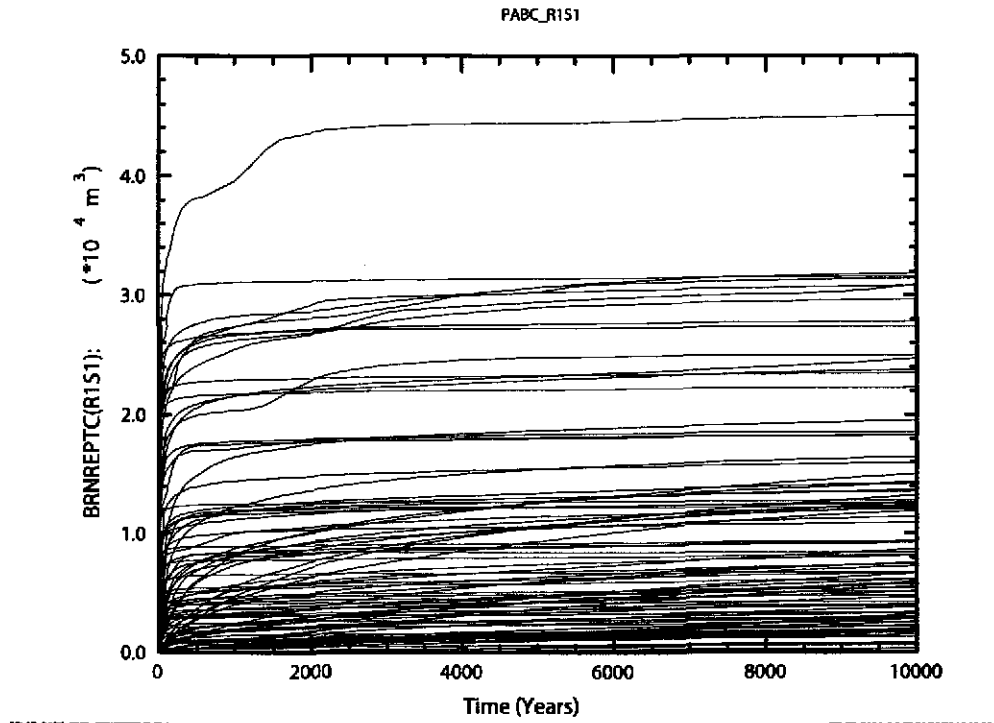
a) PABC
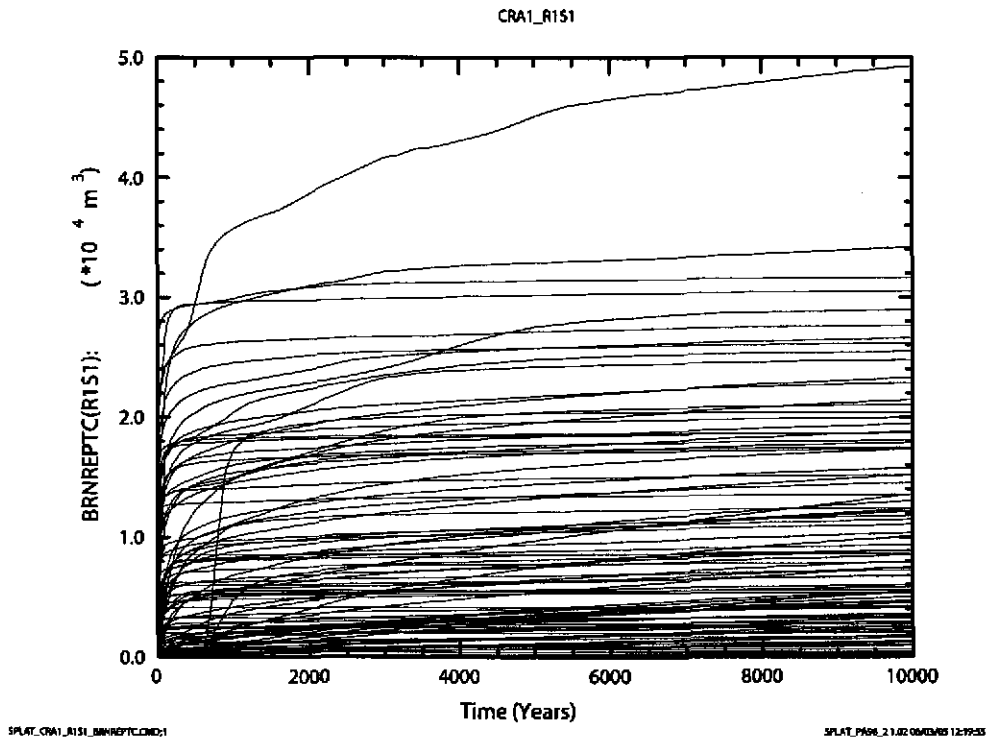
b) CRA1

Figure 6-2. Total cumulative inflow of brine (m³) into the repository versus time (years) for all 100 vectors in Replicate 1, Scenario S1. Figure a) shows results from the CRA-2004 PABC. Figure b) shows results from the CRA-2004.

a) PABC

b) CRA1
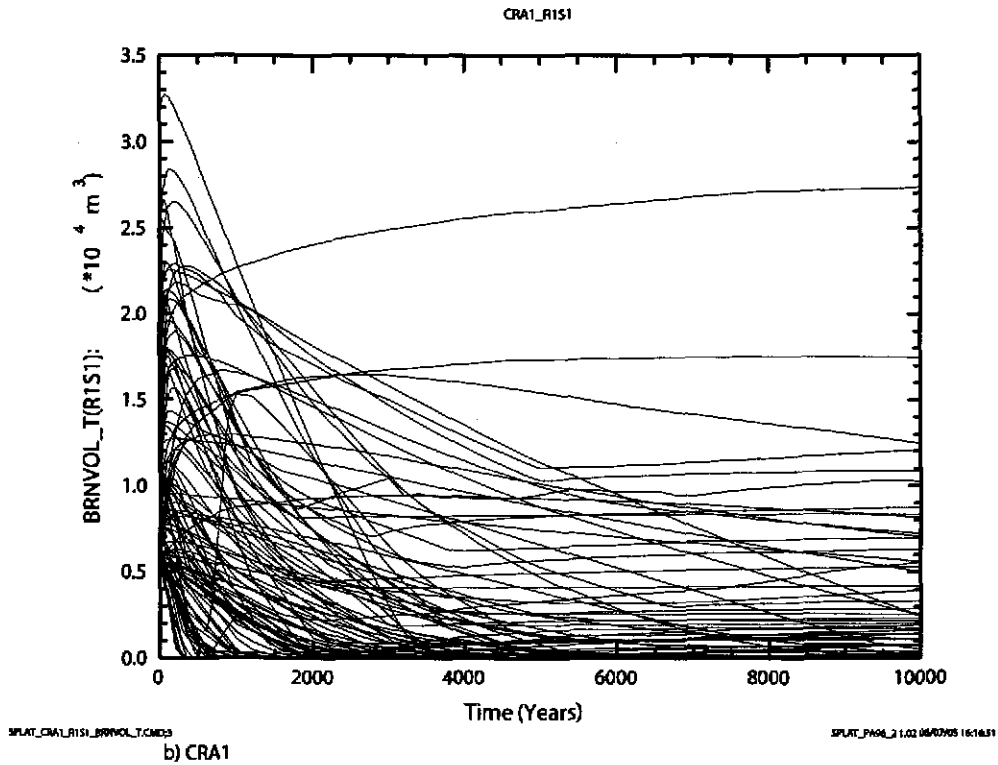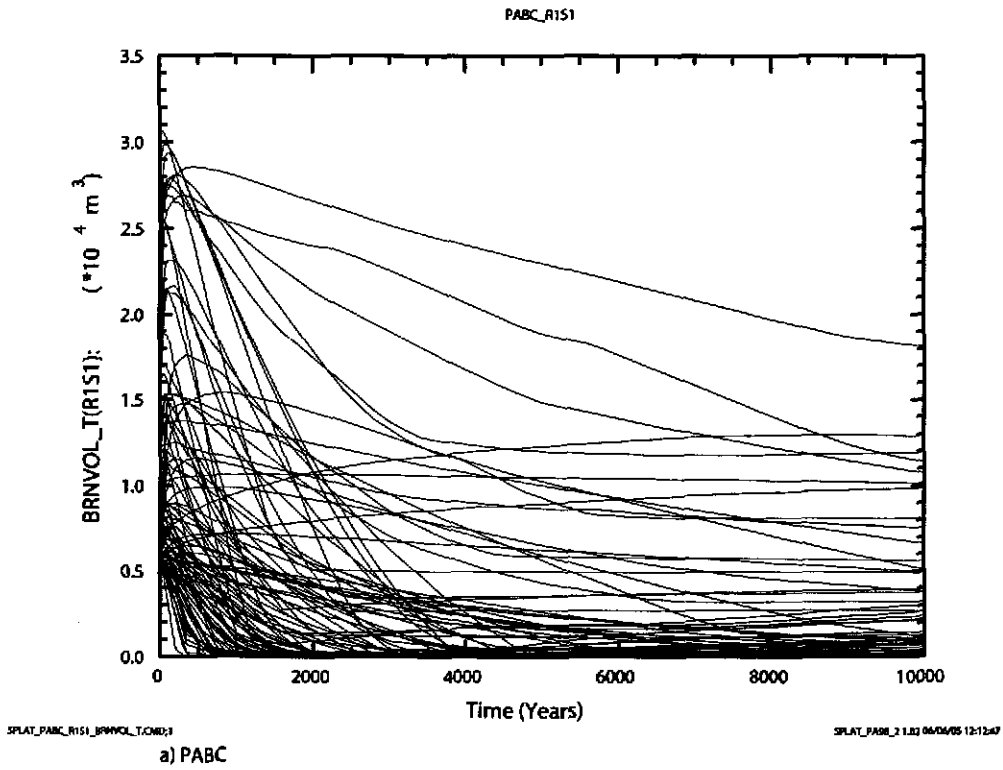
Figure 6-3. Total brine volume (m³) in all waste regions versus time (years) for all 100 vectors in Replicate 1, Scenario S1. Figure a) shows results from the CRA-2004 PABC. Figure b) shows results from the CRA-2004.
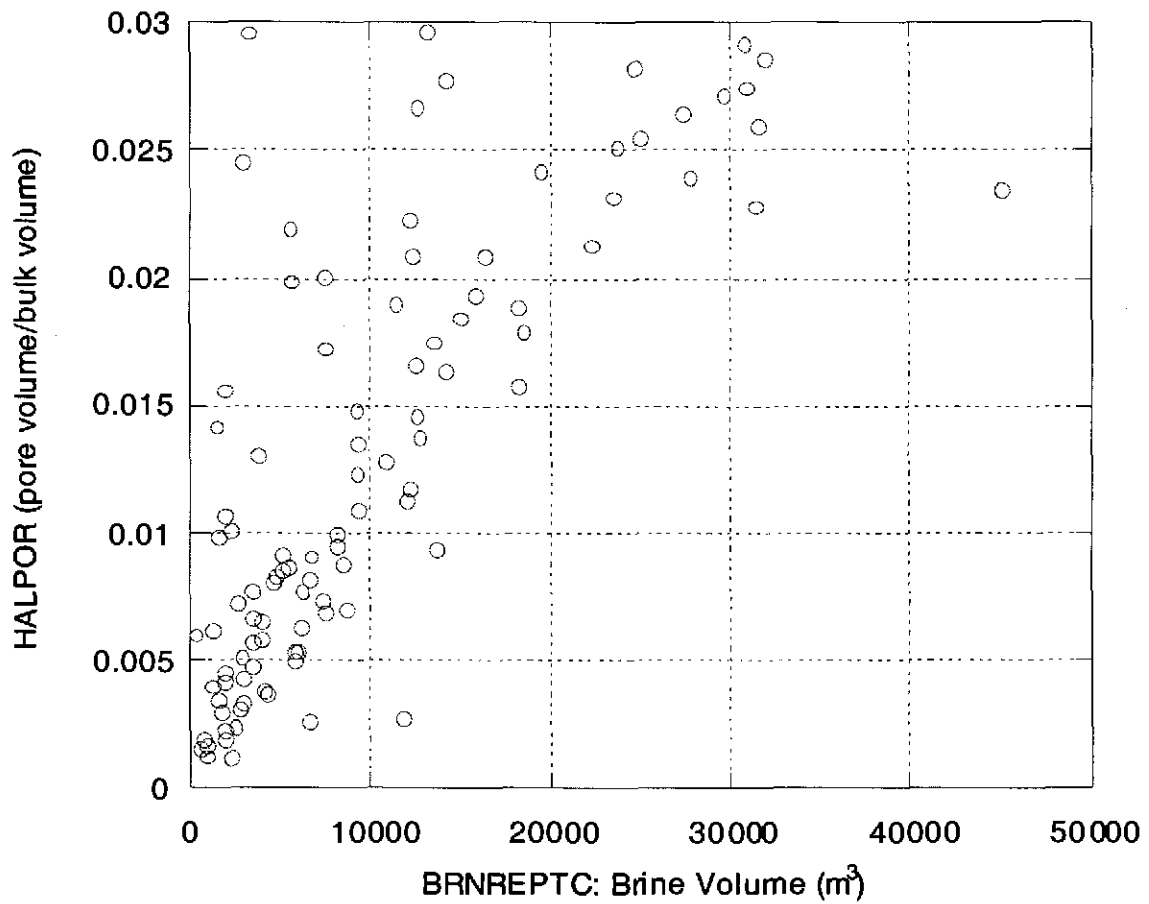
Figure 6-4. Scatter plot of halite porosity (dimensionless) versus cumulative brine inflow (m^3) into the repository for all 100 vectors in Replicate 1, Scenario S1, CRA-2004 PABC.
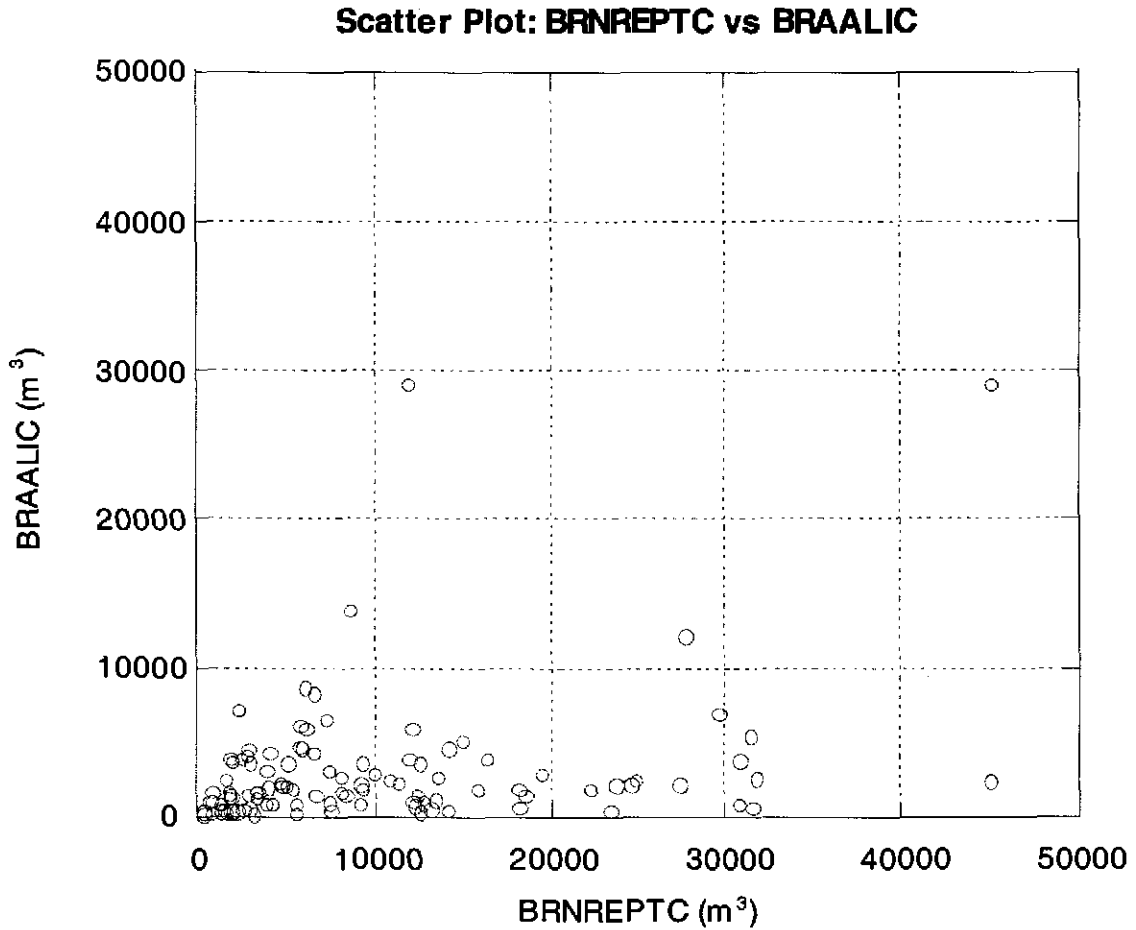
Figure 6-5. Scatter plot of total cumulative brine flow (m³) into the DRZ versus cumulative brine flow (m³) into the repository for all 100 vectors in Replicate 1, Scenario S1, CRA-2004 PABC.
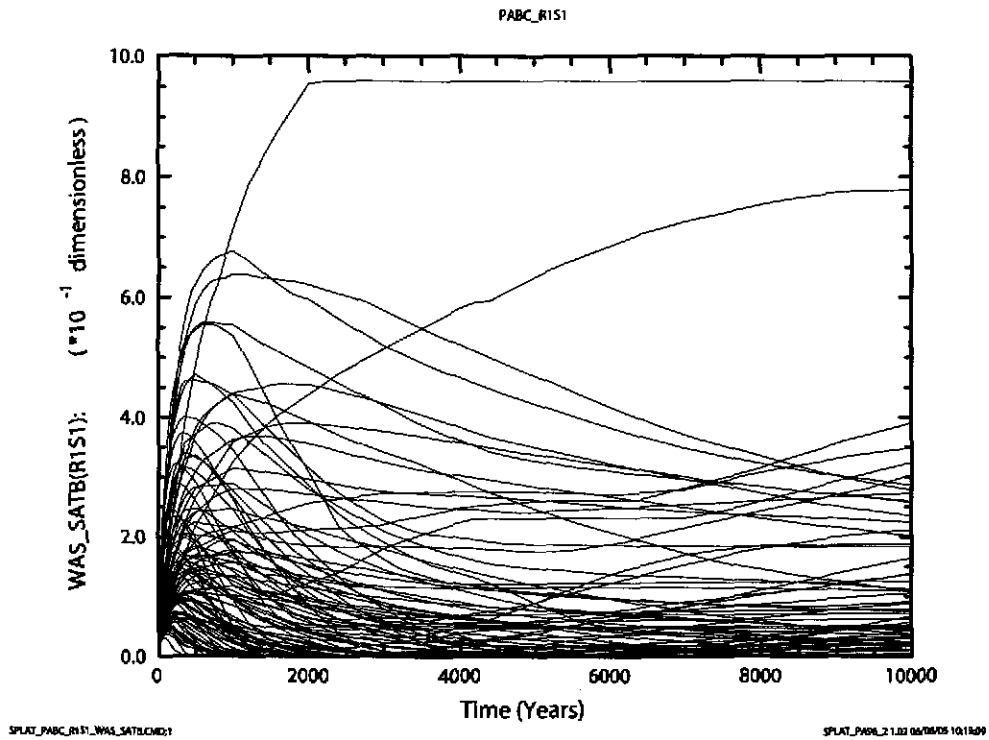
a) PABC
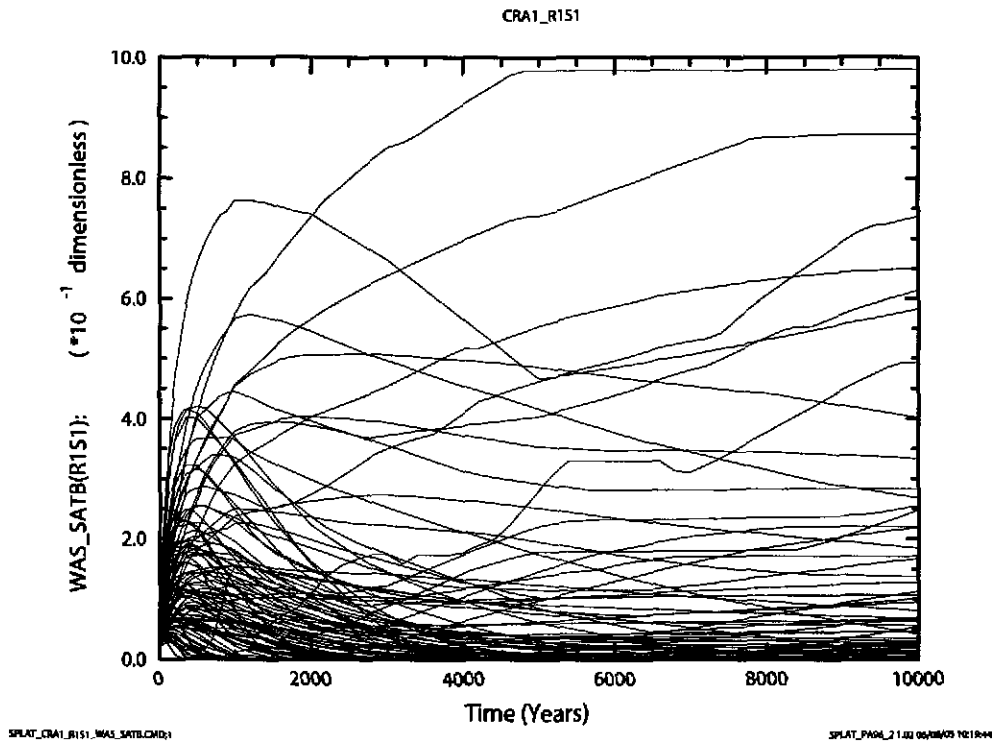
b) CRA1

Figure 6-6. Brine saturation (dimensionless) in the waste panel versus time (years) for all 100 vectors in Replicate 1, Scenario S1. Figure a) shows results from the CRA-2004 PABC. Figure b) shows results from the CRA-2004.

R1S1 Vector 28
Brine Saturation (WAS_SATB) versus
Pressure in the Waste Panel (WAS_PRES)
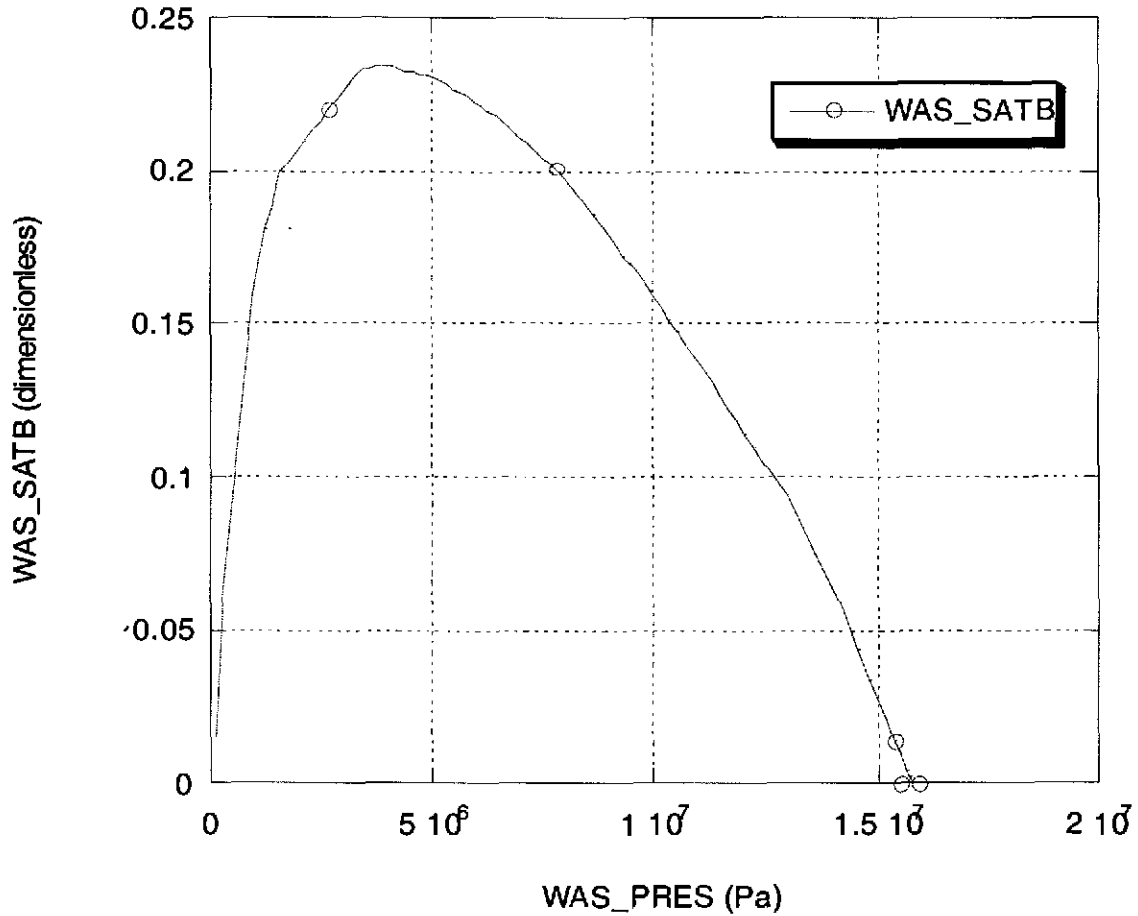
Figure 6-7. Brine saturation (dimensionless) in the waste panel versus pressure (Pa) in the waste panel for Vector 28, Replicate 1, Scenario S1, CRA-2004 PABC.

Sensitivity Analysis for Brine Saturation in the Waste Panel
CRA1BC BRAGFLO R1S1
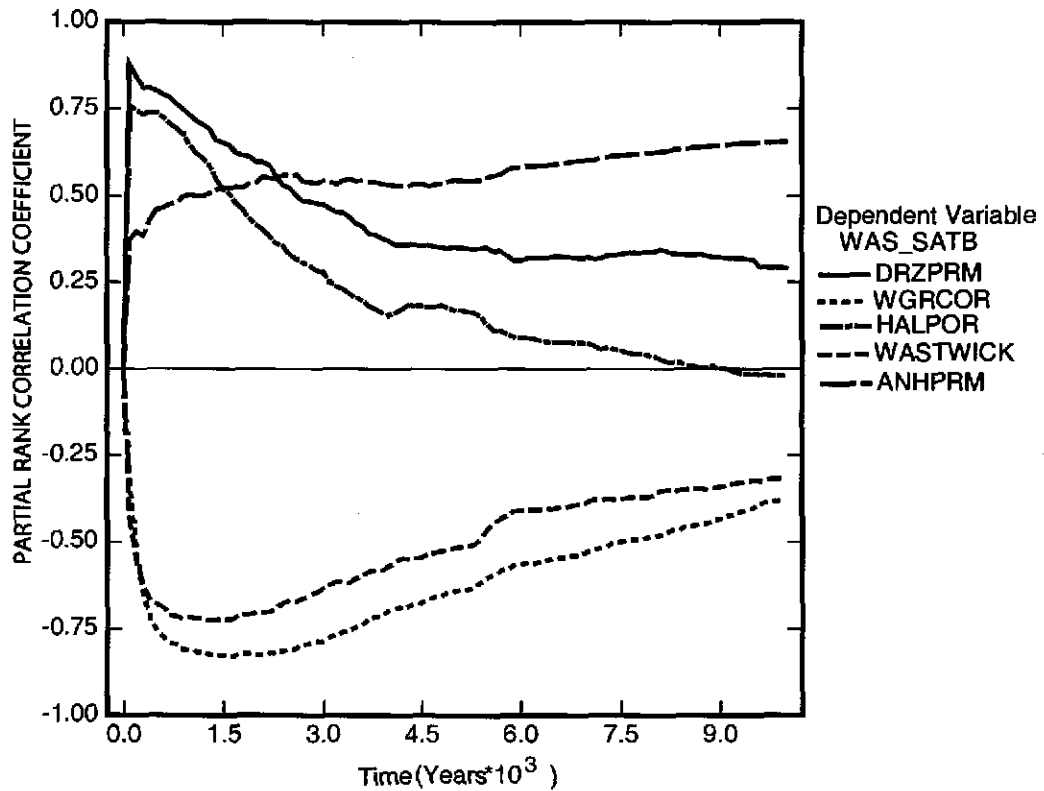
Figure 6-8. Primary correlations of brine saturation (dimensionless) in the waste panel with input parameters versus time (years), for Replicate 1, Scenario S1, CRA-2004 PABC. Table 4-2 gives a description of the names in the legend.

Information Only
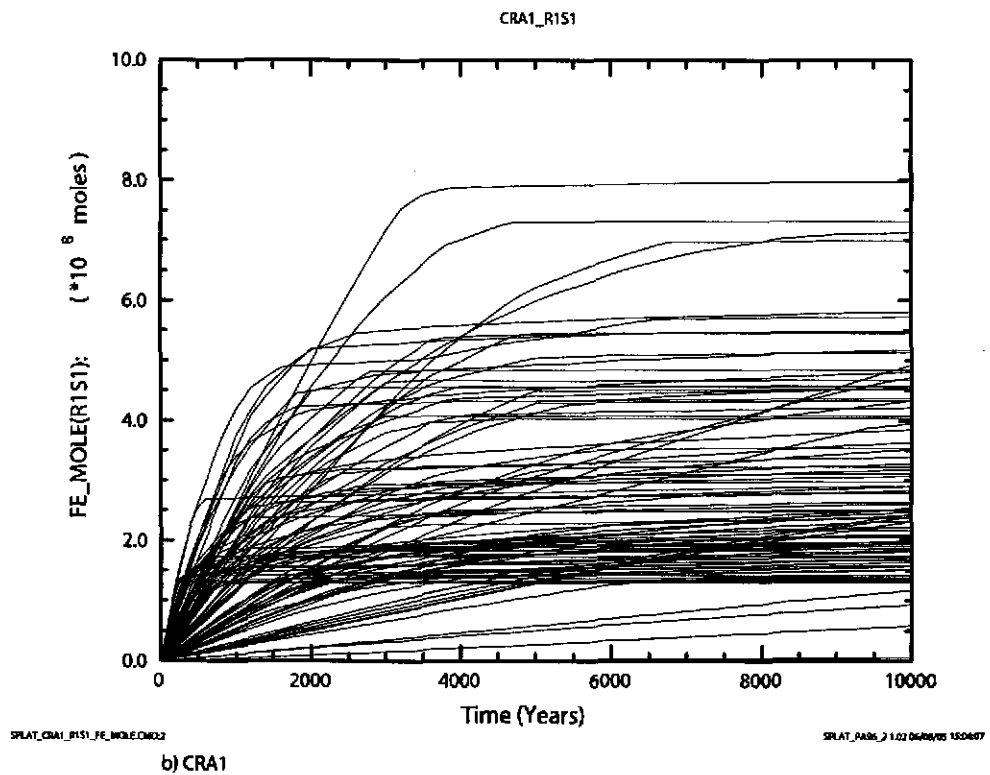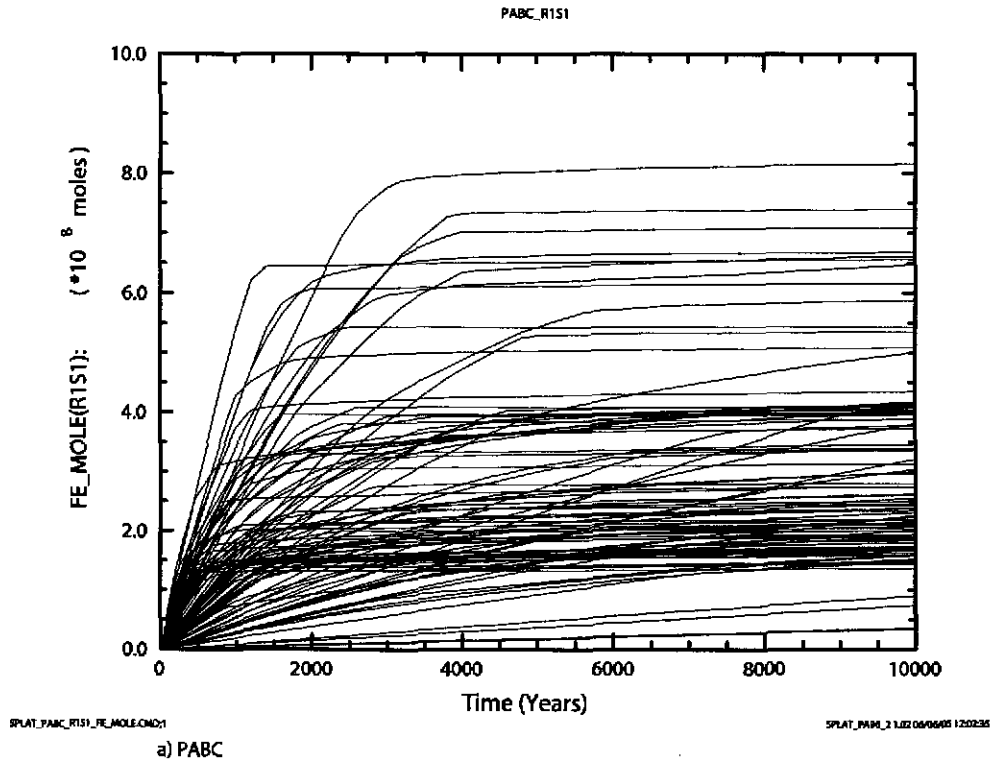
a) PABC

b) CRA1

Figure 6-9. Cumulative gas generation (moles) by iron corrosion versus time (years) for all 100 vectors in Replicate 1, Scenario S1. Figure a) shows results from the CRA-2004 PABC. Figure b) shows results from the CRA-2004.

Information Only
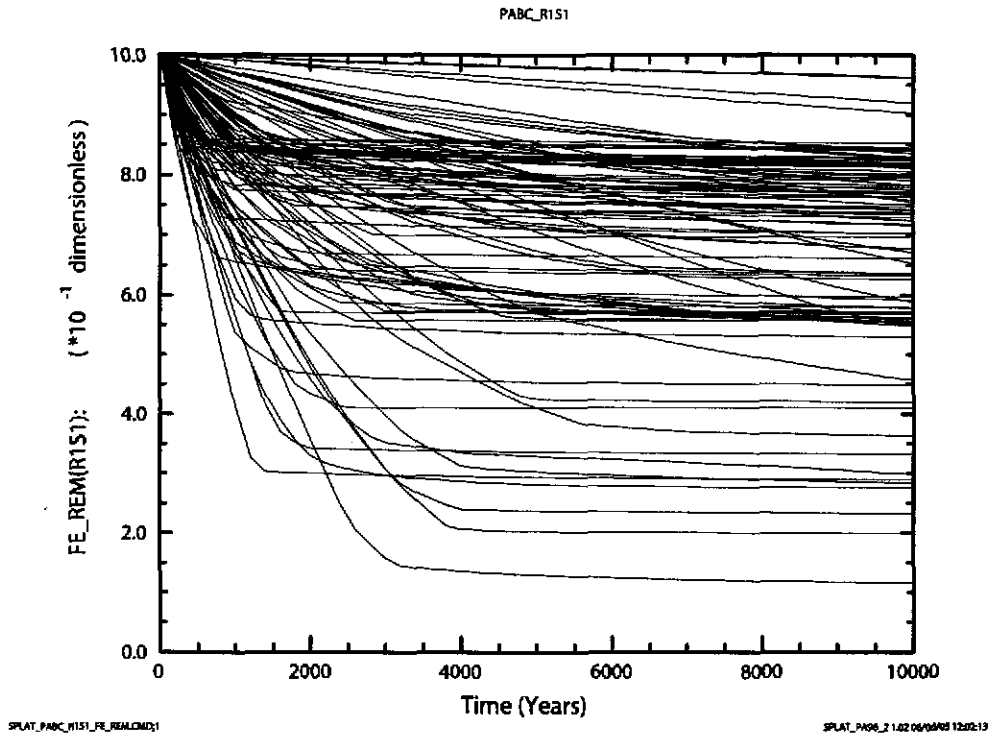
a) PABC
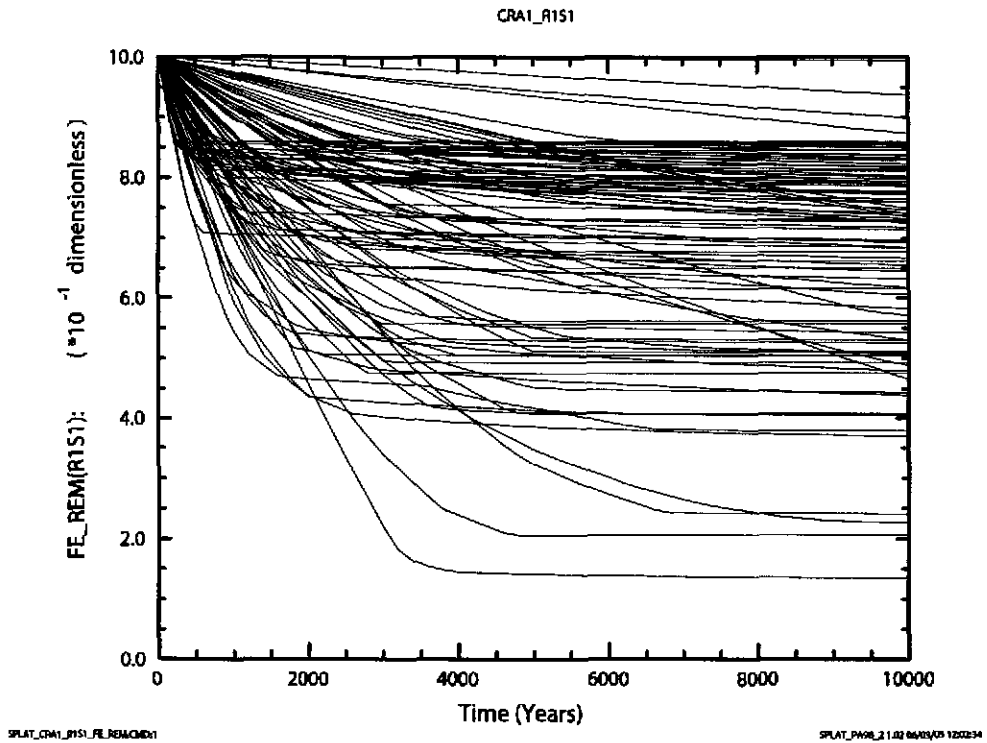
b) CRA1

Figure 6-10. Fraction of iron (dimensionless) remaining versus time (years) for all 100 vectors in Replicate 1, Scenario S1. Figure a) shows results from the CRA-2004 PABC. Figure b) shows results from the CRA-2004.

Sensitivity Analysis for Total Cumulative Gas Generation by Corrossion
CRA1BC BRAGFLO R1S1
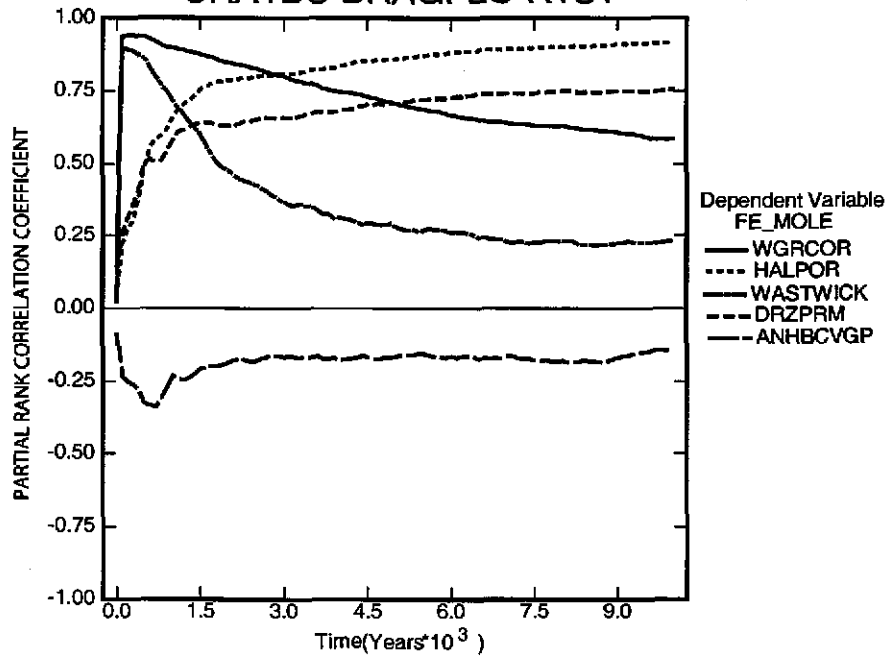
Figure 6-11. Primary correlations (dimensionless) of cumulative gas generation by corrosion with input parameters versus time (years) from the CRA-2004 PABC, Replicate 1, Scenario S1. Table 4-2 gives a description of the names in the legend.
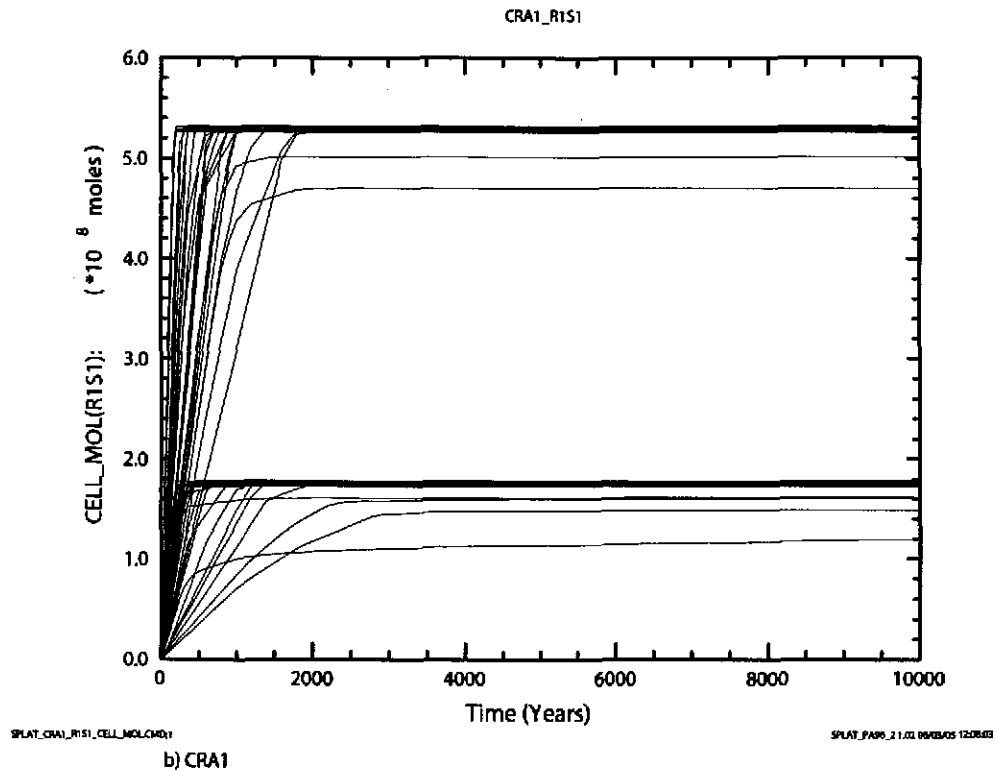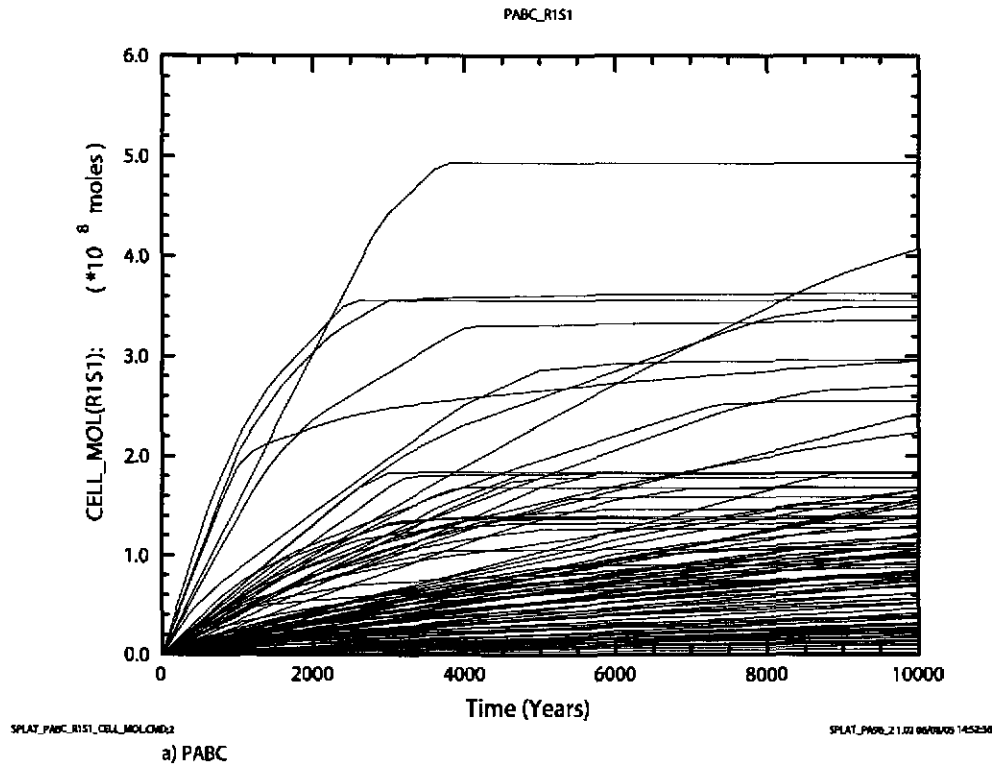
Figure 6-12. Cumulative gas generation (moles) due to microbial activity versus time (years) for all 100 vectors in Replicate 1, Scenario S1. Figure a) shows results from the CRA-2004 PABC. Figure b) shows results from the CRA-2004.

PABC_R1S1

a) PABC

CRA1_R1S1

b) CRA1
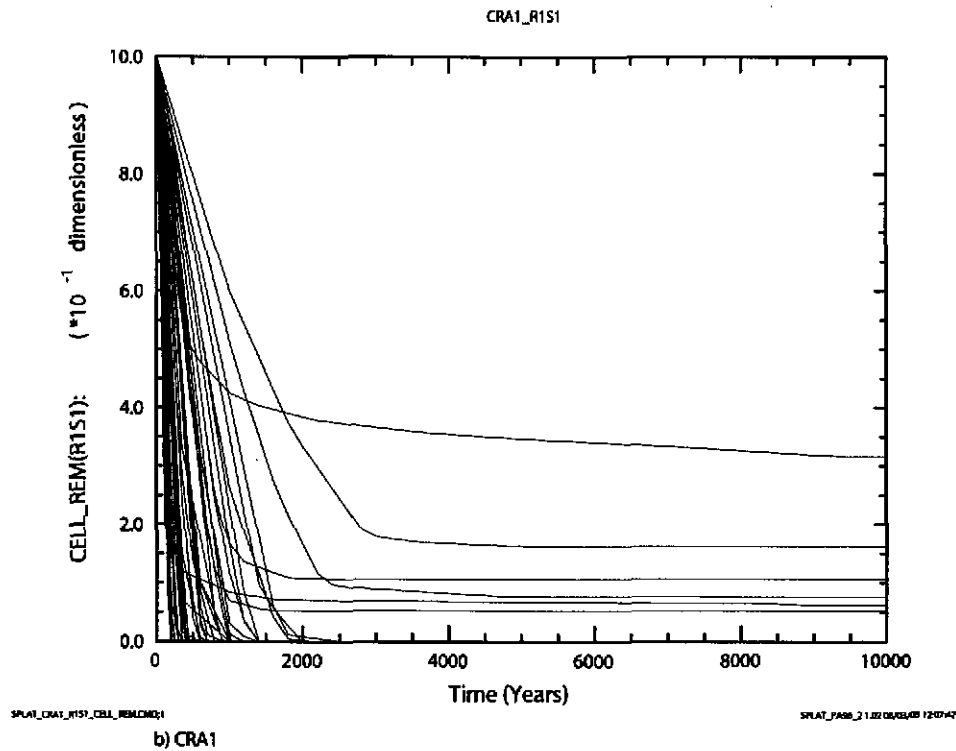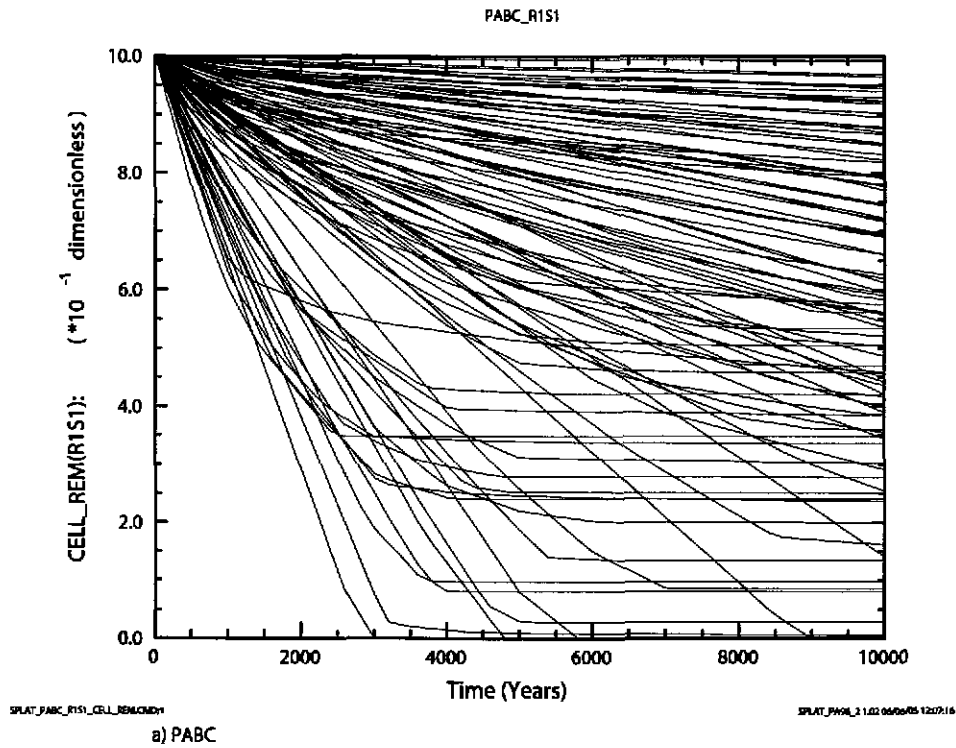
Figure 6-13. Remaining fraction of cellulosics (dimensionless) versus time (years) for all 100 vectors in Replicate 1, Scenario S1. The remaining fraction of cellulosics is either cellulose or CPR depending on the value of WAS_AREA:PROBDEG (§5.4). Figure a) shows results from the CRA-2004 PABC. Figure b) shows results from the CRA-2004.

Sensitivity Analysis for Total Cumulative Microbial Gas Generation
CRA1BC BRAGFLO R1S1
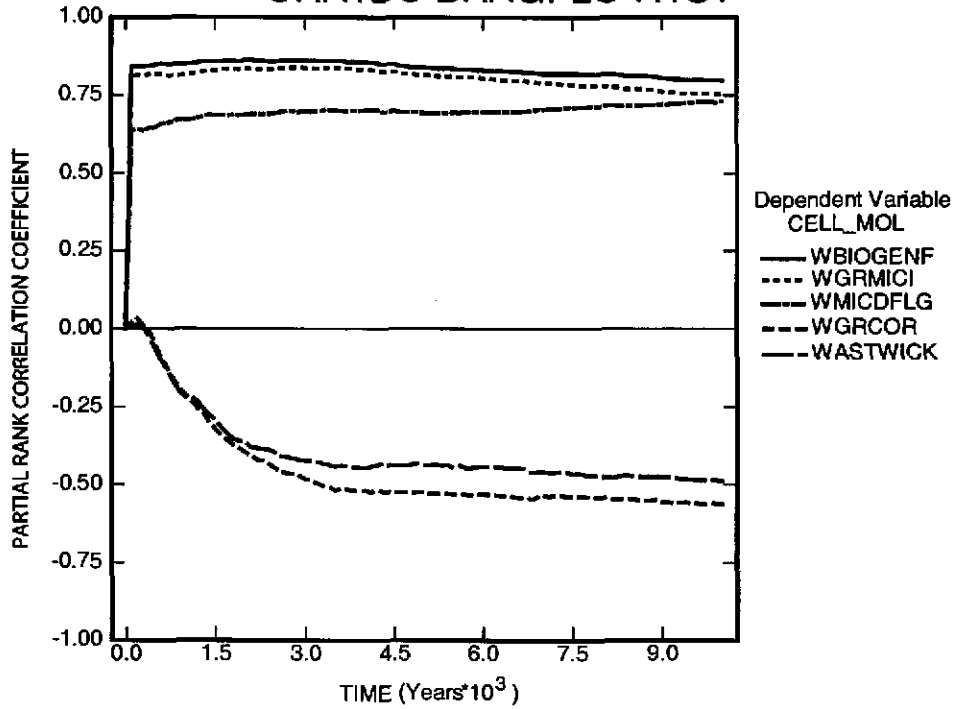
Figure 6-14. Primary correlations (dimensionless) of cumulative microbial gas generation with input parameters versus time (years), from the CRA-2004 PABC, Replicate 1, Scenario S1, CRA-2004 PABC. Table 4-2 gives a description of the names in the legend.

a) PABC

b) CRA1
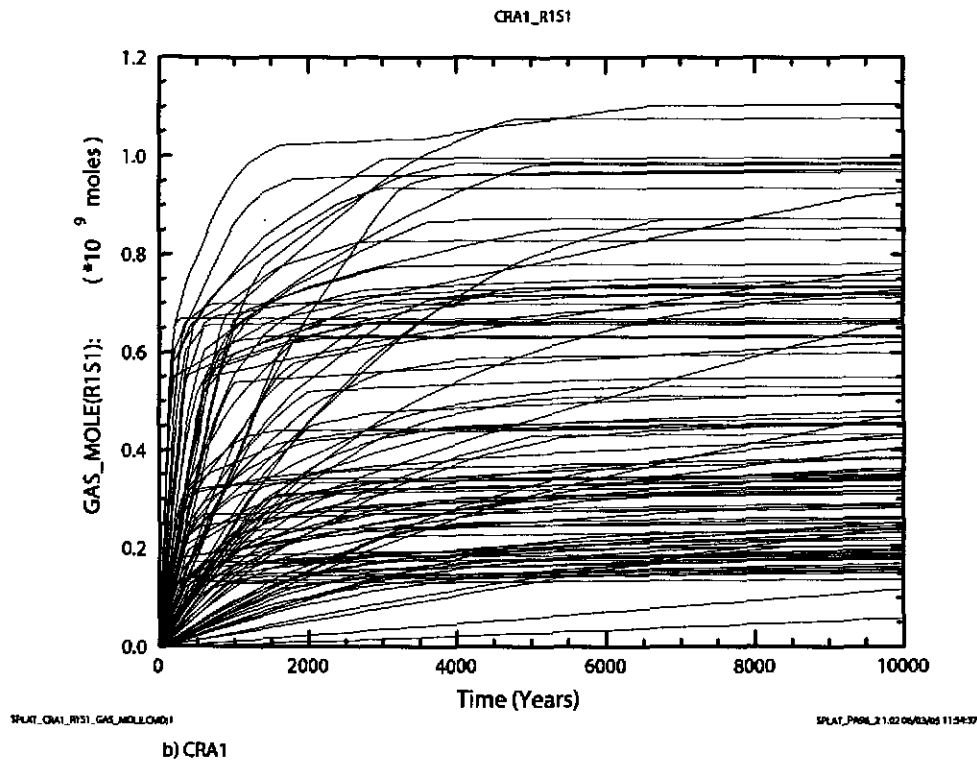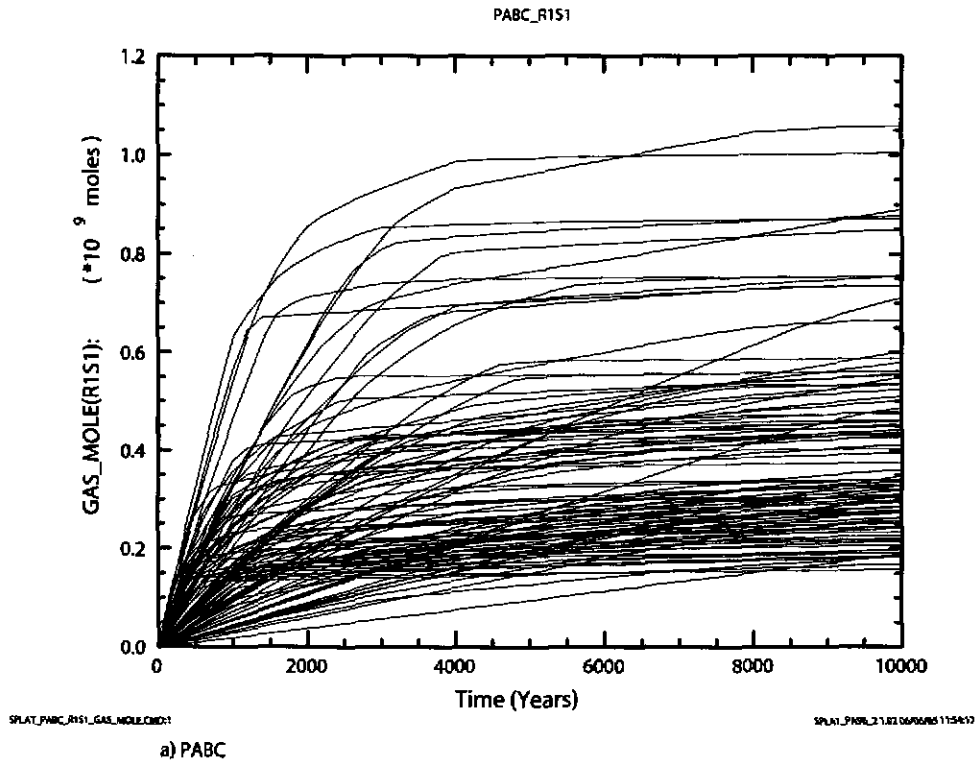
Figure 6-15. Cumulative gas generation (moles) by all processes versus time (years) for all 100 vectors in Replicate 1, Scenario S1. Figure a) shows results from the CRA-2004 PABC. Figure b) shows results from the CRA-2004.

Sensitivity Analysis for Total Cumulative Gas Generation
CRA1BC BRAGFLO R1S1
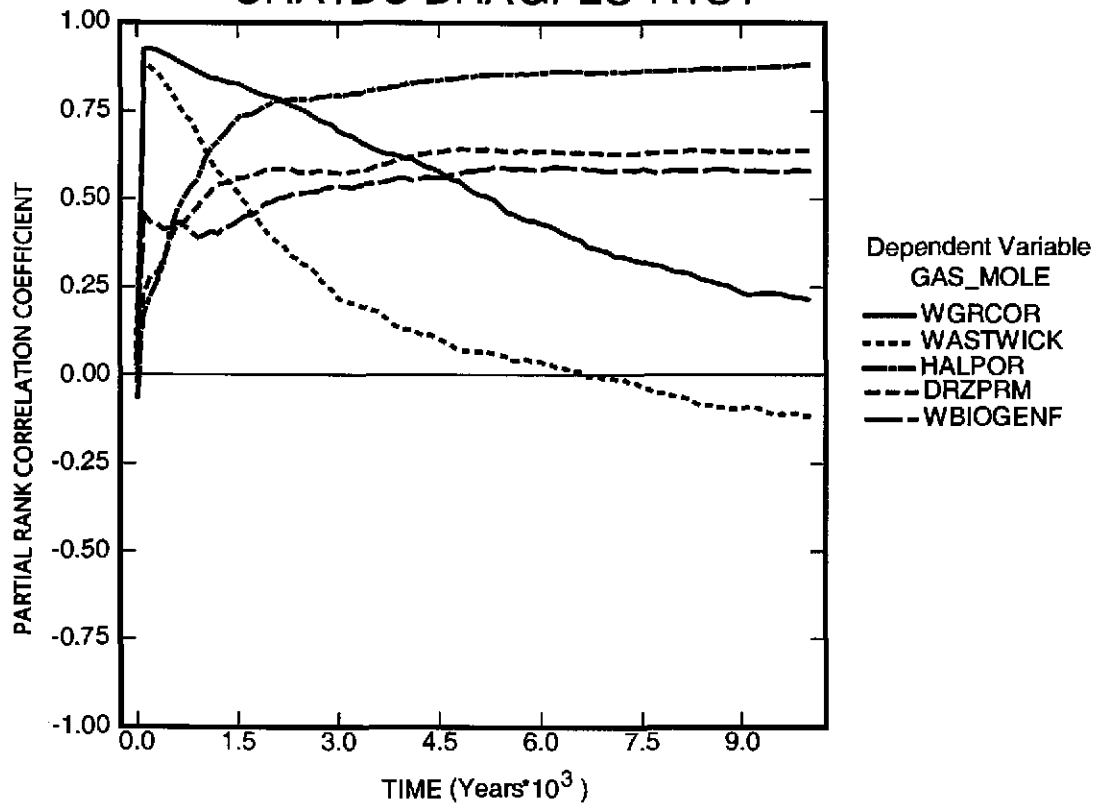
Figure 6-16. Primary correlations (dimensionless) of cumulative microbial gas generation with input parameters versus time (years) from the CRA-2004 PABC, Replicate 1, Scenario S1. Table 4-2 gives a description of the names in the legend.

PABC R1S1
Average Cumulative Gas Generation
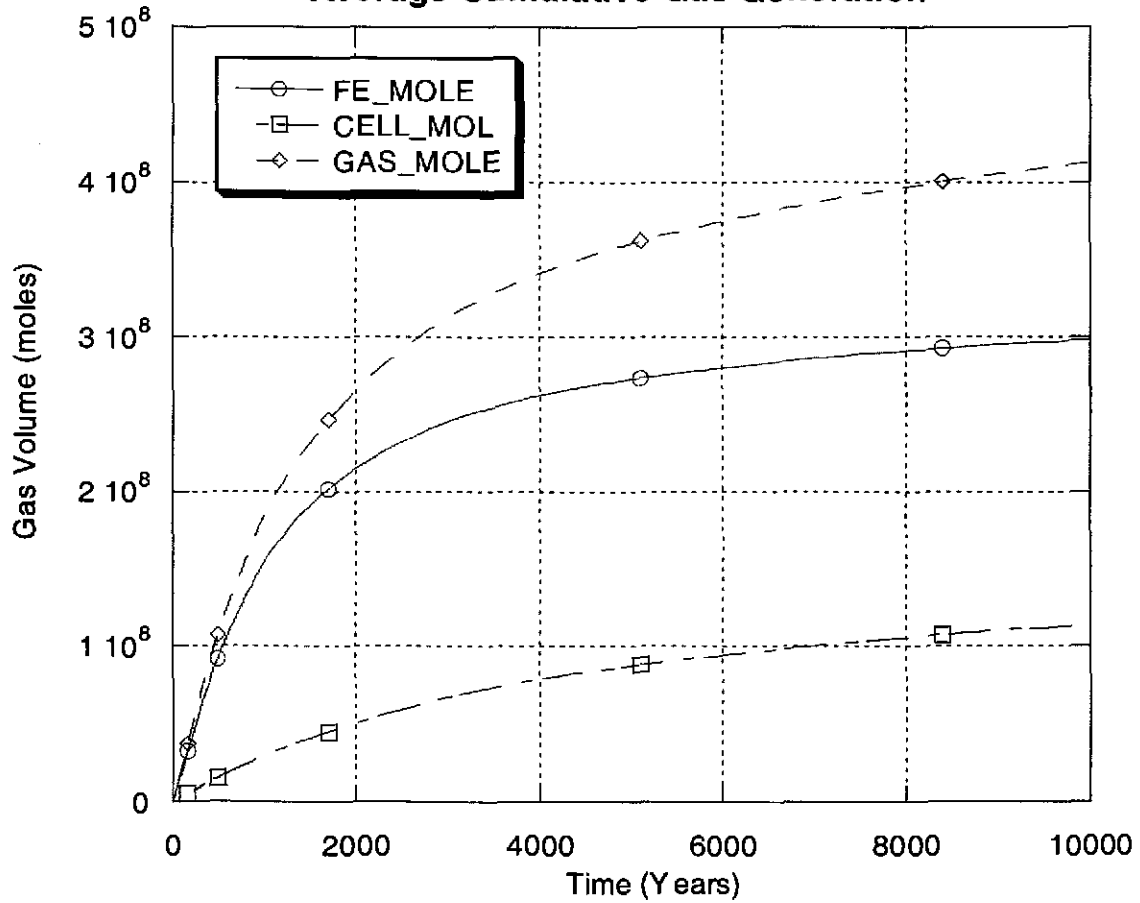
Figure 6-17. Cumulative gas generation (moles) by corrosion, by microbial activity and total versus time (years), averaged over 100 vectors from Replicate 1, Scenario S1 of the CRA-2004 PABC.
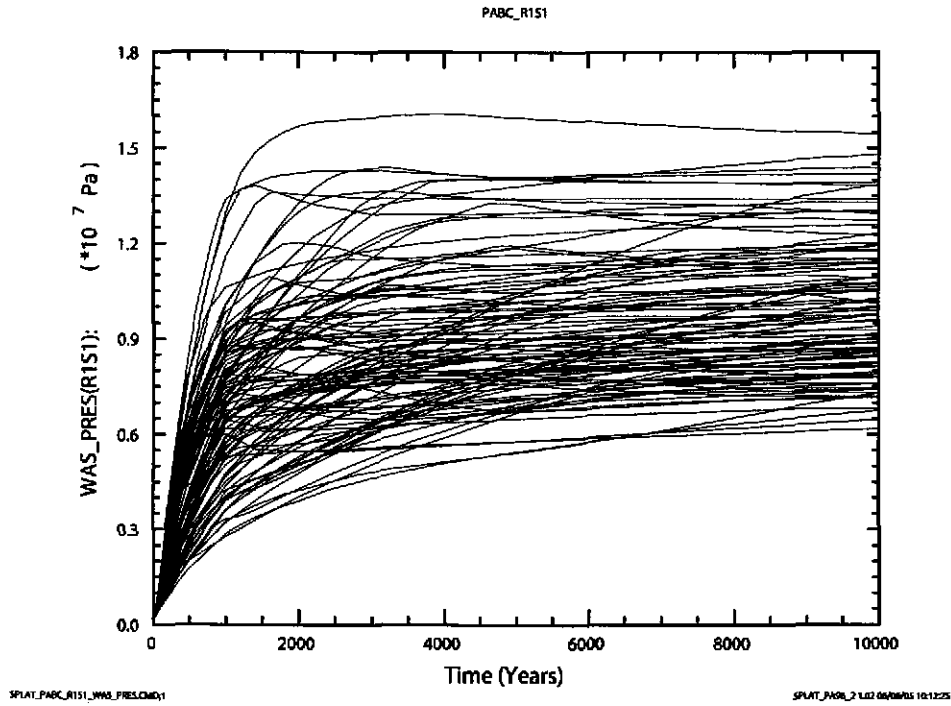
a) PABC
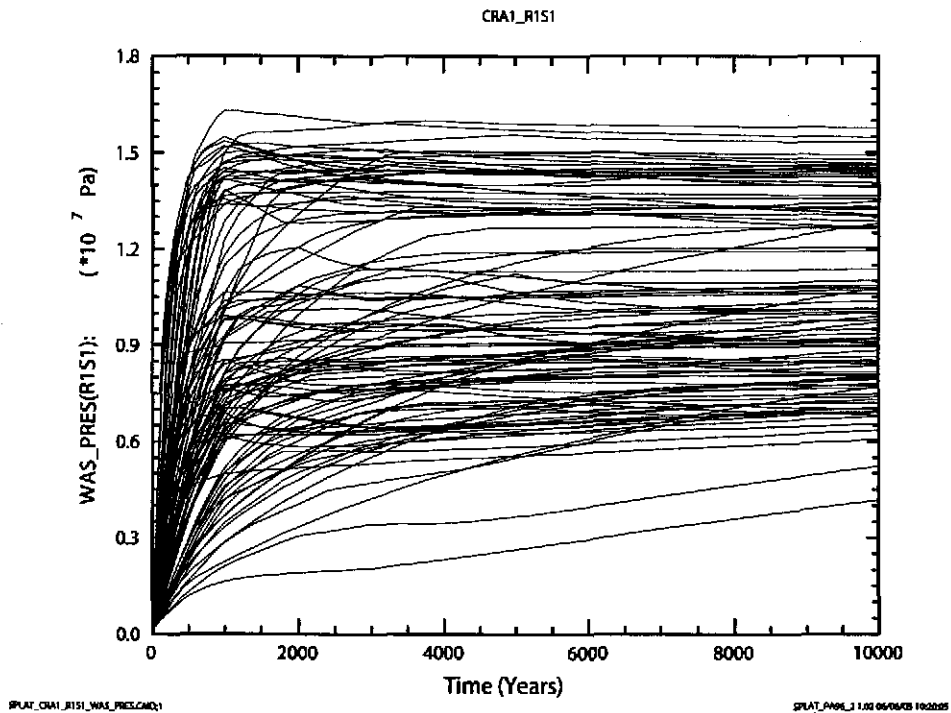
b) CRA1

Figure 6-18. Volume averaged pressure (Pa) in the waste area versus time (years) for all 100 vectors in Replicate 1, Scenario S1. Figure a) shows results from the CRA-2004 PABC. Figure b) shows results from the CRA-2004.
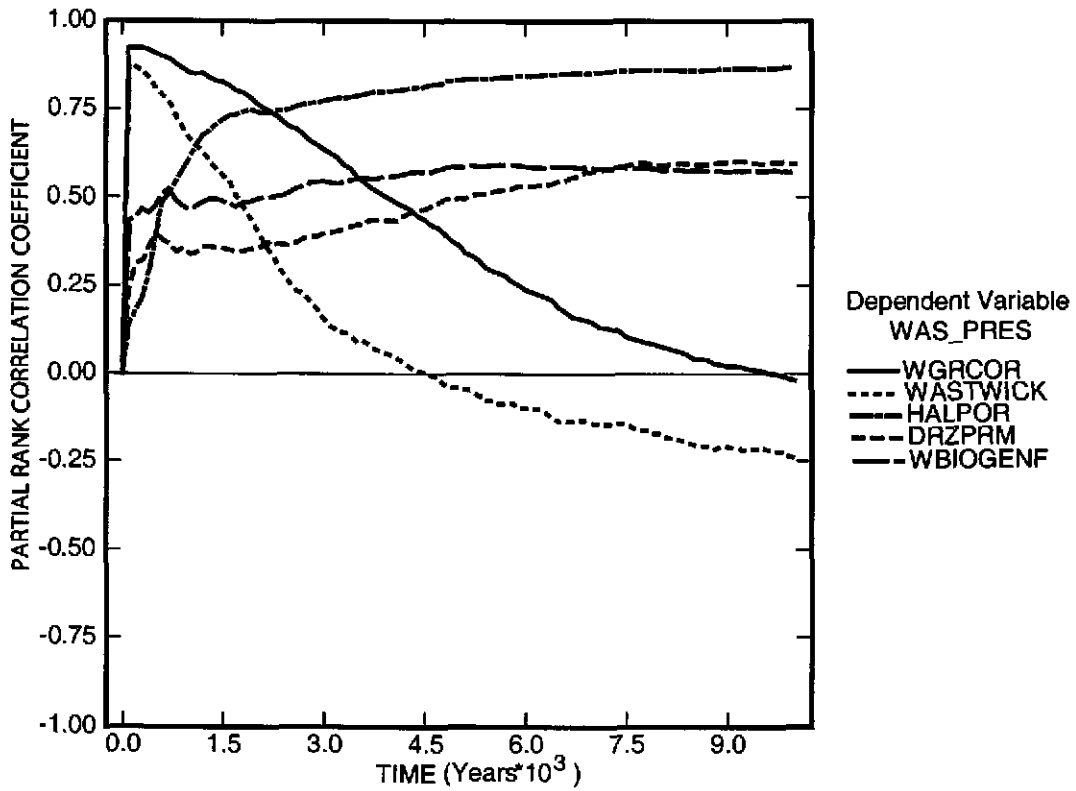
Figure 6-19. Primary correlations (dimensionless) of volume averaged pressure in the waste area with input parameters versus time (years) from the CRA-2004 PABC, Replicate 1, Scenario S1. Table 4-2 gives a description of the names in the legend.

FRACX38N(R1S1): (m)

1.0

0.0

-1.0

0   2000   4000   6000   8000   10000

Time (Years)

a) PABC

FRACX38N(R1S1): (*10² m)

4.0

3.0

2.0

1.0

0.0

0   2000   4000   6000   8000   10000
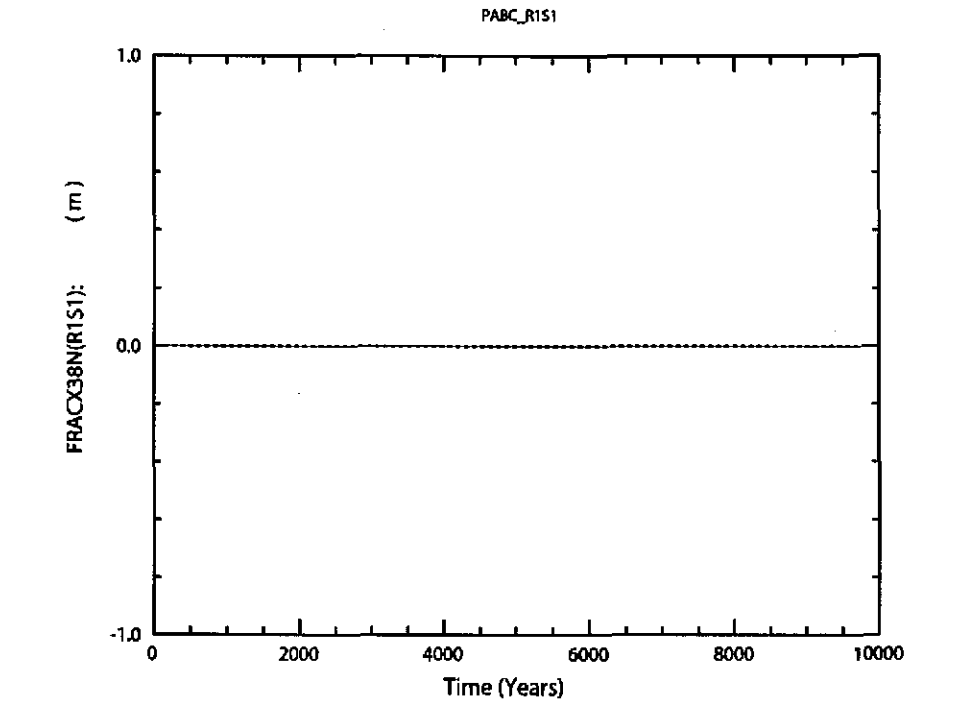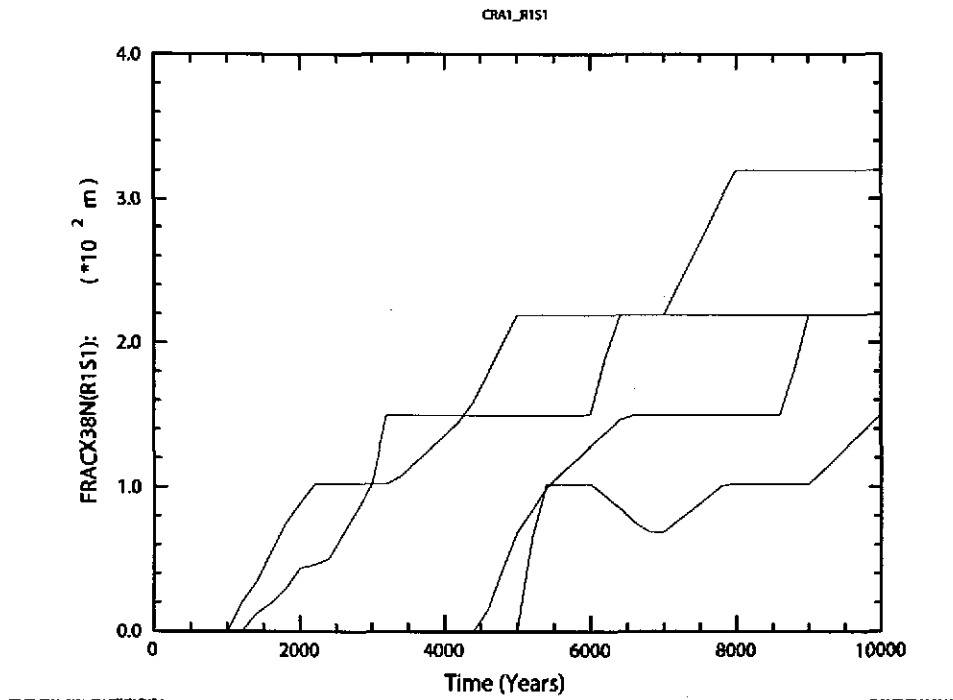
Time (Years)

b) CRA1

Figure 6-20. Fracture length (m) in MB138 north of the repository versus time (years) for all 100 vectors in Replicate 1, Scenario S1. Figure a) shows results from the CRA-2004 PABC. Figure b) shows results from the CRA-2004.

PABC_R1S1

a) PABC

CRA1_R1S1

b) CRA1
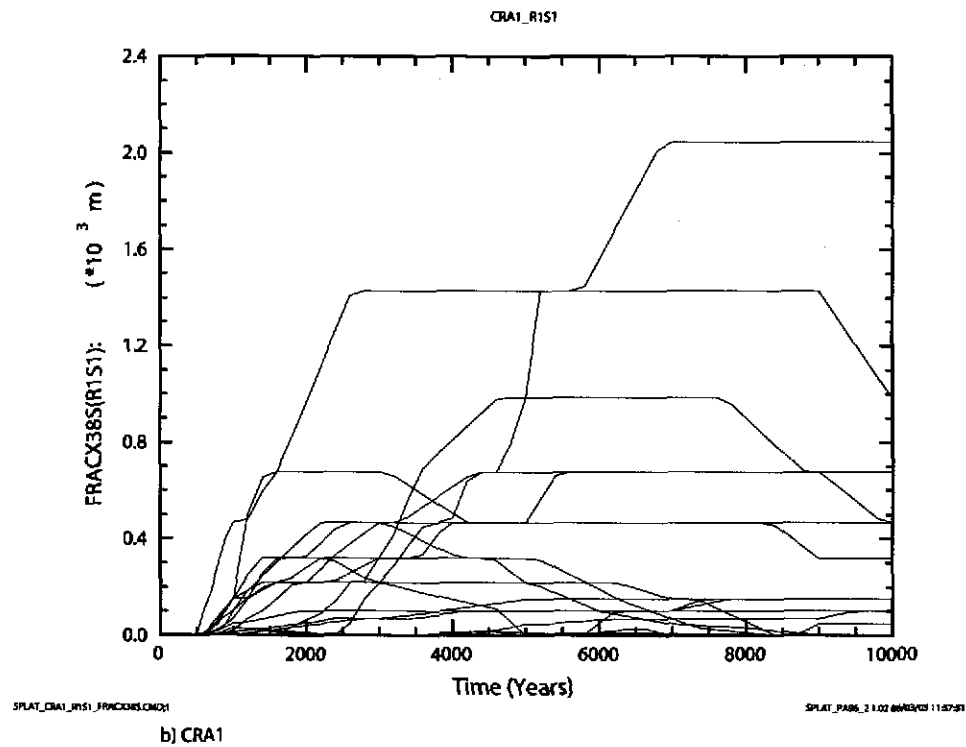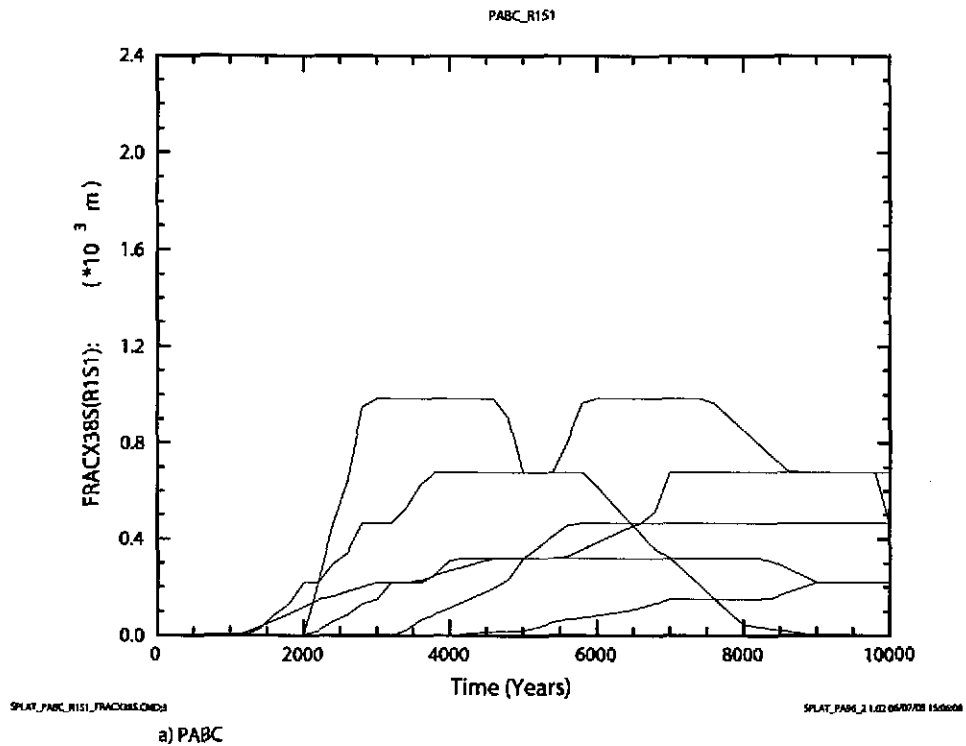
Figure 6-21. Fracture length (m) in MB138 south of the repository versus time (years) for all 100 vectors in Replicate 1, Scenario S1. Figure a) shows results from the CRA-2004 PABC. Figure b) shows results from the CRA-2004.

Figure a) PABC plot showing FRACX39N(R1S1): (*10³ m) versus Time (Years)

SPLAT_PABC_R1S1_FRACX39N.CMD;1   SPLAT_PAB8_2 1.02 06/06/05 11:57:10

a) PABC

CRA1_R1S1

SPLAT_CRA1_R1S1_FRACX39N.CMD;1   SPLAT_PAB8_2 1.02 06/07/05 19:11:56

b) CRA1
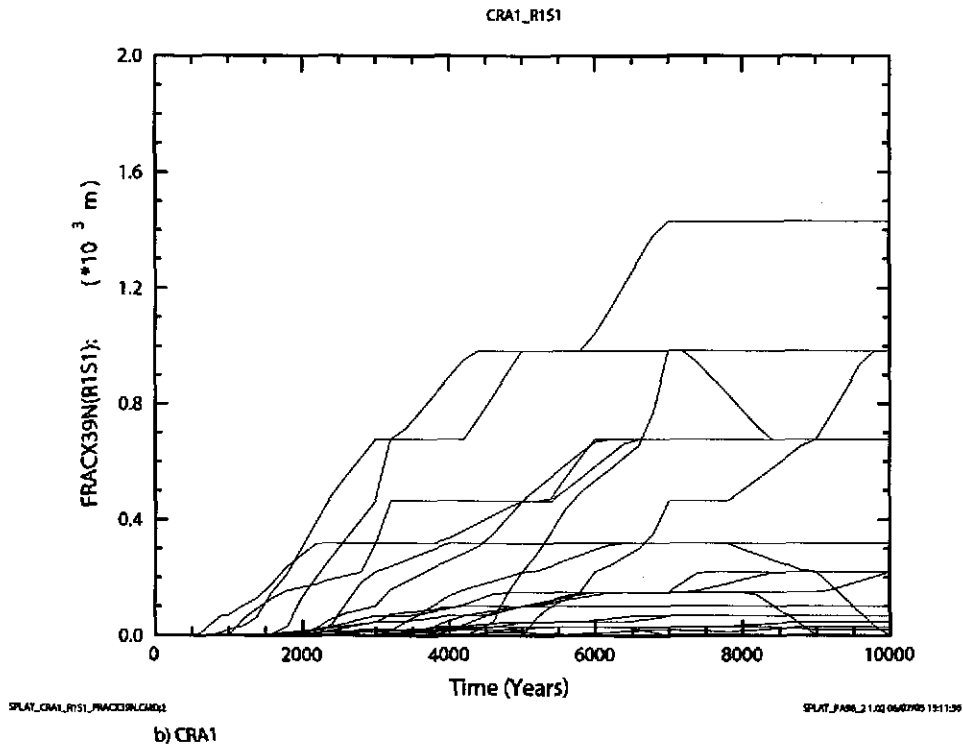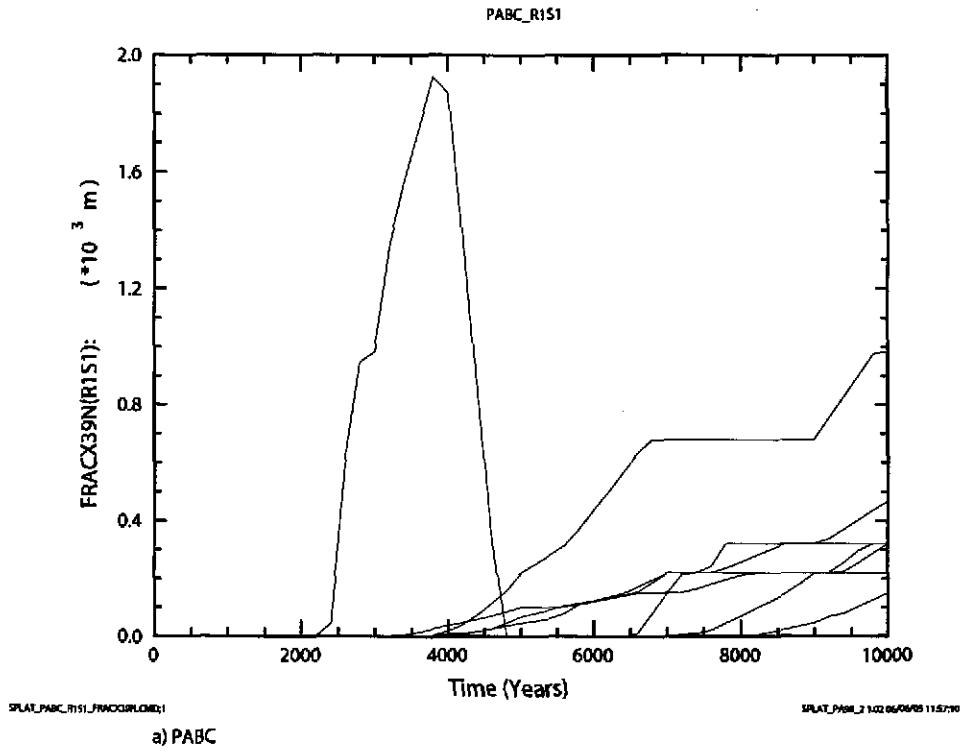
Figure 6-22. Fracture length (m) in MB139 north of the repository versus time (years) for all 100 vectors in Replicate 1, Scenario S1. Figure a) shows results from the CRA-2004 PABC. Figure b) shows results from the CRA-2004.

Page 77 of 165

a) PABC

b) CRA1
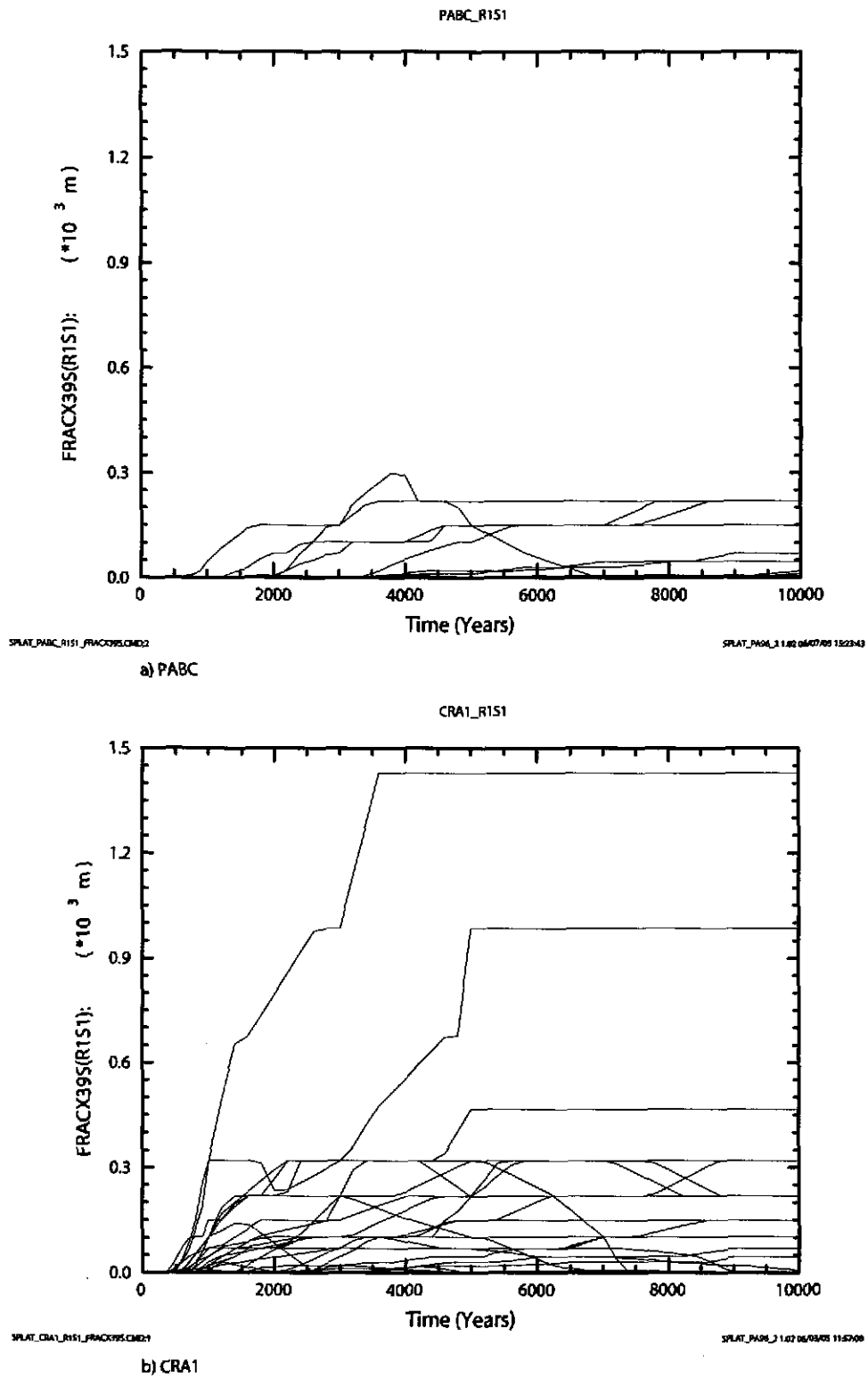
Figure 6-23. Fracture length (m) in MB139 south of the repository versus time (years) for all 100 vectors in Replicate 1, Scenario S1. Figure a) shows results from the CRA-2004 PABC. Figure b) shows results from the CRA-2004.

Information Only
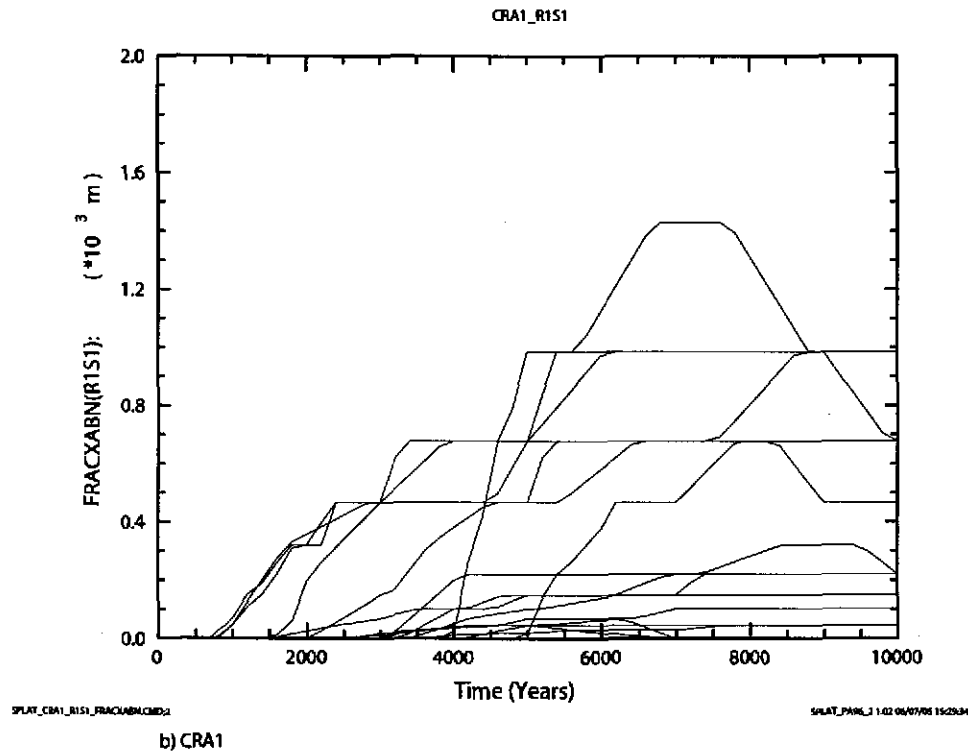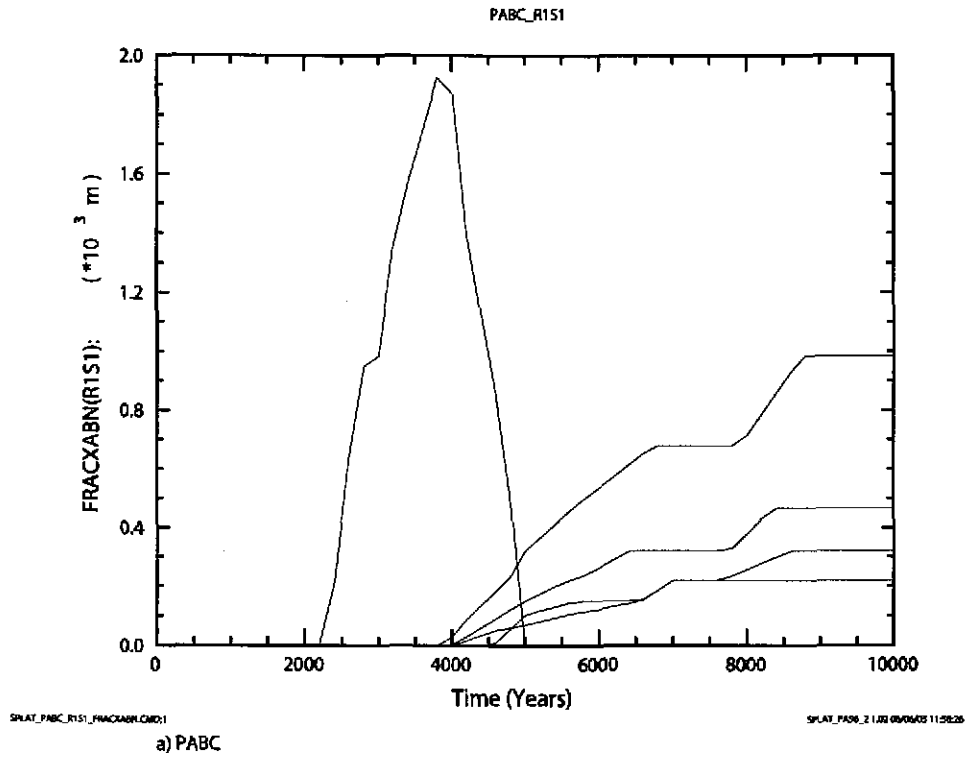
a) PABC

b) CRA1

Figure 6-24. Fracture length in Anhydrite A&B (m) north of the repository versus time (years) for all 100 vectors in Replicate 1, Scenario S1. Figure a) shows results from the CRA-2004 PABC. Figure b) shows results from the CRA-2004.
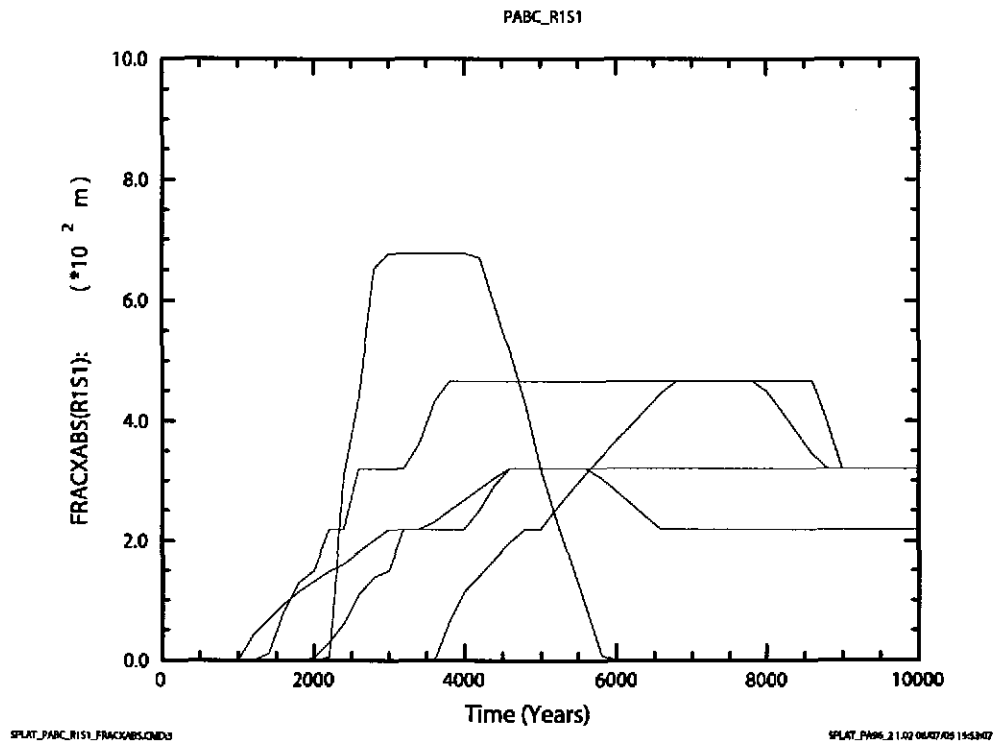
a) PABC
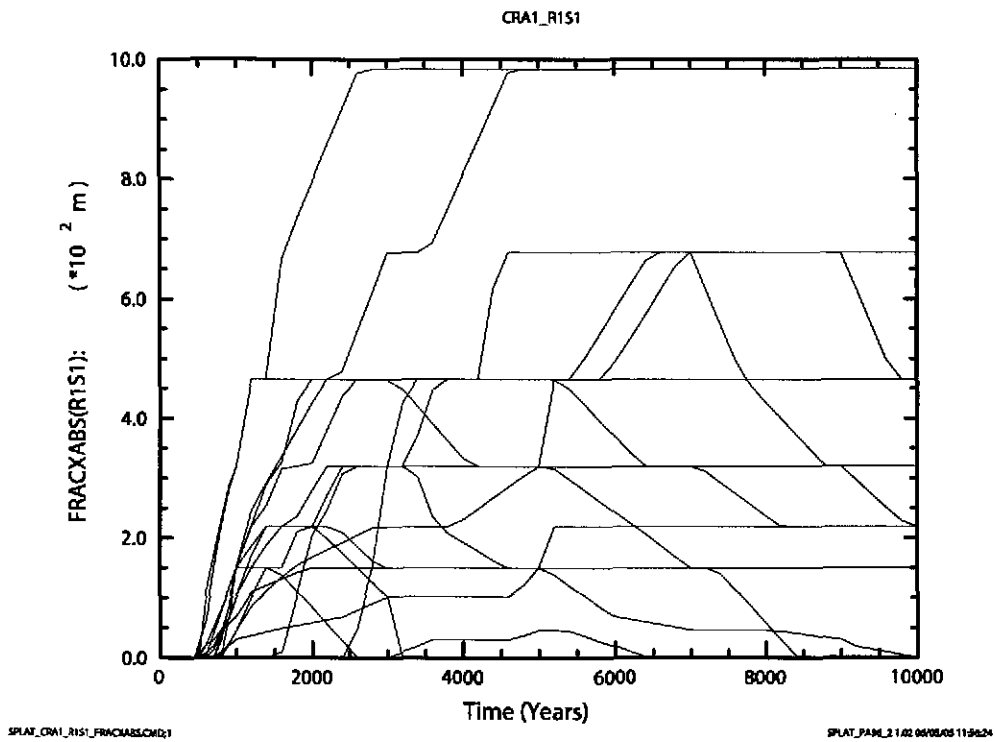
b) CRA1

Figure 6-25. Fracture length in Anhydrite A and Anhydrite B (m) south of the repository versus time (years) for all 100 vectors in Replicate 1, Scenario S1. Figure a) shows results from the CRA-2004 PABC. Figure b) shows results from the CRA-2004.

a) PABC

b) CRA1
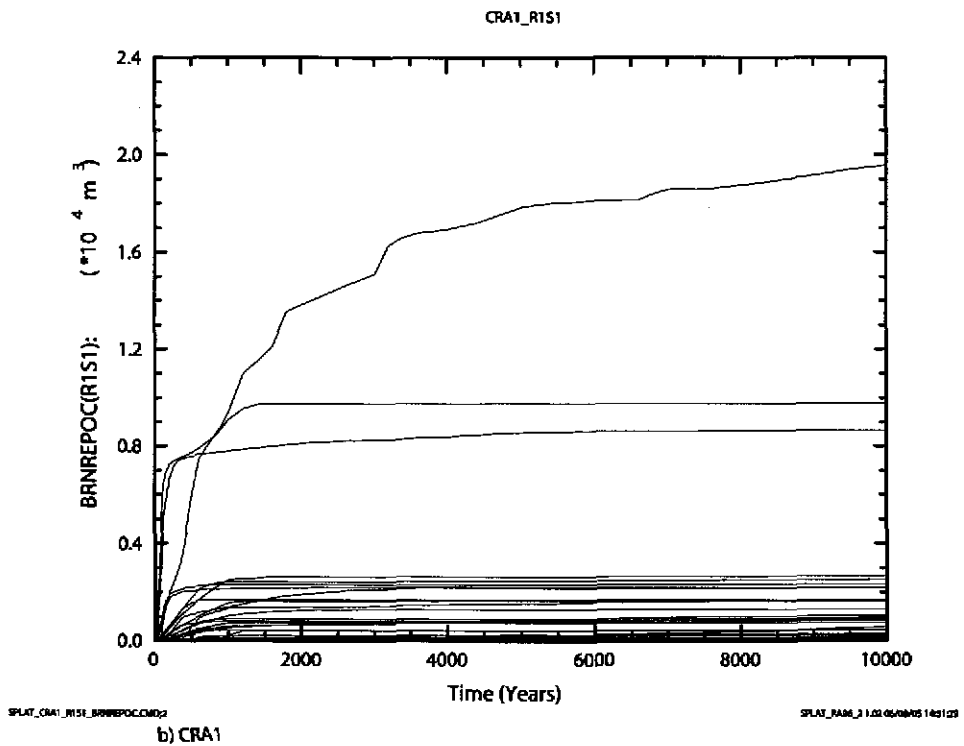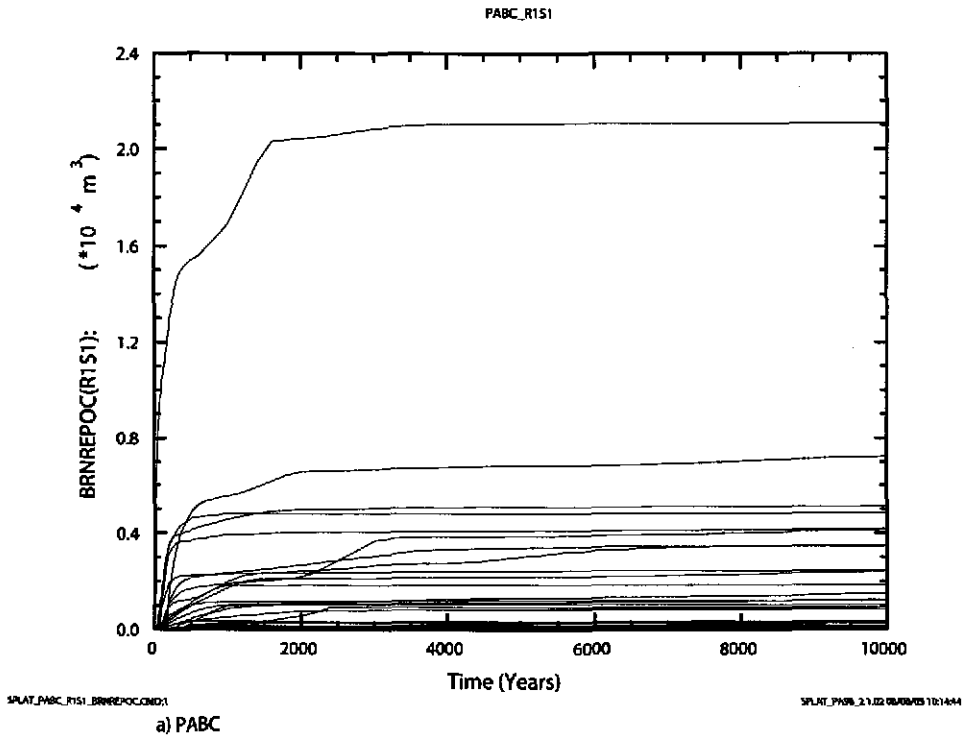
Figure 6-26. Total cumulative brine flow (m³) away from the repository versus time (years) for all 100 vectors in Replicate 1, Scenario S1. Figure a) shows results from the CRA-2004 PABC. Figure b) shows results from the CRA-2004.
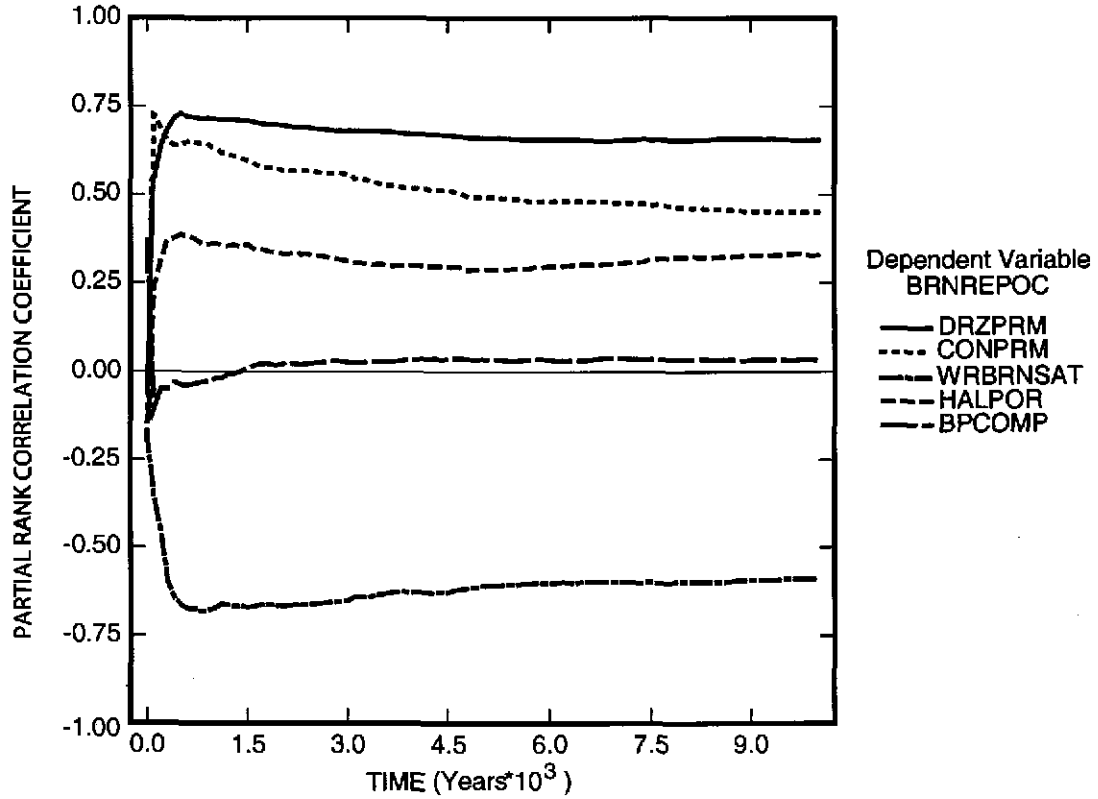
Figure 6-27. Primary correlations (dimensionless) of cumulative brine outflow from the repository with input parameters versus time (years) from the CRA-2004 PABC, Replicate 1, Scenario S1. Table 4-2 gives a description of the names in the legend.
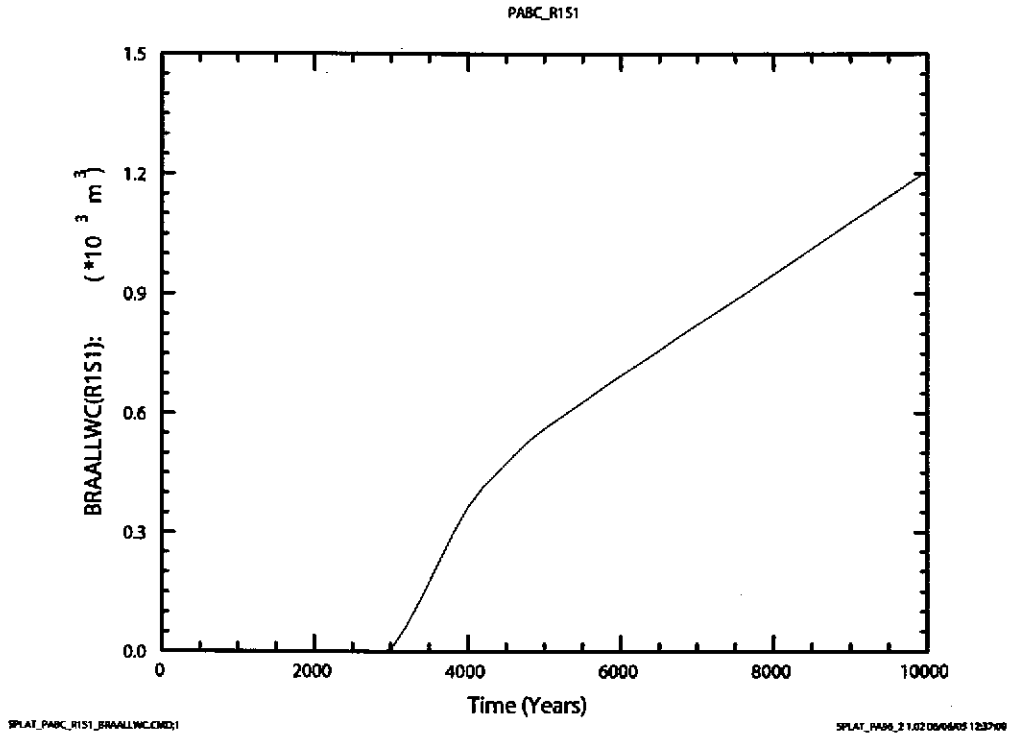
a) PABC
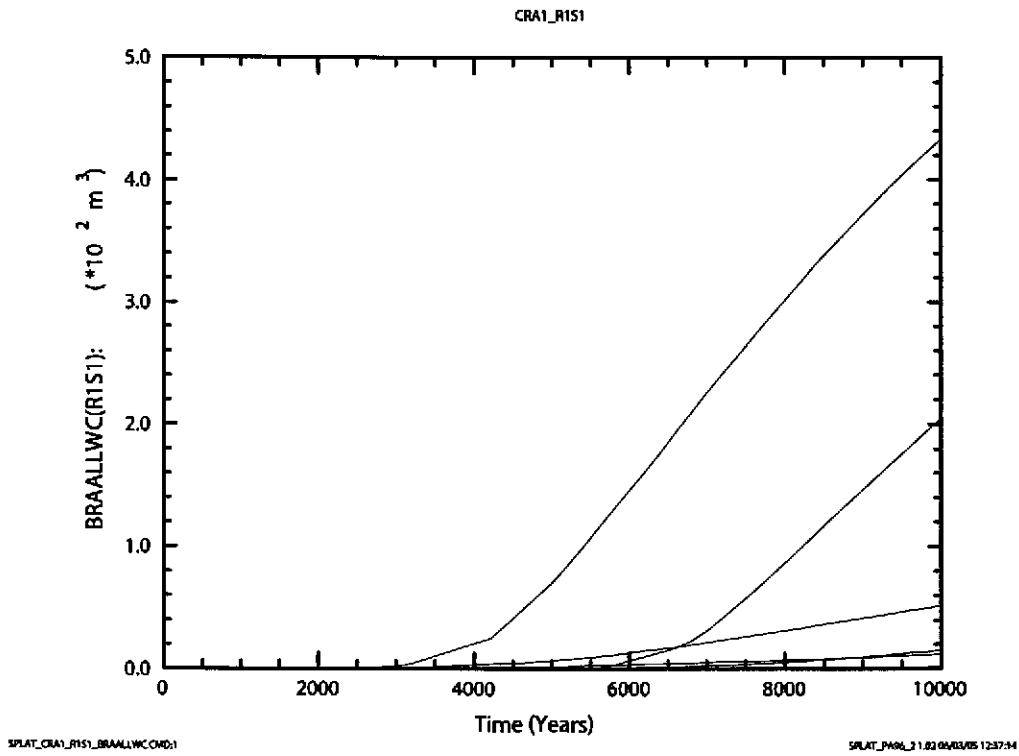
b) CRA1

Figure 6-28. Cumulative brine releases (m³) to the LWB versus time (years) for all 100 vectors in Replicate 1, Scenario S1. Figure a) shows results from the CRA-2004 PABC. Figure b) shows results from the CRA-2004.

6.4 DRILLING DISTURBANCE SCENARIOS

Scenarios S2 through S6 evaluate the possible results of drilling intrusions into the repository. It is assumed that all boreholes in the Salado Flow Analysis are drilled through the repository in search of deeper resources. The potential consequences of encountering a pressurized brine pocket in the Castile (an E1 event) are considered in Scenarios S2 and S3. Boreholes that do not encounter pressurized brine (S4 & S5) are modeled in the Salado Flow grid as terminating at the base of the repository (an E2 event). Scenario S6 evaluates an E2 event followed by an E1 event. The specific sequences of material property changes in the model are listed in the following section. After section §6.4.1, detailed results are presented for Scenario S2 and S4, which are representative of Scenarios S2-S6, except for the differences in the timing of the drilling intrusions. Brine releases to the Culebra are also presented for Scenario S6, as S6 is only used for determining the radionuclide source term to the Culebra in the PANEL application (Kanney and Leigh, 2005).

6.4.1   Sequence of Events

Five drilling disturbance scenarios are considered in this part of the Salado Flow Analysis. The sequence of events for each is summarized below:

Scenario S2 (E1 event)
> 200 years: change in lower shaft material properties.
> 350 years: borehole intrusion (E1) through the Waste Panel into a hypothetical pressurized brine reservoir in the underlying Castile Formation. Concrete borehole plugs are immediately emplaced in the borehole at the Culebra and at the surface.
> 550 years: Borehole plugs fail and the borehole (top to bottom) is assumed to have properties equivalent to sand (material: BH_SAND).
> 1,550 years: the permeability of the borehole between the repository and the Castile Formation decreases due to creep closure of the salt (material: BH_CREEP).

Scenario S3 (E1 event)
> 200 years: change in lower shaft material properties.
> 1,000 years: borehole intrusion (E1) through the Waste Panel into a hypothetical pressurized brine reservoir in the underlying Castile Formation. Concrete borehole plugs are immediately emplaced in the borehole at the Culebra and at the surface.
> 1,200 years: Borehole plugs fail and the borehole (top to bottom) is assumed to have properties equivalent to sand (material: BH_SAND).
> 2,200 years: the permeability of the borehole between the repository and the Castile Formation decreases due to creep closure of the salt (material: BH_CREEP).

Scenario S4 (E2 event)

200 years: change in lower shaft material properties.

350 years: borehole intrusion (E2) through a Waste Panel terminating at the base of the DRZ in the modeling grid (no connection to the underlying Castile Formation). Two plugs are present in the upper part of the borehole.

550 years: Borehole plugs fail and the borehole (top to bottom) is assumed to have properties equivalent to sand (material: BH_SAND).

Scenario S5 (E2 event)

200 years: change in lower shaft material properties.

1,000 years: borehole intrusion (E2) through a Waste Panel terminating at the base of the DRZ in the modeling grid (no connection to the underlying Castile Formation). Two plugs are present in the upper part of the borehole.

1,200 years: Borehole plugs fail and the borehole (top to bottom) is assumed to have properties equivalent to sand (material: BH_SAND).

Scenario S6 (E2,E1 events)

200 years: change in lower shaft material properties.

1,000 years: borehole intrusion (E2) through a Waste Panel terminating at the base of the DRZ in the modeling grid (no connection to the underlying Castile Formation) Borehole filled with sand.

2,000 years: borehole intrusion (E1) through a Waste Panel into a hypothetical pressurized brine reservoir in the underlying Castile Formation

2,200 years: Borehole plugs fail and the borehole (top to bottom) is assumed to have properties equivalent to sand (material: BH_SAND).

3,200 years: the permeability of the borehole between the repository and the Castile Formation decreases due to creep closure of the salt (material: BH_CREEP).

6.4.2 Halite Creep

Drilling intrusions have relatively little effect on the range of porosities in the repository compared to the undisturbed scenario, because most creep closure occurs prior to the drilling event. However, changes in pressure due to the intrusion do have a small but recognizable impact on porosity, which is the primary measure of creep closure in the waste areas. Figure 6-29 and Figure 6-30 show the volume averaged porosity in all waste areas versus time for Scenarios S2 and S4, for the CRA-2004 PABC and the CRA-2004. There is little difference in the two analyses, which is confirmed by statistics given in Table 6-12.

Table 6-12. Statistics of porosity at 10,000 years for Replicate R1, Scenarios S2 and S4 for the CRA-2004 and CRA-2004 PABC.

W_R_POR (dimensionless)	CRA-2004		CRA-2004 PABC	
	S2	S4	S2	S4
Maximum	2.23E-01	2.24E-01	2.11E-01	2.04E-01
Average	1.44E-01	1.20E-01	1.51E-01	1.26E-01
Minimum	9.14E-02	5.32E-02	9.76E-02	5.71E-02

6.4.3 Brine Inflow

Table 6-13 summarizes statistics for S2 and S4 for BRNREPTC, the cumulative brine flow into the repository. The average inflows for the CRA-2004 PABC and the CRA-2004 differ only slightly for Scenarios S2 and S4. The maximum brine inflow in S2 is greater in the CRA-2004 PABC than in the CRA-2004. This is likely due to the fact that pressures in the CRA-2004 PABC rise more slowly than in the CRA-2004, leading to a greater driving force (gradient) for brine to flow into the repository.

Table 6-13 Statistics for cumulative brine flow into the repository at 10,000 years Replicate R1, Scenarios S2 and S4 for the CRA-2004 and CRA-2004 PABC.

(BRNREPTC) (m^3)	CRA-2004		CRA-2004 PABC	
	S2	S4	S2	S4
Maximum	1.64E+05	5.15E+04	1.99E+05	4.71E+04
Average	2.95E+04	1.31E+04	3.19E+04	1.31E+04
Minimum	3.64E+03	3.89E+02	9.32E+03	8.05E+02

Figure 6-31 and Figure 6-32 show plots of brine flow into the repository versus time for all 100 vectors in Scenarios S2 and S4 for the CRA-2004 PABC and the CRA-2004 The graphs visually confirm the statistics listed above in Table 6-13.

Figure 6-33 and Figure 6-34 show the total volume of brine in the repository versus time for all 100 vectors in replicate 1. The results from Scenario S2 show a spike in brine volume at the intrusion time as one would expect. The volume then decreases with time due to increasing pressure, associated brine flow up the borehole, and brine consumption from steel corrosion. The results for Scenario S4 show a similar decrease after the borehole plugs fail. Scenario S4 has no intrusion into the Castile brine pocket.

6.4.4 Brine Saturation

Figure 6-35 and Figure 6-36 show brine saturation (WAS_SATB) in the Waste Panel versus time for all 100 vectors, for Scenarios S2 and S4, for the CRA-2004 PABC and the CRA-2004. The direct consequence of greater brine inflow associated with a drilling intrusion is higher brine saturation in the waste areas. For Scenario S2, brine saturation in the Waste Panel increases immediately to a value close to 1 after a drilling intrusion into a pressurized brine pocket in the Castile (350 years).

Figure 6-37 shows the PRCC's for brine saturation in the Waste Panel WAS_SATB for Scenario S2. Figure 6-38 shows the PRCC's for Scenario S4. The permeability of the DRZ (DRZPRM) and the borehole (BHPERM) exhibit the largest positive correlations. High permeability in these materials allows brine to flow into the waste areas. Negative correlations with the steel corrosion rate (WGRCOR) and the waste wicking factor (WASTWICK) are evident because high values of these parameters lead to faster brine consumption.

6.4.5   Gas Generation

Table 6-14 summarizes average cumulative gas generation information at 10,000 years for Scenarios S2 and S4. The lower microbial gas-generation rates lead to slightly less gas produced by microbial activity in the CRA-2004 PABC compared to the CRA-2004 Drilling intrusions do not appreciably affect gas generation by microbial activity, but gas generation by corrosion is greater in the E1 scenario (S2) than in the E2 (S4) scenario. The increase is due to increased availability of brine, which is a limiting factor for corrosion. At 10,000 years, the average brine saturation in the Waste Panel (WAS_SATB) in the E1 scenario is greater than in the E2 scenario.

Table 6-14. **Brine saturation and cumulative gas generation at 10,000 years averaged over 100 vectors for Replicate R1 for the CRA-2004 and CRA-2004 PABC.**

Property	CRA-2004		CRA-2004 PABC	
	S2	S4	S2	S4
WAS_SATB (dimensionless)	7.21E-01	3.52E-01	8.00E-01	3.76E-01
GAS_MOLE (moles)	5.25E+08	5.00E+08	4.83E+08	4.48E+08
FE_MOLE (moles)	3.50E+08	3.26E+08	3.57E+08	3.24E+08
CELL_MOL (moles)	1.74E+08	1.74E+08	1.26E+08	1.24E+08

Figure 6-39 and Figure 6-40 show the cumulative amount of gas produced by iron corrosion versus time, and Figure 6-43 and Figure 6-44 show the fraction of iron remaining versus time. The results for gas produced by iron corrosion in the CRA-2004 PABC are very similar to that of the CRA-2004. Figure 6-41 and Figure 6-42 show the PRCC's for gas generation by iron corrosion versus time. Variables such as the steel corrosion rate (WGRCOR), halite porosity (HALPOR), DRZ permeability (DRZPRM), and the waste wicking factor (WASTWICK) show the highest positive correlations with gas generation by iron corrosion. These correlations make sense because these variables all influence the net gas generation rate from corrosion. The borehole permeability (BHPERM) shows a strong positive correlation in S4, presumably because it serves as a

conduit for brine to enter the repository from the lower DRZ (bore hole does not penetrate the castile brine pocket in S4).

Figure 6-45 and Figure 6-46 show the cumulative amount of gas produced by microbial gas generation, Figure 6-49 and Figure 6-50 show the fraction of cellulosics (cellulose or CPR depending on the value of WAS_AREA:PROBDEG, see §5.4). A stark difference between CRA-2004 and CRA-2004 PABC results is evident. This is due to the new significantly lower microbial gas-generation rates. In the CRA-2004 most cellulosic material was consumed within a few hundred years. In the CRA-2004 PABC, many vectors have cellulose remaining after 10,000 years. Figure 6-47 and Figure 6-48 show the PRCC's for the cumulative amount of gas generation by microbial activity versus time. Besides variables that are directly related to the rate of microbial gas-generation (BIOGENFC, GRATMICI), the only variables with an important correlation are the corrosion rate and the wicking factor. It's interesting to note that the wicking factor and the iron corrosion rate both have negative correlations with microbial gas generation. This is consistent with Figure 6-37 and Figure 6-38 which show that brine saturation in the Waste Area (WAS_SATB) is negatively correlated with the wicking factor and the iron corrosion rate thus leading to microbial gas generation at the humid rate which is lower than the indundated rate.

Figure 6-51 and Figure 6-52 show the cumulative amount of gas produced versus time by all gas-generation processes. The differences between the CRA-2004 and the CRA-2004 PABC are noticeable but small. Figure 6-53 and Figure 6-54 show the PRCC's for total cumulative gas generation by all processes versus time. Halite porosity has the largest positive correlation, owing to the fact that corrosion now accounts for more gas generation than microbial activity.

6.4.6 Pressure

Pressures in the disturbed scenarios are identical to pressures in the undisturbed scenarios until the drilling intrusion occurs. Following the intrusion pressures in the Waste Panel tend to change rapidly, especially once the borehole plugs fail 200 years after the intrusion. Table 6-15 shows statistics of the volume average pressure in the Waste Panel at 10,000 years. The average pressure in Scenario S2 is slightly higher in the CRA-2004 PABC compared to the CRA-2004, owing to the higher brine saturation. Average pressures in Scenario S4 are lower in the CRA-2004 PABC than in the CRA-2004, due to the lower microbial-gas-generation rates.

Table 6-15. Statistics on the volume averaged pressure in the waste panel at 10,000 years for Replicate R1 for the CRA-2004 and CRA-2004 PABC.

WAS_PRES (Pa)	CRA-2004		CRA-2004 PABC	
	S2	S4	S2	S4
Maximum	1.52E+07	1.52E+07	1.42E+07	1.35E+07
Average	8.14E+06	6.15E+06	8.53E+06	6.39E+06
Minimum	2.32E+06	9.85E+05	4.70E+06	1.21E+06

Figure 6-55 and Figure 6-56 show the volume averaged pressure in the Waste Panel (WAS_PRES) versus time for all 100 vectors in replicate R1, for the CRA-2004

PABC and the CRA-2004. As the figures indicate there aren't significant differences between the two analyses. Figure 6-57 and Figure 6-58 show PRCC's for WAS_PRES versus time for Scenarios S2 and S4. The figures indicate that borehole permeability has the strongest negative correlation, as this is the primary means by which pressure may escape the repository. Castile brine pocket pressure has a strong positive correlation with pressure at the time of an intrusion, which subsequently decreases with time.

6.4.7 Rock Fracturing

The consequence of rock fracturing is modeled in the DRZ and marker beds with a model that alters the permeability of these units as pressures increase above a fracture initiation pressure. Figure 6-59 through
Figure 6-70 show the fracturing length in marker beds 138, 139 and Anhydrite A&B, north and south of the repository. The plots show a large but transient fracture length at around 3000 years. This event occurs in vector 53 as in Scenario S1 (see §6.3.7).

6.4.8 Brine Flow Out of the Repository

Figure 6-71 and Figure 6-72 show cumulative brine flow out of the Waste Panel. Figure 6-73 and Figure 6-74 show cumulative brine flow away from the repository (BRNREPOC) versus time for Scenarios S2 and S4, for the CRA-2004 PABC and the CRA-2004. The results indicate that cumulative brine flow is slightly higher in the CRA-2004 PABC analysis compared to the CRA-2004. This is confirmed by statistics at 10,000 years given below in Table 6-16. The only exception is the minimum brine outflow in S2, which was greater in the CRA-2004 PABC than in the CRA-2004.

Table 6-16. Statistics on cumulative brine flow out of the repository at 10,000 years for Replicate R1 for CRA-2004 and CRA-2004 PABC.

BRNREPOC (m³)	CRA-2004		CRA-2004 PABC	
	S2	S4	S2	S4
Maximum	1.54E+05	1.91E+04	1.78E+05	2.13E+04
Average	1.33E+04	1.27E+03	1.48E+04	1.36E+03
Minimum	1.35E+01	3.52E+00	8.20E+02	1.41E+00

Figure 6-75 and Figure 6-76 show PRCC's for BRNREPOC versus time for Scenario S2 and S4. In both scenarios, DRZ and borehole permeability have the strongest positive correlations. For S2, the iron corrosion rate has the largest negative correlation due to brine consumption by corrosion. In S4, the residual brine saturation has the largest negative correlation, which is consistent with the repository having a lower brine saturation compared to S2 (as shown in Table 6-14 and Figure 6-36).
Figure 6-77 and Figure 6-78 show the cumulative brine release to the Culebra formation in Scenarios S2 and S4. Figure 6-79 and Figure 6-80 show cumulative brine release to the LWB. Table 6-17 gives statistics on these releases at 10,000 years for S2, S4 and S6. Scenario S6 was included here because releases to the Culebra were slightly higher in S6 compared to S2, and because the results of S6 are only used to determine the

radionuclide source term to the Culebra in the PANEL application (Kanney and Leigh, 2005). The results indicate higher releases to the Culebra and lower releases to the LWB in the CRA-2004 PABC compared to the CRA-2004.

Table 6-18 shows statistics on cumulative brine releases to the Magenta and the Dewey lake for scenarios S2 and S6. For this table ALGEBRACDB had to be rerun to include these output variables. The ALGEBRACDB code was run under run control with input file ALG3_BF_CRA1BC.INP, which is stored CMS library LIBCRA1BC_BF, in the ANALYSIS class. The output ALG3_BF_CRA1BC_R1_Ss_Vvvv.CDB files were stored in the CMS library LIBCRA1BC_BFR1Ss in the ANALYSIS class, where s = 1,...6, and vvv = 001,... 100.

The results shown in Table 6-18 show that the maximum cumulative brine releases to the Magenta and Dewey Lake over the 10,000-year regulatory period are three to four orders of magnitude lower than releases to the Culebra. In looking at the results of Table 6-17 and Table 6-18, it's important to note that the Los Medanos, Tamarisk, and Forty Niner are set in the WIPP PAPDB to be essentially impermeable to liquid and gas flow in order to maximize the amount of brine flow into the Culebra. This modeling approach was designed to add conservatism (Dotson, 1996) to radionuclide release calculations since the Culebra is known to be the most transmissive unit above the repository. However, treating the Tamarisk and Forty-niner units as impermeable should also over-estimate brine flow to the Magenta.

Table 6-17. Statistics on cumulative brine releases to the Culebra, and the LWB at 10,000 years for Replicate R1, for the CRA-2004 and CRA-2004 PABC. BRNBHRCC and BRAALLWC are variables calculated in the ALG2 post-processing step (see Table 4-1 and Appendix B).

Cumulative brine releases to the Culebra BRNBHRCC (m^3)	CRA-2004		CRA-2004 PABC		
	S2	S4	S2	S4	S6
Maximum	1.52E+05	5.67E+03	1.72E+05	1.46E+03	1.75E+05
Average	9.17E+03	2.82E+02	9.51E+03	1.09E+02	9.58E+03
Minimum	6.61E-01	1.09E-02	6.35E-01	2.27E-01	4.04E+00

Cumulative brine releases to the LWB BRAALLWC (m^3)	CRA-2004		CRA-2004 PABC	
	S2	S4	S2	S4
Maximum	3.74E+02	4.07E+02	8.28E+02	7.42E+02
Average	3.81E+00	4.12E+00	8.31E+00	7.43E+00
Minimum	1.96E-06	1.95E-06	4.96E-05	4.96E-05

Table 6-18. Statistics on cumulative brine releases to the Magenta and the Dewey Lake at 10,000 years for replicate R1 of the CRA-2004 PABC. BRNBHUP4 and BRNBHUP6 are variables that were calculated in a ALG3 post-processing step that is described above in section 6.4.8.

Cumulative brine releases to the Magenta BRNBHUP4 (m^3)	CRA-2004 PABC	
	S2	S6
Maximum	4.19E+00	8.53E-05
Average	1.34E-01	1.10E-05
Minimum	2.20E-19	6.28E-19

Cumulative brine releases to the Dewey Lake BRNBHUP6 (m^3)	CRA-2004 PABC	
	S2	S6
Maximum	5.75E-01	0.00E+00
Average	3.12E-02	0.00E+00
Minimum	0.00E+00	0.00E+00

6.4.9 Figures for §6.4

PABC_R1S2

SPLAT_PABC_R1S2_W_R_POR.CHD;1   SPLAT_PA96_2 1/2 06/06/05 11:52:23

a) PABC

CRA1_R1S2

SPLAT_CRA1_R1S2_W_R_POR.CHD;1   SPLAT_PA96_2 1.02 06/06/05 10:21:59
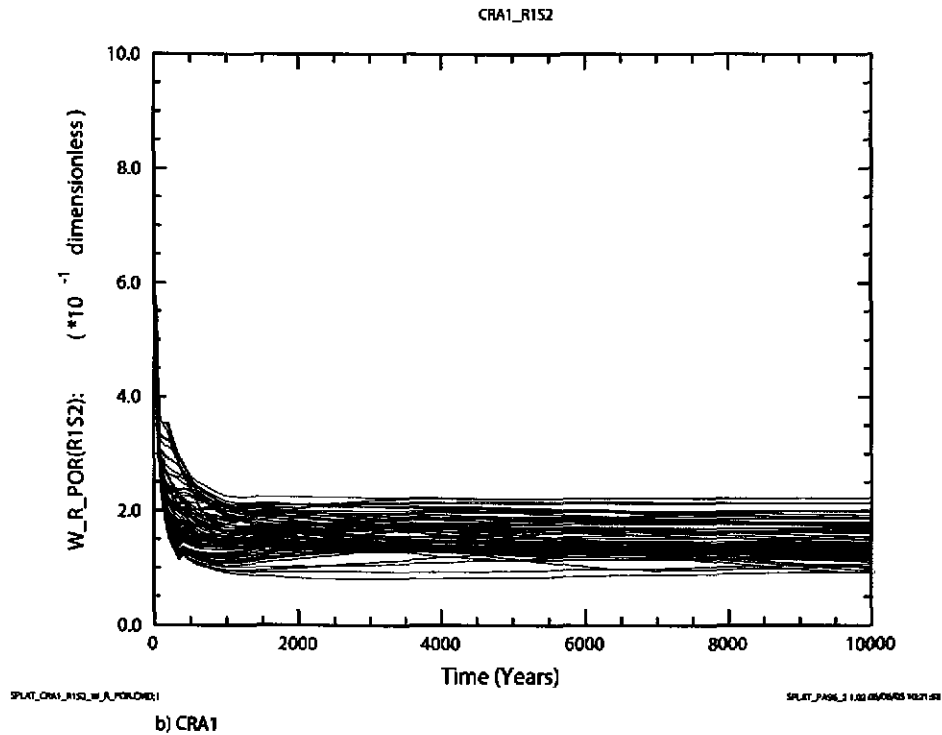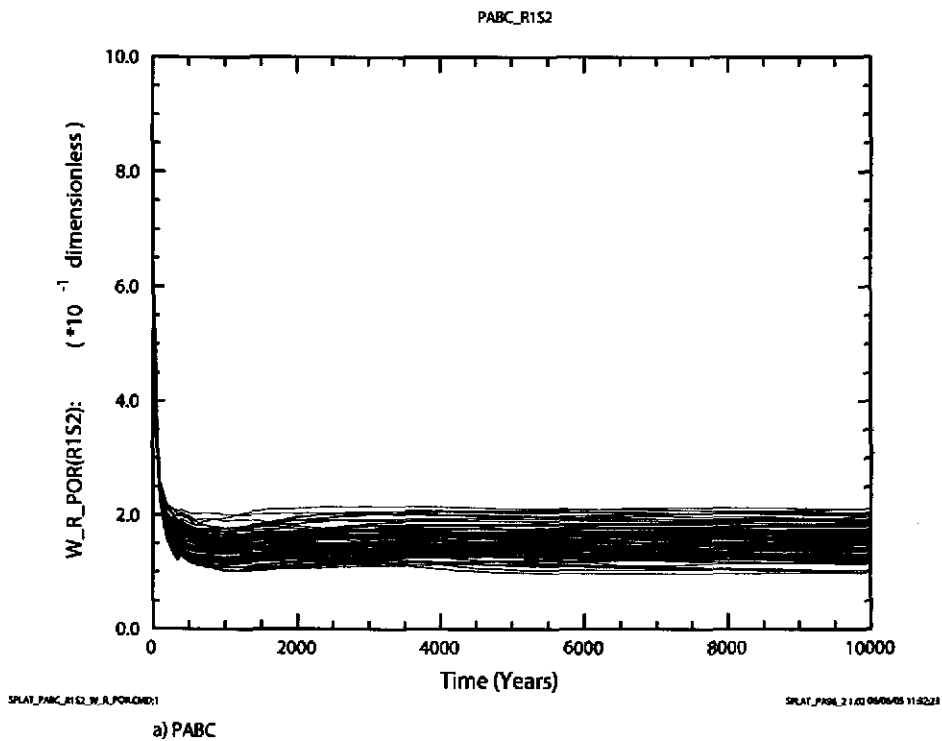
b) CRA1

Figure 6-29. Volume averaged porosity (dimensionless) in all waste regions versus time (years) for all 100 vectors in Replicate 1, Scenario S2. Figure a) shows results from the CRA-2004 PABC. Figure b) shows results from the CRA-2004.

Information Only
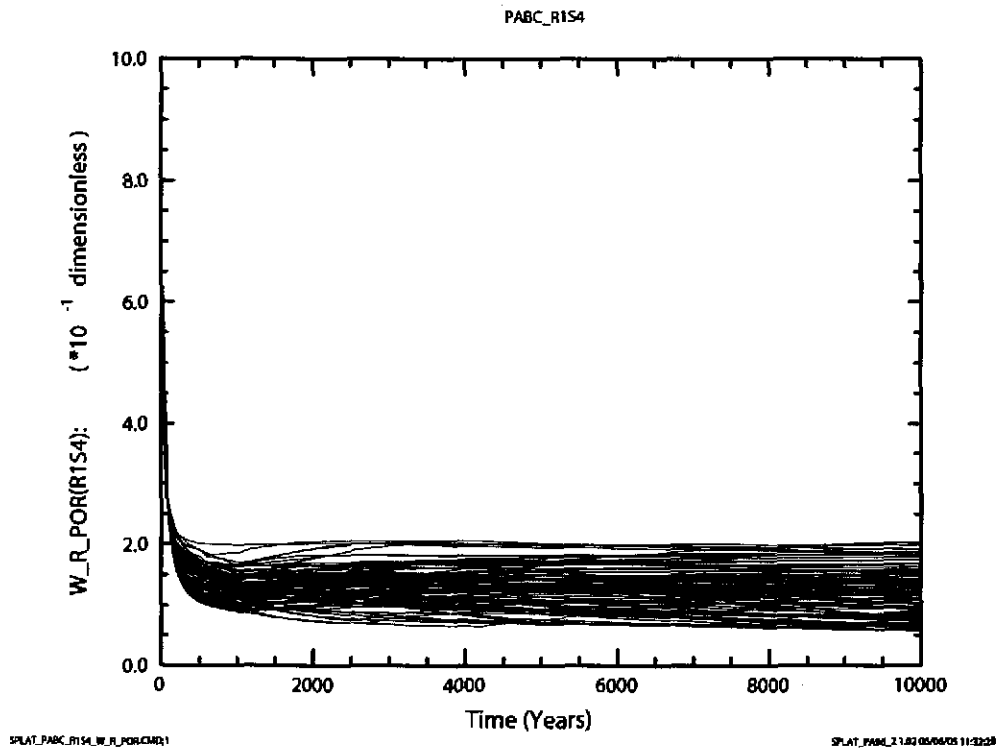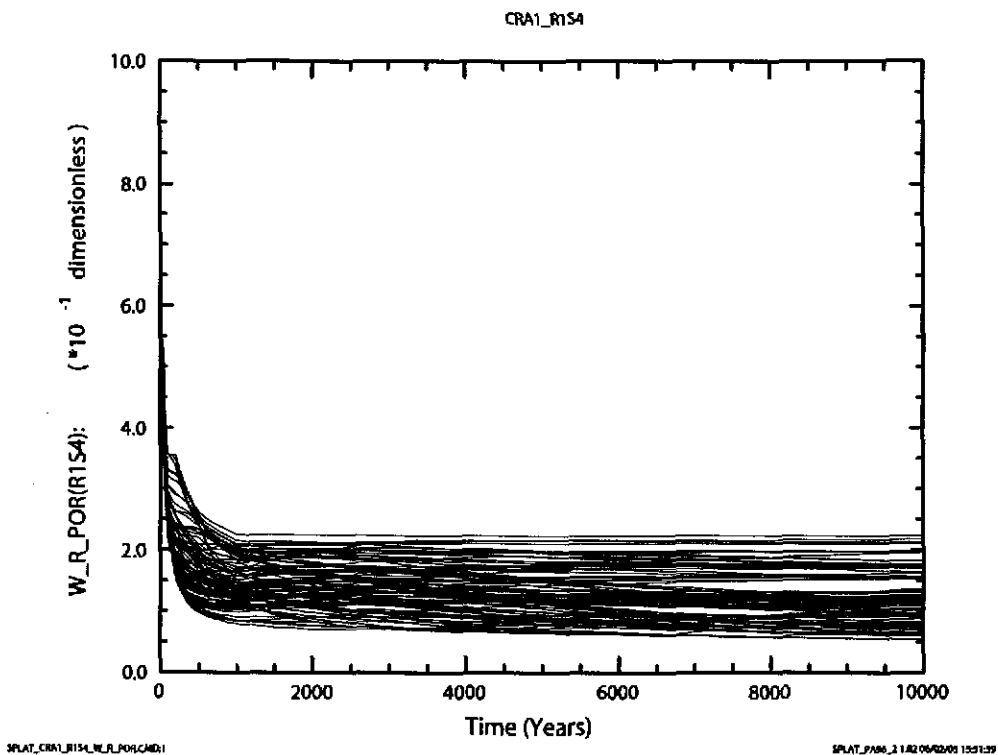
a) PABC

b) CRA1

Figure 6-30. Volume averaged porosity (dimensionless) in all waste regions versus time (years) for all 100 vectors in Replicate 1, Scenario S4. Figure a) shows results from the CRA-2004 PABC. Figure b) shows results from the CRA-2004.

Information Only
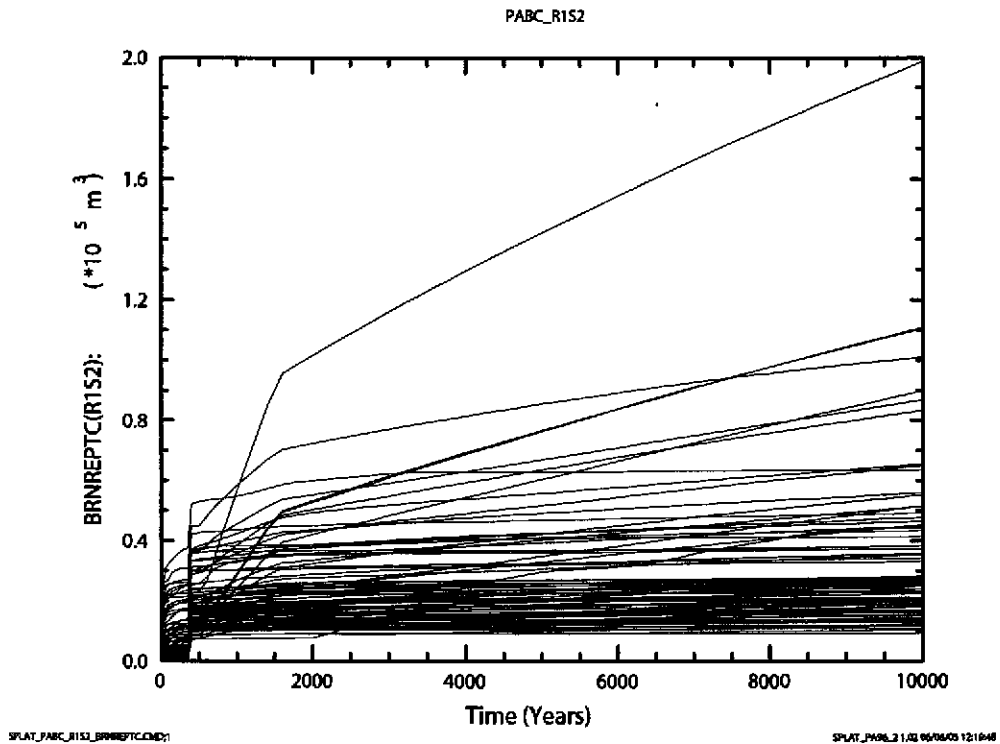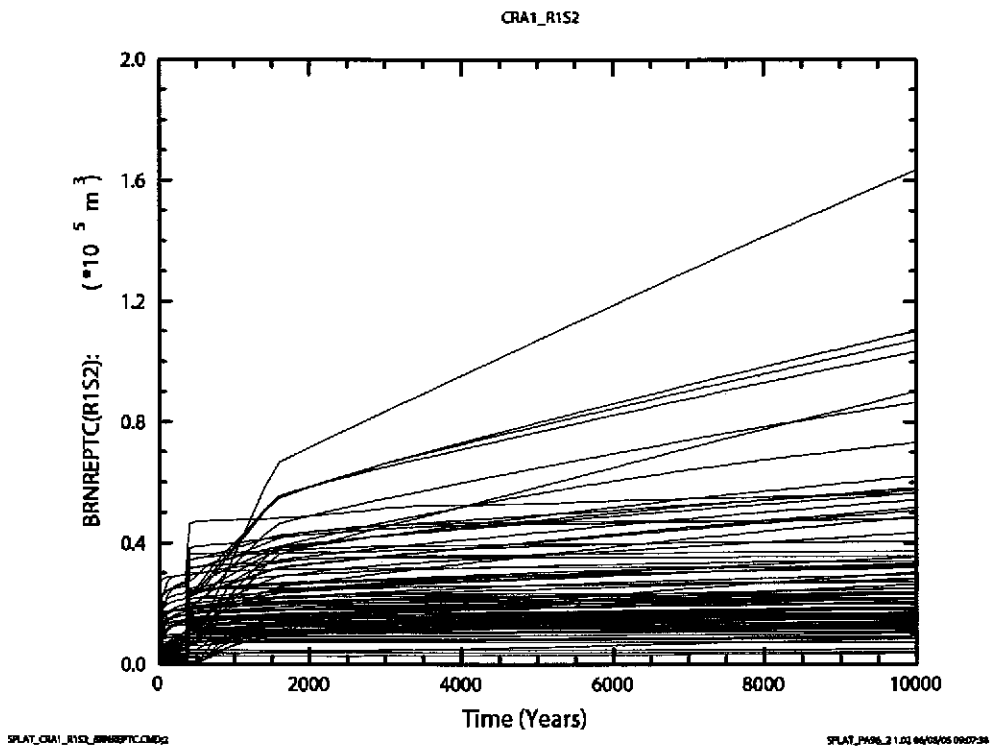
a) PABC

b) CRA1

Figure 6-31. Total cumulative inflow (m³) of brine into the repository versus time (years) for all 100 vectors in Replicate 1, Scenario S2. Figure a) shows results from the CRA-2004 PABC. Figure b) shows results from the CRA-2004.
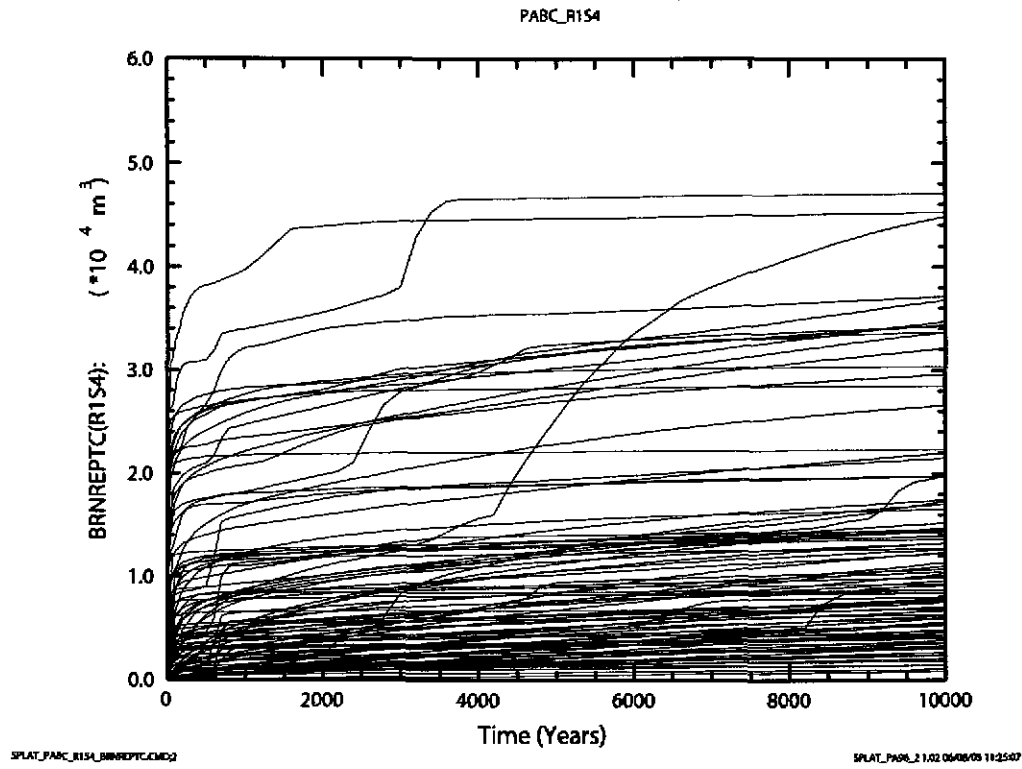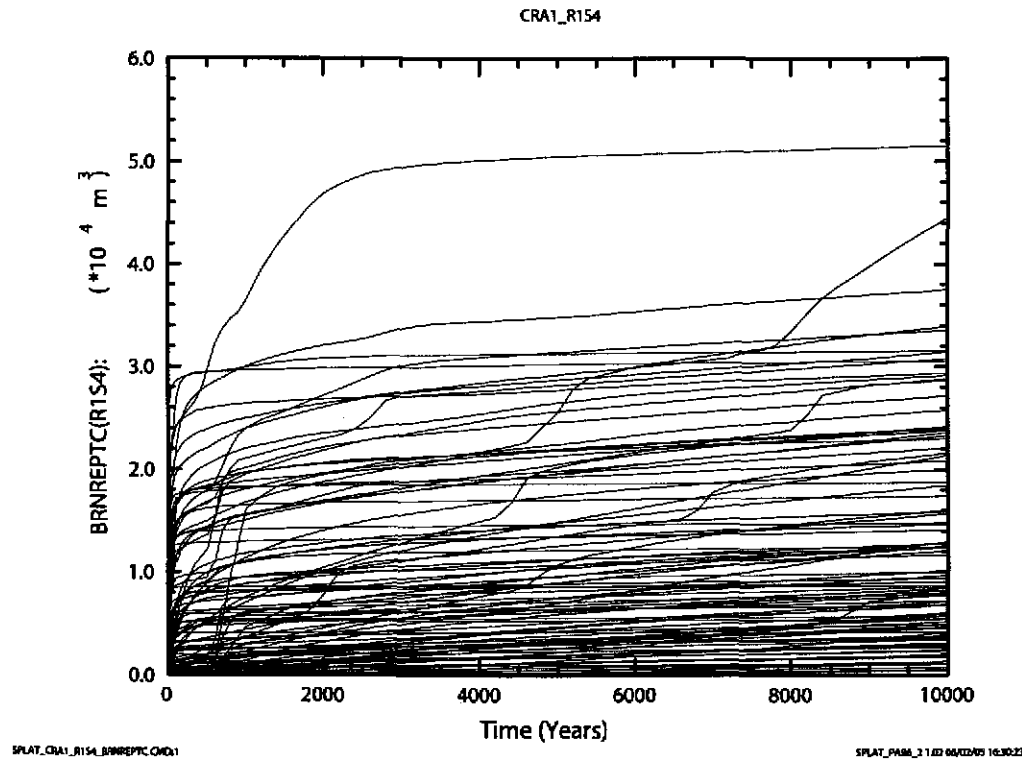
a) PABC

b) CRA1

Figure 6-32. Total cumulative inflow of brine (m³) into the repository versus time (years) for all 100 vectors in Replicate 1, Scenario S4.   Figure a) shows results from the CRA-2004 PABC.   Figure b) shows results from the CRA-2004.
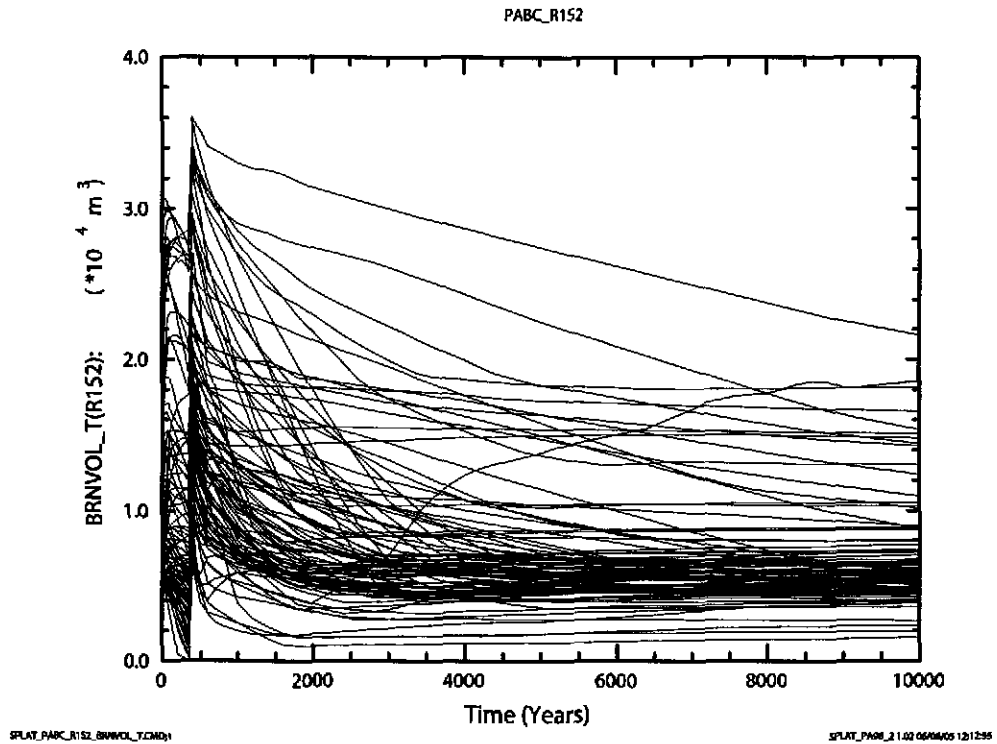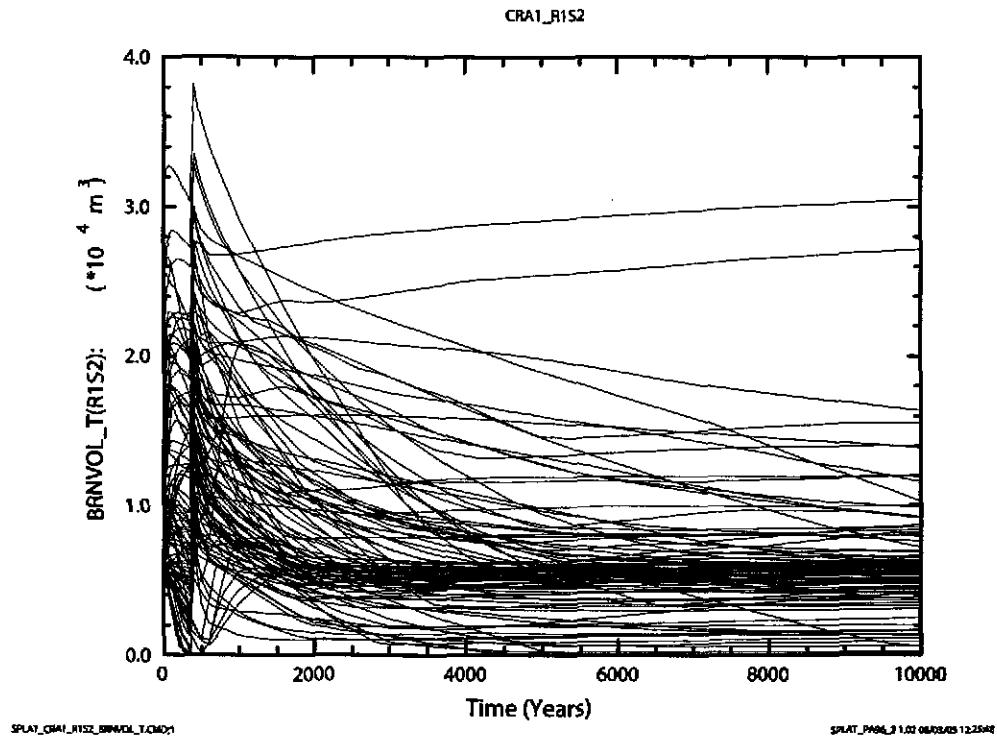
a) PABC

b) CRA1

Figure 6-33. Total volume (m³) of brine in the repository versus time (years) for all 100 vectors in Replicate 1, Scenario S2. Figure a) shows results from the CRA-2004 PABC. Figure b) shows results from the CRA-2004.
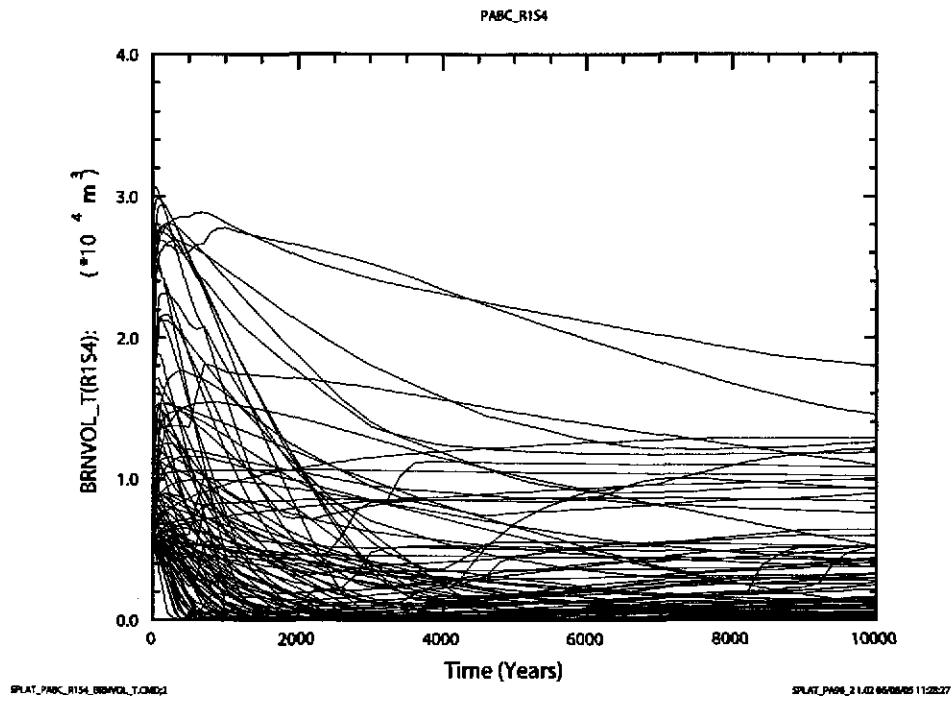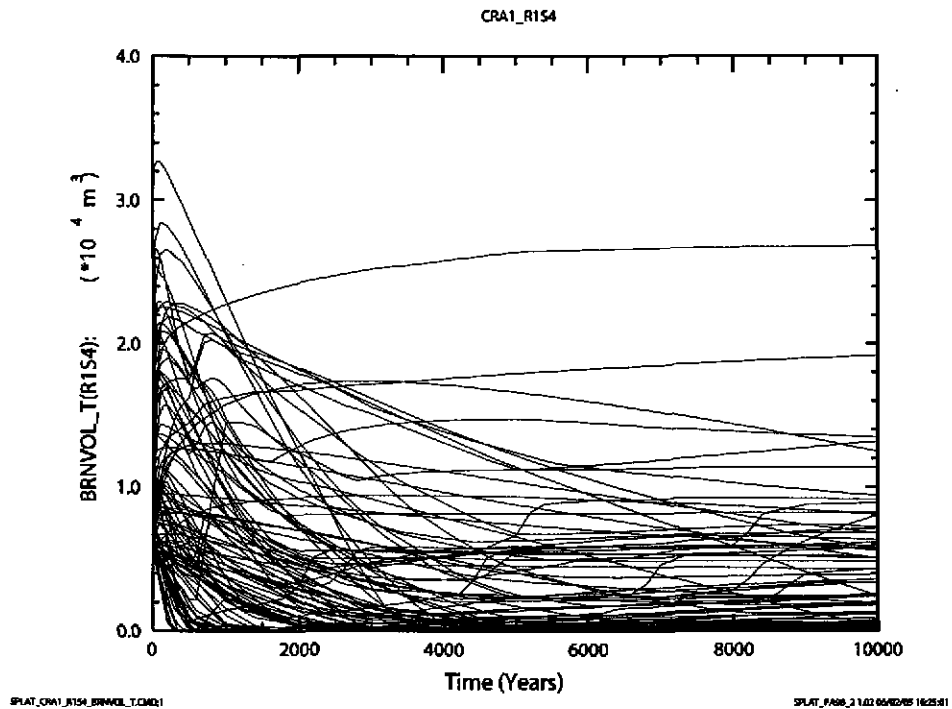
a) PABC

b) CRA1

Figure 6-34. Total volume (m³) of brine in the repository versus time (years) for all 100 vectors in Replicate 1, Scenario S4. Figure a) shows results from the CRA-2004 PABC. Figure b) shows results from the CRA-2004.

Information Only

SPLAT_PABC_R1S2_WAS_SATB.CMD;1   SPLAT_PABC_2 1.02 08/08/05 11:38:13

a) PABC

SPLAT_CRA1_R1S2_WAS_SATB.CMD;1   SPLAT_PABC_2 1.02 08/08/05 10:19:18
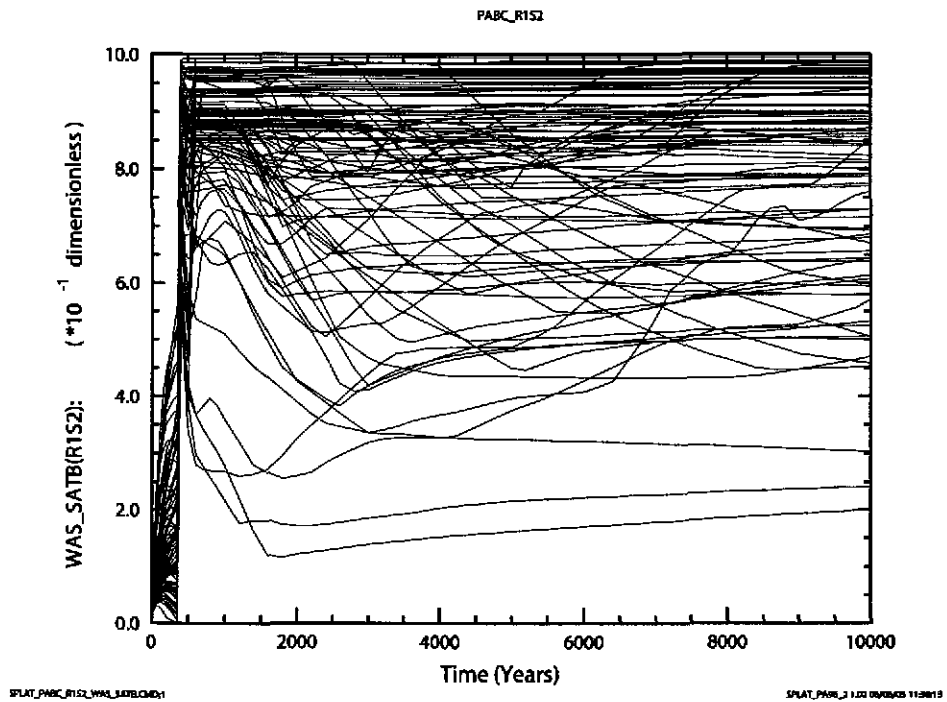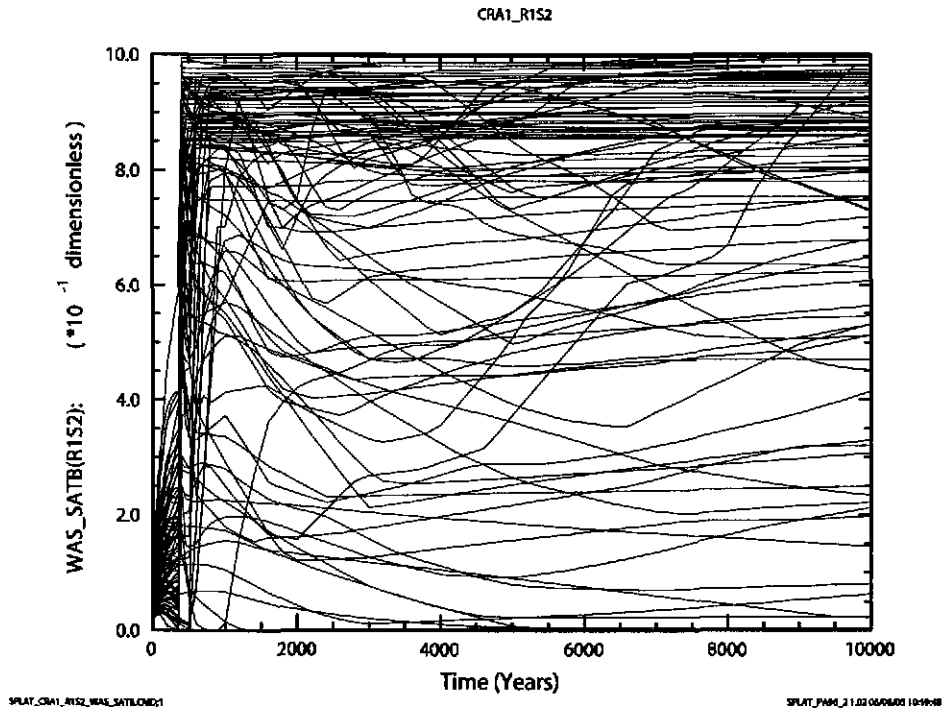
b) CRA1

Figure 6-35. Brine saturation (dimensionless) in the Waste Panel versus time (years) for all 100 vectors in Replicate 1, Scenario S2. Figure a) shows results from the CRA-2004 PABC. Figure b) shows results from the CRA-2004.

Information Only

SPLAT_PABC_R1S4_WAS_SATB.CMD:1   SPLAT_PA98_2 1.02 06/08/05 11:30:17

a)PABC

CRA1_R1S4

SPLAT_CRA1_R1S4_WAS_SATB.CMD:1   SPLAT_PA98_2 1.02 06/02/05 15:49:57

b) CRA1
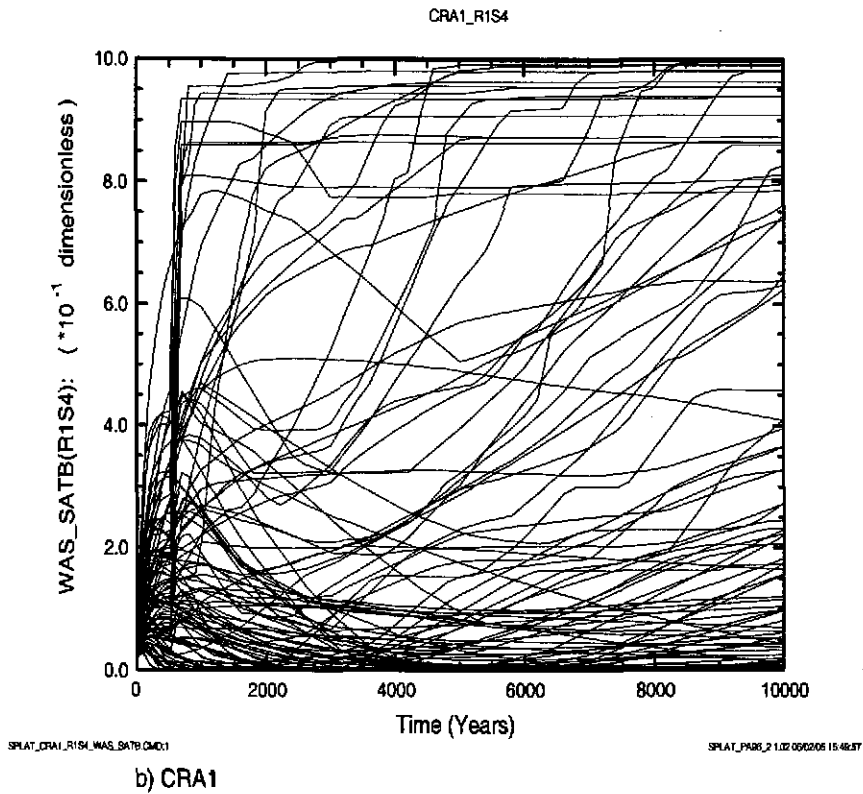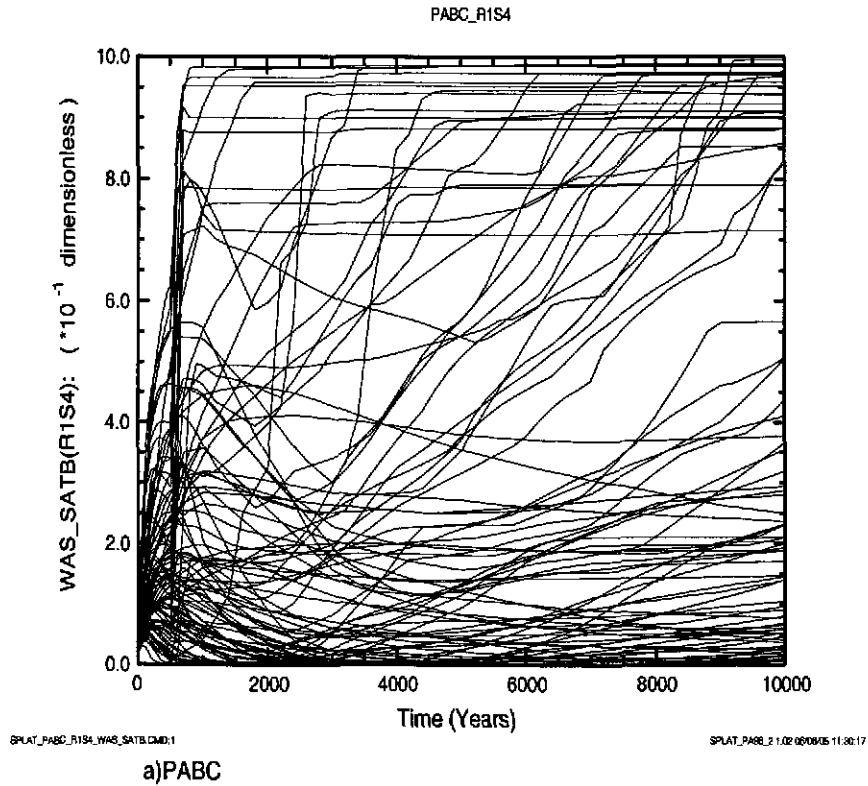
Figure 6-36. Brine saturation (dimensionless) in the waste panel versus time (years) for all 100 vectors in Replicate 1, Scenario S4. Figure a) shows results from the CRA-2004 PABC. Figure b) shows results from the CRA-2004.

PCCSRC_S2.INP;3

PCCSRC_PA96 2.21 06/08/05 10:19
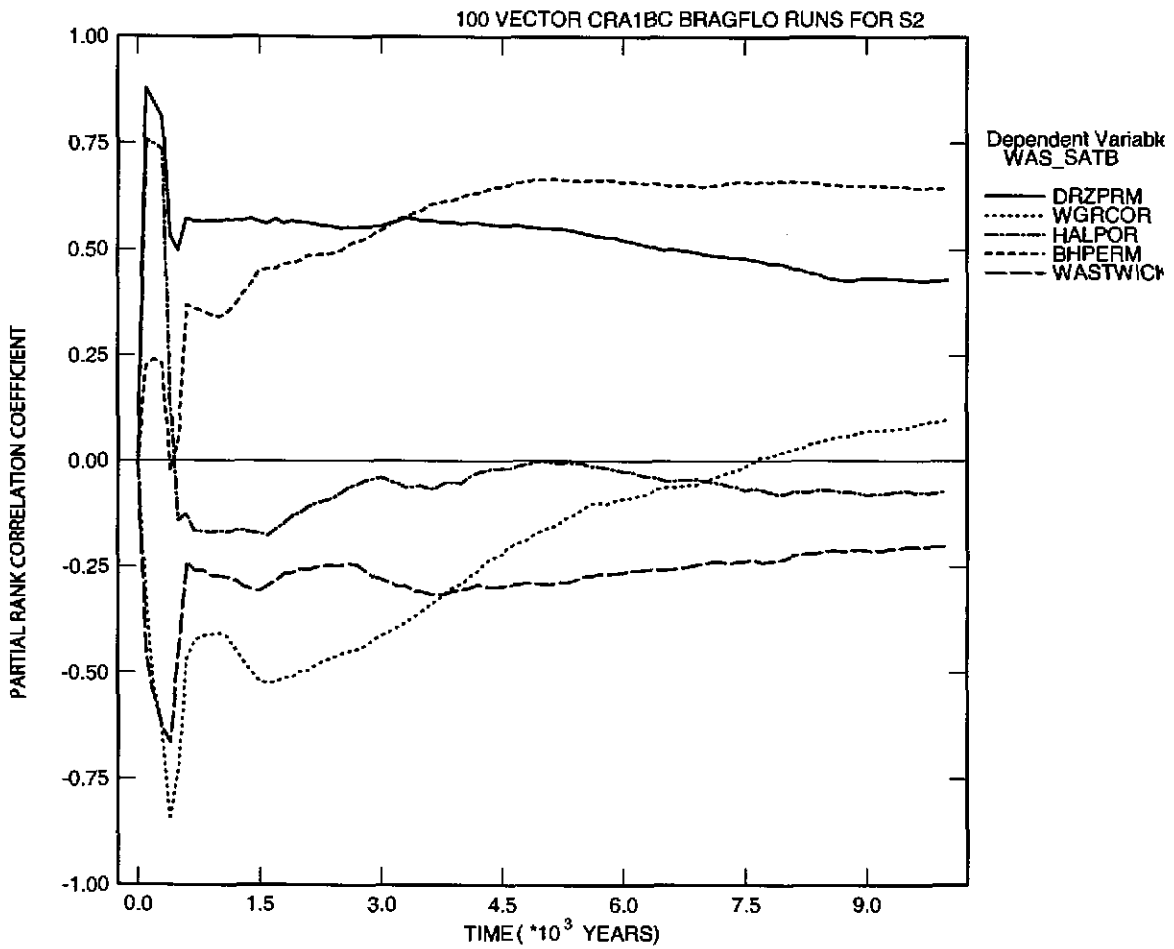
Figure 6-37. Primary correlations of brine saturation (dimensionless) in the Waste Panel with input parameters versus time (years) from the CRA-2004 PABC, Replicate 1, Scenario S2. Table 4-2 gives a description of the names in the legend.
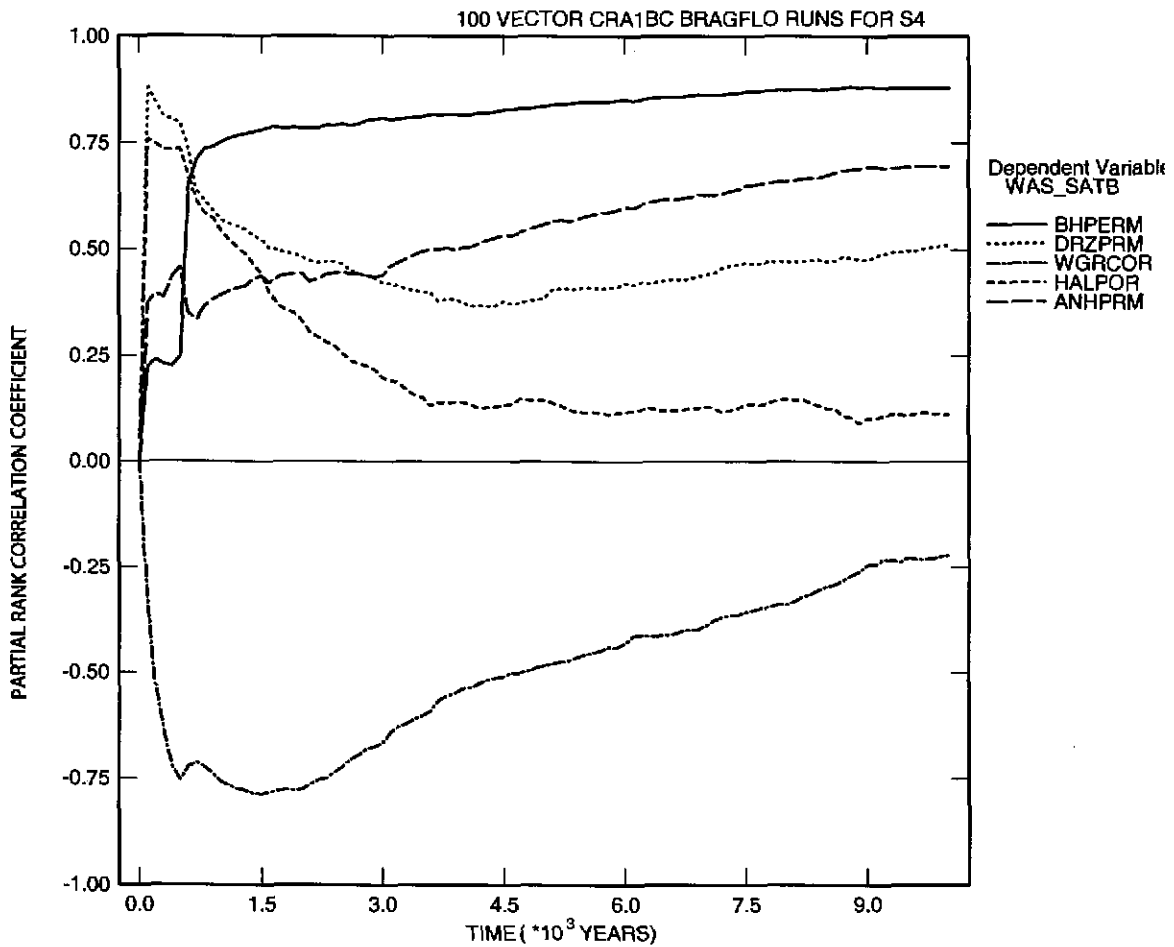
PCCSRC_S4.INP;2

PCCSRC_PA96 2.21 06/08/05 10:23

Figure 6-38. Primary correlations of brine saturation (dimensionless) in the waste panel with input parameters versus time (years) from the CRA-2004 PABC, Replicate 1, Scenario S4. Table 4-2 gives a description of the names in the legend.
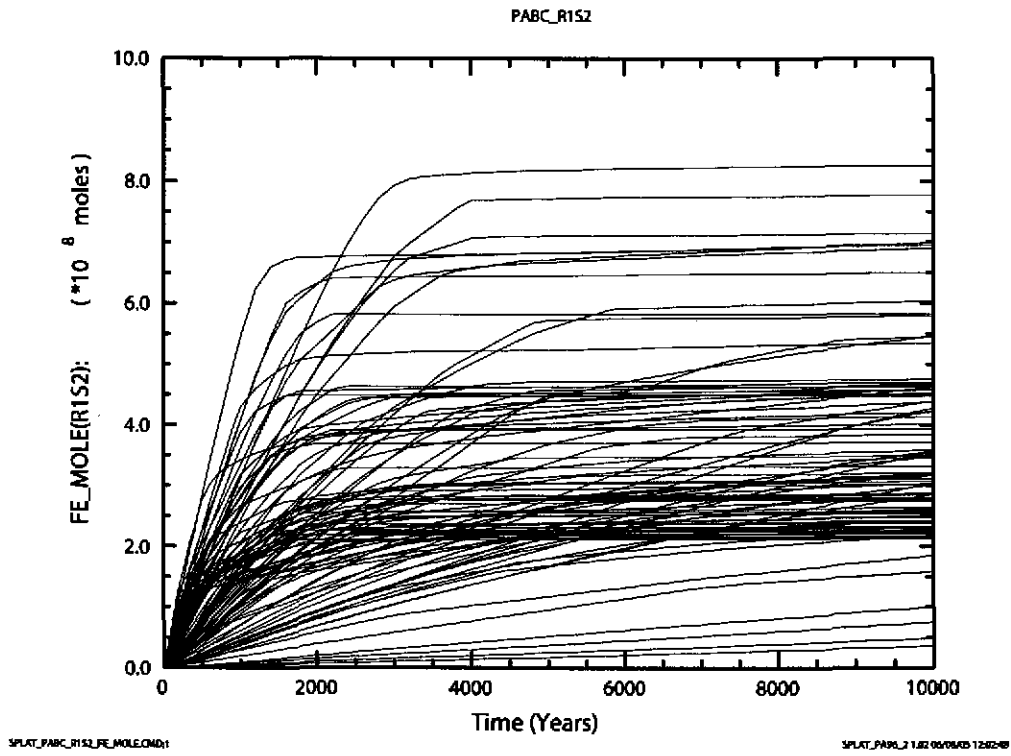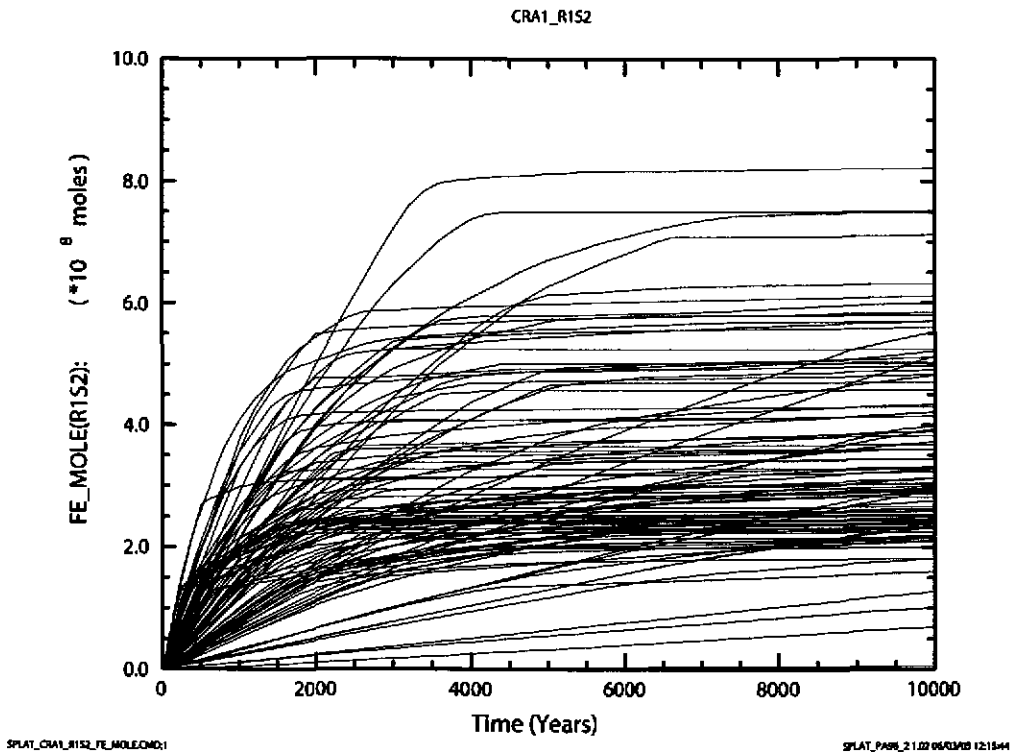
a) PABC

b) CRA1

Figure 6-39. Cumulative moles of gas (moles) produced by iron corrosion versus time (years) for all 100 vectors in Replicate 1, Scenario S2. Figure a) shows results from the CRA-2004 PABC. Figure b) shows results from the CRA-2004.
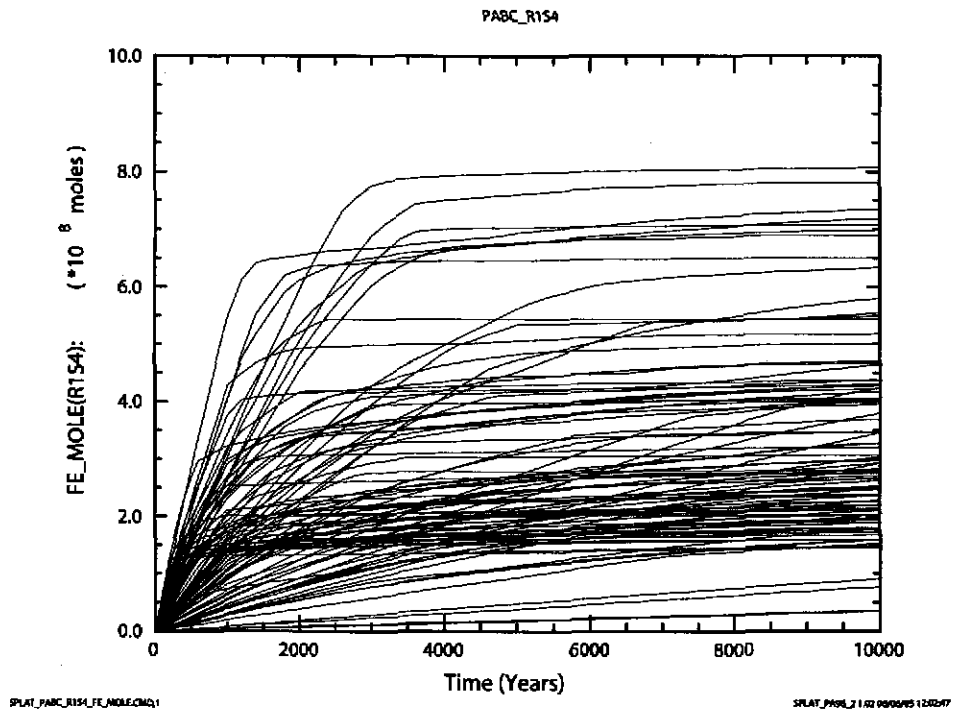
a) PABC
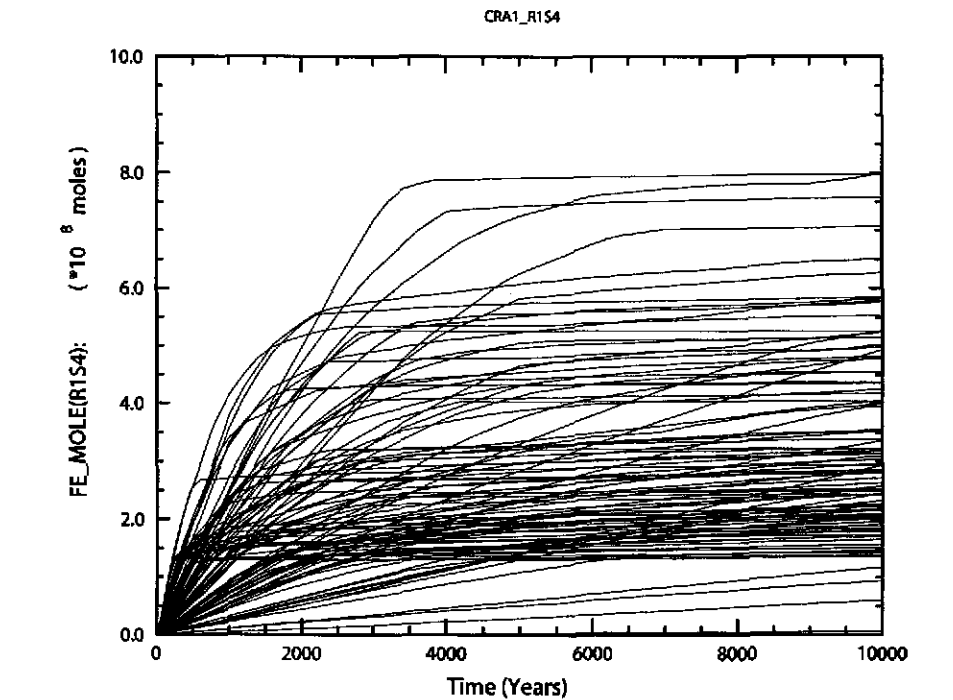
b) CRA1

Figure 6-40. Cumulative moles of gas (moles) produced by iron corrosion versus time (years) for all 100 vectors in Replicate 1, Scenario S4. Figure a) shows results from the CRA-2004 PABC. Figure b) shows results from the CRA-2004.

PCCSRC_S2.INP;3

PCCSRC_PA96 2.21 06/08/05 10:19
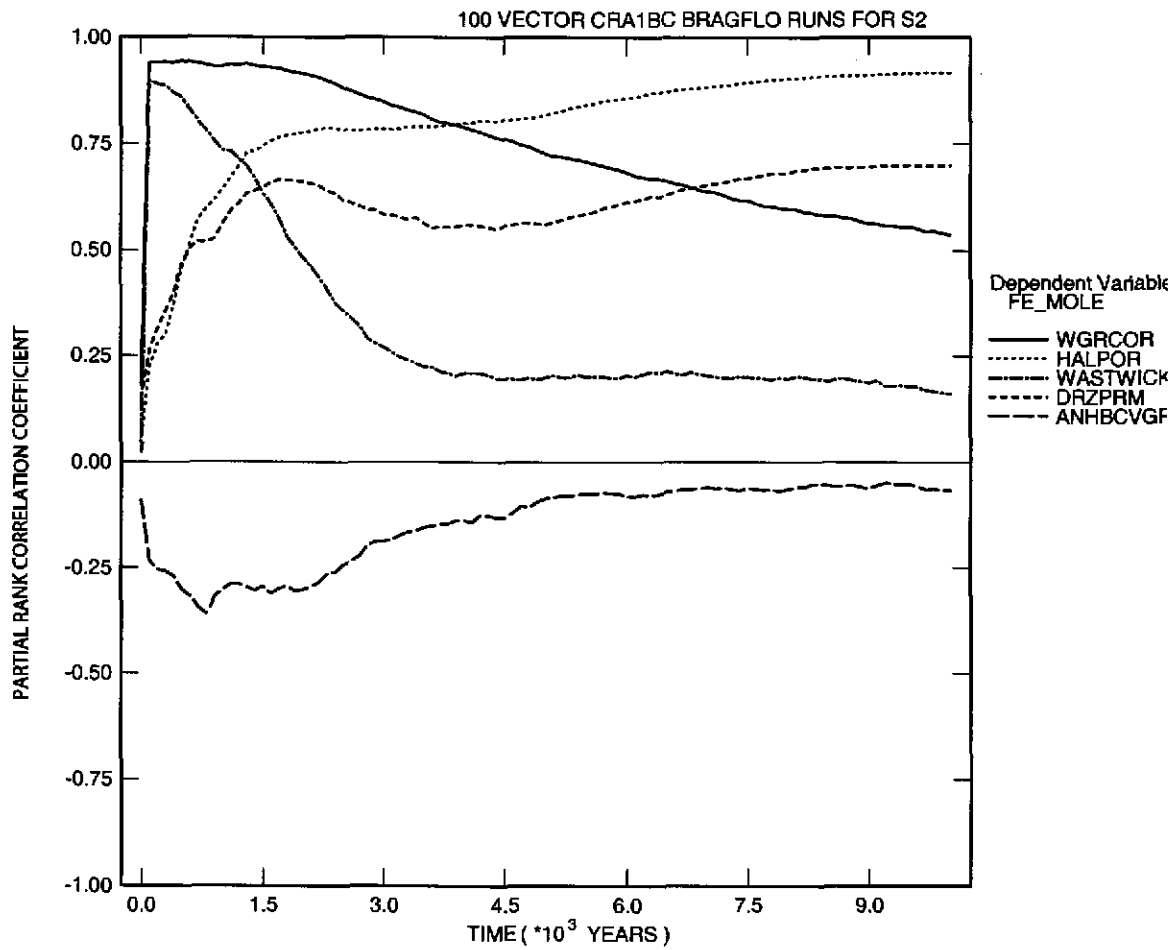
Figure 6-41. Primary correlations of cumulative amount (moles) of gas produced by iron corrosion in the waste panel with input parameters versus time (years) from the CRA-2004 PABC, Replicate 1, Scenario S2. Table 4-2 gives a description of the names in the legend.

PCCSRC_S4.INP;2   PCCSRC_PA96 2.21 06/08/05 10:23
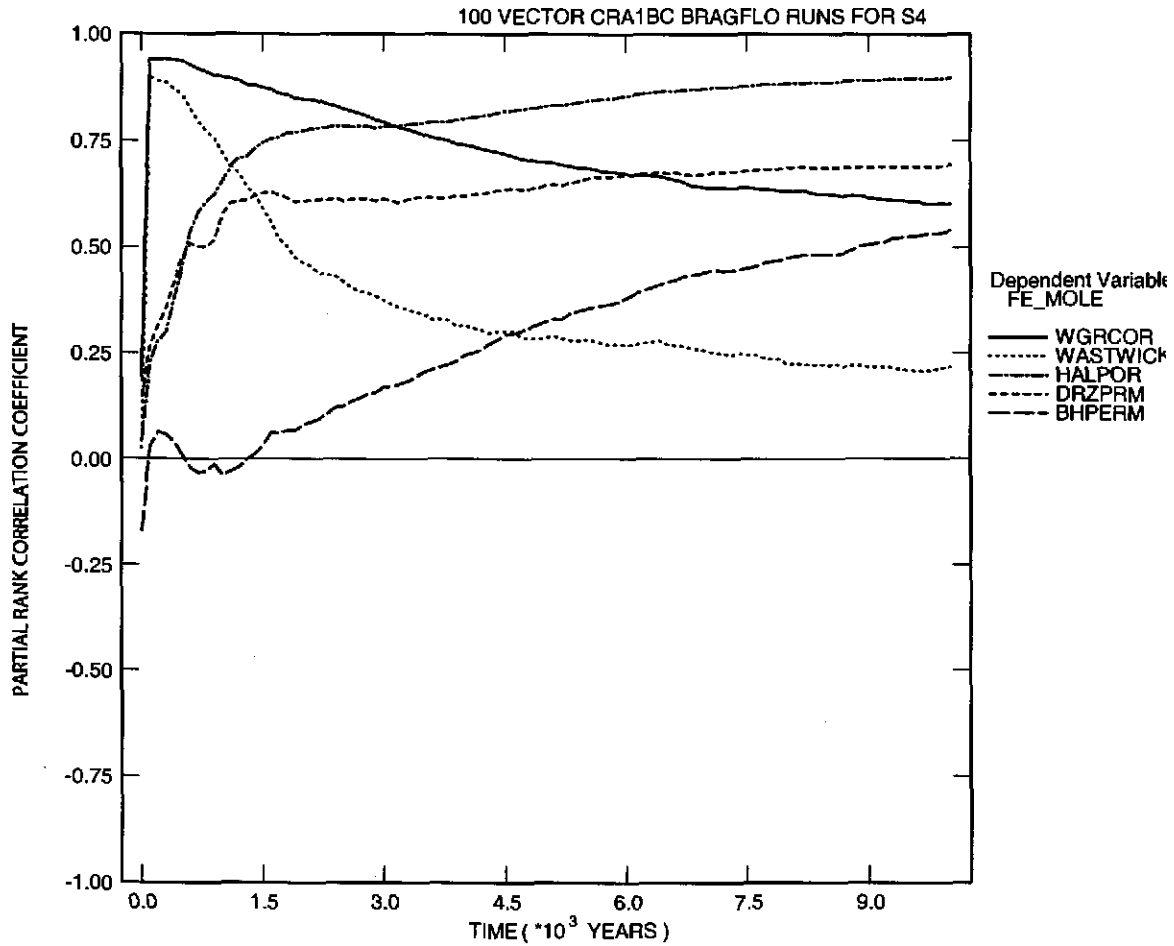
Figure 6-42. Primary correlations of cumulative amount (moles) of gas produced by iron corrosion in the waste panel with input parameters versus time (years) from the CRA-2004 PABC, Replicate 1, Scenario S4. Table 4-2 gives a description of the names in the legend.
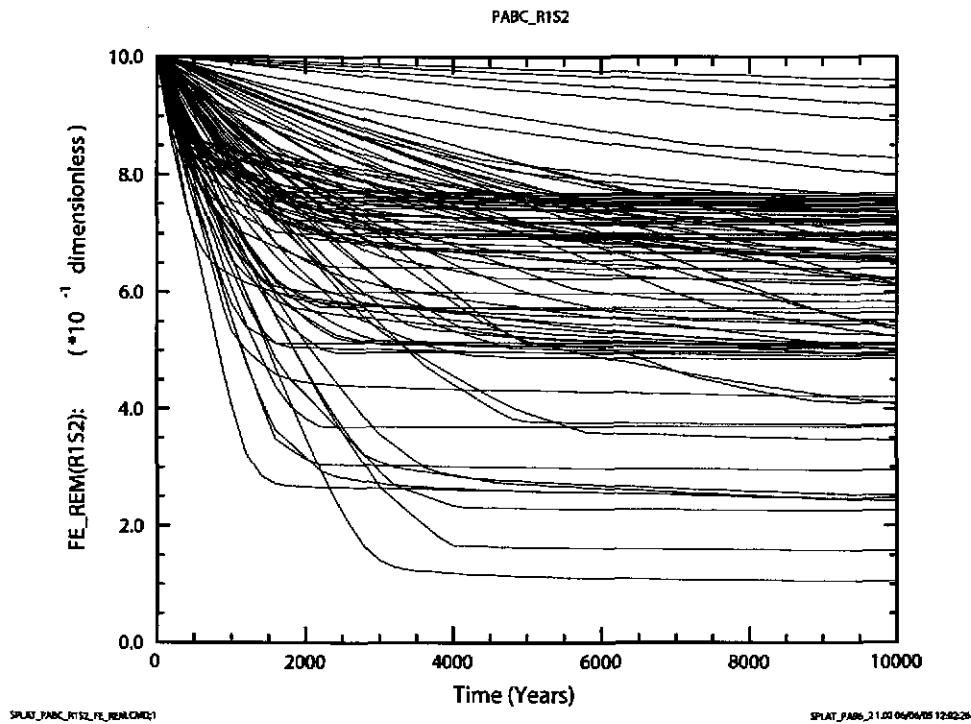
a) PABC
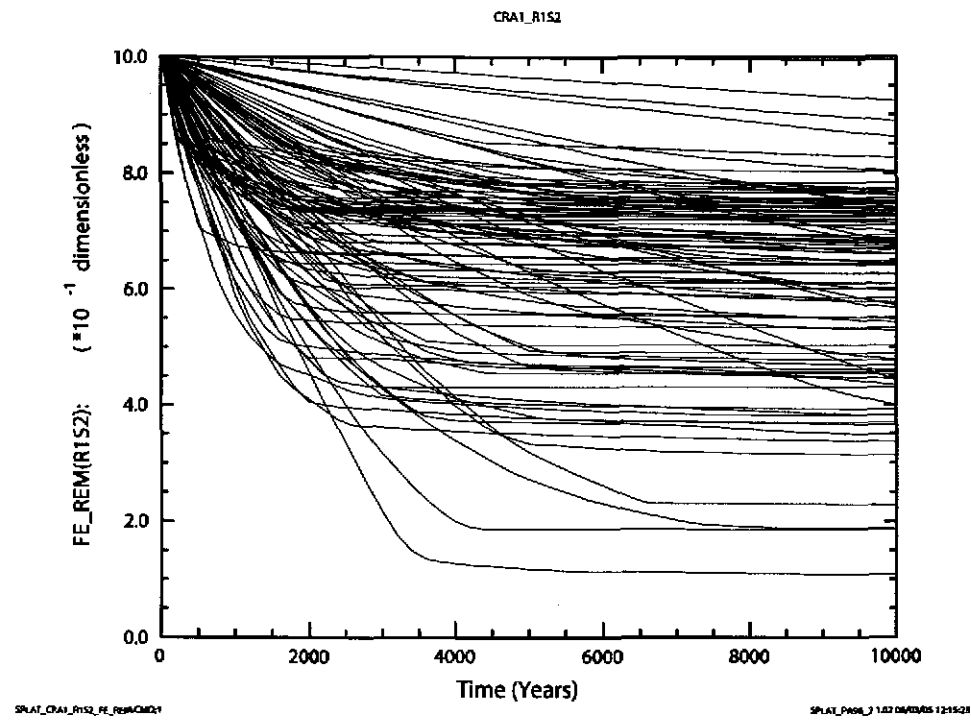
b) CRA1

Figure 6-43. Fraction of iron (dimensionless) remaining versus time (years) for all 100 vectors in Replicate 1, Scenario S2. Figure a) shows results from the CRA-2004 PABC. Figure b) shows results from the CRA-2004.

PABC_R1S4

SPLAT_PABC_R1S4_FE_REM.CMD:1   SPLAT_PA96_2 1.02 06/06/01 12:02:25

a) PABC

CRA1_R1S4

SPLAT_CRA1_R1S4_FE_REM.CMD:1   SPLAT_PA96_2 1.02 06/02/03 14:16:50

b) CRA1
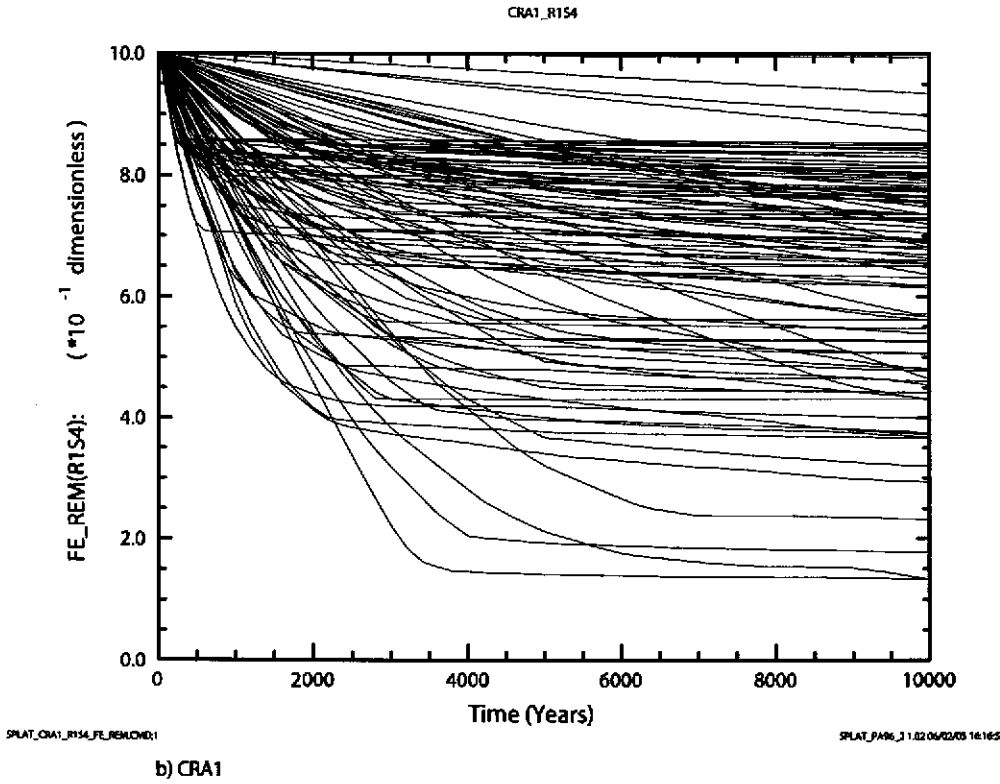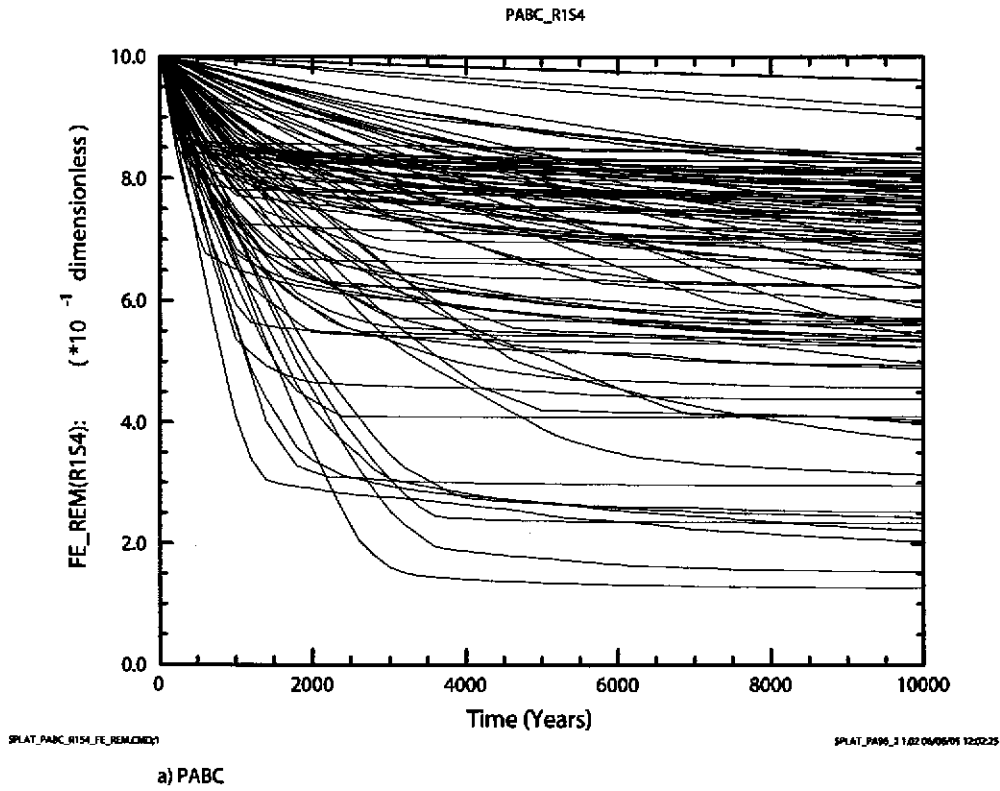
Figure 6-44. Fraction of iron (dimensionless) remaining versus time (years) for all 100 vectors in Replicate 1, Scenario S4. Figure a) shows results from the CRA-2004 PABC. Figure b) shows results from the CRA-2004.
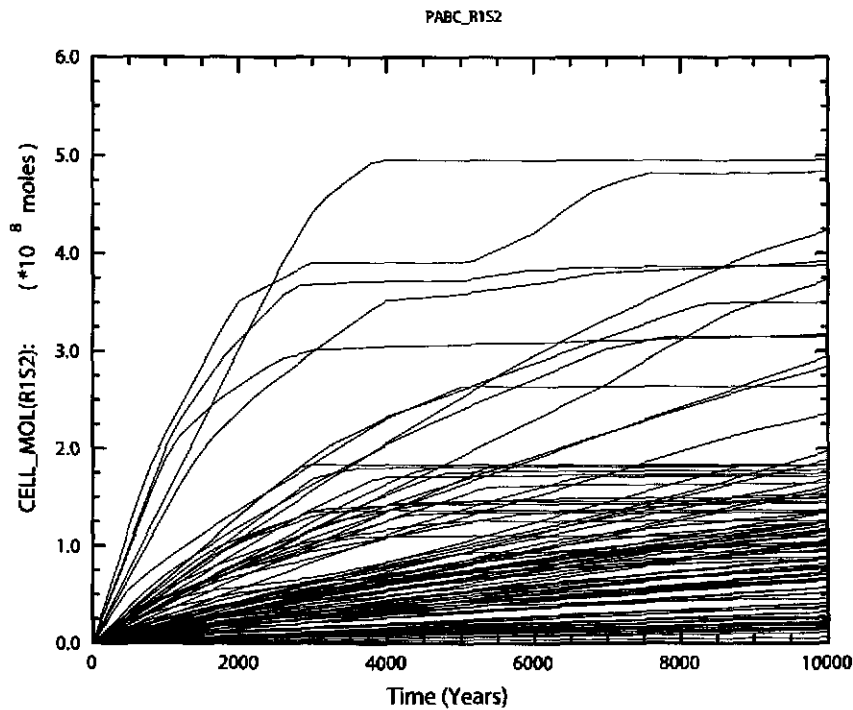
a) PABC
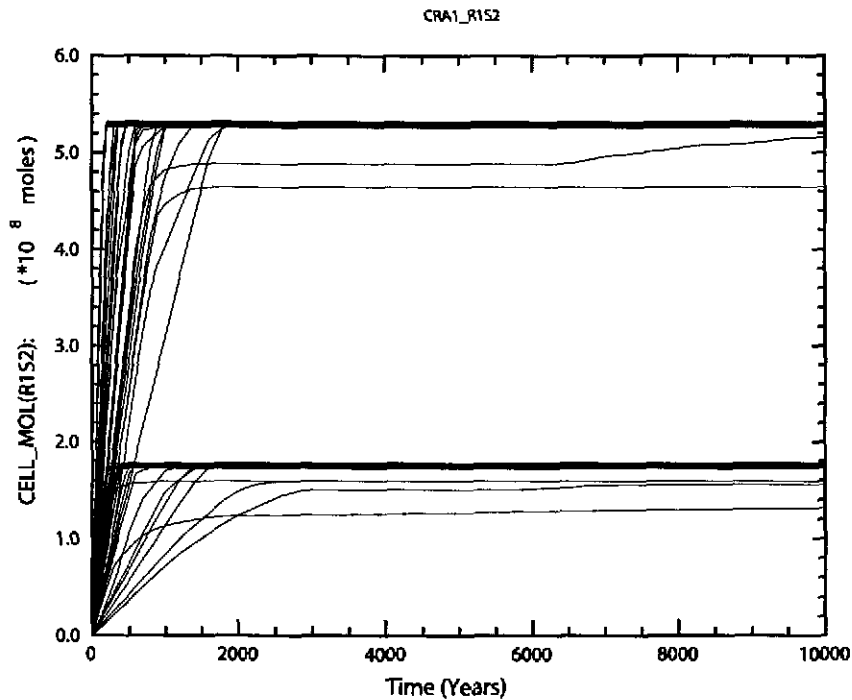
CRA1_R1S2

b) CRA1

Figure 6-45. Cumulative amount of gas (moles) produced by microbial gas generation versus time (years) for all 100 vectors in Replicate 1, Scenario S2. Figure a) shows results from the CRA-2004 PABC. Figure b) shows results from the CRA-2004.
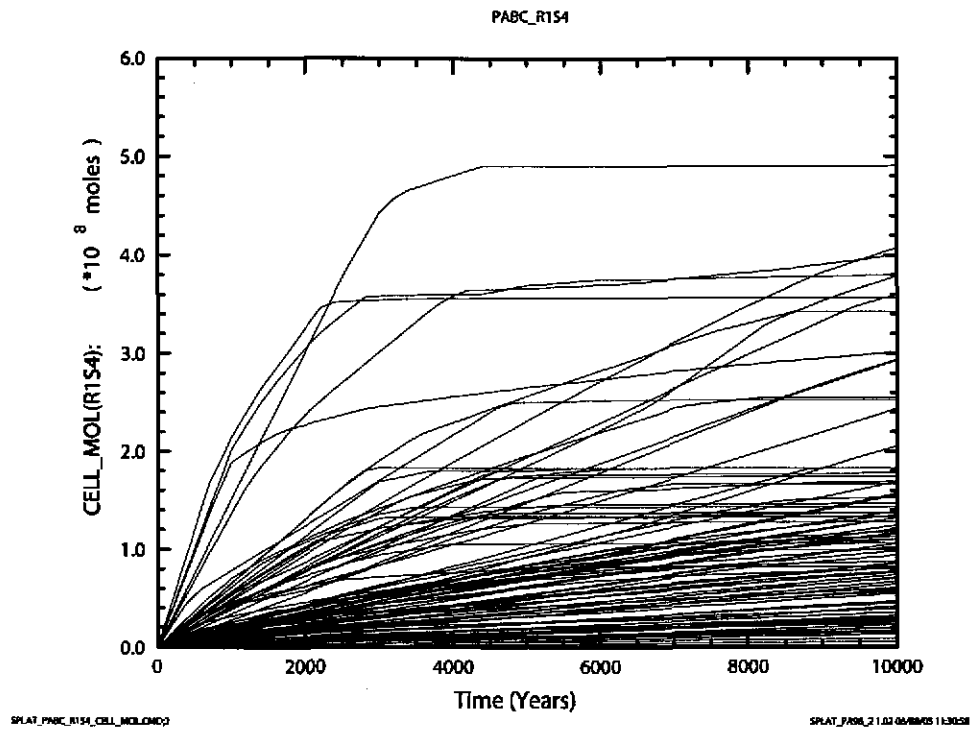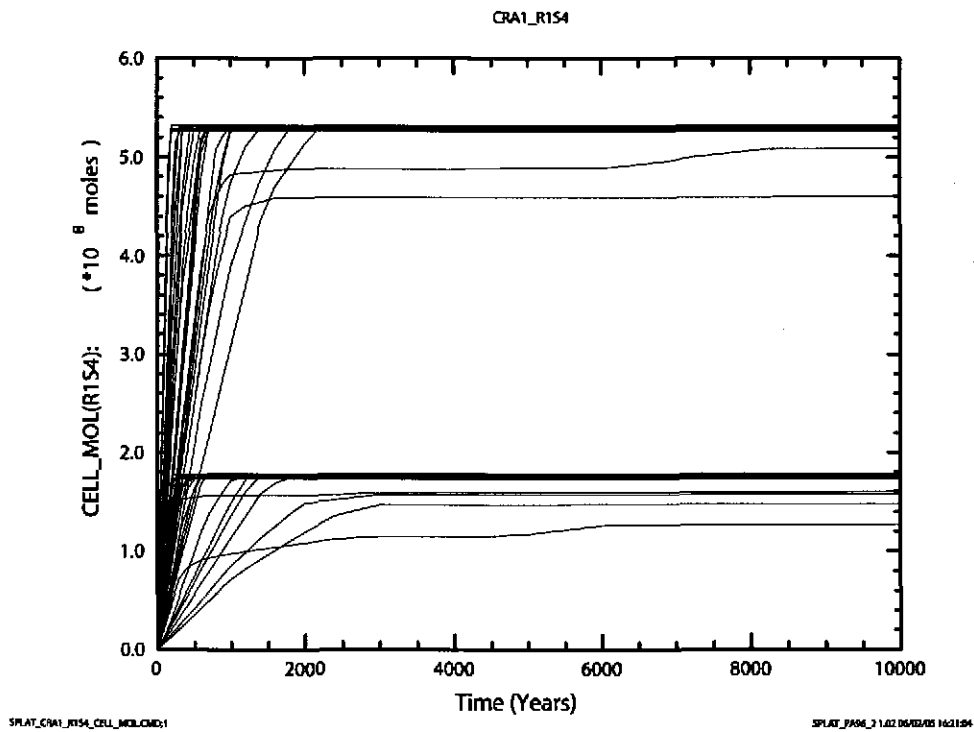
Figure 6-46. Cumulative amount of gas (moles) produced by microbial gas generation versus time (years) for all 100 vectors in Replicate 1, Scenario S4. Figure a) shows results from the CRA-2004 PABC. Figure b) shows results from the CRA-2004.
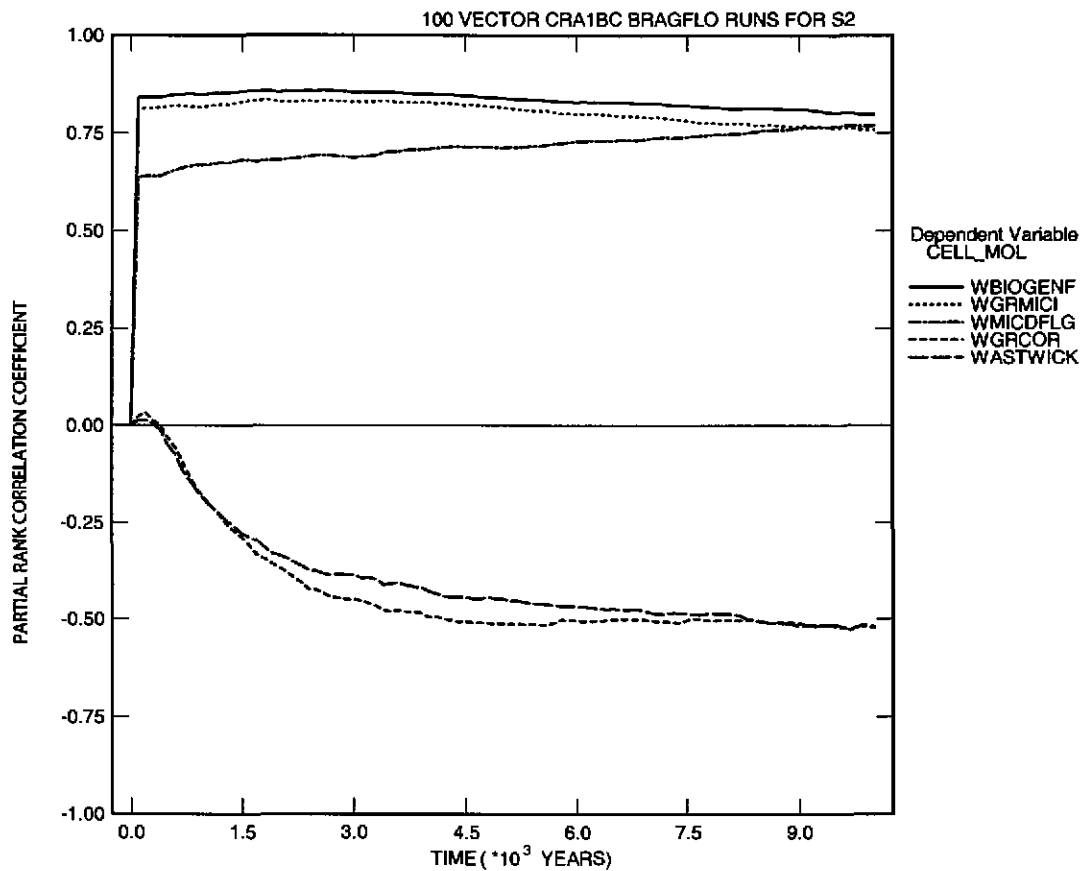
Figure 6-47. Primary correlations of cumulative amount (moles) of gas produced by microbial gas generation in the waste panel with input parameters versus time (years) from the CRA-2004 PABC, Replicate 1, Scenario S2. Table 4-2 gives a description of the names in the legend.
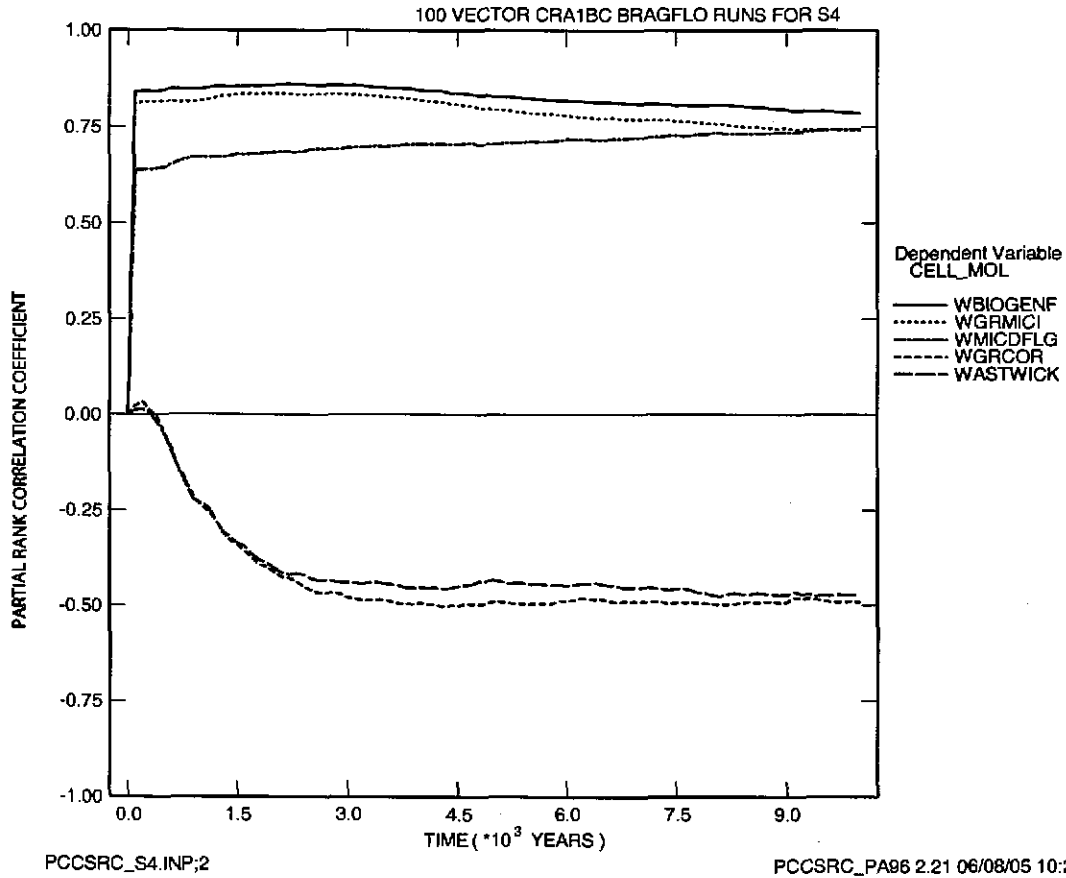
Figure 6-48. Primary correlations of cumulative amount (moles) of gas produced by microbial gas generation in the Waste Panel with input parameters versus time (years) from the CRA-2004 PABC, Replicate 1, Scenario S2. Table 4-2 gives a description of the names in the legend.

a) PABC

b) CRA1
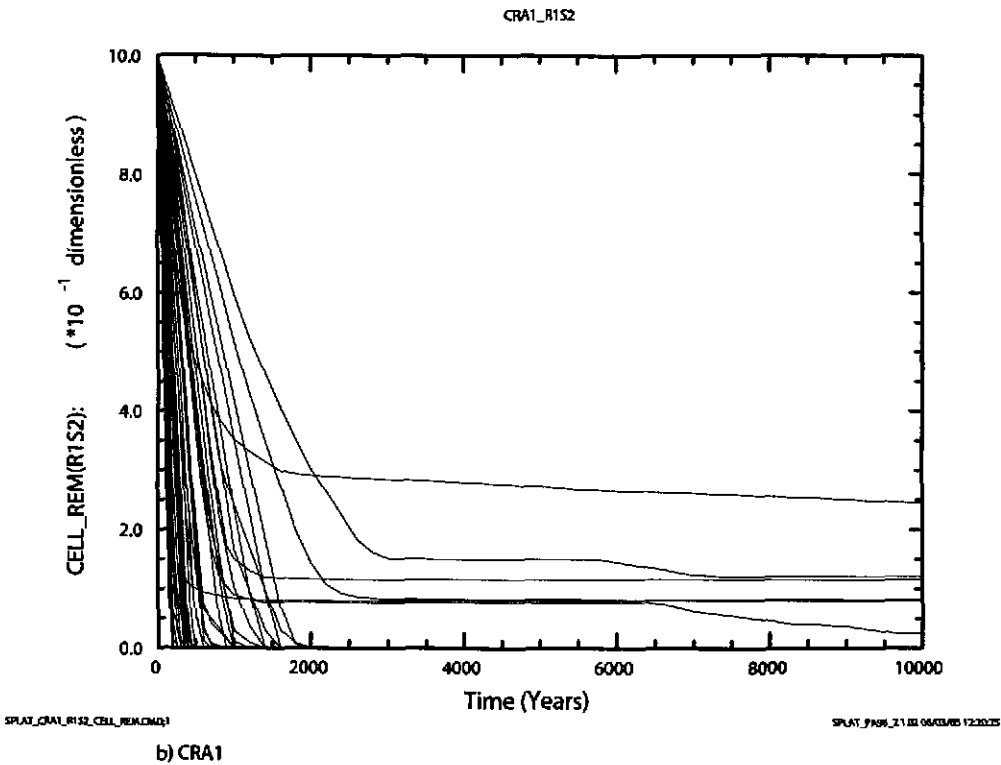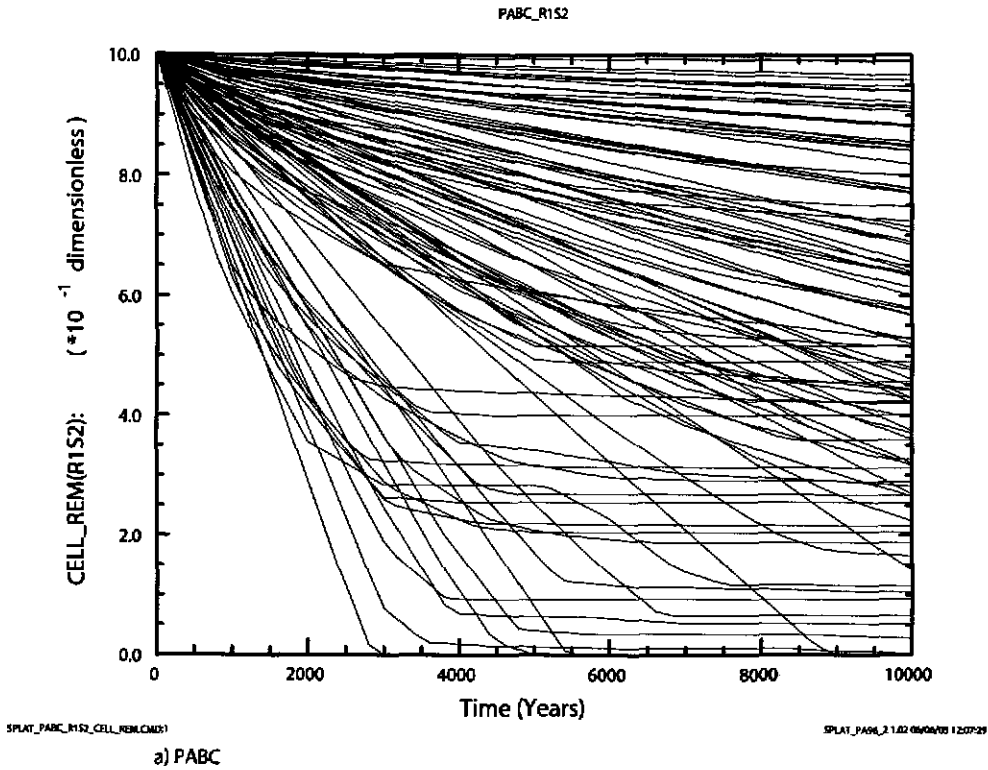
Figure 6-49. Fraction of cellulosics (dimensionless) remaining versus time (years) for all 100 vectors in Replicate 1, Scenario S2. Fraction of cellulosics is either cellulose or CPR depending on the value of WAS_AREA:PROBDEG (see §5.4). Figure a) shows results from the CRA-2004 PABC. Figure b) shows results from the CRA-2004.

a) PABC

b) CRA1
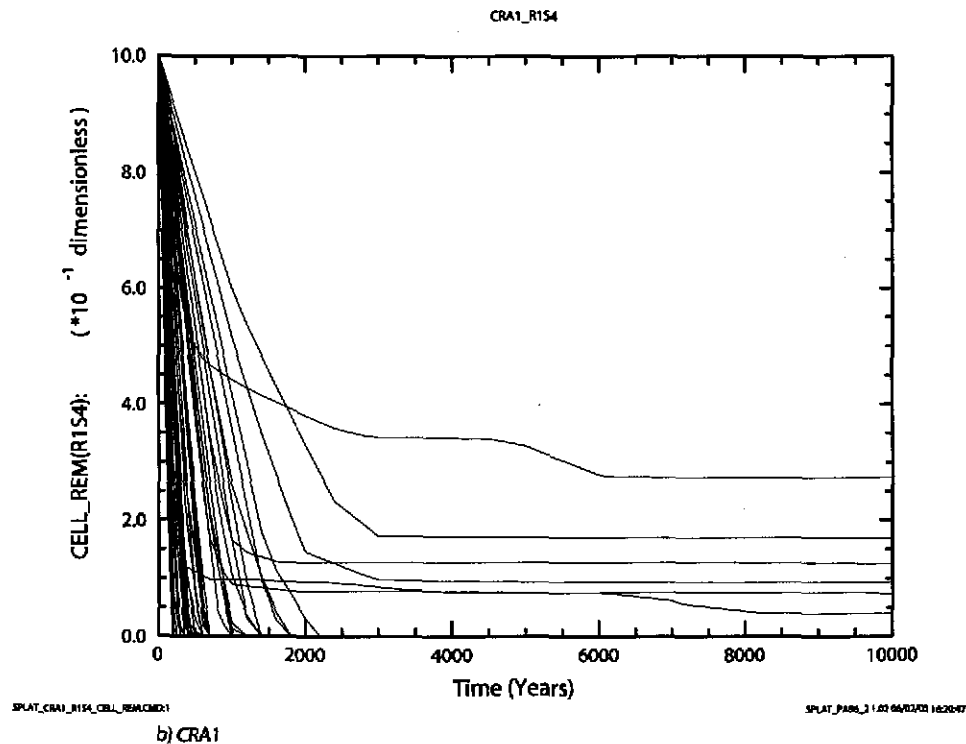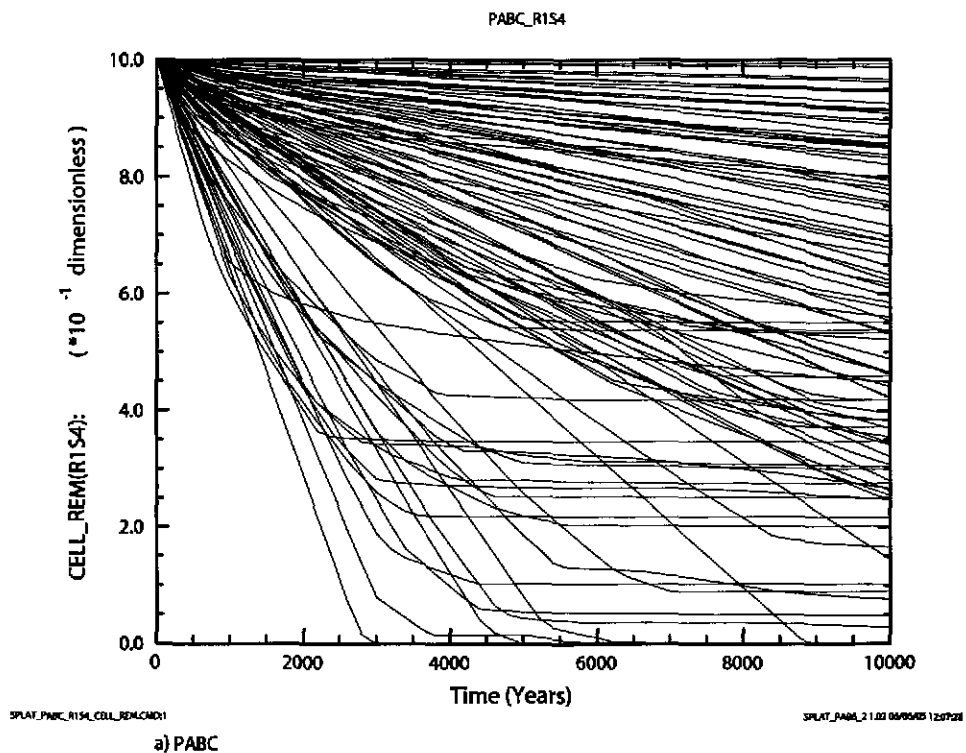
Figure 6-50. Fraction of cellulosics (dimensionless) remaining versus time (years) for all 100 vectors in Replicate 1, Scenario S4. Fraction of cellulosics is either cellulose or CPR depending on the value of WAS_AREA:PROBDEG (§5.4). Figure a) shows results from the CRA-2004 PABC. Figure b) shows results from the CRA-2004.
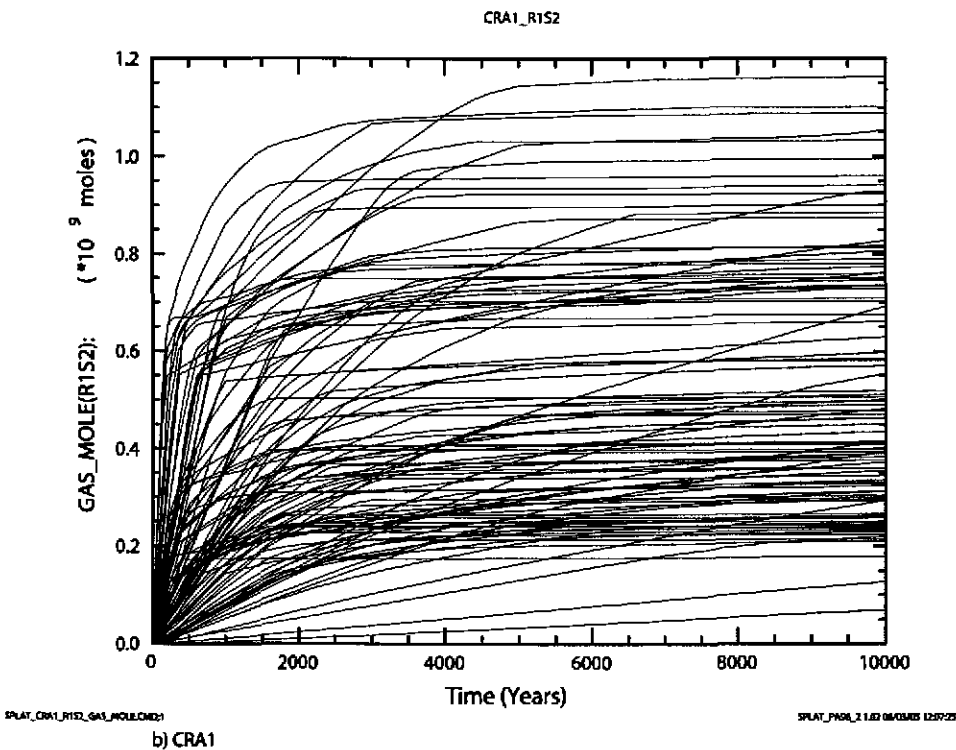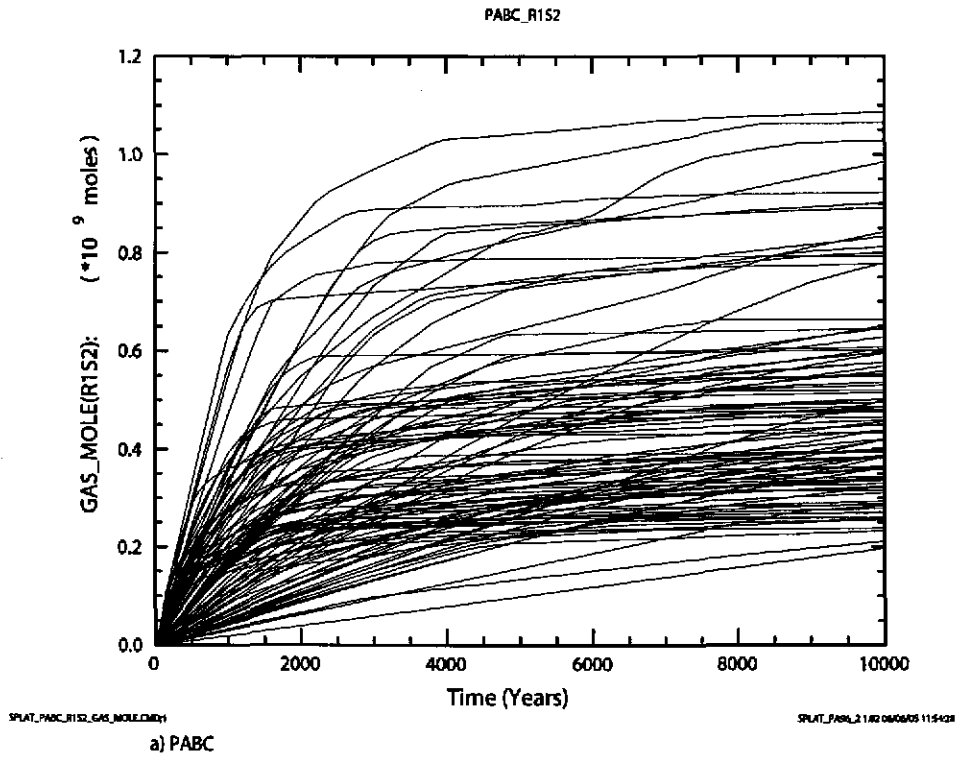
Figure 6-51. Total cumulative amount of gas (moles) generated versus time (years) for all 100 vectors in Replicate 1, Scenario S2. Figure a) shows results from the CRA-2004 PABC. Figure b) shows results from the CRA-2004.
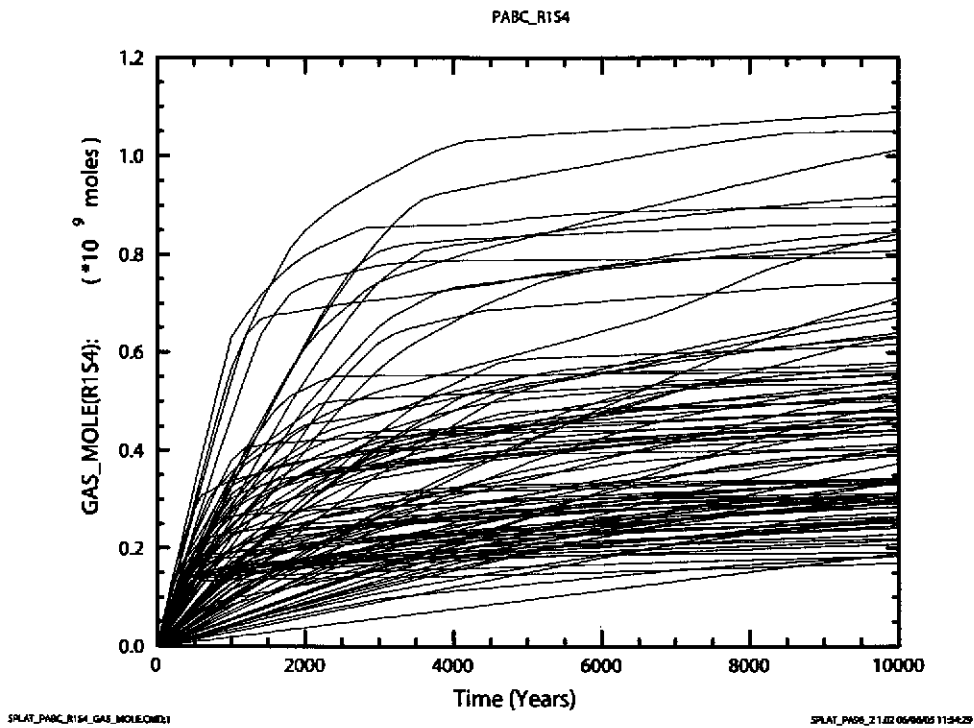
a) PABC
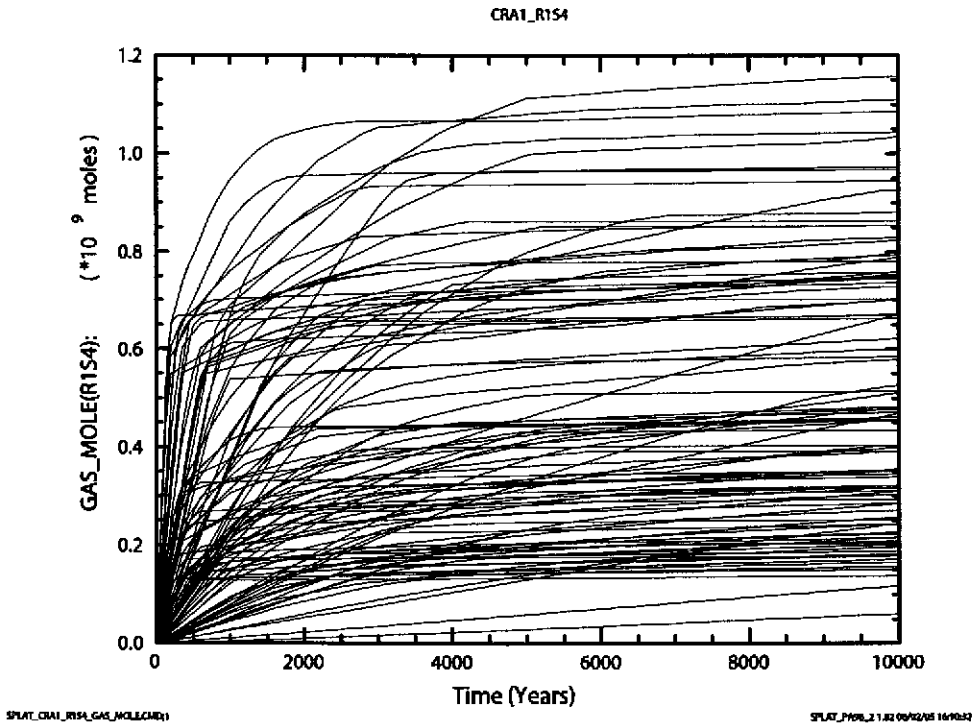
b) CRA1

Figure 6-52. Total cumulative amount of gas (moles) generated versus time (years) for all 100 vectors in Replicate 1, Scenario S4. Figure a) shows results from the CRA-2004 PABC. Figure b) shows results from the CRA-2004.
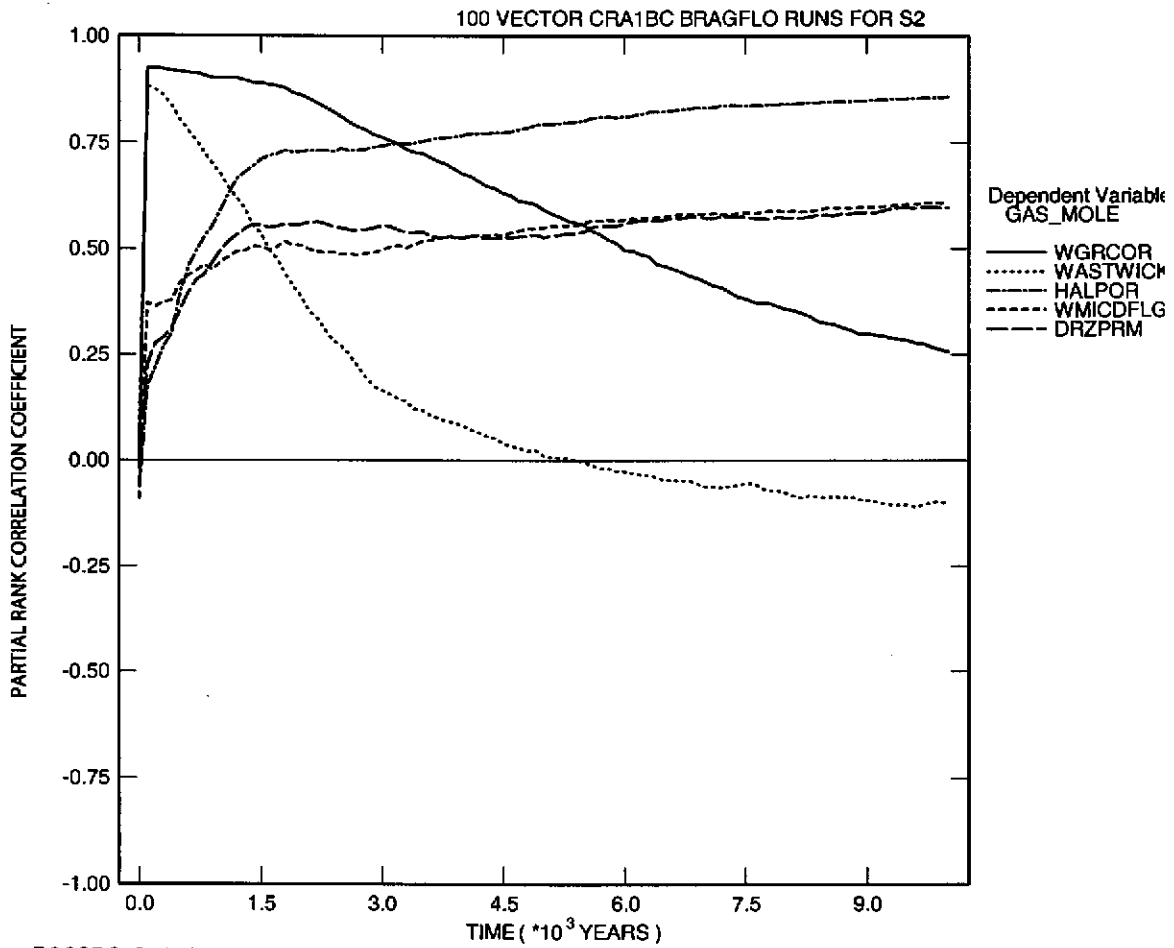
Figure 6-53. Primary correlations of cumulative amount (moles) of gas produced in the waste panel with input parameters, versus time (years) from the CRA-2004 PABC Replicate 1, Scenario S2. Table 4-2 gives a description of the names in the legend.
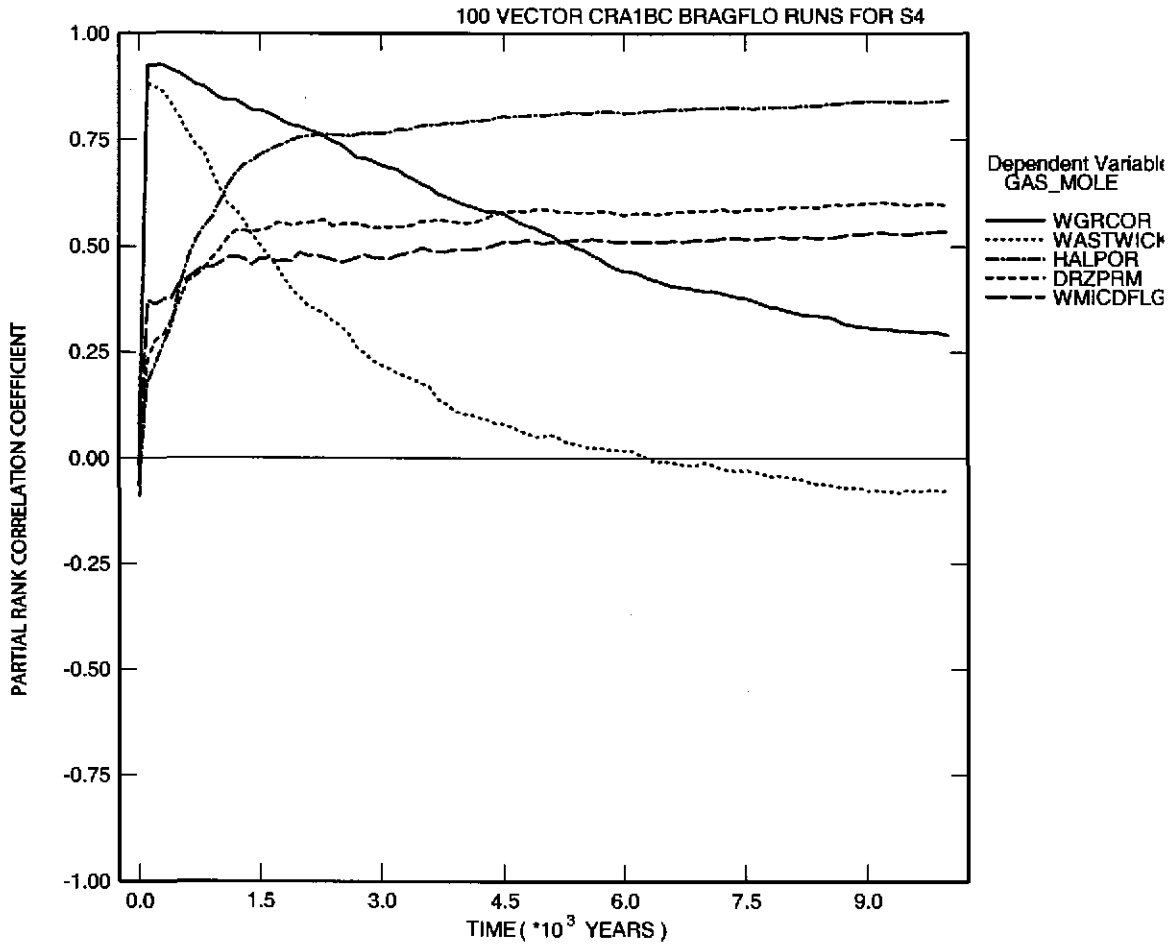
Figure 6-54. Primary correlations of cumulative amount (moles) of gas produced in the Waste Panel with input parameters, versus time (years) from the CRA-2004 PABC Replicate 1, Scenario S4. Table 4-2 gives a description of the names in the legend.

a) PABC

b) CRA1
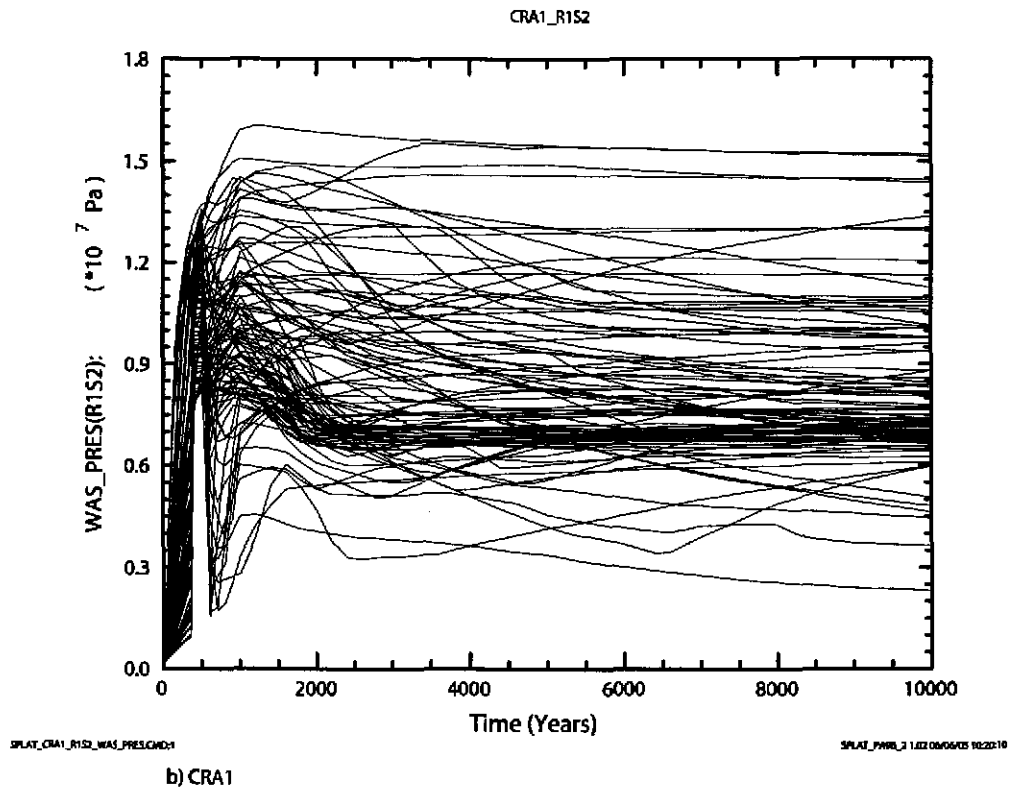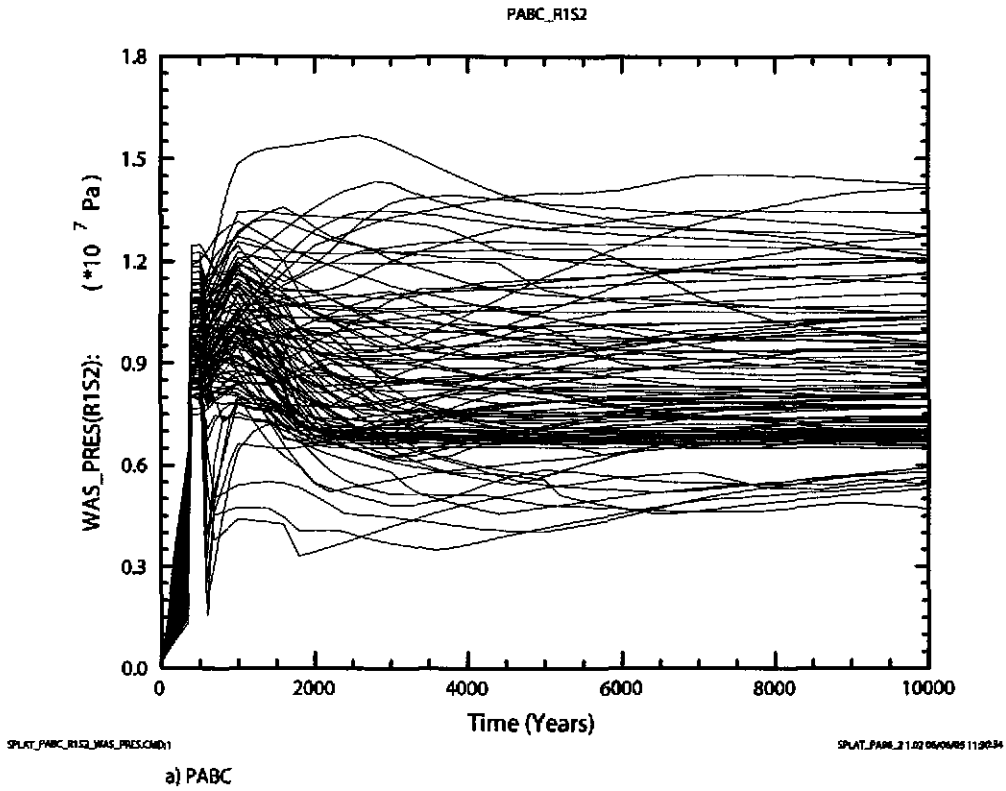
Figure 6-55. Volume averaged pressure (Pa) in the waste area versus time (years) for all 100 vectors in Replicate 1, Scenario S2. Figure a) shows results from the CRA-2004 PABC. Figure b) shows results from the CRA-2004.

a) PABC

b) CRA1
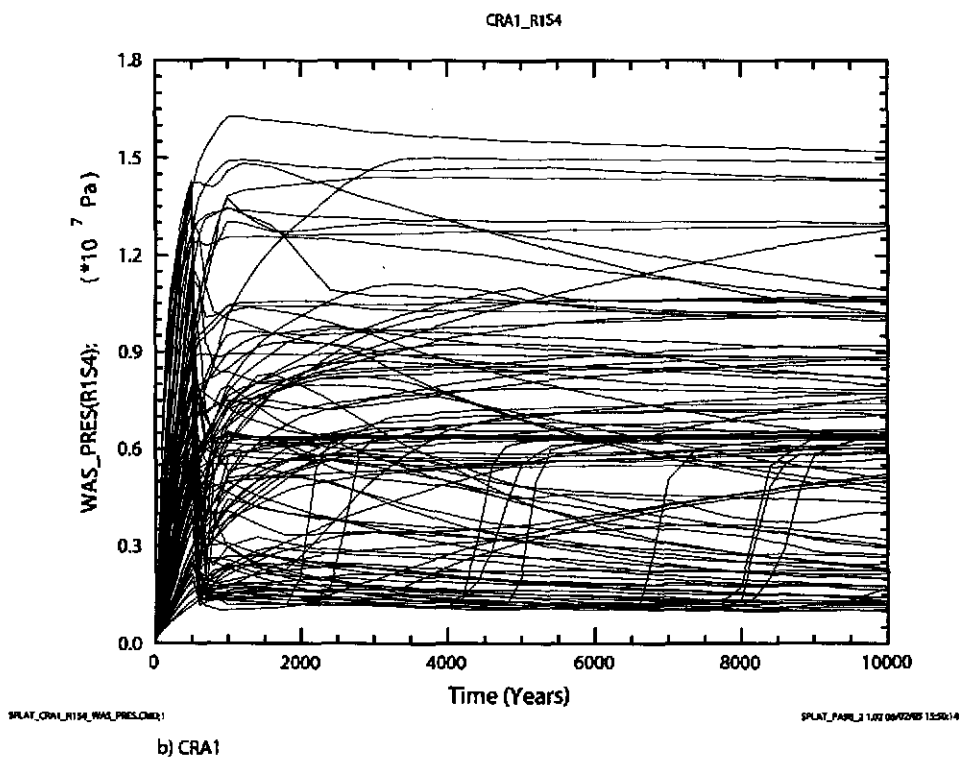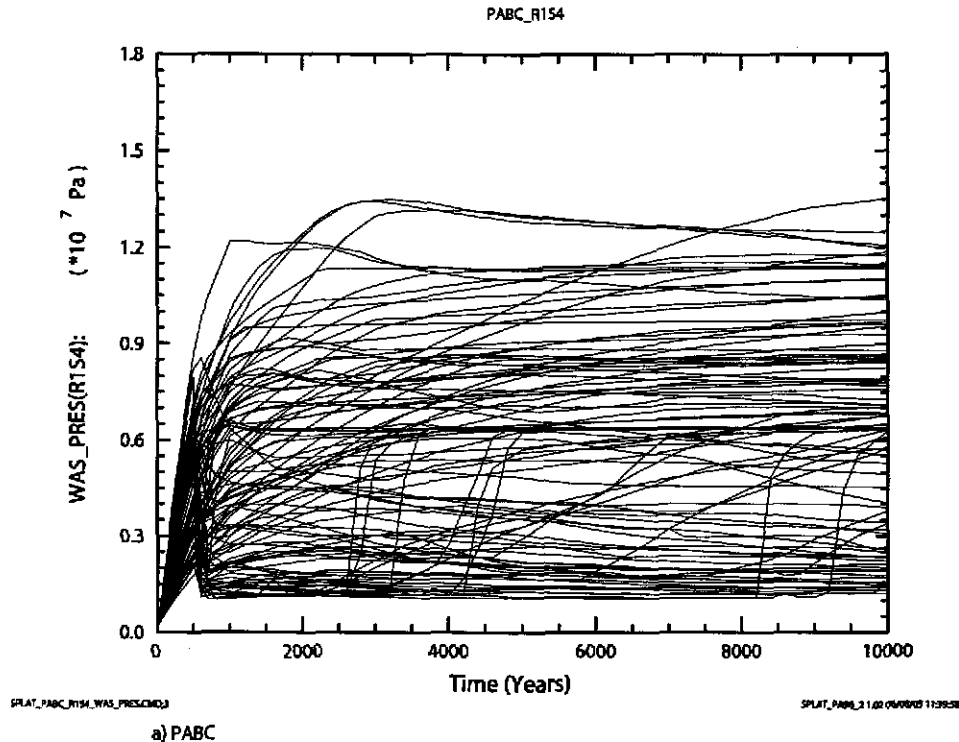
Figure 6-56. Volume averaged pressure (Pa) in the waste area versus time (years) for all 100 vectors in Replicate 1, Scenario S4. Figure a) shows results from the CRA-2004 PABC. Figure b) shows results from the CRA-2004.
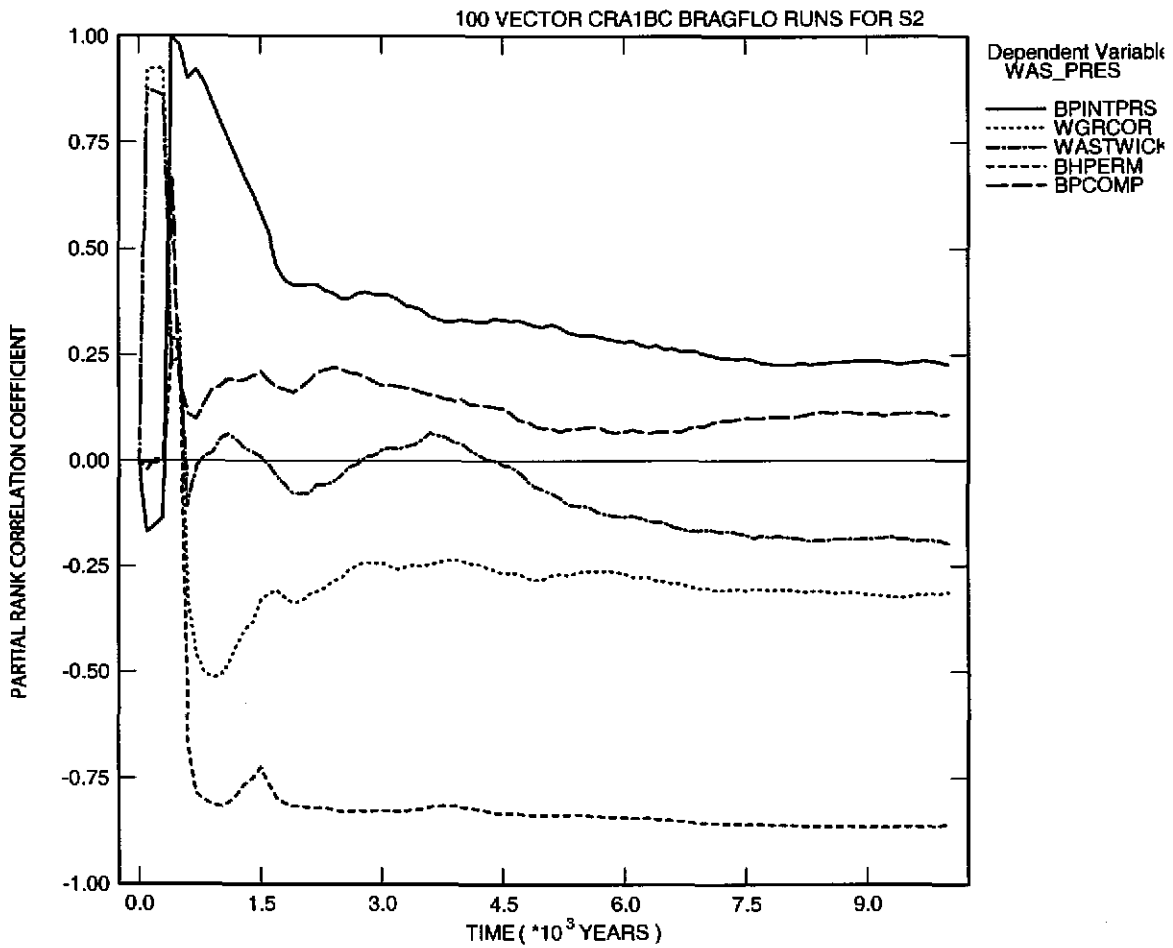
Figure 6-57. Primary correlations (dimensionless) of volume averaged pressure in the waste panel with input parameters versus time (years) from the CRA-2004 PABC Replicate 1, Scenario S2. Table 4-2 gives a description of the names in the legend.
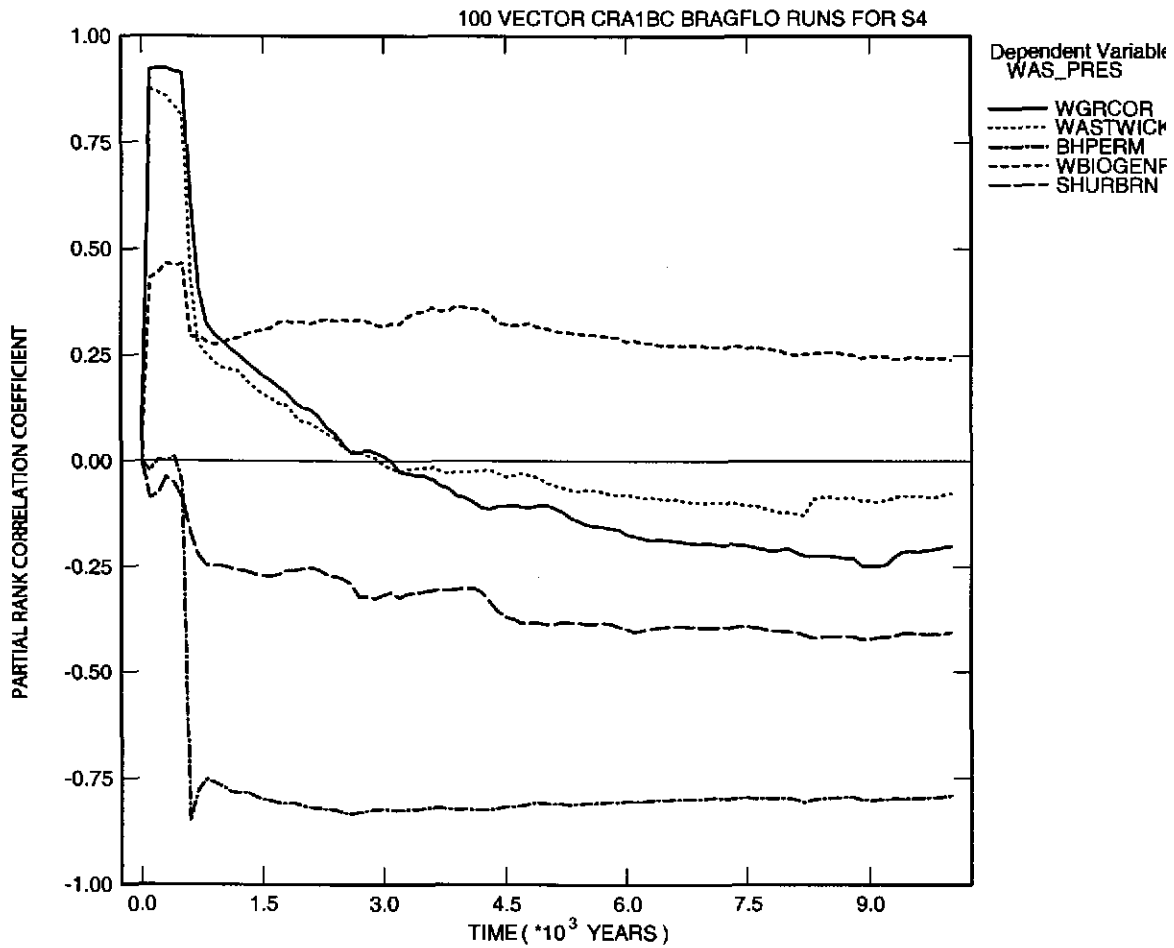
Figure 6-58. Primary correlations (dimensionless) of volume averaged pressure in the waste panel with input parameters versus time (years) from the CRA-2004 PABC Replicate 1, Scenario S4. Table 4-2 gives a description of the names in the legend.

PABC_R1S2

a) PABC

CRA1_R1S2
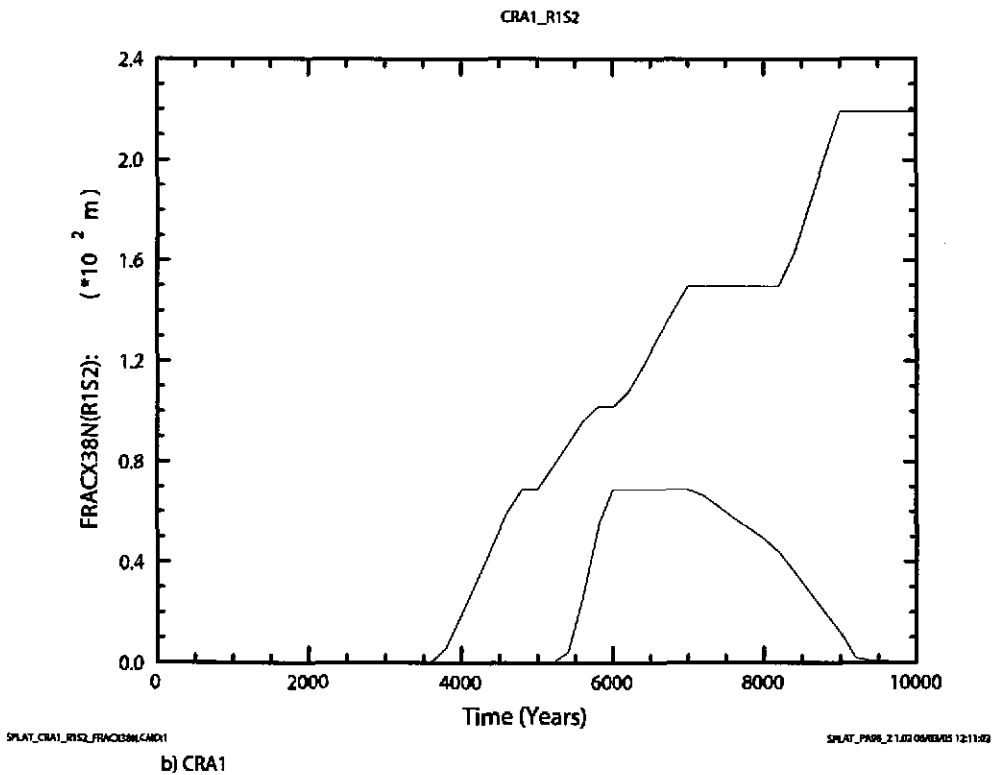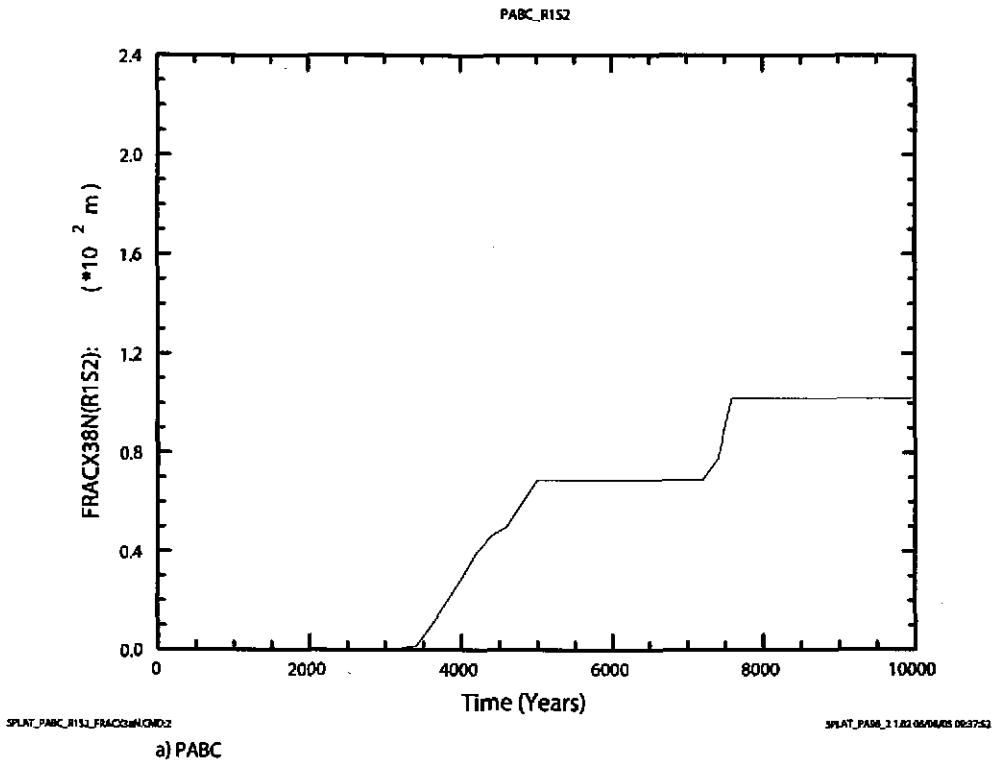
b) CRA1

Figure 6-59. Fracture length (m) in MB138, north of the repository versus time (years) for all 100 vectors in Replicate 1, Scenario S2. Figure a) shows results from the CRA-2004 PABC. Figure b) shows results from the CRA-2004.

PABC_R1S4

a) PABC

CRA1_R1S4
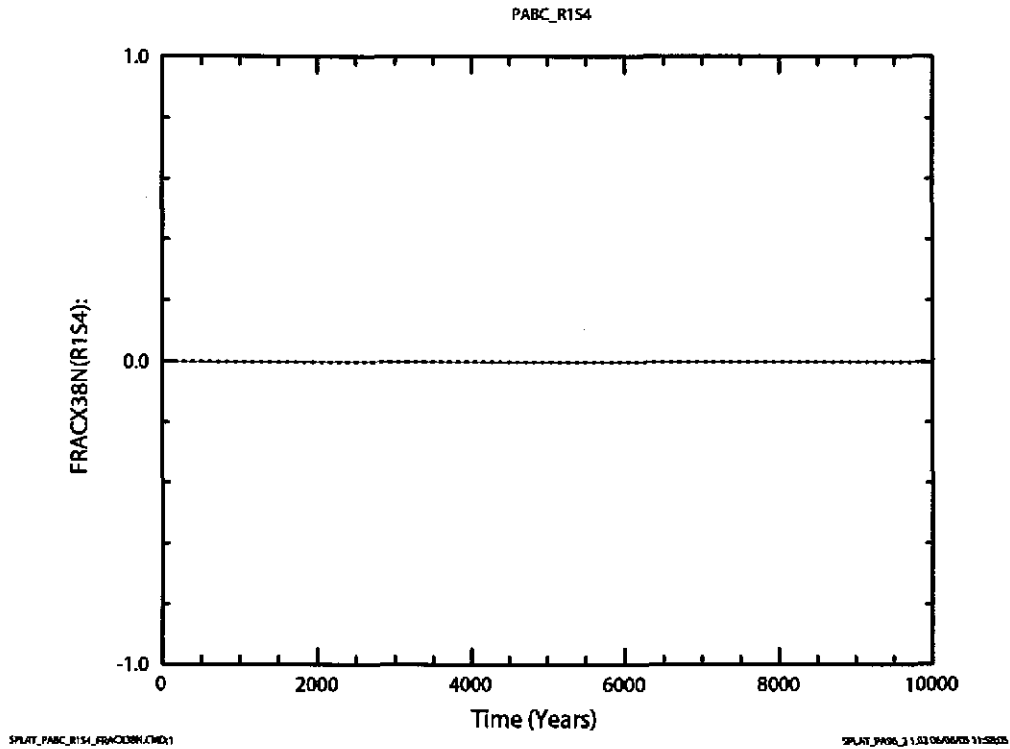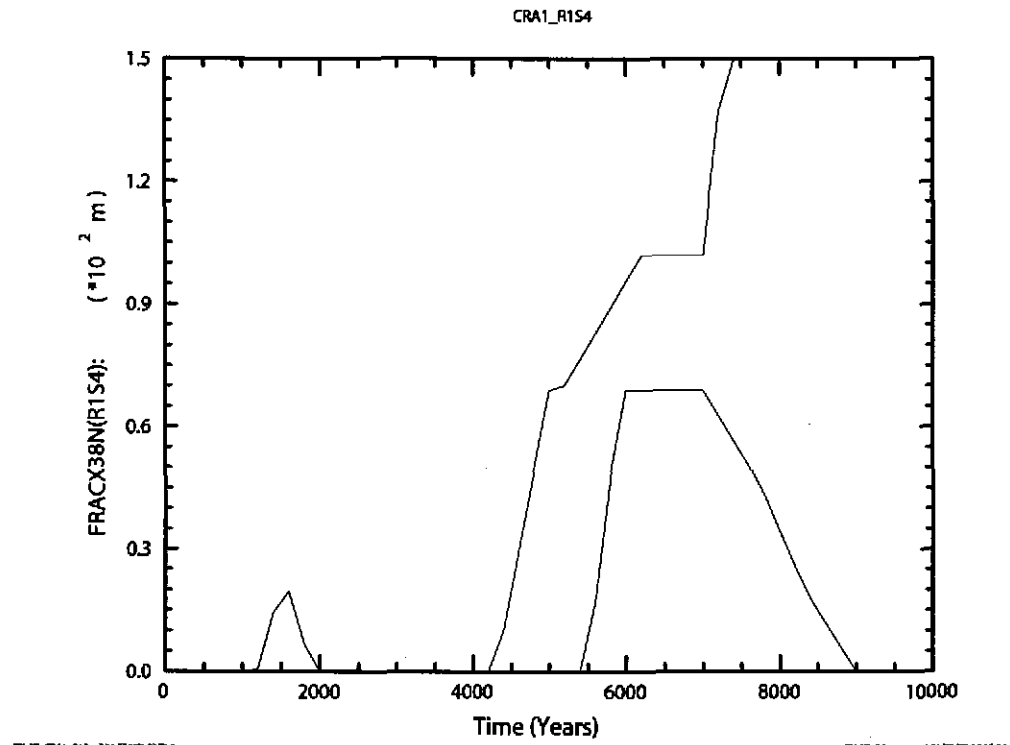
b) CRA1

Figure 6-60. Fracture length (m) in MB138, north of the repository versus time (years) for all 100 vectors in Replicate 1, Scenario S4. Figure a) shows results from the CRA-2004 PABC. Figure b) shows results from the CRA-2004.
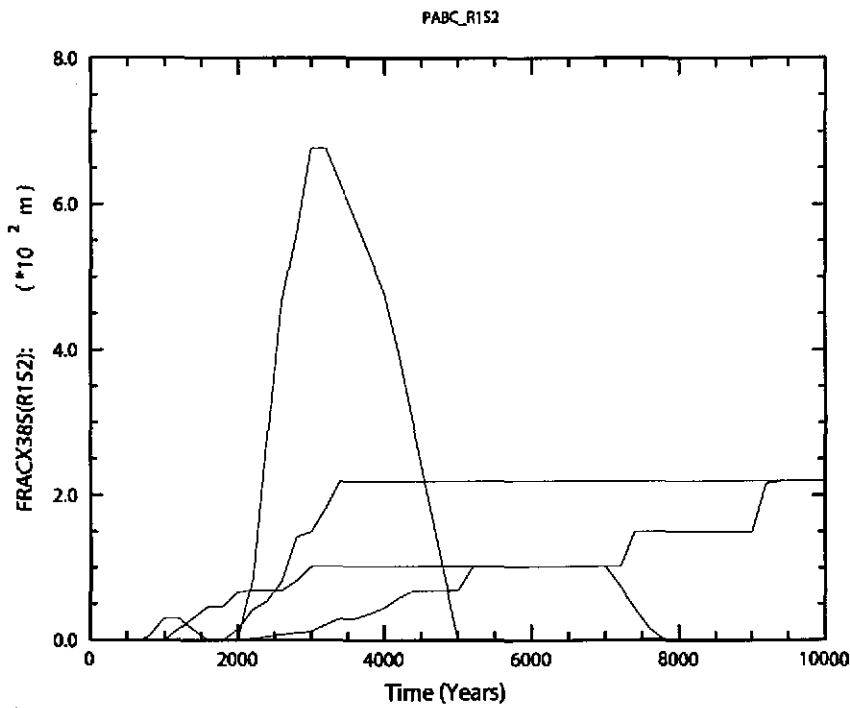
a) PABC
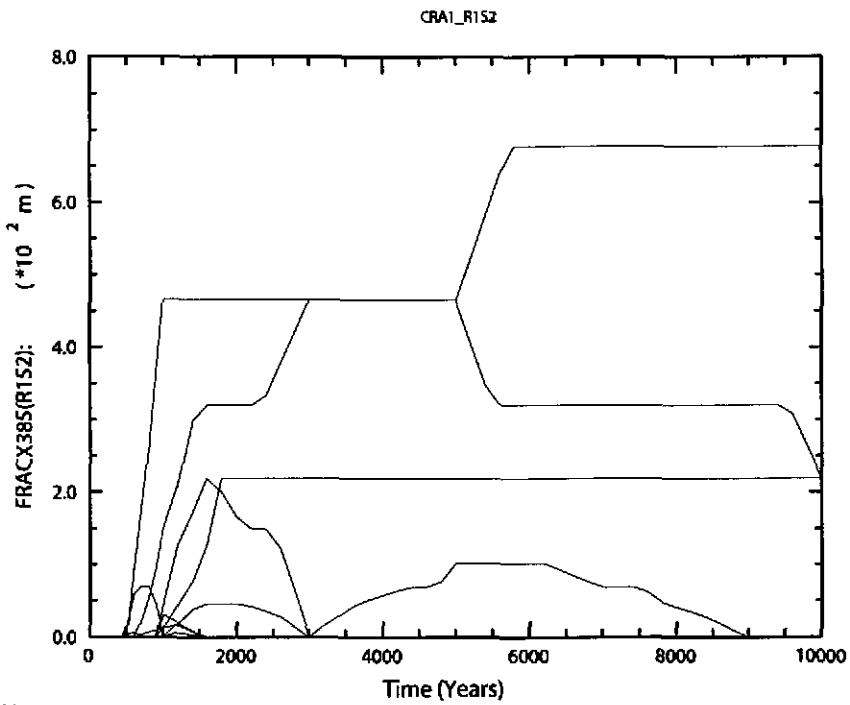
b) CRA1

Figure 6-61. Fracture length (m) in MB138, south of the repository versus time (years) for all 100 vectors in Replicate 1, Scenario S2. Figure a) shows results from the CRA-2004 PABC. Figure b) shows results from the CRA-2004.
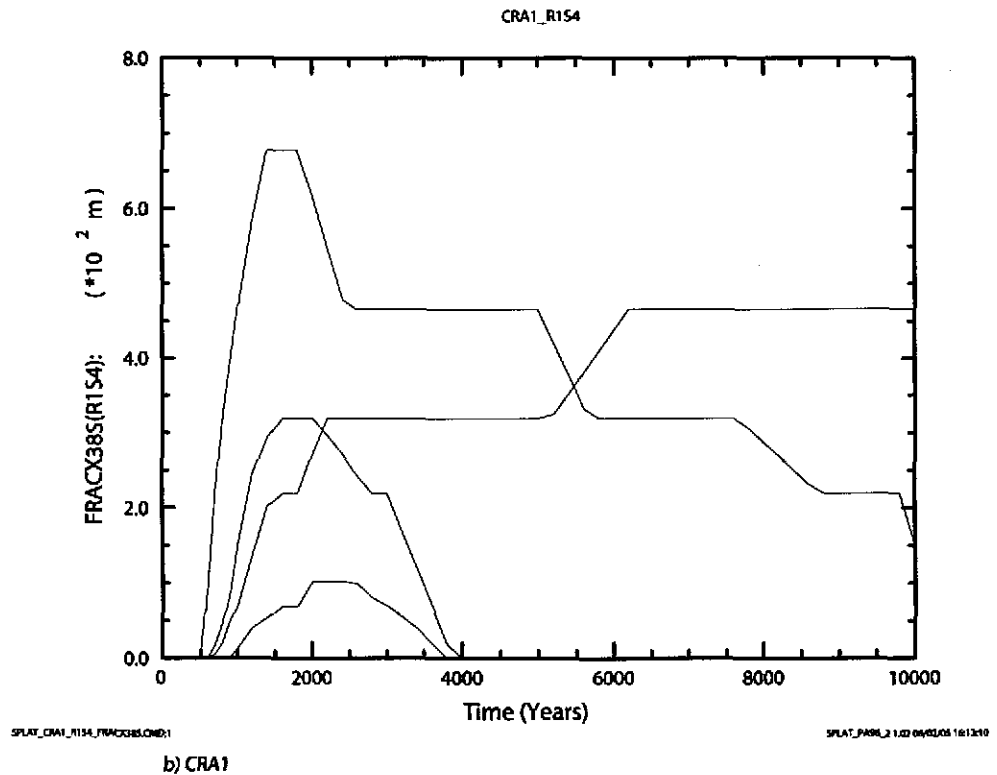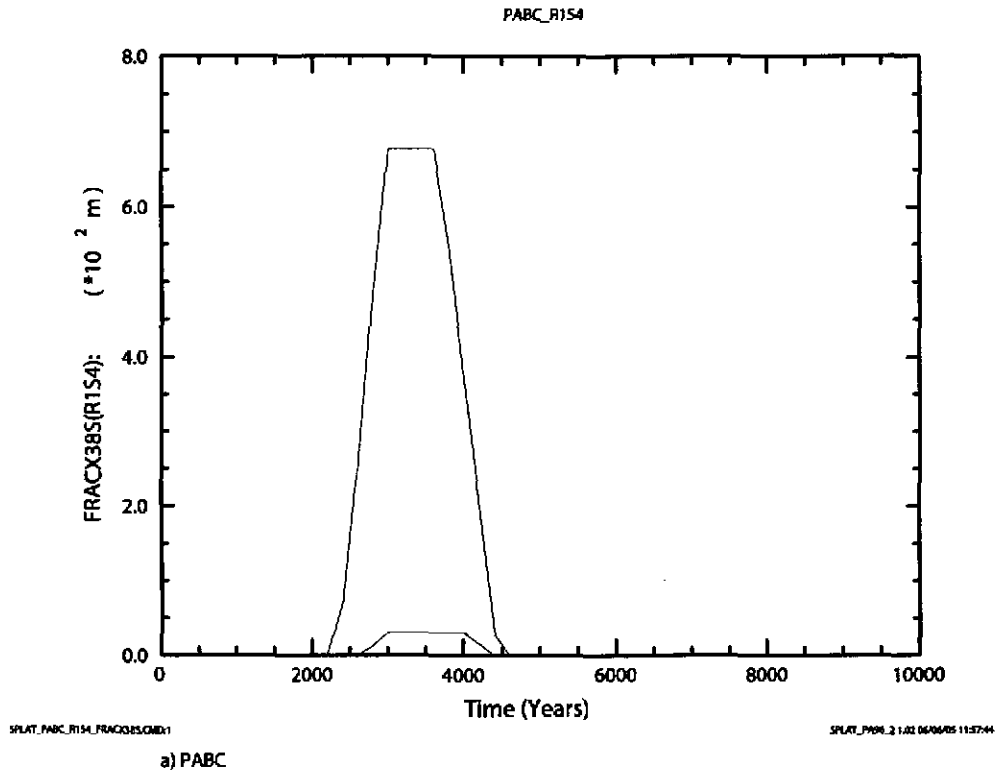
a) PABC

b) CRA1

Figure 6-62. Fracture length (m) in MB138, south of the repository versus time (years) for all 100 vectors in Replicate 1, Scenario S4. Figure a) shows results from the CRA-2004 PABC. Figure b) shows results from the CRA-2004.
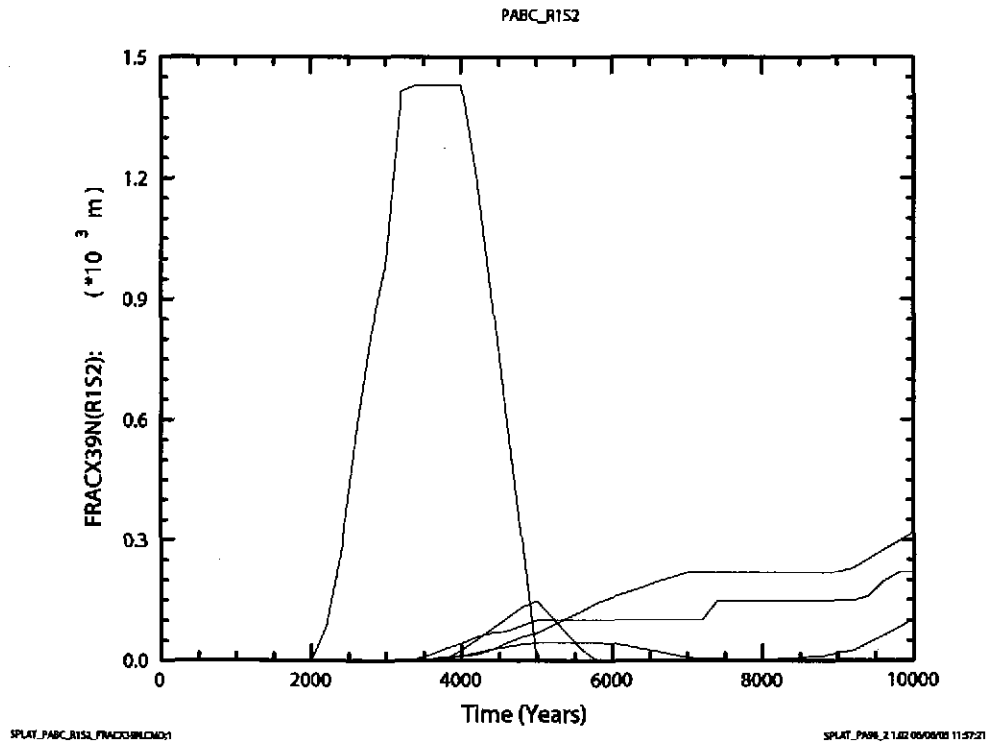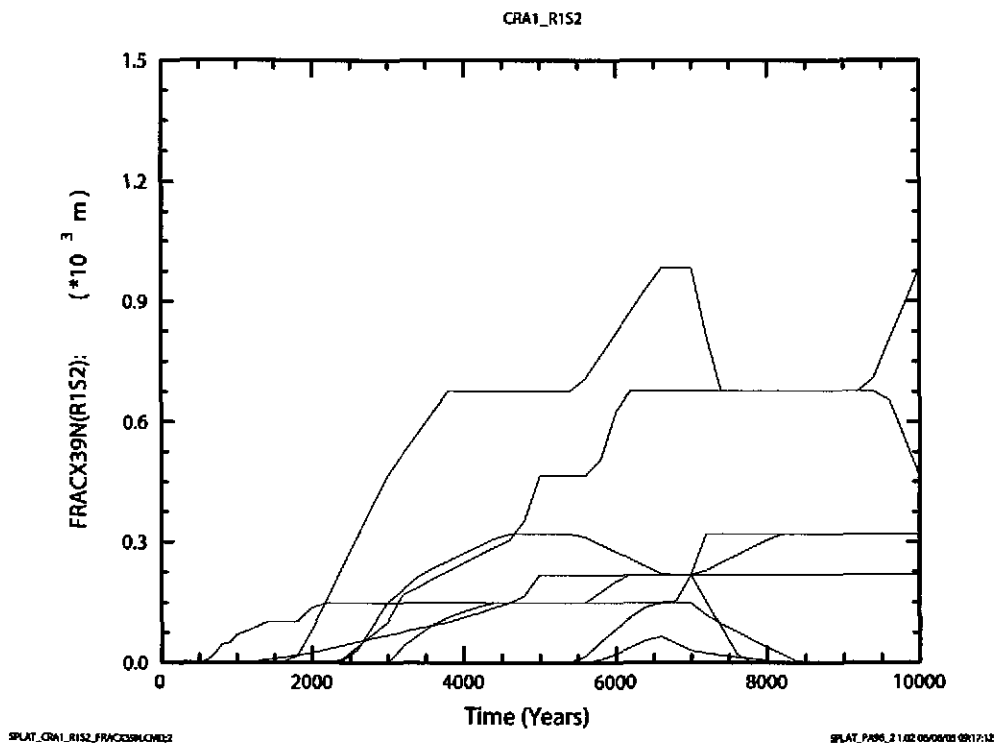
a) PABC

b) CRA1

Figure 6-63. Fracture length (m) in MB139, north of the repository versus time (years) for all 100 vectors in Replicate 1, Scenario S2. Figure a) shows results from the CRA-2004 PABC. Figure b) shows results from the CRA-2004.
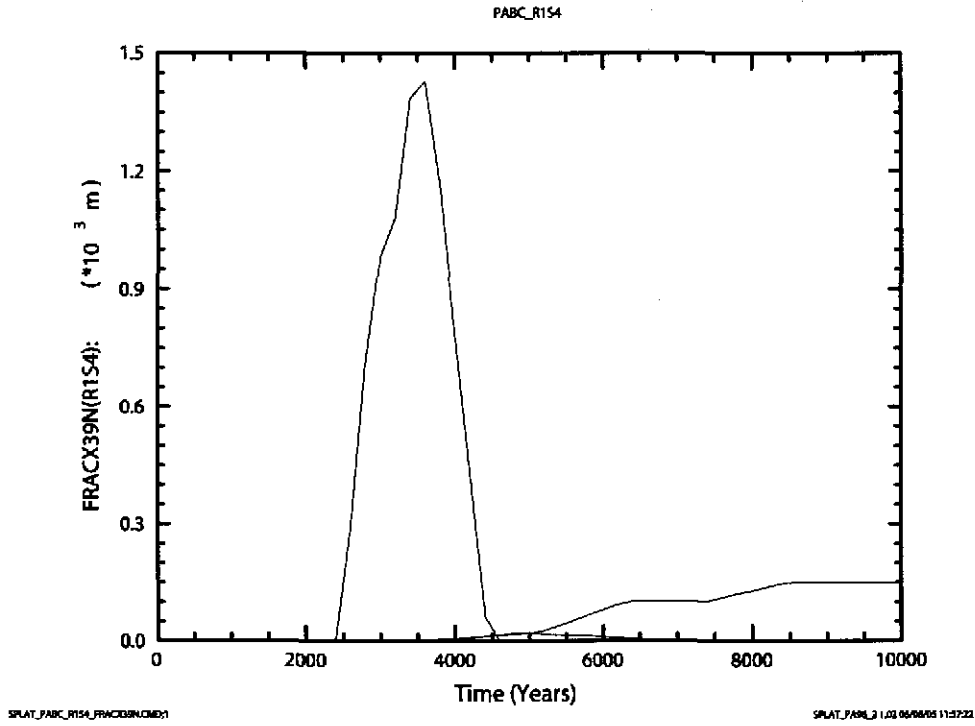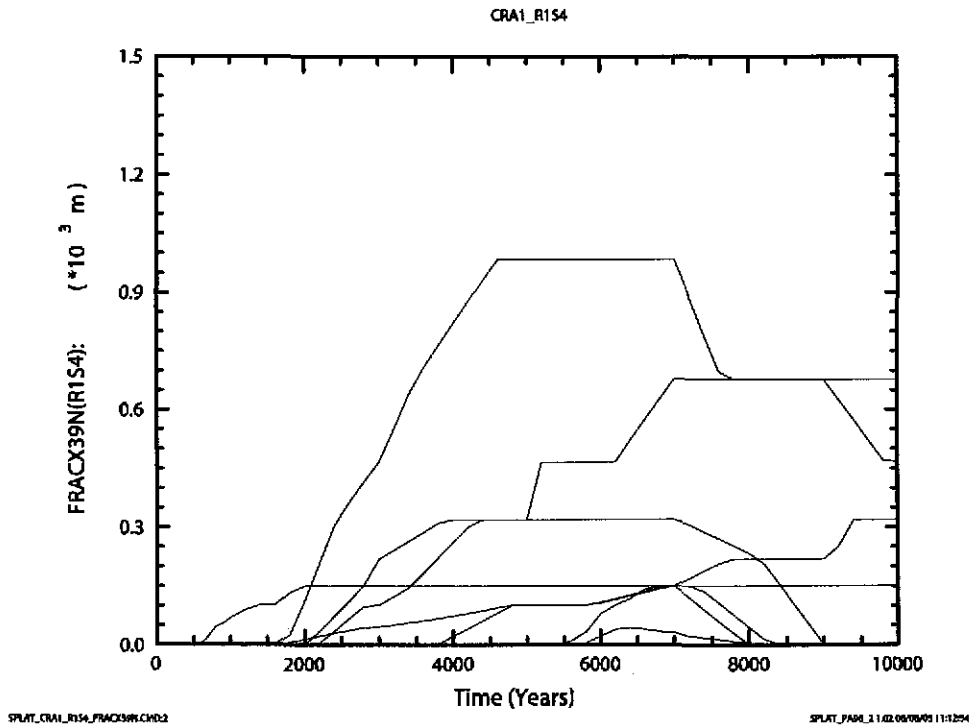
a) PABC

b) CRA1

Figure 6-64. Fracture length (m) in MB139, north of the repository versus time (years) for all 100 vectors in Replicate 1, Scenario S4. Figure a) shows results from the CRA-2004 PABC. Figure b) shows results from the CRA-2004.
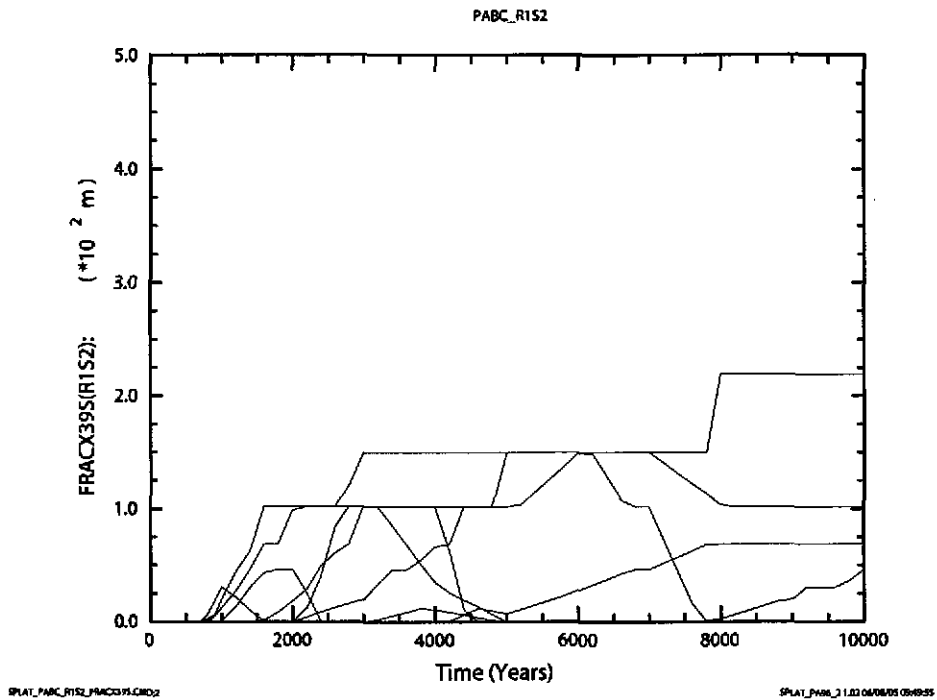
a) PABC
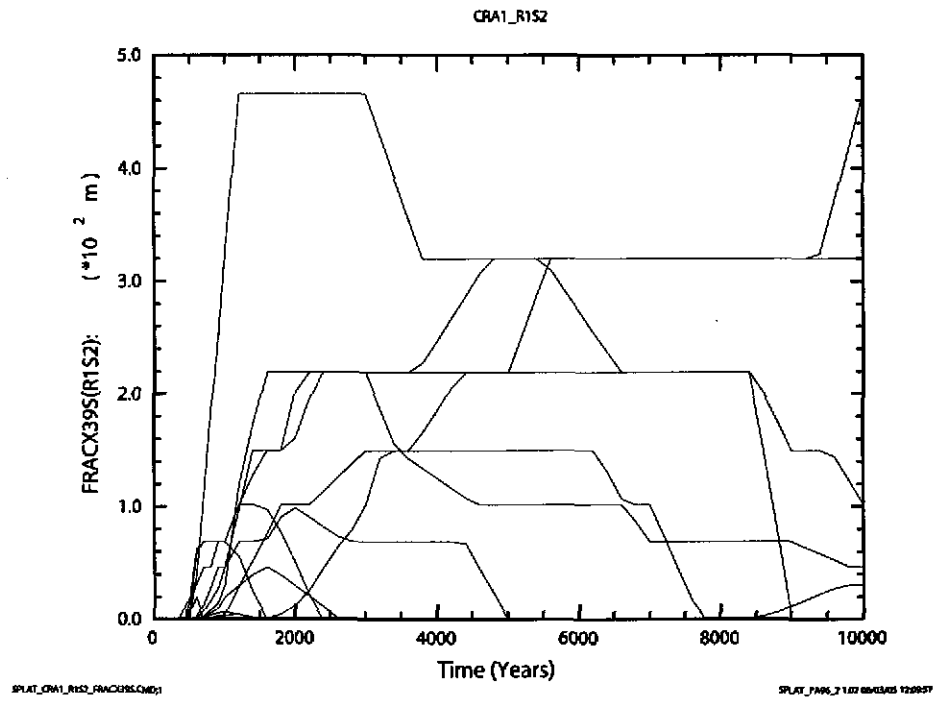
b) CRA1

Figure 6-65. Fracture length (m) in MB139, south of the repository versus time (years) for all 100 vectors in Replicate 1, Scenario S2. Figure a) shows results from the CRA-2004 PABC. Figure b) shows results from the CRA-2004.
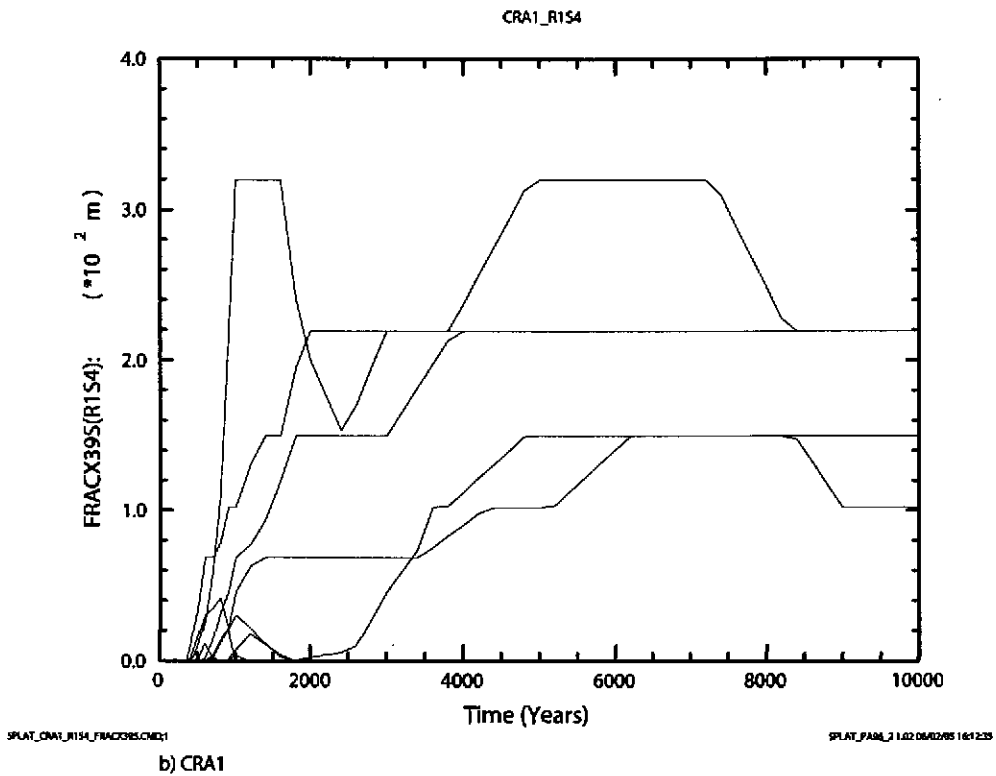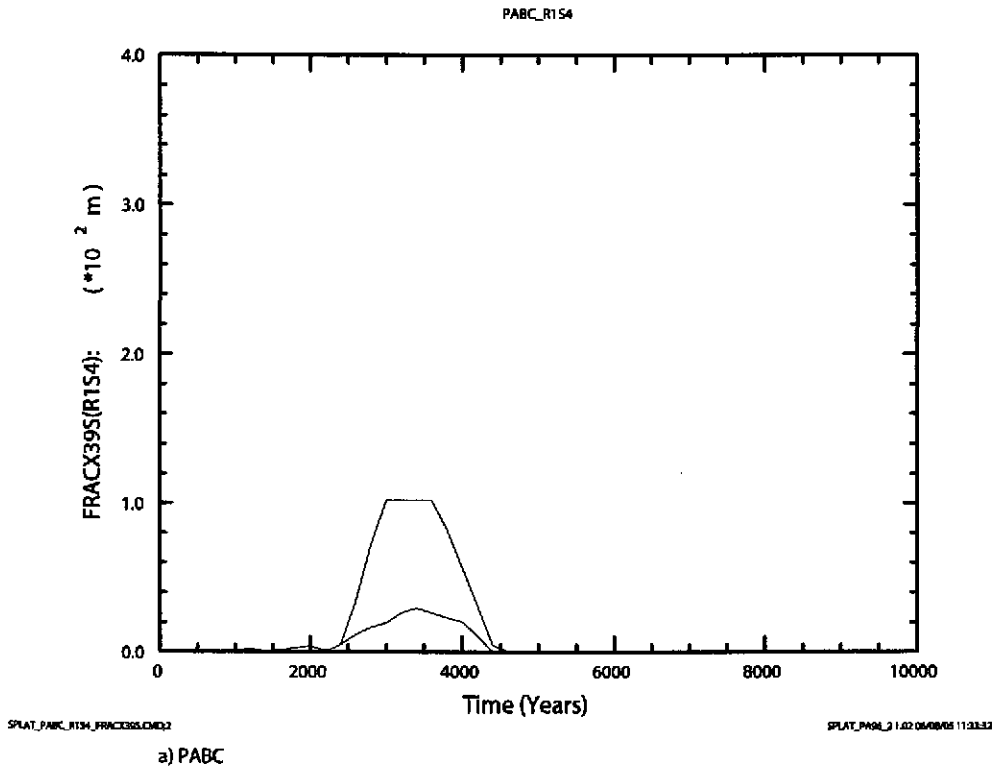
a) PABC

b) CRA1

Figure 6-66. Fracture length (m) in MB139, south of the repository versus time (years) for all 100 vectors in Replicate 1, Scenario S4. Figure a) shows results from the CRA-2004 PABC. Figure b) shows results from the CRA-2004.

PABC_R1S2

a) PABC

CRA1_R1S2
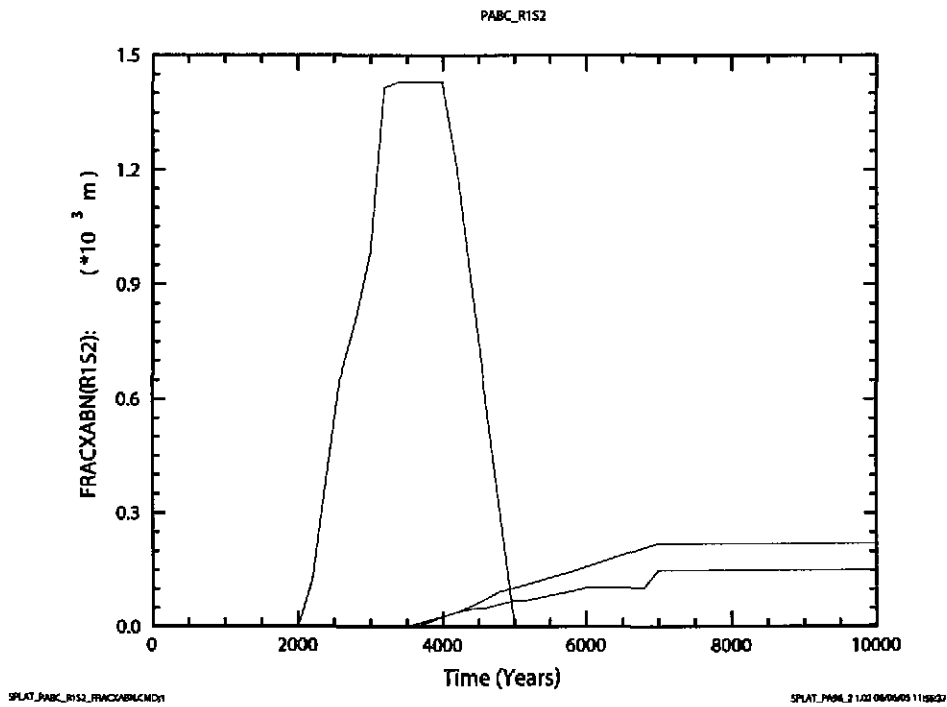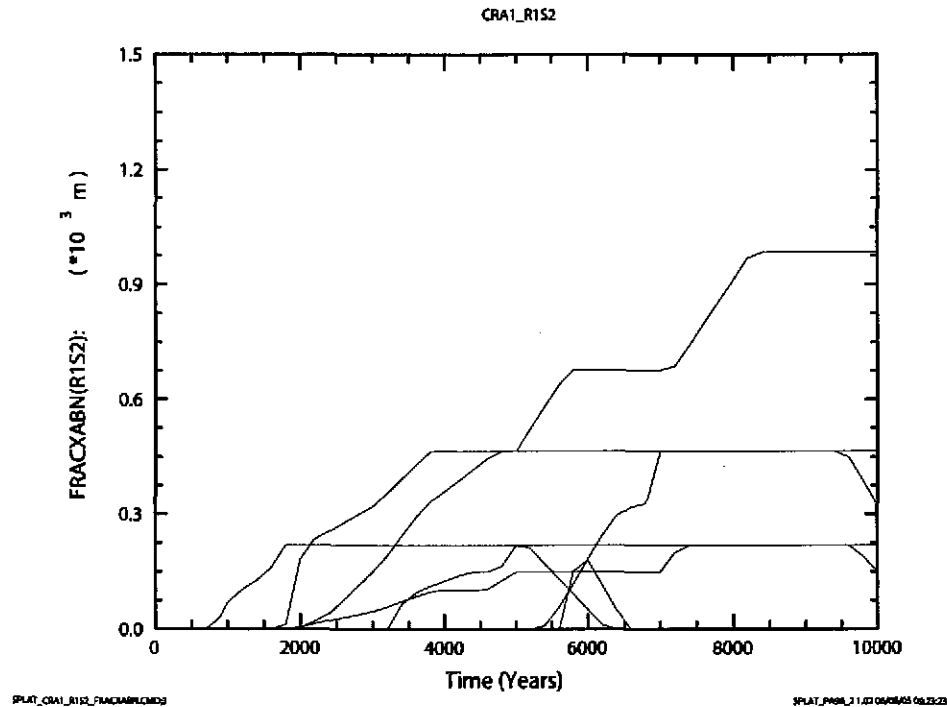
b) CRA1

Figure 6-67. Fracture length (m) in Anhydrite A&B, north of the repository versus time (years) for all 100 vectors in Replicate 1, Scenario S2. Figure a) shows results from the CRA-2004 PABC. Figure b) shows results from the CRA-2004.
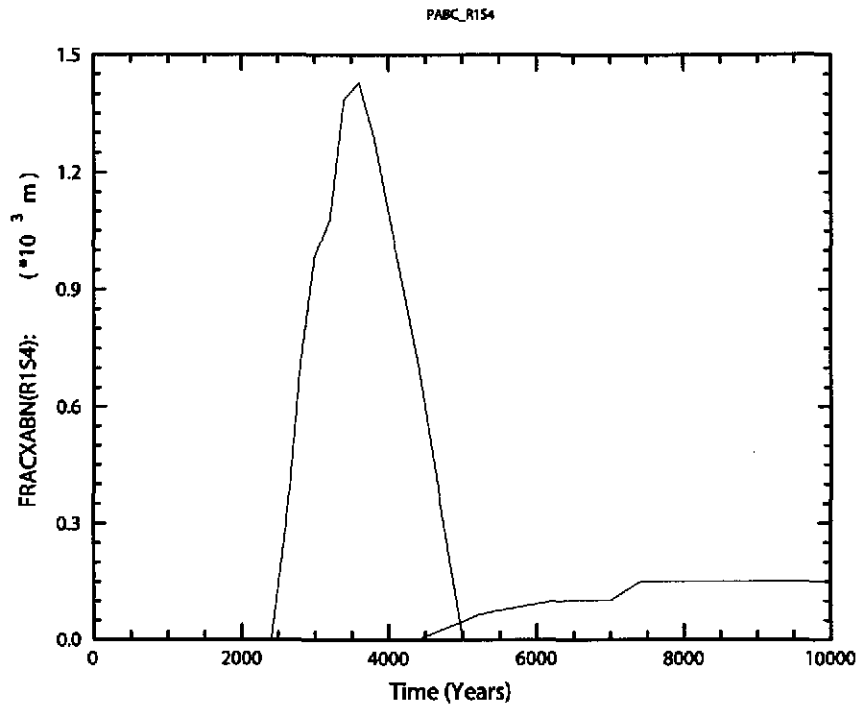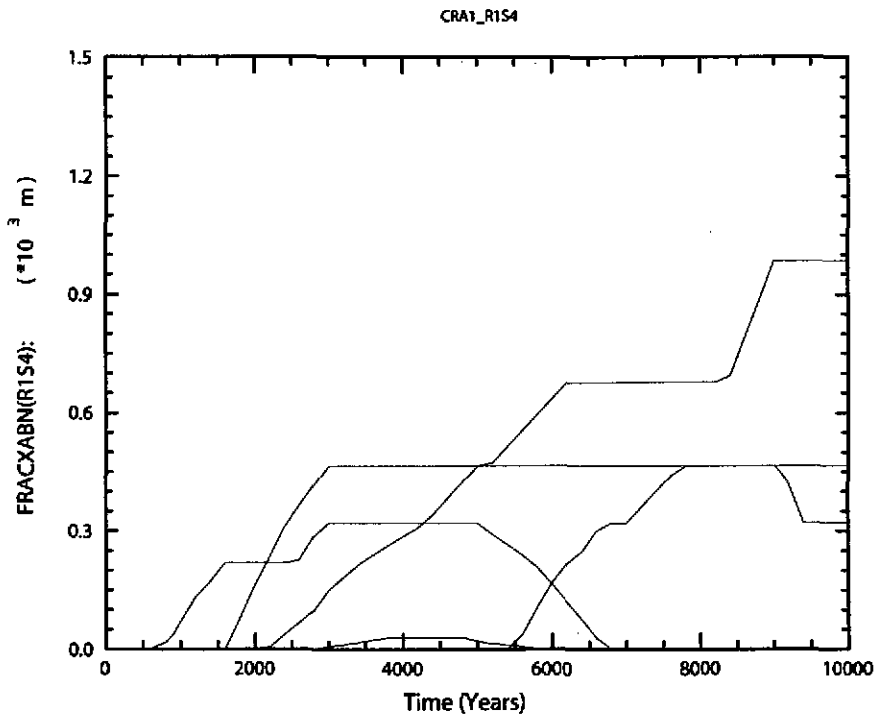
a) PABC

b) CRA1

Figure 6-68. Fracture length (m) in Anhydrite A&B, north of the repository versus time (years) for all 100 vectors in Replicate 1, Scenario S4. Figure a) shows results from the CRA-2004 PABC. Figure b) shows results from the CRA-2004.
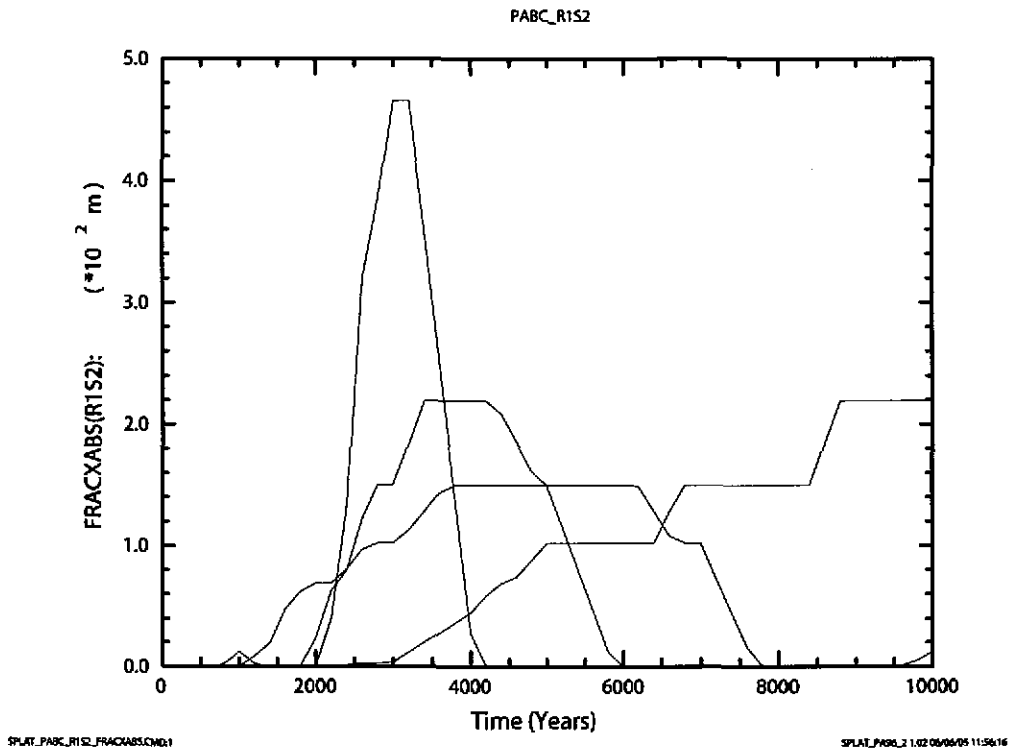
a) PABC
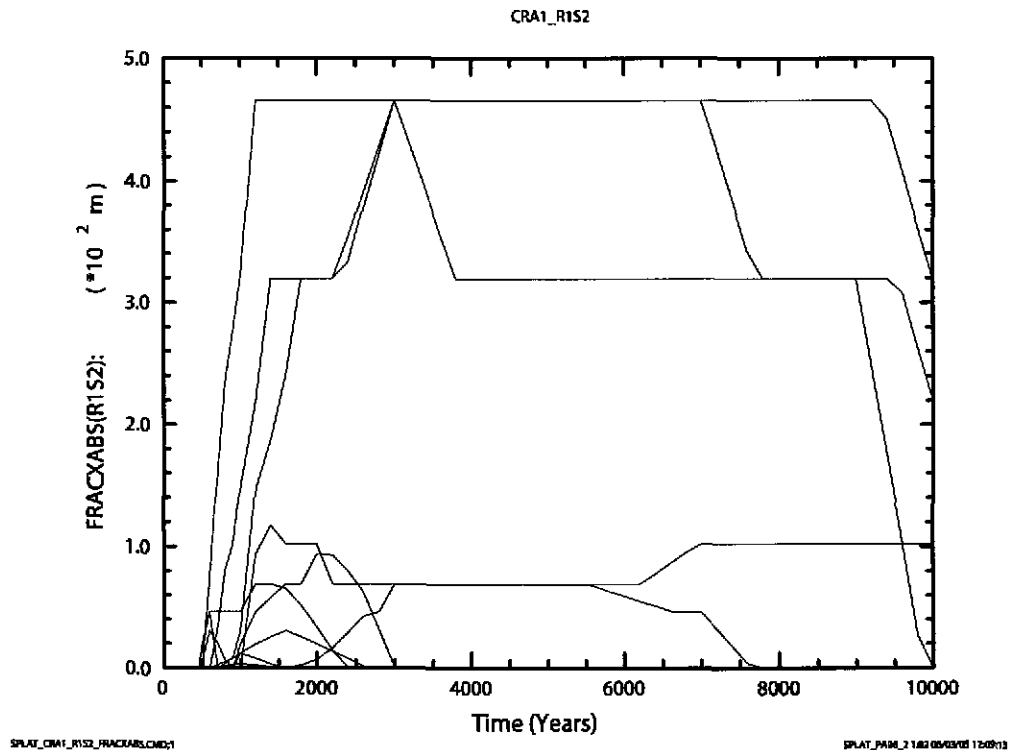
b) CRA1

Figure 6-69. Fracture length (m) in Anhydrite A&B, south of the repository versus time (years) for all 100 vectors in Replicate 1, Scenario S2. Figure a) shows results from the CRA-2004 PABC. Figure b) shows results from the CRA-2004.

PABC_R1S4

a) PABC

CRA1_R1S4
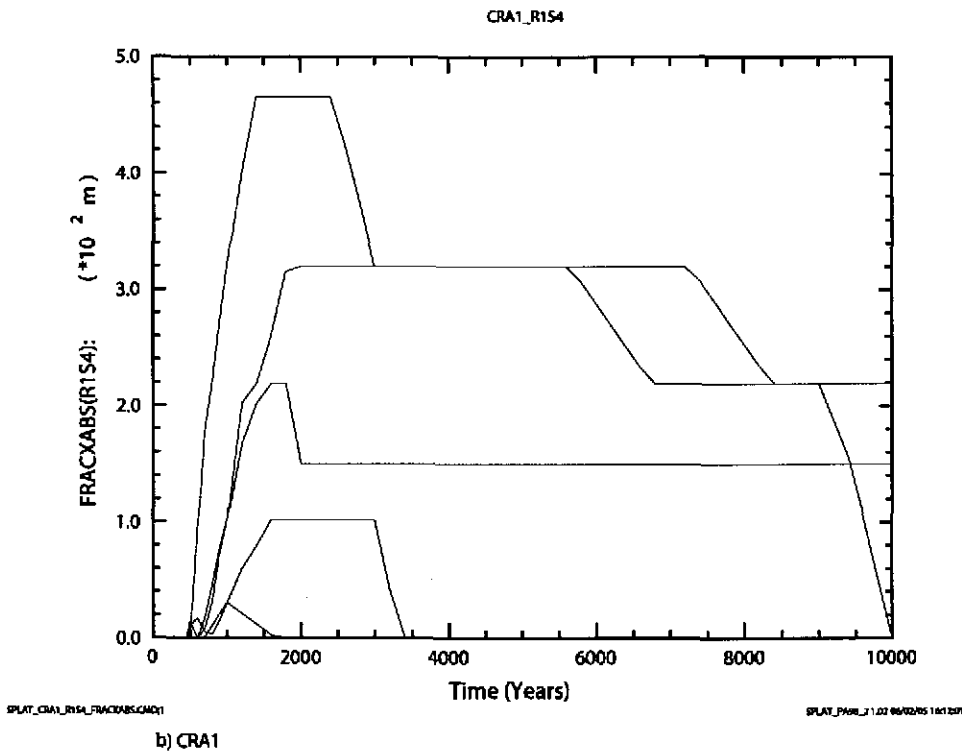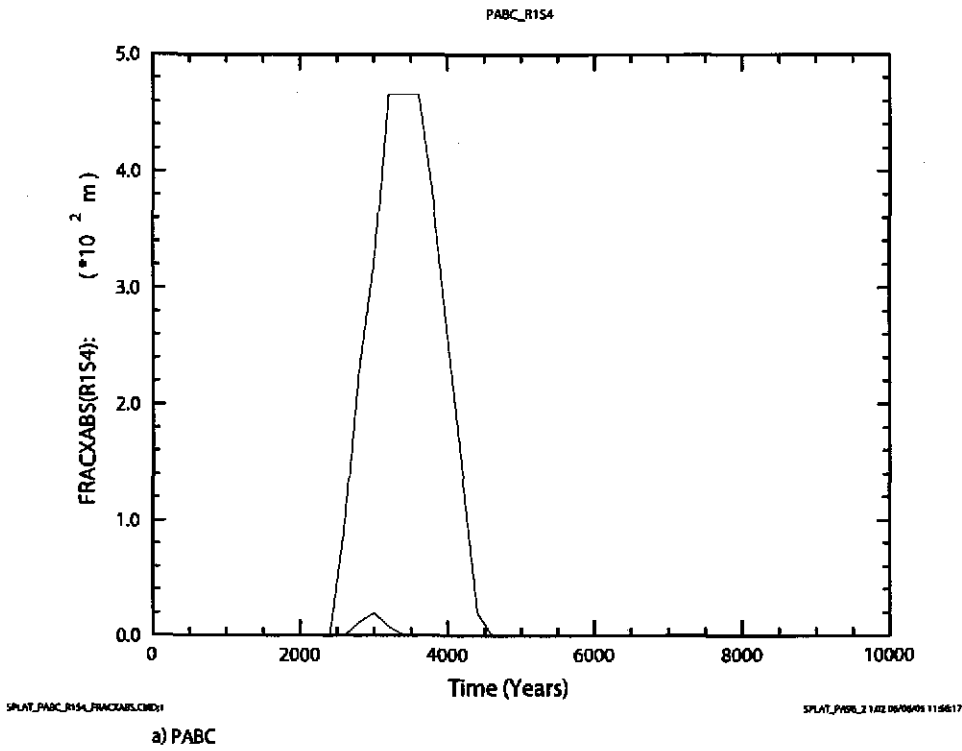
b) CRA1

Figure 6-70. Fracture length (m) in Anhydrite A&B, south of the repository versus time (years) for all 100 vectors in Replicate 1, Scenario S4. Figure a) shows results from the CRA-2004 PABC. Figure b) shows results from the CRA-2004.
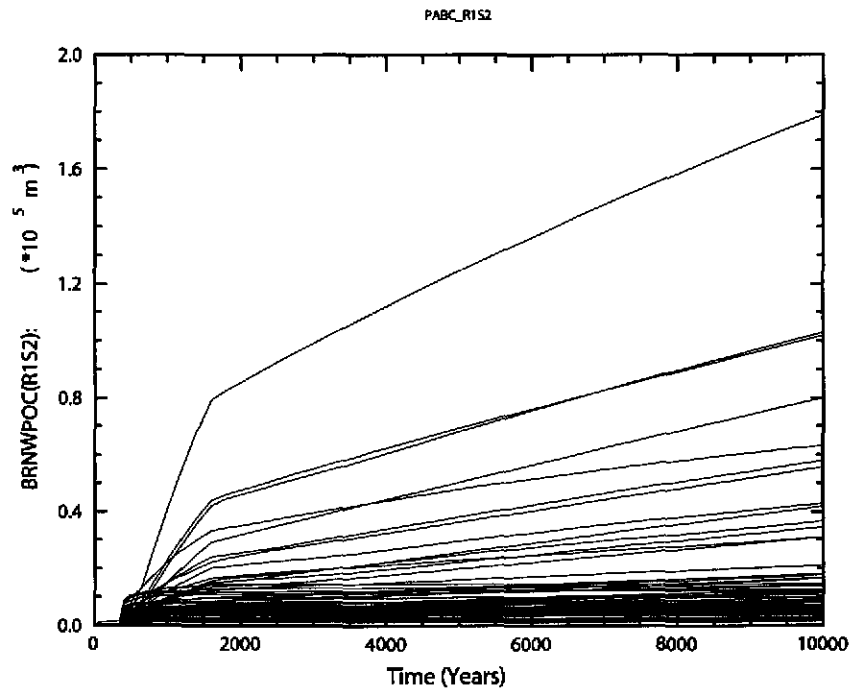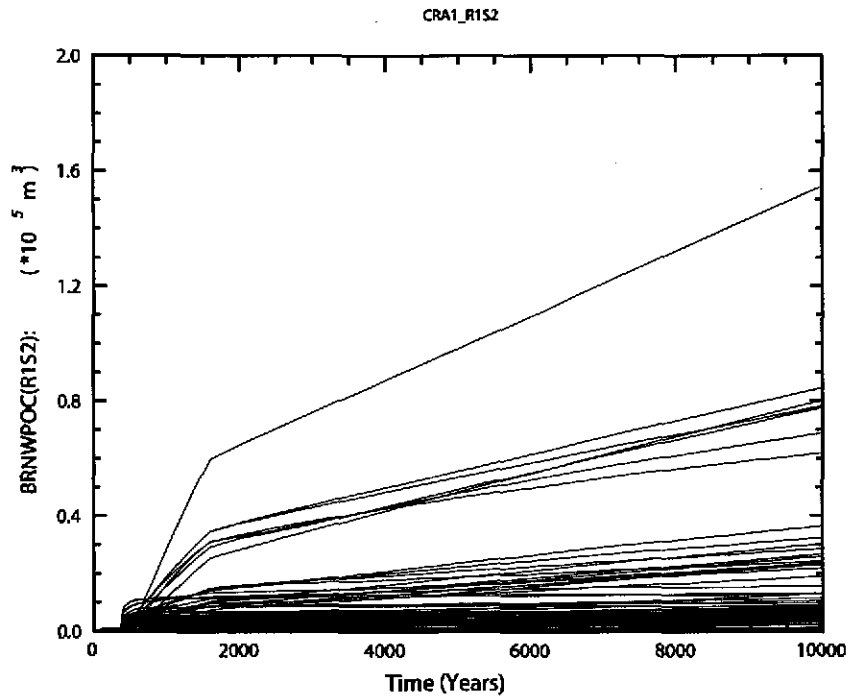
a) PABC

b) CRA1

Figure 6-71. Total cumulative brine flow (m³) out of the waste panel versus time (years) for all 100 vectors in Replicate 1, Scenario S2. Figure a) shows results from the CRA-2004 PABC. Figure b) shows results from the CRA-2004.
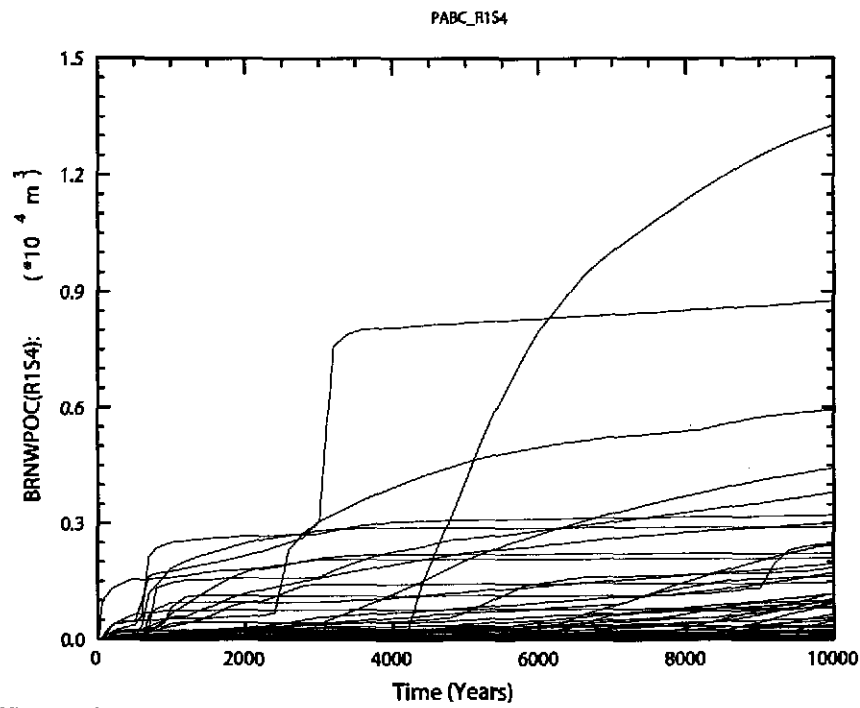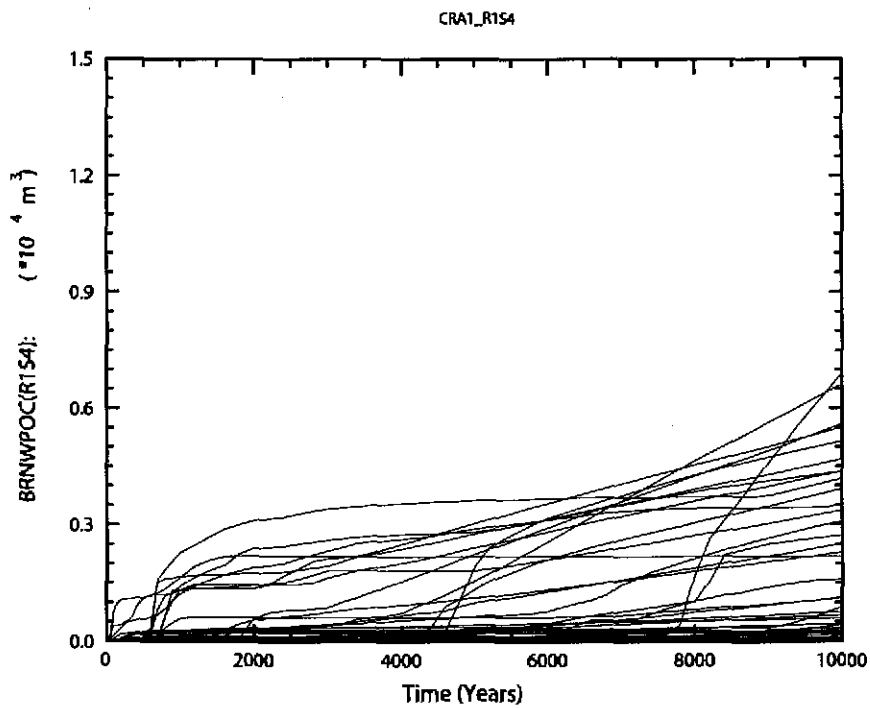
a) PABC

b) CRA1

Figure 6-72. Total cumulative brine flow (m^3) out of the Waste Panel, versus time (years) for all 100 vectors in Replicate 1, Scenario S4. Figure a) shows results from the CRA-2004 PABC. Figure b) shows results from the CRA-2004.
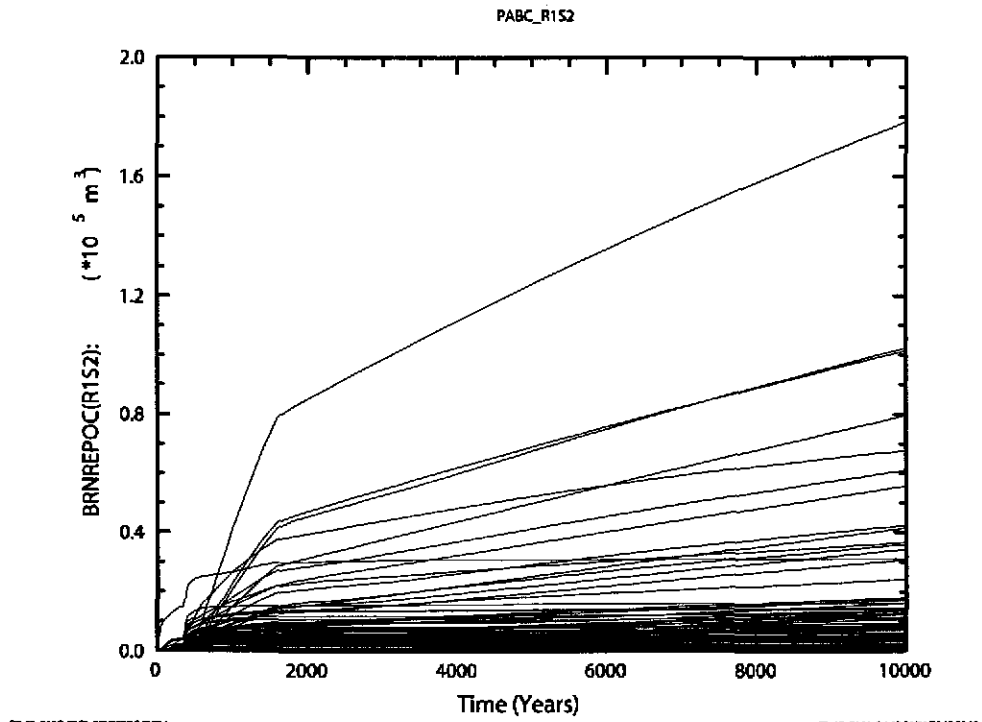
a) PABC
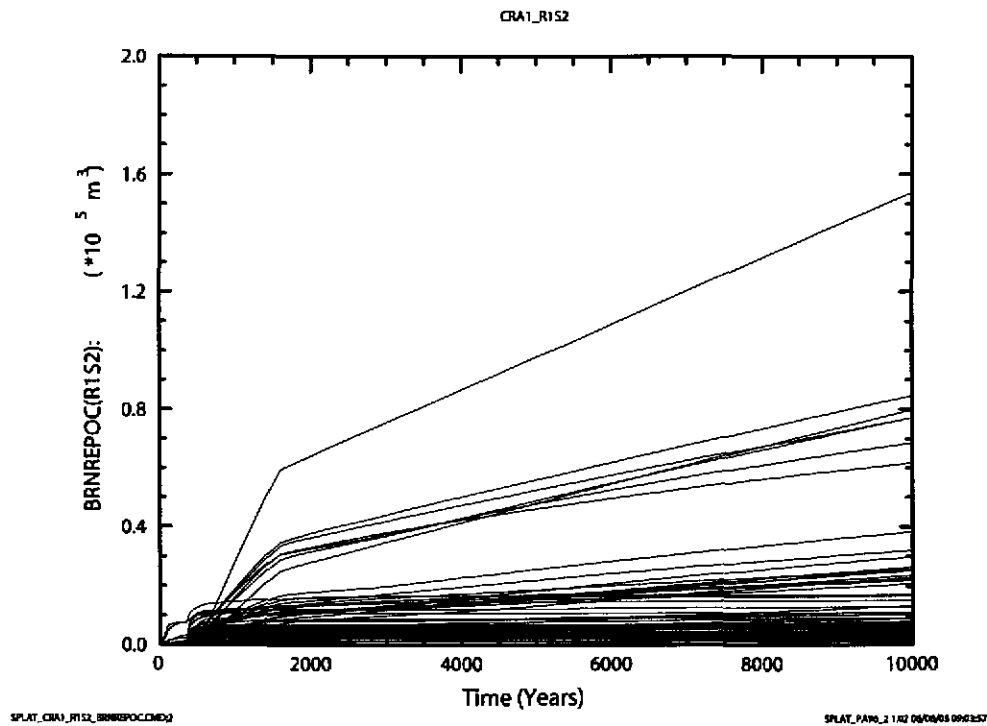
b) CRA1

Figure 6-73. Cumulative brine flow (m³) out of the repository versus time (years) for all 100 vectors in Replicate 1, Scenario S2. Figure a) shows results from the CRA-2004 PABC. Figure b) shows results from the CRA-2004.

a) PABC

b) CRA1
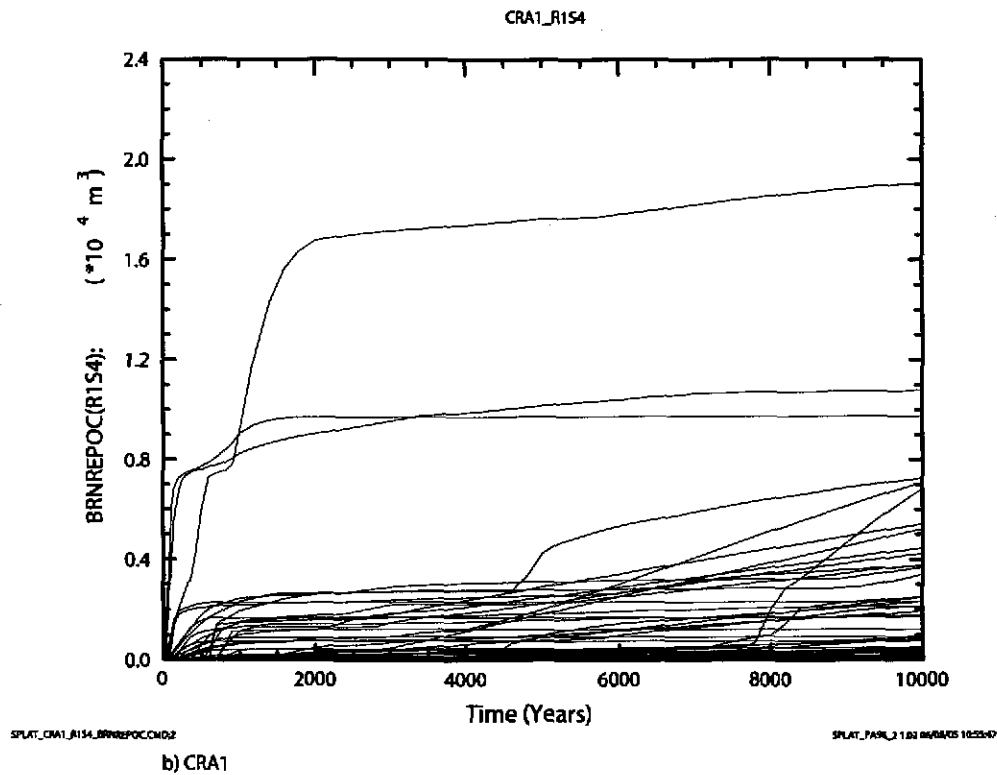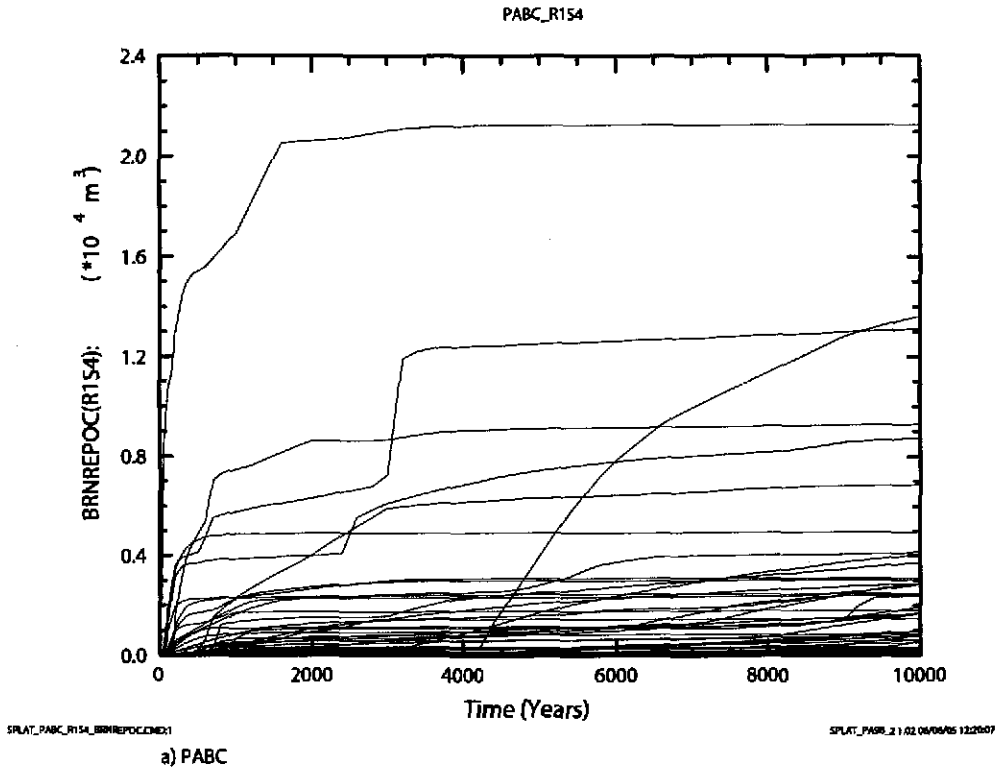
Figure 6-74. Cumulative brine flow (m³) out of the repository versus time (years) for all 100 vectors in Replicate 1, Scenario S4. Figure a) shows results from the CRA-2004 PABC. Figure b) shows results from the CRA-2004.
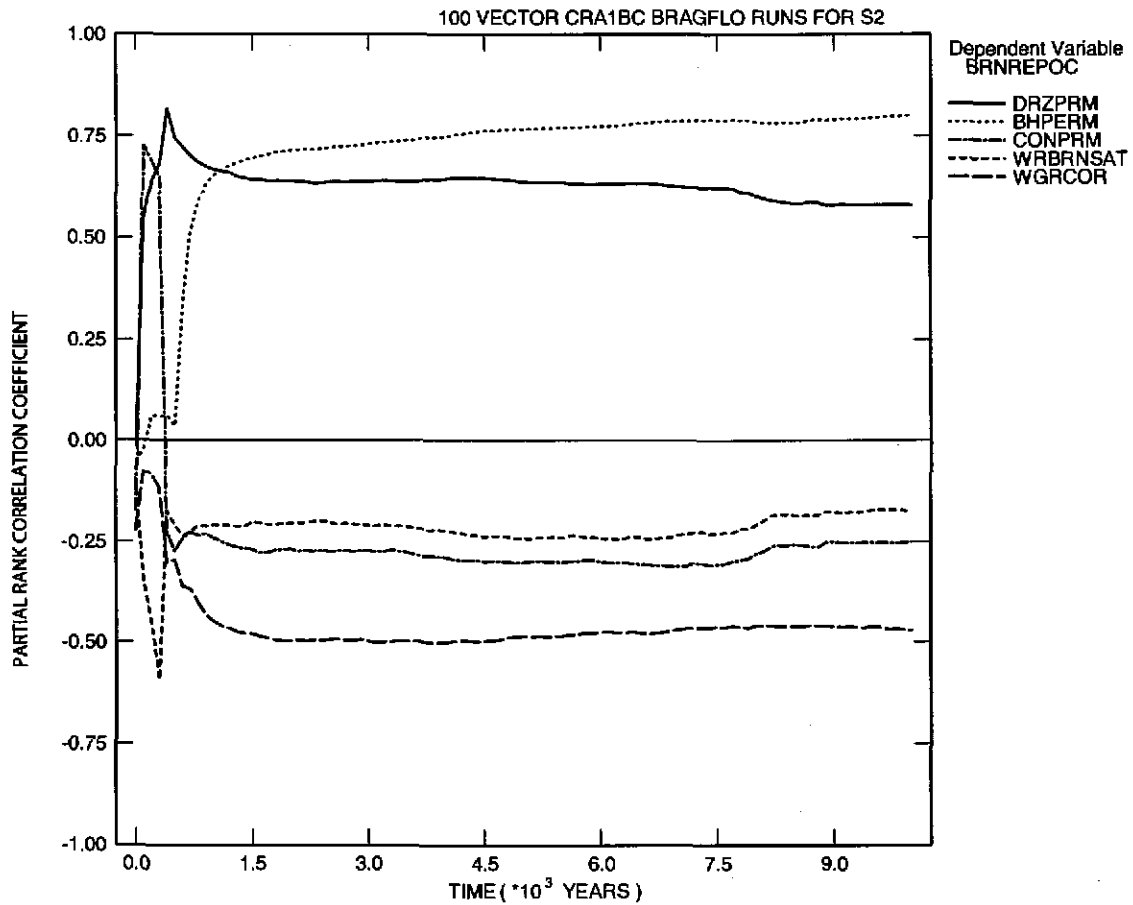
PCCSRC_S2.INP;3   PCCSRC_PA96 2.21 06/08/05 10:1:

Figure 6-75. Primary correlations (dimensionless) of brine flow out of the repository with input parameters versus time (years) from the CRA-2004 PABC Replicate 1, Scenario S2. Table 4-2 gives a description of the names in the legend.
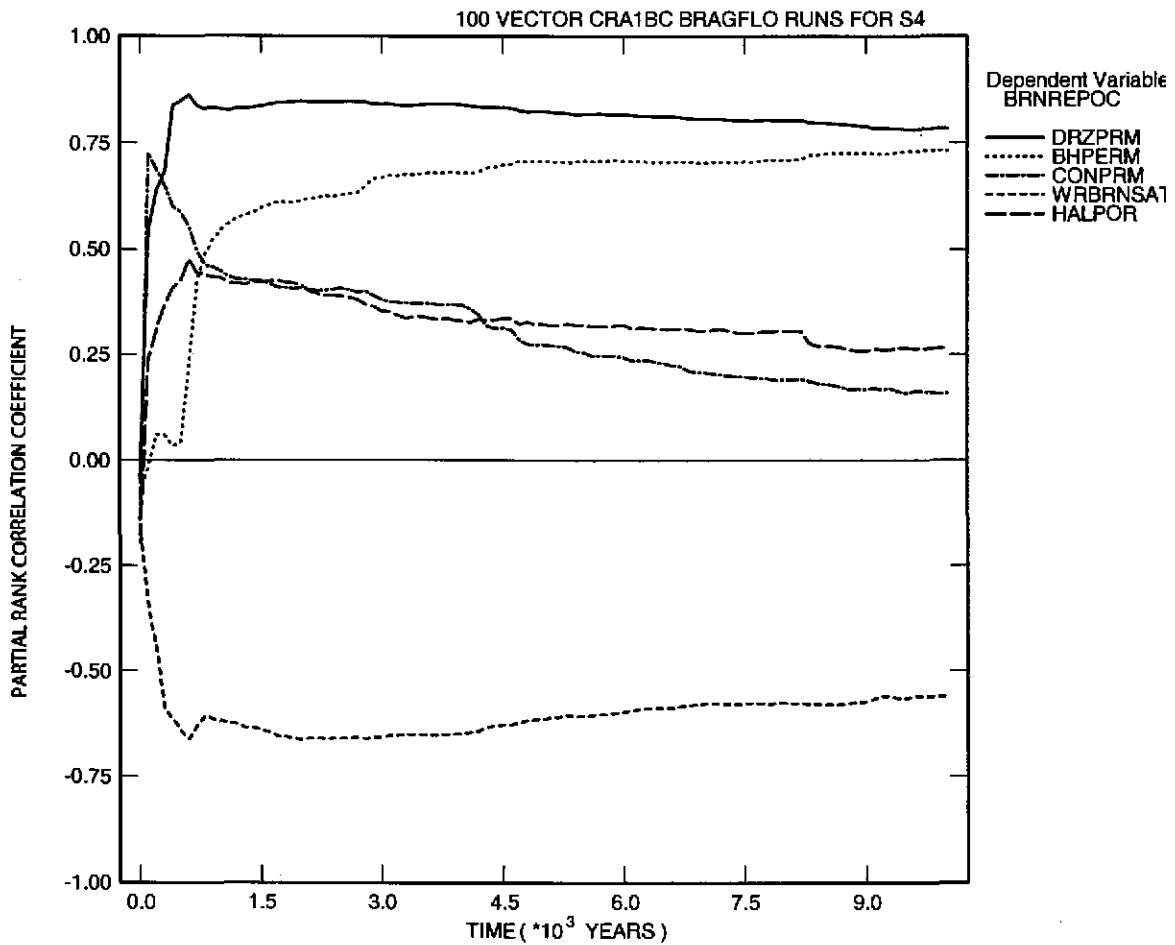
PCCSRC_S4.INP;2   PCCSRC_PA96 2.21 06/08/05 10:23

Figure 6-76. Primary correlations (dimensionless) of brine flow out of the repository with input parameters versus time (years) from the CRA-2004 PABC Replicate 1, Scenario S4. Table 4-2 gives a description of the names in the legend.
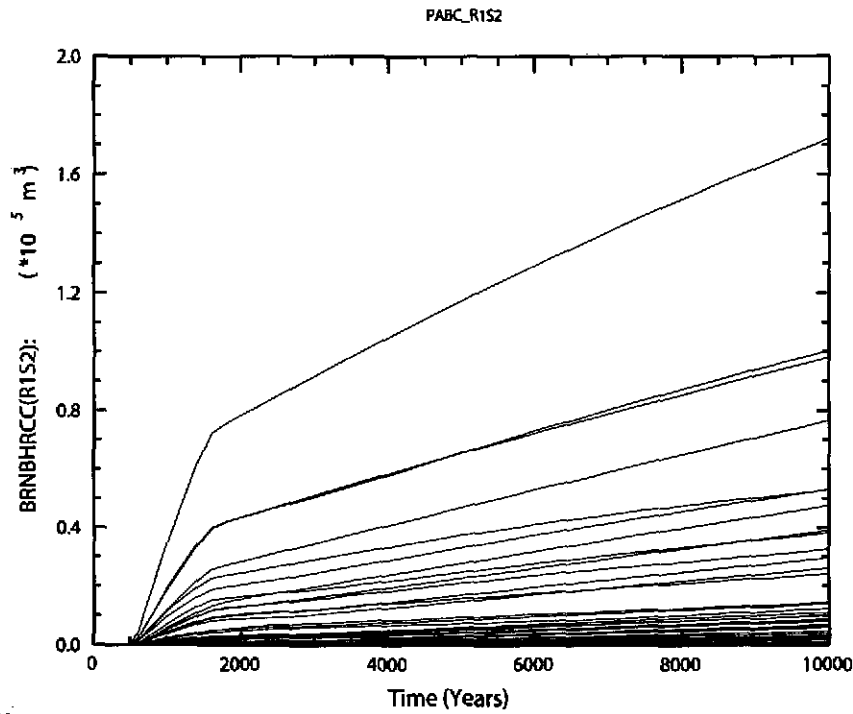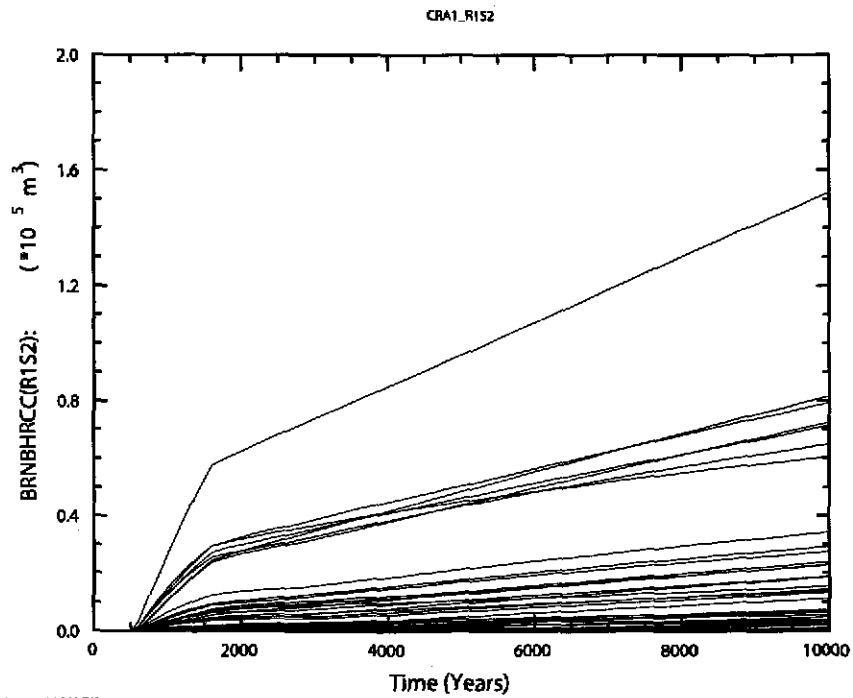
a) PABC

b) CRA1

Figure 6-77. Cumulative brine flow (m³) to the Culebra formation versus time (years) for all 100 vectors in Replicate 1, Scenario S2. Figure a) shows results from the CRA-2004 PABC. Figure b) shows results from the CRA-2004.
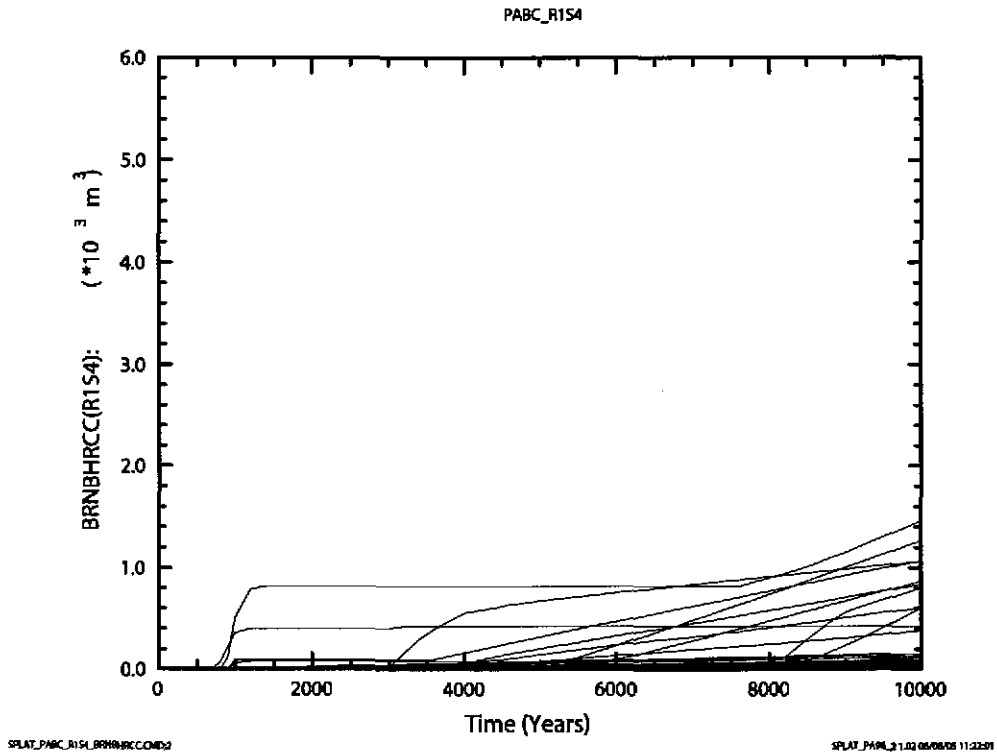
a) PABC
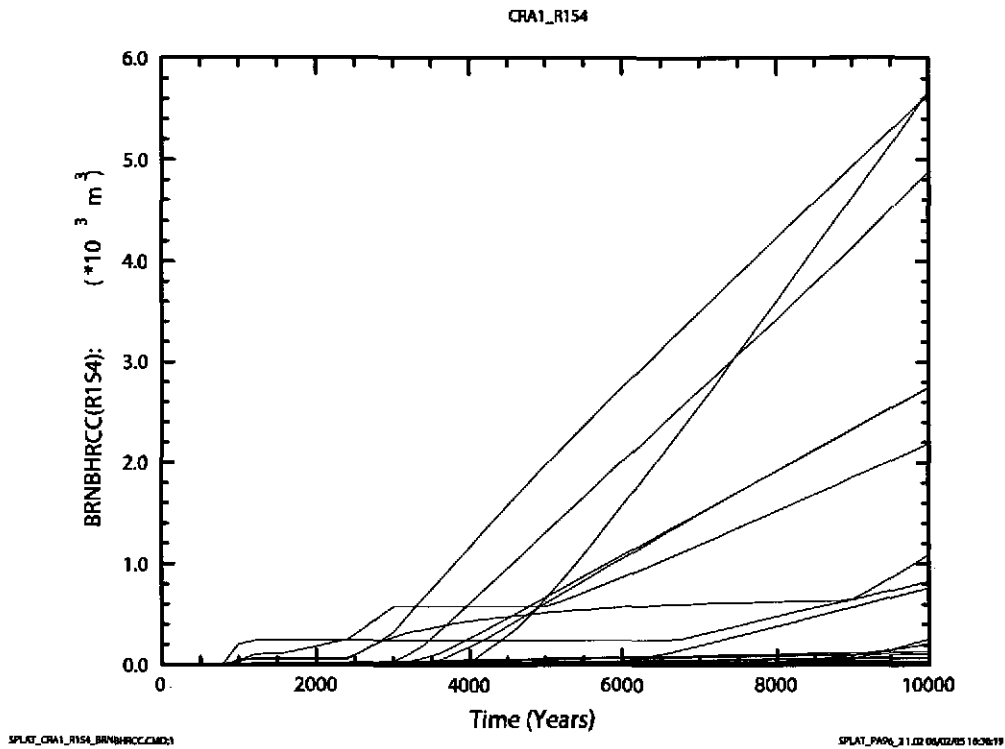
b) CRA1

Figure 6-78. Cumulative brine flow (m³) to the Culebra formation versus time (years) for all 100 vectors in Replicate 1, Scenario S4. Figure a) shows results from the CRA-2004 PABC. Figure b) shows results from the CRA-2004.

Information Only

PABC_R1S2

a) PABC

CRA1_R1S2
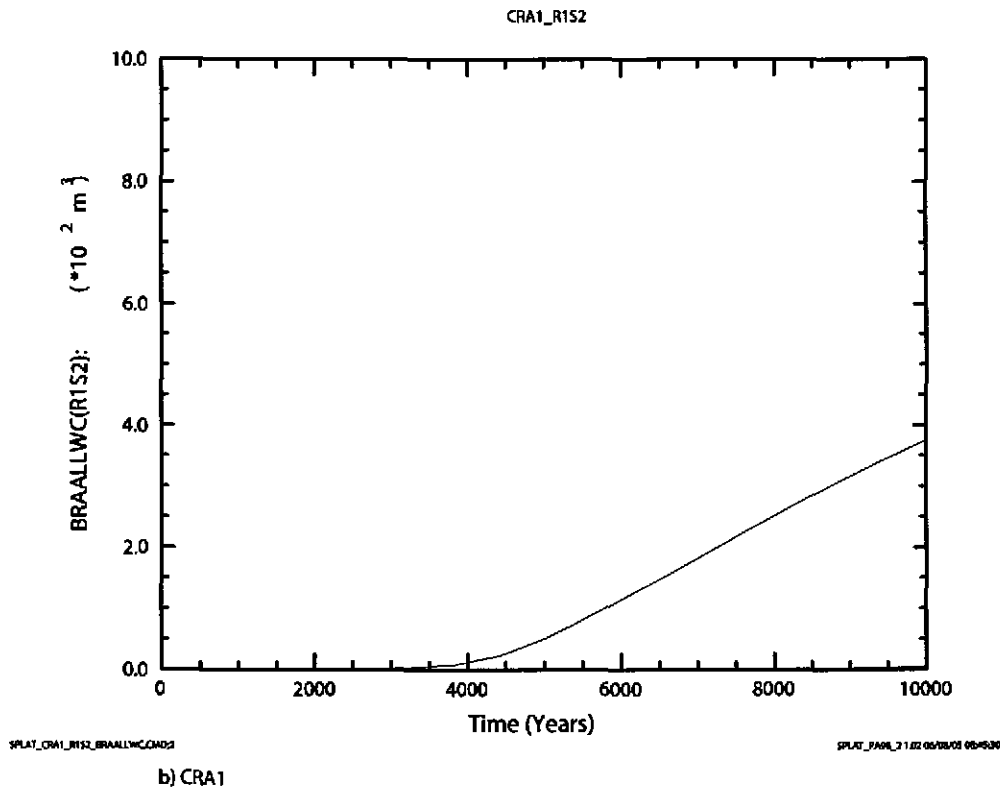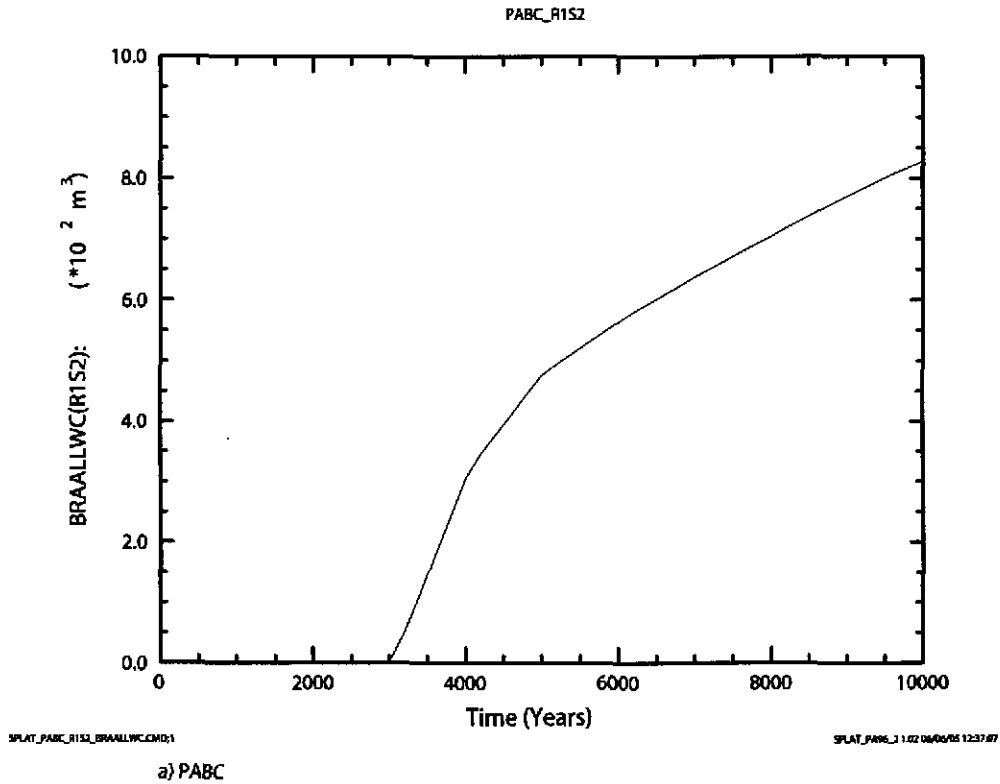
b) CRA1

Figure 6-79. Cumulative brine flow (m³) to the LWB versus time (years) for all 100 vectors in Replicate 1, Scenario S2. Figure a) shows results from the CRA-2004 PABC. Figure b) shows results from the CRA-2004.
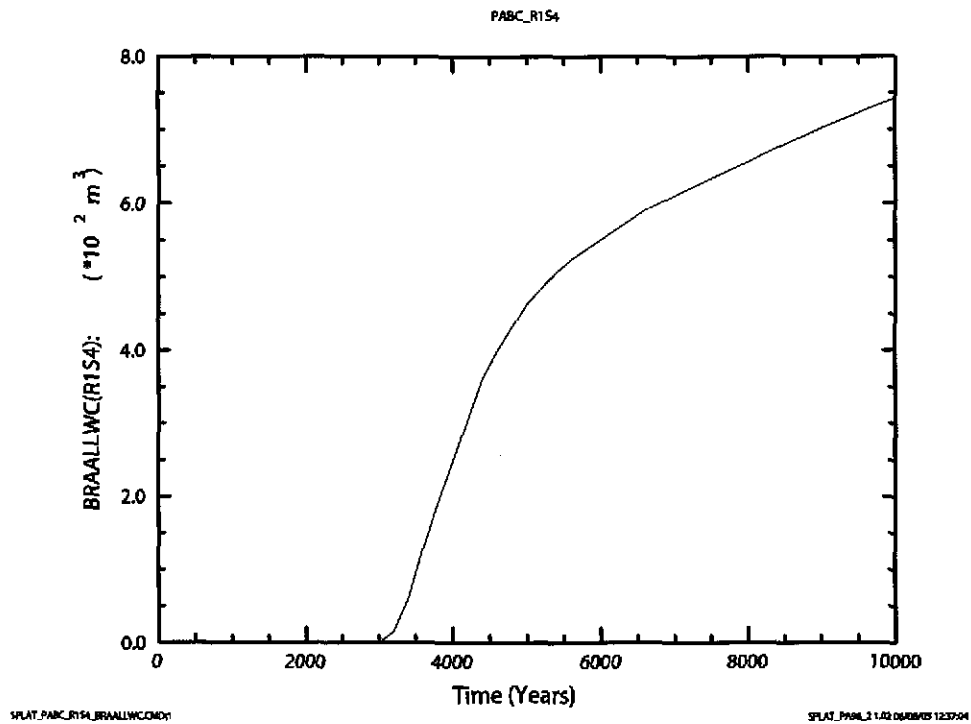
a) PABC
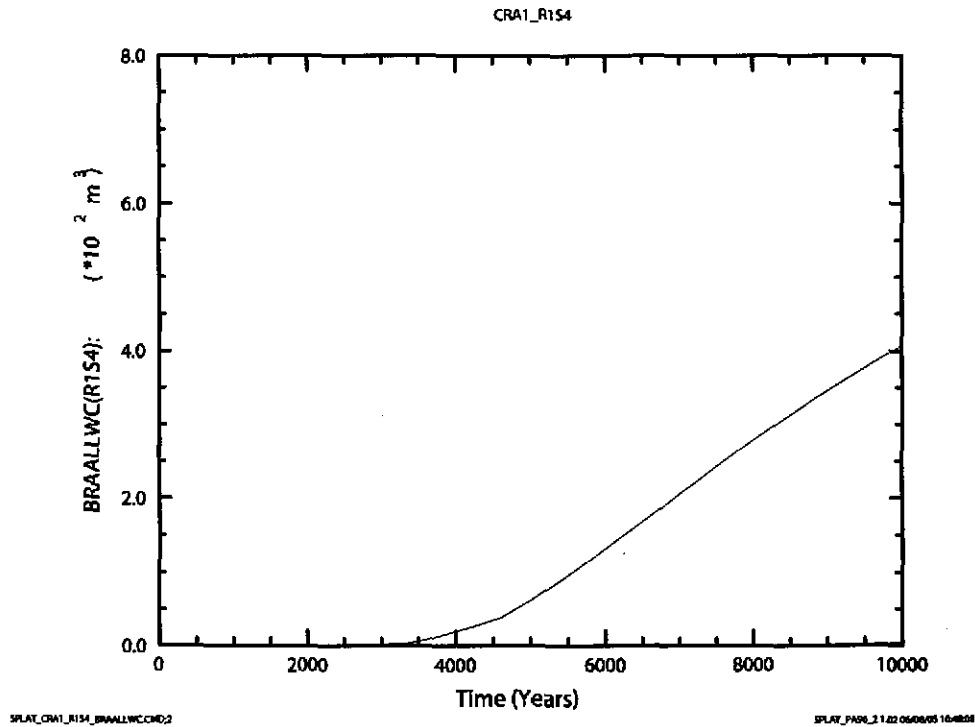
b) CRA1

Figure 6-80. Cumulative brine flow (m³) to the LWB versus time (years) for all 100 vectors in Replicate 1, Scenario S4. Figure a) shows results from the CRA-2004 PABC. Figure b) shows results from the CRA-2004.

6.5 COMPARISON OF REPLICATES

The Salado Flow Analysis employs three replicates to confirm the statistical reliability of the primary analysis of Replicate 1. Each is composed of the same six scenarios, but each replicate uses a different Latin Hypercube set of sampled input parameters.

Comparison of results from the three replicates is based upon three key output variables. These variables are chosen because of their importance to other models, which calculate releases that are tallied in the final CCDFs. All of these variables are discussed in detail for replicate 1 in §6:

- WAS_SATB - brine saturation in the waste panel
- WAS_PRES - pressure in the waste panel
- BRNREPOC - cumulative brine flow away from the repository

Figure 6-81 and Figure 6-82 show volume averaged pressure in the Waste Panel (WAS_PRES) versus time, averaged over 100 vectors, from Scenario S1, replicates 1-3, from the CRA-2004 PABC and the CRA-2004 The differences in the replicates are about the same relative magnitude in the two analyses. Figure 6-83 and Figure 6-84 show the brine saturation in the Waste Panel (WAS_SATB) versus time for the same set of analyses as Figure 6-81. Figure 6-85 and Figure 6-86 show the cumulative brine flow away from the repository (BRNREPOC) for the same set of analyses as Figure 6-81. The differences between replicates are greater for WAS_SATB and BRNREPOC than for WAS_PRES but no greater in the CRA-2004 PABC than was seen in the CRA-2004.
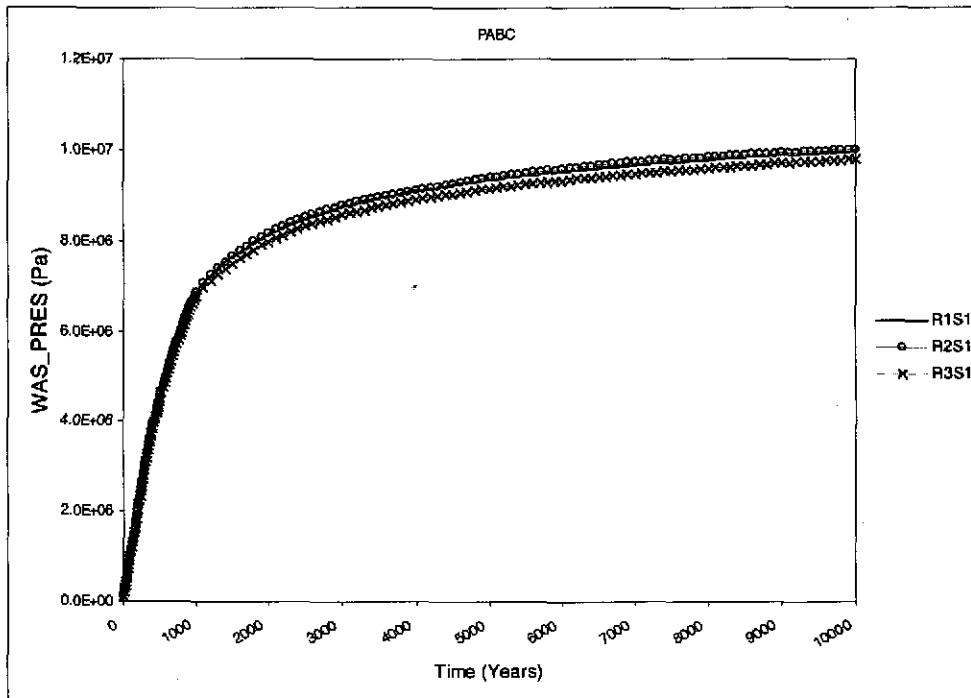
Figure 6-81. Volume averaged pressure (Pa) in the waste area versus time (years) from the CRA-2004 PABC, *Scenario* S1, Replicates 1-3.
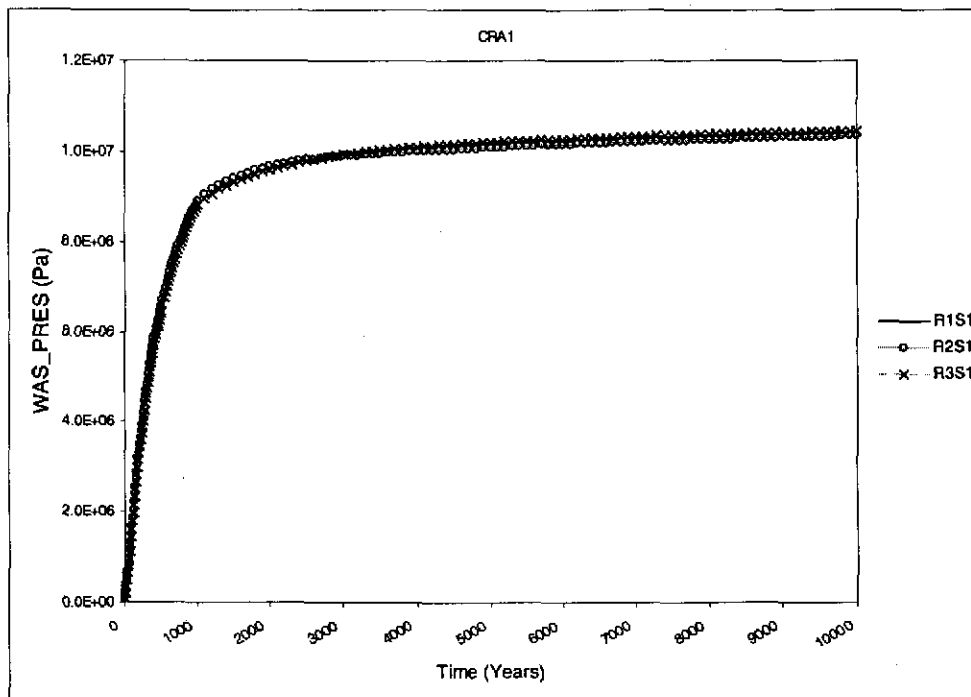
Figure 6-82. Volume averaged pressure (Pa) in the waste area versus time (years) from the CRA-2004 PABC, *Scenario* S1, Replicates 1-3.
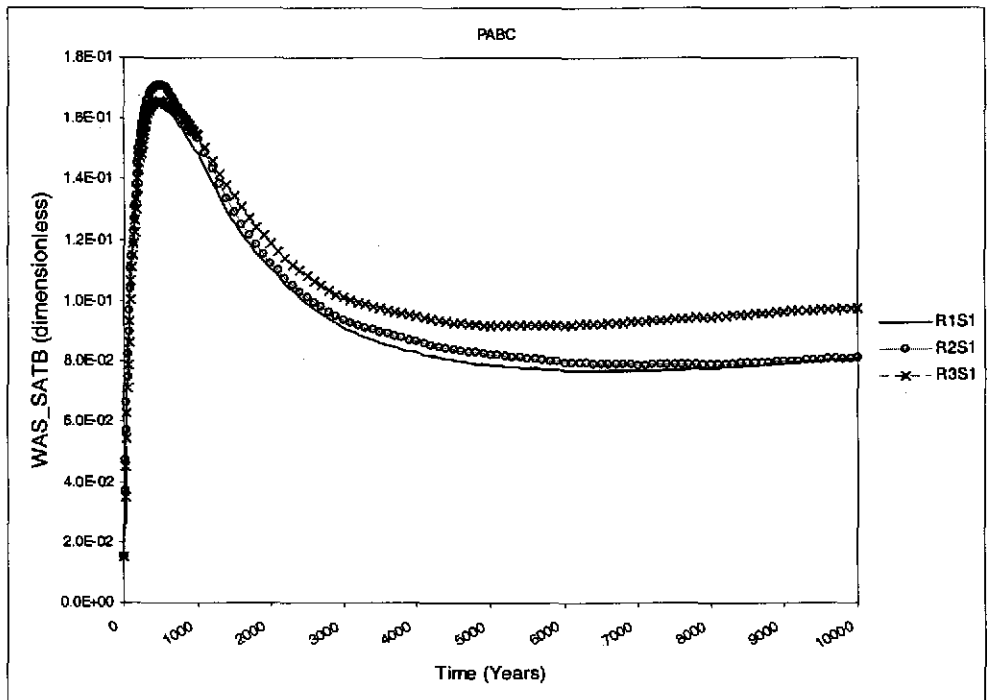
Figure 6-83. Volume-averaged brine saturation (dimensionless) in the waste panel versus time (years)) from the CRA-2004 PABC, Scenario S1, Replicates 1-3. Note that brine saturation axis maximum is set at 0.18 to emphasize the differences.
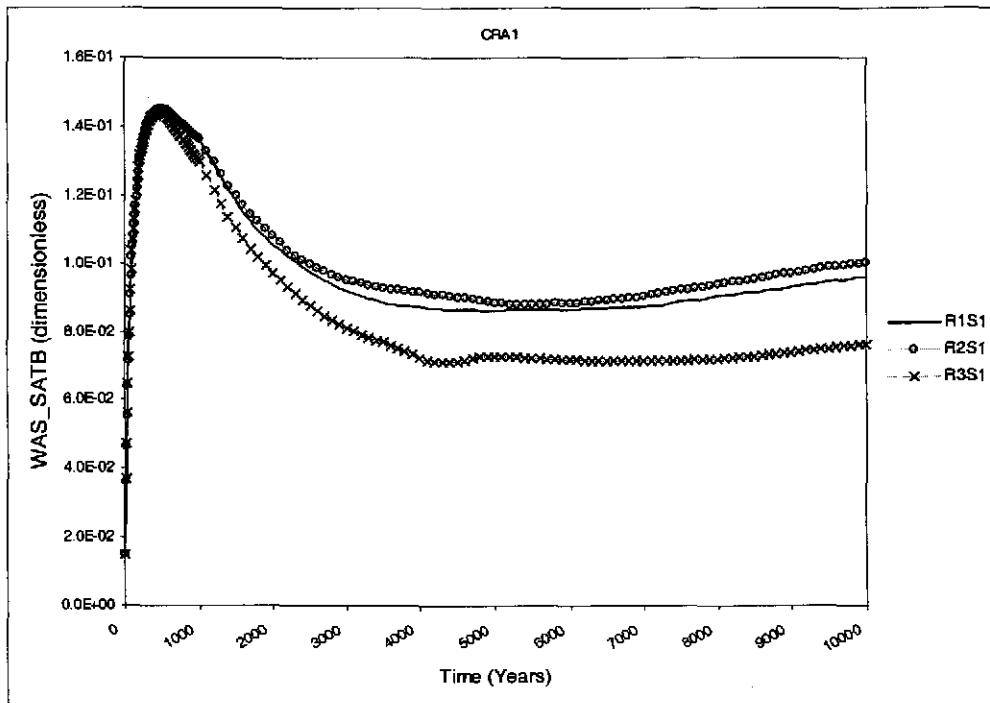
Figure 6-84. Volume-averaged brine saturation (dimensionless) in the waste panel versus time (years)) from the CRA-2004 PABC, Scenario S1, Replicates 1-3. Note that brine saturation axis maximum is set at 0.16 to emphasize the differences.
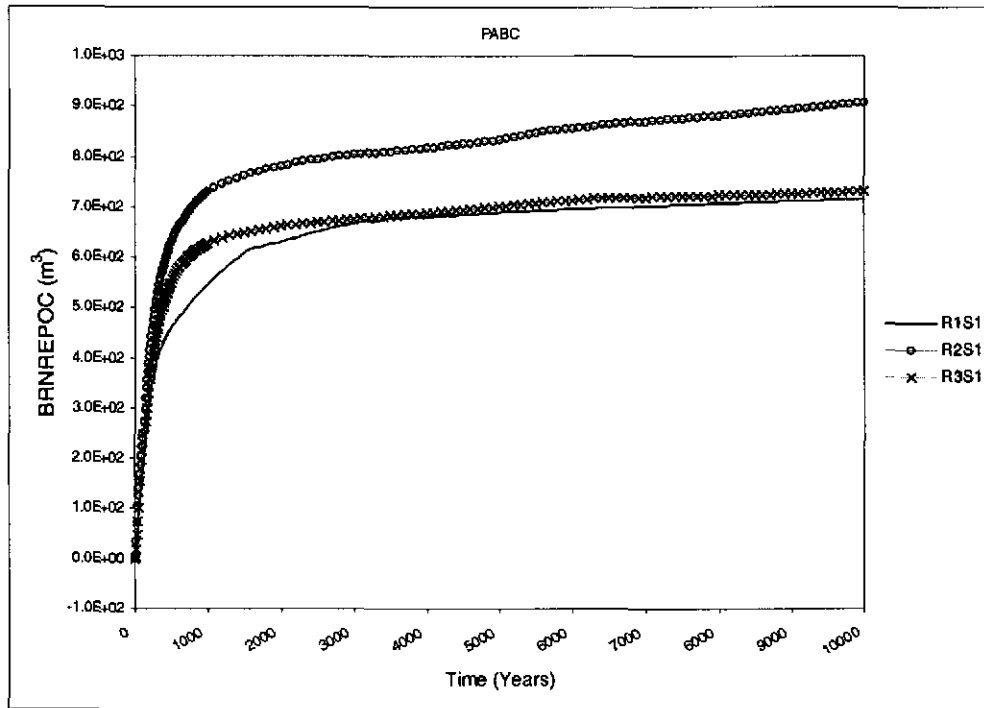
Figure 6-85. Cumulative brine flow (m³) away from the repository versus time (years) from the CRA-2004 PABC, Scenario S1, Replicates 1-3.
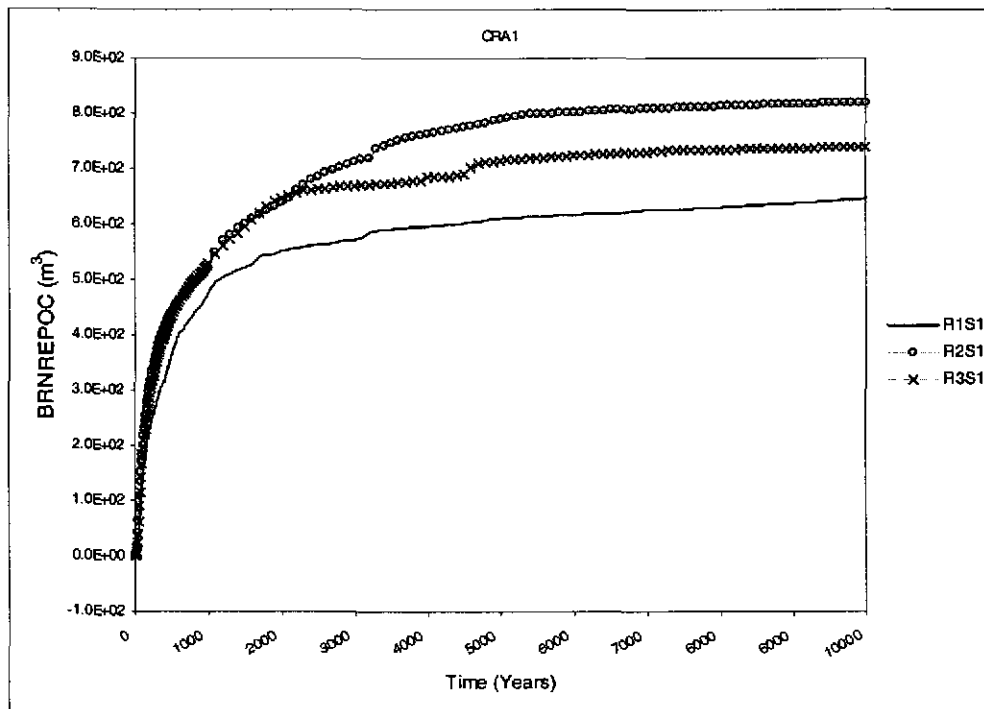
Figure 6-86. Cumulative brine flow (m³) away from the repository versus time (years) from the CRA-2004 PABC, Scenario S1, Replicates 1-3.

7 SUMMARY AND CONCLUSIONS

The BRAGFLO analysis contained herein provides essential outputs that are needed by other PA process models in order to calculate total releases from the repository. Results of the CRA-2004 PABC and CRA-2004 were compared. For the S1 scenario, pressures and saturations in the CRA-2004 PA and the CRA-2004 PABC were similar at 10,000 years. Pressures tended to increase more slowly in the CRA-2004 PABC due to the new lower microbial gas generation rates, which may affect Spallings and DBR releases that occur at short times.

8   REFERENCES

Brush, L. H. (2004). Implications of New (Post-CCA) Information for The Probability of Significant Microbial Activity In the WIPP. Sandia National Laboratory, Albuquerque, NM. ERMS 536205.

Caporuscio, F., J. Gibbons and E. Oswald (2002). Waste Isolation Pilot Plant: Salado Flow Conceptual Models Peer Review Report. U.S. Department of Energy, Carlsbad Area Office, Office of Regulatory Compliance, Carlsbad, NM. ERMS 523783.

Caporuscio, F., J. Gibbons and E. Oswald (2003). Waste Isolation Pilot Plant: Salado Flow Conceptual Models Final Peer Review Report. U.S. Department of Energy, Carlsbad Area Office, Office of Regulatory Compliance, Carlsbad, NM. ERMS 526879.

Cotsworth, E. (2004a). EPA's CRA completeness comments, 2nd set. U.S. Environmental Protection Agency, Washington, DC. ERMS 537187.

Cotsworth, E. (2004b). EPA's CRA completeness comments, 3rd set. U.S. Environmental Protection Agency, Washington, DC. ERMS 536771.

Cotsworth, E. (2004c). EPA received CRA on March 26, 2004. U.S. Environmental Protection Agency., Washington, DC. ERMS 535554.

Cotsworth, E. (2004d). Fourth Set of CRA Comments (December 17, 2004 Letter to Lloyd Piper, Acting Manger. Carlsbad Field Office, U.S. Department of Energy). U.S. Environmental Protection Agency, Washington, DC. ERMS #540236.

Cotsworth, E. (2005). EPA letter on conducting the performance assessment baseline change (PABC) verification test. U.S. EPA, Office of Radiation and Indoor Air, Washington, D.C. ERMS 538858.

Crawford, B. (2005). Waste Material Densities in TRU Waste Streams from TWBID Revision 2.1 Version 3.13, Data Version D.4.15. Los Alamos National Laboratory, Carlsbad, NM. ERMS 539323.

Detwiler, P. (2004a). DOE Letter #4: Response to CRA Comments (September 29, 2004 Letter to E. Cotsworth, Director, Office of Radiation and Indoor Air, U.S. Environmental Protection Agency). U.S. Department of Energy, Carlsbad, NM. ERMS #540237.

Detwiler, P. (2004b). DOE Letter #5: Response to CRA Comments (October 20, 2004 Letter to E. Cotsworth, Director, Office of Radiation and Indoor Air, U.S. Environmental Protection Agency). U.S. Department of Energy, Carlsbad, NM. ERMS #540238.

Detwiler, P. (2004c). DOE Letter #6: Response to CRA Comments (November 1, 2004 Letter to E. Cotsworth, Director, Office of Radiation and Indoor Air, U.S. Environmental Protection Agency). U.S. Department of Energy, Carlsbad, NM. ERMS #540239.

Detwiler, P. (2004d). Partial response to Environmental Protection Agency (EPA) May 20, 2004 letter on CRA. U.S. Department of Energy, Carlsbad, NM. ERMS 537372.

Detwiler, P. (2004e). Partial response to Environmental Protection Agency (EPA) May 20, 2004 letter on CRA, [1st response submittal to EPA]. U.S. Department of Energy, Carlsbad, NM. ERMS 537430.

Detwiler, P. (2004f). Response to Environmental Protection Agency (EPA) July 12, 2004 letter on CRA. U.S. Department of Energy, Carlsbad, NM. ERMS 537369.

Dotson, L. (1996). Memo to M. Tierney, Parameter Values for Forty-Niner, Tamarisk, and Unnamed Lower Members of the Rustler Formation (Addundum to Records # 21,22, 23, 24). Sandia National Laboratory, Carlsbad, NM. ERMS# 232291.

Francis, A. J., J. B. Gillow and M. R. Giles (1997). Microbial Gas Generation Under Expected Waste Isolation Pilot Plant Repository Conditions. Sandia National Laboratories, Albuquerque, NM. SAND96-2582. ERMS 244883.

Gilkey, A. P. (1995). User's Manual for PCCSRC, Version 2.21, Document Version 1.00. Sandia National Laboratories, Albuquerque, NM. ERMS 227773.

Gilkey, A. P. (1996). User's Manual for ALGEBRACDB, Version 2.35, Document Version 1.01. Sandia National Laboratories, Albuquerque, NM. ERMS 241864.

Gilkey, A. P. (2001). User's Manual and Criteria Form for MATSET, Version 9.10. Sandia National Laboratory, Carlsbad, NM. ERMS# 519736.

Gitlin, B. (2005). Fifth Set of CRA Comments (February 3, 2005 Letter to Ines Triay, Acting Manger. U.S. Environmental Protection Agency, Washington, DC. ERMS #540240.

Hansen, C. W. (2004). Software Problem Report (SPR) form 04-006 for LHS Version 2.41. Sandia National Laboratories, Carlsbad, NM. ERMS 536209.

Hansen, C. W. and C. Leigh (2002). A Reconciliation of the CCA and PAVT Parameter Baselines, Revision 2. Sandia National Laboratories, Carlsbad, NM. ERMS 524694.

Hansen, C. W., C. Leigh, D. Lord and J. S. Stein (2002). BRAGFLO Results for the Technical Baseline Migration. Sandia National Laboratories, Carlsbad, NM. ERMS 523209.

Helton, J. C., J. E. Bean, et al. (1998). Uncertainty and Sensitivity Analysis Results Obtained in the 1996 Performance Assessment for the Waste Isolation Pilot Plant. Sandia National Laboratories, Albuquerque, NM. SAND98-0365 ERMS #252619.

Kanney, J. F. and C. D. Leigh (2005). Analysis Plan for Post CRA PA Baseline Calculation AP-122. Sandia National Laboratory, Carlsbad, NM. ERMS# 539624.

Long, J. J. (2004). Execution of Performance Assessment for the Compliance Recertification Application (CRA1), Revision 1. Sandia National Laboratories, Carlsbad, NM. ERMS 536616.

Long, J. J. and J. F. Kanney (2005). Execution of Performance Assessment Codes for the CRA-2004 Performance Assessment Baseline Calculation. Sandia National Laboratory, Carlsbad, NM.

Monod, J. (1949). "The growth of bacterial cultures." Annual Review of Microbiology 3: 371-394.

Nemer, M. B. (2005). Updated Value of WAS_AREA:PROBDEG; April 20, 2005 memo to David Kessel. Sandia National Laboratory, Carlsbad, NM. ERMS 539441.

Nemer, M. B., J. S. Stein and W. Zelinski (2005). Analysis Report for BRAGFLO Preliminary Modeling Results With New Gas Generation Rates Based Upon Recent Experimental Results. Sandia National Laboratory, Carlsbad, NM. ERMS 539437.

Nemer, M. B. and W. Zelinski (2005). Analysis Report for BRAGFLO Modeling Results with the removal of Methanogenesis from the Microbial-Gas-Generation Model. Sandia National Laboratory, Carlsbad, NM. ERMS 538748.

Patterson, R. (2005). DOE Letter #9: Response to CRA Comments (March 18, 2005 Letter to E. Cotsworth, Director, Office of Radiation and Indoor Air, U.S. Environmental Protection Agency). U.S. Department of Energy, Carlsbad, NM. ERMS# 540241.

Piper, L. (2004). DOE Letter #7: Response to CRA Comments (December 23, 2004 Letter to E. Cotsworth, Director, Office of Radiation and Indoor Air, U.S. Environmental Protection Agency). U.S. Department of Energy, Carlsbad, NM. ERMS #540242.

Rath, J. (1995). ICSET, Version 2.21ZO, Version Date 9/14/95, User's Manual. Sandia National Laboratories, Albuquerque, NM. ERMS 223329.

Rechard, R. P., A. P. Gilkey, H. J. Iuzzolino, D. K. Rudeen and K. A. Byle (1990). Programmer's Manual for CAMCON: Compliance Assessment Methodology Controller, SAND90-1984. Sandia National Laboratory, Albuquerque, NM. ERMS# 224600.

Shuldberg, H. K. (1995). User's Manual for GENMESH, Version 6.07, Document Version 1.00. Sandia National Laboratories, Albuquerque, NM. ERMS 223291.

SNL (1996). Verification of 2-D Radial Flaring Using 3-D Geometry. Sandia National Laboratories, Albuquerque, NM. ERMS 230840.

SNL (1997). Final, Supplemental Summary of EPA-Mandated Performance Assessment Verification Test (All Replicates) and Comparison with the Compliance Certification Application Calculations. ERMS 414879.

Stein, J. S. (2002). Methodology Behind the TBM BRAGFLO Grid." Memorandum to M.K. Knowles, May 13, 2002. Sandia National Laboratories, Carlsbad, NM. ERMS 522373.

Stein, J. S. (2003a). User's Manual for BRAGFLO Version 5.00, Document Version 5.00. Sandia National Laboratories, Carlsbad, NM. ERMS 525702.

Stein, J. S. (2003b). User's Manual for PREBRAG Version 7.00, Document Version 7.00. Sandia National Laboratories, Carlsbad, NM. ERMS 526643.

Stein, J. S. and M. B. Nemer (2005). Analysis Plan for Updating the Microbial Degradation Rates for performance Assessment, AP-116. Sandia National Laboratory, Albuquerque, NM. ERMS 538596.

Stein, J. S. and W. Zelinski (2003a). Analysis Package for BRAGFLO: Compliance Recertification Application. Sandia National Laboratories, Carlsbad, NM. ERMS 530163.

Stein, J. S. and W. P. Zelinski (2003b). Analysis Report for: Testing of a Proposed BRAGFLO Grid to be used for the Compliance Recertification Application Performance Assessment Calculations. Sandia National Laboratories, Carlsbad, NM. ERMS 526868.

Triay, I. R. (2005). DOE Letter #8: Response to CRA Comments (January 19, 2005 Letter to E. Cotsworth, Director, Office of Radiation and Indoor Air, U.S. Environmental Protection Agency). U.S. Department of Energy, Carlsbad Field Office, Carlsbad, NM. ERMS #540243.

U. S. DOE (1980). Final Environmental Impact Statement: Waste Isolation Pilot Plant. U.S. Department of Energy, Assistant Secretary for Defense Programs, Vols. 1-2., Washington, D.C. DOE/EIS-0026, ERMS 238839.

U. S. DOE (1990). Final Supplement: Environmental Impact Statement, Waste Isolation Pilot Plant. U.S. Department of Energy, Office of Environmental Restoration and Waste Management. Vols. 1-13, Washington, D.C. DOE/EIS-0026-FS, ERMS 247955 and 243022.

U. S. DOE (1993). Waste Isolation Pilot Plant Strategic Plan. U.S. Department of Energy, Washington, D.C. ERMS 251353.

U. S. DOE (1996). Title 40 CFR Part 191 Compliance Certification Application for the Waste Isolation Pilot Plant. U.S. Department of Energy, Waste Isolation Pilot Plant Carlsbad Area Office, Carlsbad, NM. DOE/CAO-1996-2184.

U. S. DOE (2002). January 31'st, 2002 Technical baseline Report: Compliance Monitoring and Repository Investigations, Milestone RI110. U.S. Department of Energy Waste Isolation Pilot Plant, Carlsbad, NM. ERMS 520467.

U.S. DOE (1996). Title 40 CFR Part 191 Compliance Certification Application for the Waste Isolation Pilot. U.S. Department of Energy Waste Isolation Pilot Plant, Carlsbad Area Office, Carlsbad, NM. DOE/CAO-1996-2184.

U.S. DOE (2004). Title 40 CFR Part 191 Compliance Recertification Application for the Waste Isolation Pilot. U.S. Department of Energy Waste Isolation Pilot Plant, Carlsbad Field Office, Carlsbad, NM. DOE/WIPP 2004-3231.

U.S. EPA (1996). 40 CFR 194. Criteria for the Certification and Recertification of the Waste Isolation Pilot Plant's Compliance with the 40 CFR Part 191 Disposal Regulations; Final Rule. U.S. Environmental Protection Agency, Washington, DC. ERMS 241579.

Vugrin, E., T. Kirchner, J. Stein and B. Zelinski (2005). Analysis Report for Modifying Parameter Distributions for S_MB139:COMP_RCK and S_MB139:SAT_RGAS. Sandia National Laboratory, Carlsbad, NM. ERMS# 539301.

Vugrin, E. D. (2004). Software Problem Report (SPR) 2004-09 for LHS Version 2.41. Sandia National Laboratories, Carlsbad, NM. ERMS 538239.

Vugrin, E. D. (2005a). Change Control Form for LHS Version 2.41 to 2.42. Sandia National Laboratories, Carlsbad, NM. ERMS 538375.

Vugrin, E. D. (2005b). Design Document for LHS Version 2.42 Document Version 2.42. Sandia National Laboratories, Carlsbad, NM. ERMS 538371.

Vugrin, E. D. (2005c). Implementation Document for LHS Version 2.42 Document Version 2.42. Sandia National Laboratories, Carlsbad, NM. ERMS 538373.

Vugrin, E. D. (2005d). Installation and Checkout Form for LHS Version 2.42. Sandia National Laboratories, Carlsbad, NM. ERMS 538376.

Vugrin, E. D. (2005e). Requirements Document for LHS Version 2.42 Document Version 2.42. Sandia National Laboratories, Carlsbad, NM. ERMS 538369.

Vugrin, E. D. (2005f). User's Manual for LHS Version 2.42 Document Version 2.42. Sandia National Laboratories, Carlsbad, NM. ERMS 538374.

Vugrin, E. D. (2005g). Verification and Validation Plan/Validation Document for LHS Version 2.42 Document Version 2.42. Sandia National Laboratories, Carlsbad, NM. ERMS 538370.

Wang, Y. and L. Brush (1996). Estimates of Gas-Generation Parameters for the Long-Term WIPP Performance Assessment. Sandia National Laboratory, Albuquerque, NM. ERMS 231943.

Wang, Y. and L. Brush (2002). Gas Generation Parameters Required for BRAGFLO. Sandia National Laboratory, Albuquerque, NM. ERMS 230819.

APPENDIX A: INVENTORY OF CELLULOSE PLASTICS AND RUBBER

Here the CPR inventory is tabulated and converted to moles of organic carbon. Table 0-1 lists the various types of CPR materials in the WIPP repository and their total masses. All values were obtained from the WIPP parameter database.

Table 0-1. Cellulosics inventory from the 2004 CRA PA. The volume of the contact-handled waste and the volume of the remote-handled waste were obtained from WAS_AREA:VOLCHW and WAS_AREA:VOLRHW respectively in the parameter database

Type of cellulosics	contact (CH) or remote handled (RH)	WAS_AREA property in the parameter database	Density (kg/m^3)	Volume (m^3)	Total mass (kg)
CELL	CH	DCELLCHW	60	1.68500E+05	1.01100E+07
-	RH	DCELLRHW	9.3	7080	6.58440E+04
-	Total	-	-	-	1.01758E+07
RUB	CH	DRUBBCHW	13	1.68500E+05	2.19050E+06
-	RH	DRUBBRHW	6.7	7080	4.74360E+04
-	Total	-	-	-	2.23794E+06
PLAS	CH	DPLASCHW+DPLSCCHW	60	1.68500E+05	1.01100E+07
-	RH	DPLASRHW+DPLSCRHW	11.1	7080	7.85880E+04
-	Total	-	-	-	1.01886E+07

Given the total masses of the three types of CPR materials, cellulose, rubber and plastic, we can find their equivalent amounts of cellulose using conversion factors (Wang and Brush, 1996). This is accomplished in Table 0-2.

Table 0-2. Conversion of the masses of cellulose, plastics, and rubber into equivalent amounts of cellulose. Conversion factors were obtained from Wang and Brush, 1996a.

Type of material	Mass (kg)	Conversion factor	Converted mass (kg)
cell	1.01758E+07	1	1.01758E+07
rubber	2.23794E+06	1	2.23794E+06
plastics	1.01886E+07	1.7	1.73206E+07
Total	-	-	2.97344E+07

Thus given the total equivalent mass of cellulosics 2.97344E+07 kg, we convert to total moles of organic carbon by

$$mol\ C = kg\ cellulose \times \frac{1000\ mol\ cellulose}{162\ kg\ cellulose} \times \frac{6\ mol\ C}{mol\ cellulose}, \tag{9}$$

where 162/1000 is the molecular weight of cellulose in mol/kg and there are 6 mol of organic carbon in 1 mol of cellulose ($C_6H_{10}O_5$). Inserting the total mass 2.97344E+07 kg into equation (9) yields 1.10127E+09 mol organic C.

Given the total mol of organic carbon 1.10127E+09 mol, and the new inventory of nitrate (4.31E+07) from

Table 5-1, equations (3)-(4) yield the maximum moles of gas that can be produced,

$$mol\ gas = \frac{2.4\,N_2}{4.8\,NO_3^-} 4.31E + 07\,mol\,NO_3^- + \frac{3\,H_2S}{6\,C}\left(1.10E + 09molC - \frac{6\,C}{4.8\,NO_3^-}4.31E + 07\,mol\,NO_3^-\right) = 5.45E + 08 \qquad (10)$$

In the above equation the first term is the amount of gas produced by denitrification, the second term is the amount of gas produced by sulfate reduction. Thus the fraction of gas produced by denitrification is

$$\frac{2.4\,N_2}{4.8\,NO_3^-}4.31E + 07\,mol\,NO_3^- \Big/ 5.45E + 08\,mol\,gas = 0.04. \qquad (11)$$

APPENDIX B: ALGEBRACDB (ALG2) OUTPUT VARIABLES IN STEP 5

Name	Type/Units	Description
FE_KG	Steel (kg)	Remaining Mass Of Steel
CELL_KG	Cellulose (kg)	Remaining Mass Of Cellulose
FE_REM	Fraction of Initial Steel	Remaining Fraction Of Steel
CELL_REM	Fraction of Initial Cellulose	Remaining Fraction Of Cellulose
FE_MOLE	Gas (moles)	Cumulative Gas Generation By Corrosion
CELL_MOL	Gas (moles)	Cumulative Gas Generation By Total Microbial Activity
GAS_MOLE	Gas (moles)	Cumulative Total Gas Generation
CELL_M_H	Gas (moles)	Cumulative Gas Generation By Microbial Activity In A Humid Environment
CELL_M_I	Gas (moles)	Cumulative Gas Generation By Microbial Activity In An Inundated Environment
C_M_HI_T	Gas (moles)	Cumulative Gas Generation By Total Microbial Activity
FE_MOL_D	Gas (moles/drum)	Cumulative Gas Generation By Corrosion
CEL_MH_D	Gas (moles/drum)	Cumulative Gas Generation By Microbial Activity In A Humid Environment
CEL_MI_D	Gas (moles/drum)	Cumulative Gas Generation By Microbial Activity In An Inundated Environment
CELMOL_D	Gas (moles/drum)	Cumulative Gas Generation By Total Microbial Activity (CELL_MOL/DRUMTOT)
C_MHIT_D	Gas (moles/drum)	Cumulative Gas Generation By Total Microbial Activity (C_M_HI_T/DRUMTOT)
GASMOL_D	Gas (moles/drum)	Cumulative Total Gas Generation
GAS_FE_V	Gas Volume (m^3)	Cumulative Gas Generation By Corrosion
GAS_CMH	Gas Volume (m^3)	Cumulative Gas Generation By Humid Microbial Activity
GAS_CMI	Gas Volume (m^3)	Cumulative Gas Generation By Inundated Microbial Activity
GAS_C_V	Gas Volume (m^3)	Cumulative Gas Generation By Total Microbial Activity (CELL_MOL)
C_MHIT_V	Gas Volume (m^3)	Cumulative Gas Generation By Total Microbial Activity (C_M_HI_T)
GAS_VOL	Gas Volume (m^3)	Cumulative Total Gas Generation
WAS_PRES	Pressure (Pa)	Volume-Averaged Pressure: Waste Panel
SRR_PRES	Pressure (Pa)	Volume-Averaged Pressure: RoR South

Name	Type/Units	Description
NRR_PRES	Pressure (Pa)	Volume-Averaged Pressure: RoR North
REP_PRES	Pressure (Pa)	Volume-Averaged Pressure: RoR (North + South)
OPS_PRES	Pressure (Pa)	Volume-Averaged Pressure: Ops Region
EXP_PRES	Pressure (Pa)	Volume-Averaged Pressure: Exp Region
W_R_PRES	Pressure (Pa)	Volume-Averaged Pressure: All Waste Regions
B_P_PRES	Pressure (Pa)	Volume-Averaged Pressure: Castille Brine Pocket
PORVOL_T	Pore Volume (m^3)	Total Pore Volume In The Repository
BRNVOL_W	Brine Volume (m^3)	Brine Volume: Waste Panel
BRNVOL_S	Brine Volume (m^3)	Brine Volume: RoR South
BRNVOL_N	Brine Volume (m^3)	Brine Volume: RoR North
BRNVOL_R	Brine Volume (m^3)	Brine Volume: RoR (North + South)
BRNVOL_T	Brine Volume (m^3)	Brine Volume: All Waste Regions
BRNVOL_O	Brine Volume (m^3)	Brine Volume: Ops Region
BRNVOL_E	Brine Volume (m^3)	Brine Volume: Exp Region
BRNVOL_A	Brine Volume (m^3)	Brine Volume: All Excavated Areas
WAS_SATG	Gas Saturation (dimensionless)	Volume-Averaged Gas Saturation: Waste Panel
SRR_SATG	Gas Saturation (dimensionless)	Volume-Averaged Gas Saturation: Ror South
NRR_SATG	Gas Saturation (dimensionless)	Volume-Averaged Gas Saturation: Ror North
REP_SATG	Gas Saturation (dimensionless)	Volume-Averaged Gas Saturation: Ror (North + South)
OPS_SATG	Gas Saturation (dimensionless)	Volume-Averaged Gas Saturation: Ops Region
EXP_SATG	Gas Saturation (dimensionless)	Volume-Averaged Gas Saturation: Exp Region
W_R_SATG	Gas Saturation (dimensionless)	Volume-Averaged Gas Saturation: All Waste Regions
B_P_SATG	Gas Saturation (dimensionless)	Volume-Averaged Gas Saturation: Castille Brine Pocket
WAS_SATB	Brine Saturation (dimensionless)	Volume-Averaged Brine Saturation: Waste Panel
SRR_SATB	Brine Saturation (dimensionless)	Volume-Averaged Brine Saturation: RoR South
NRR_SATB	Brine Saturation (dimensionless)	Volume-Averaged Brine Saturation: RoR North
REP_SATB	Brine Saturation (dimensionless)	Volume-Averaged Brine Saturation: RoR (North + South)
OPS_SATB	Brine Saturation (dimensionless)	Volume-Averaged Brine Saturation: Ops Region
EXP_SATB	Brine Saturation (dimensionless)	Volume-Averaged Brine Saturation: Exp Region
W_R_SATB	Brine Saturation (dimensionless)	Volume-Averaged Brine Saturation: All Waste Regions

Name	Type/Units	Description
B_P_SATB	Brine Saturation (dimensionless)	Volume-Averaged Brine Saturation: Castille Brine Pocket
WAS_POR	Porosity (dimensionless)	Volume-Averaged Porosity: Waste Panel
SRR_POR	Porosity (dimensionless)	Volume-Averaged Porosity: RoR South
NRR_POR	Porosity (dimensionless)	Volume-Averaged Porosity: RoR North
REP_POR	Porosity (dimensionless)	Volume-Averaged Porosity: RoR (North + South)
OPS_POR	Porosity (dimensionless)	Volume-Averaged Porosity: Ops Region
EXP_POR	Porosity (dimensionless)	Volume-Averaged Porosity: Exp Region
W_R_POR	Porosity (dimensionless)	Volume-Averaged Porosity: All Waste Regions
BRN_RMV	Brine Volume (m^3)	Brine Consumed
BRNREPTC	Brine Volume (m^3)	Total Brineflow Into Repository
BRNWPIC	Brine Volume (m^3)	Total Brineflow Into Waste Panel
BRNSRRIC	Brine Volume (m^3)	Total Brineflow Into RoR South
BRNNRRIC	Brine Volume (m^3)	Total Brineflow Into RoR North
BRNRRIC	Brine Volume (m^3)	Total Brineflow Into RoR (North + South)
BRNORIC	Brine Volume (m^3)	Total Brineflow Into Ops Region
BRNEAIC	Brine Volume (m^3)	Total Brineflow Into Exp Region
BRNREPOC	Brine Volume (m^3)	Total Brinflow Out Of Repository
BRNREPNC	Brine Volume (m^3)	Net Brineflow Into Repository
BRNWPOC	Brine Volume (m^3)	Total Brinflow Out Of Waste Panel
BRNWPNC	Brine Volume (m^3)	Net Brineflow Into Waste Panel
BRNSRROC	Brine Volume (m^3)	Total Brinflow Out Of RoR South
BRNSRRNC	Brine Volume (m^3)	Net Brineflow Into RoR South
BRNNRROC	Brine Volume (m^3)	Total Brinflow Out Of RoR North
BRNNRRNC	Brine Volume (m^3)	Net Brineflow Into RoR North
BRNRROC	Brine Volume (m^3)	Total Brinflow Out Of RoR (North + South)
BRNRRNC	Brine Volume (m^3)	Net Brineflow Into RoR (North + South)
BRNOROC	Brine Volume (m^3)	Total Brinflow Out Of Ops Region
BRNORNC	Brine Volume (m^3)	Net Brineflow Into Ops Region
BRNEAOC	Brine Volume (m^3)	Total Brinflow Out Of Exp Region
BRNEANC	Brine Volume (m^3)	Net Brineflow Into Exp Region

Name	Type/Units	Description
BRNBHUPP	Brine Volume (m^3)	Brineflow Up Borehole: Bottom Of Waste Panel (@Element 1410)
BRNBHUPC	Brine Volume (m^3)	Brineflow Up Borehole: Bottom Of Upper DRZ (@Element 1168)
BRNBHRCC	Brine Volume (m^3)	Brineflow Up Borehole: Culebra/Unamed Contact (@Element 1845)
BRNBHRUC	Brine Volume (m^3)	Brineflow Up Borehole: Dewey Lake/49er Contact (@Element 1979)
BRNBHRSC	Brine Volume (m^3)	Brineflow Up Borehole: Santa Rosa (@Element 2155)
BNBHLDRZ	Brine Volume (m^3)	Brineflow Up Borehole: Bottom Of Lower DRZ (@Element 1111)
BNBHUDRZ	Brine Volume (m^3)	Brineflow Up Borehole: Top Of Upper DRZ (@Element 1493)
BRNSHRSC	Brine Volume (m^3)	Brineflow up shaft: Santa Rosa (@element 1364)
BNSHDSCZ	Brine Volume (m^3)	Brineflow down shaft: Santa Rosa (@element 1496)
BRNSHRUC	Brine Volume (m^3)	Brineflow up shaft: Dewey Lake/49er Contact (@element 1493)
BNSHDRUZ	Brine Volume (m^3)	Brineflow Down Shaft: Dewey Lake/49er Contact (@Element 1493)
BRNSHRCC	Brine Volume (m^3)	Brineflow up Shaft: Culebra/unamed Contact (@element 1489)
BNSHDRCC	Brine Volume (m^3)	Brineflow down Shaft: Culebra/unamed Contact (@element 1489)
BNSHUDRZ	Brine Volume (m^3)	Brineflow up Shaft: MB138/U_DRZ Contact (@element 1381)
BNSHDDRZ	Brine Volume (m^3)	Brineflow down Shaft: MB138/U_DRZ Contact (@element 1381)
BRNSHABC	Brine Volume (m^3)	Brineflow Up Shaft: Anhy AB/CONC_MON Contact (@element 1315)
BNSHDABC	Brine Volume (m^3)	Brineflow down Shaft: Anhy AB/CONC_MON Contact (@element 1315)
BRM38NIC	Brine Volume (m^3)	Total Lateral Brineflow Out Of MB Toward Repository: MB 138, North
BRAABNIC	Brine Volume (m^3)	Total Lateral Brineflow Out Of MB Toward Repository: Anhydrite A & B, North
BRM39NIC	Brine Volume (m^3)	Total Lateral Brineflow Out Of MB Toward Repository: MB 139, North
BRM38SIC	Brine Volume (m^3)	Total Lateral Brineflow Out Of MB Toward Repository: MB 138, South
BRAABSIC	Brine Volume (m^3)	Total Lateral Brineflow Out Of MB Toward Repository: Anhydrite A & B, South
BRM39SIC	Brine Volume (m^3)	Total Lateral Brineflow Out Of MB Toward Repository: MB 139, South
BRAALIC	Brine Volume (m^3)	Total Lateral Brineflow Out Of MB Toward Repository: All Marker Beds
BRM38NOC	Brine Volume (m^3)	Total Lateral Brineflow Into MB Away From Repository: MB 138, North
BRAABNOC	Brine Volume (m^3)	Total Lateral Brineflow Into MB Away From Repository: Anhydrite A & B, North
BRM39NOC	Brine Volume (m^3)	Total Lateral Brineflow Into MB Away From Repository: MB 139, North
BRM38SOC	Brine Volume (m^3)	Total Lateral Brineflow Into MB Away From Repository: MB 138, South

Name	Type/Units	Description
BRAABSOC	Brine Volume (m^3)	Total Lateral Brineflow Into MB Away From Repository: Anhydrite A & B, South
BRM39SOC	Brine Volume (m^3)	Total Lateral Brineflow Into MB Away From Repository: MB 139, South
BRAALOC	Brine Volume (m^3)	Total Lateral Brineflow Into MB Away From Repository: All Marker Beds
BRM38NNC	Brine Volume (m^3)	Net Lateral Brineflow Through MB: MB 138, North
BRAABNNC	Brine Volume (m^3)	Net Lateral Brineflow Through MB: Anhydrite A & B, North
BRM39NNC	Brine Volume (m^3)	Net Lateral Brineflow Through MB: MB 139, North
BRM38SNC	Brine Volume (m^3)	Net Lateral Brineflow Through MB: MB 138, South
BRAABSNC	Brine Volume (m^3)	Net Lateral Brineflow Through MB: Anhydrite A & B, South
BRM39SNC	Brine Volume (m^3)	Net Lateral Brineflow Through MB: MB 139, South
BRAALNC	Brine Volume (m^3)	Net Lateral Brineflow Into DRZ Through All Anhydrite Layers
GASBHUPC	Gas Volume (m^3)	Cumulative Gas Flow Up Borehole: Top Of Waste Panel
GASBHUDZ	Gas Volume (m^3)	Cumulative Gas Flow Up Borehole: Top Of Upper DRZ
GSSHUSCC	Gas Volume at Reference Conditions (m^3)	Gas flow up shaft (@element 1496 Santa Rosa)
GSSHRRUC	Gas Volume at Reference Conditions (m^3)	Gas Flow Up Shaft (@Element 1493 49er/Dewey Lake)
GSSHUCUC	Gas Volume at Reference Conditions (m^3)	Gas flow up shaft (@element 1489 unnamed/Culebra)
GSSHUDRZ	Gas Volume at Reference Conditions (m^3)	Gas flow up shaft (@element 1381 U_DRZ/Upper 138)
GASSHABC	Gas Volume at Reference Conditions (m^3)	Gas flow up shaft (@element 1315 Anhy AB/CONC_MON)
GSM38NOC	Gas Volume at Reference Conditions (m^3)	Total Gas Flow Through MB Away From Repository: MB 138, North
GSAABNOC	Gas Volume at Reference Conditions (m^3)	Total Gas Flow Through MB Away From Repository: Anhydrite A & B, North
GSM39NOC	Gas Volume at Reference Conditions (m^3)	Total Gas Flow Through MB Away From Repository: MB 139, North
GSM38SOC	Gas Volume at Reference Conditions (m^3)	Total Gas Flow Through MB Away From Repository: MB 138, South
GSAABSOC	Gas Volume at Reference Conditions (m^3)	Total Gas Flow Through MB Away From Repository: Anhydrite A & B, South
GSM39SOC	Gas Volume at Reference Conditions (m^3)	Total Gas Flow Through MB Away From Repository: MB 139, South
GSAALOC	Gas Volume at Reference Conditions (m^3)	Total Gas Flow Through MB Away From Repository: All Marker Beds

Name	Type/Units	Description
FRACX38N	Fracture Length (m)	Interbed Fracturing: Length Of Fracture Zone: MB 138, North
FRACXABN	Fracture Length (m)	Interbed Fracturing: Length Of Fracture Zone: Anhydrite A & B, North
FRACX39N	Fracture Length (m)	Interbed Fracturing: Length Of Fracture Zone: MB 139, North
FRACX38S	Fracture Length (m)	Interbed Fracturing: Length Of Fracture Zone: MB 138, South
FRACXABS	Fracture Length (m)	Interbed Fracturing: Length Of Fracture Zone: Anhydrite A & B, South
FRACX39S	Fracture Length (m)	Interbed Fracturing: Length Of Fracture Zone: MB 139, South
VFRAC38N	Fracture volume (m^3)	Interbed Fracturing: Vol Of Fracturing Zone: MB 138, North
VFRACABN	Fracture volume (m^3)	Interbed Fracturing: Vol Of Fracturing Zone: Anhydrite A & B, North
VFRAC39N	Fracture volume (m^3)	Interbed Fracturing: Vol Of Fracturing Zone: MB 139, North
VFRAC38S	Fracture volume (m^3)	Interbed Fracturing: Vol Of Fracturing Zone: MB 138, South
VFRACABS	Fracture volume (m^3)	Interbed Fracturing: Vol Of Fracturing Zone: Anhydrite A & B, South
VFRAC39S	Fracture volume (m^3)	Interbed Fracturing: Vol Of Fracturing Zone: MB 139, South
VFRACTMB	Fracture volume (m^3)	Total MB Fracture Vol: All Marker Beds
APERM38N	Permeability (m^2)	Vol-Averaged Permeability In Fracture Zone: MB 138, North
APERMABN	Permeability (m^2)	Vol-Averaged Permeability In Fracture Zone: Anhydrite A & B, North
APERM39N	Permeability (m^2)	Vol-Averaged Permeability In Fracture Zone: MB 139, North
APERM38S	Permeability (m^2)	Vol-Averaged Permeability In Fracture Zone: MB 138, South
APERMABS	Permeability (m^2)	Vol-Averaged Permeability In Fracture Zone: Anhydrite A & B, South
APERM39S	Permeability (m^2)	Vol-Averaged Permeability In Fracture Zone: MB 139, South
PVOLI38N	Permeability (m^2)	Increase In Pore Vol In Fracture Zone: MB 138, North
PVOLIABN	Permeability (m^2)	Increase In Pore Vol In Fracture Zone: Anhydrite A & B, North
PVOLI39N	Permeability (m^2)	Increase In Pore Vol In Fracture Zone: MB 139, North
PVOLI38S	Permeability (m^2)	Increase In Pore Vol In Fracture Zone: MB 138, South
PVOLIABS	Permeability (m^2)	Increase In Pore Vol In Fracture Zone: Anhydrite A & B, South
PVOLI39S	Permeability (m^2)	Increase In Pore Vol In Fracture Zone: MB 139, South
PVOLI_T	Permeability (m^2)	Total Frac Zone Pore Vol Increase: All Marker Beds
BRNVOL_B	Brine Volume (m^3)	Brine Vol: Castille Brine Pocket
BNBHDNUZ	Brine Volume (m^3)	Downward Brine Flow: Borehole At Top Of MB 138
BRNBHDNC	Brine Volume (m^3)	Downward Brine Flow: Borehole At Top Of Waste Panel

Name	Type/Units	Description
FEKG_W	Steel (kg)	Steel Mass Remaining: Waste Panel
CELLKG_W	Cellulose (kg)	Cellulose Mass Remaining: Waste Panel
FEREM_W	Fraction of Initial Iron & Steel	Fraction Steel Remaining: Waste Panel
CELREM_W	Fraction of Initial Cellulose	Fraction Cellulose Remaining: Waste Panel
GASMOL_W	Gas (moles)	Total Number Of Moles Of Gas Generated: Waste Panel
GASVOL_W	Gas at Reference Conditions (m^3) Total	Gas Volume Generated: Waste Panel
PORVOL_W	Pore volume (m^3)	Total Pore Volume: Waste Panel
BRNM38I	Brine Volume (m^3)	Total Brineflow Out Of MB, Towards Repository: MB 138
BRNAABI	Brine Volume (m^3)	Total Brineflow Out Of MB, Towards Repository: Anhydrite A & B
BRNM39I	Brine Volume (m^3)	Total Brineflow Out Of MB, Towards Repository: MB 139
BRNM38O	Brine Volume (m^3)	Total Brineflow Into MB, Away From Respository: MB 138
BRNAABO	Brine Volume (m^3)	Total Brineflow Into MB, Away From Respository: Anhydrite A & B
BRNM39O	Brine Volume (m^3)	Total Brineflow Into MB, Away From Respository: MB 139
BRN_RMVW	Brine Volume (m^3)	Brine Consumed: Waste Panel
BRN_RMSR	Brine Volume (m^3)	Brine Consumed: RoR South
BRN_RMNR	Brine Volume (m^3)	Brine Consumed: RoR North
BRN_RMVR	Brine Volume (m^3)	Brine Consumed: RoR (North + South)
FEREM_SR	Fraction of Initial Iron & Steel	Fraction Of Steel Remaining: RoR South
CELREM_S	Fraction of Initial Cellulose	Fraction Of Cellulose Remaining: RoR South
FEREM_NR	Fraction of Initial Iron & Steel	Fraction Of Steel Remaining: RoR North
CELREM_N	Fraction of Initial Cellulose	Fraction Of Cellulose Remaining: RoR North
FEREM_R	Fraction of Initial Iron & Steel	Fraction Of Steel Remaining: RoR (North + South)
CELREM_R	Fraction of Initial Cellulose	Fraction Of Cellulose Remaining: RoR (North + South)
GASMOL_S	Gas (moles)	Total Number Of Moles Of Gas Generated: RoR South
GASMOL_N	Gas (moles)	Total Number Of Moles Of Gas Generated: RoR North
GASMOL_R	Gas (moles)	Total Number Of Moles Of Gas Generated: RoR (North + South)
BRWI_XBH	Brine Volume (m^3)	Cumulative Brineflow Into Waste Panel, Excluding Borehole
SAL_BR_T	Fraction of Total Brine Inflow	(Salado Brine Inflow)/(Total Brine Inflow): DRZ
SAL_BR_U	Fraction of Unconsumed Brine Inflow	(Salado Brine Inflow)/(Unconsumed Brine Inflow): DRZ
SB_TB_WP	Fraction of Total Brine Inflow	(Salado Brine Inflow)/(Total Brine Inflow): Waste Panel

Name	Type/Units	Description
SB_UB_WP	Fraction of Unconsumed	Brine Inflow: (Salado Brine Inflow)/(Unconsumed Brine Inflow): Waste Panel
BRNBHUMC	Brine Volume (m^3)	Brineflow Up: Borehole At Magenta Dolomite
BRNSHUMC	Brine Volume (m^3)	Brineflow Up: Shaft At Magenta Dolomite
BRM38NLW	Brine Volume (m^3)	Total Outward Brineflow In MBs Across LWB: MB 138, North
BRAABNLW	Brine Volume (m^3)	Total Outward Brineflow In MBs Across LWB: Aanhydrite A & B, North
BRM39NLW	Brine Volume (m^3)	Total Outward Brineflow In MBs Across LWB: MB 139, North
BRM38SLW	Brine Volume (m^3)	Total Outward Brineflow In MBs Across LWB: MB 138, South
BRAABSLW	Brine Volume (m^3)	Total Outward Brineflow In MBs Across LWB: Anhydrite A & B, South
BRM39SLW	Brine Volume (m^3)	Total Outward Brineflow In MBs Across LWB: MB 139, South
BRAALLWC	Brine Volume (m^3)	Total Outward Brineflow In MBs Across LWB: All Marker Beds
FR_TG_C	Fraction of Total Gas	Fraction Of Total Gas Due To Steel Corrosion: All Waste Regions
FR_TG_M	Fraction of Total Gas	Fraction Of Total Gas Due To Total Microbial Activity: All Waste Regions
FR_TG_H	Fraction of Total Gas	Fraction Of Total Gas Due To Humid Microbial Activity: All Waste Regions
FR_TG_I	Fraction of Total Gas	Fraction Of Total Gas Due To Inundated Microbial Activity: All Waste Regions
FR_MG_H	Fraction of Total Gas	Fraction Of Microbial Activity Gas From Humid Conditions: All Waste Regions
FR_MG_I	Fraction of Total Gas	Fraction Of Microbial Activity Gas From Inundated Conditions: All Waste Regions
PORVOL_S	Pore volume (m^3)	Total Pore Vol: RoR South
PORVOL_N	Pore volume (m^3)	Total Pore Vol: RoR North
PORVOL_R	Pore volume (m^3)	Total Pore Vol: RoR (North + South)